Agrociencia

eISSN: 2521-9766

VOLUME 59, NUMBER 8 | November 16 - December 31, 2025 | MEXICO

In Memoriam

Jane Goodall

1934 – 2025

AGRICULTURA
SECRETARIA DE AGRICULTURA

COPYRIGHT AND RELATED RIGHTS, **Volume 59, Number 8, November 16 - December 31, 2025**, Agrociencia is a semi-monthly publication edited by Colegio de Postgraduados. Carretera Mexico-Texcoco, Km 36.5, Montecillo, Texcoco, State of Mexico. C. P. 56264. Phone: 5959284427. www.colpos.mx. Editor in chief: Dr. Fernando Carlos Gómez Merino. Reservations of Rights to Exclusive Use 04-2021-031913431800-203. eISSN: 2521-9766, granted by the National Copyright Institute. Last modification date, **December 31, 2025**.

All correspondence (subscription information, sales, advertising, author contributions, etc.) should be addressed to:

Central Office:

Agrociencia
Guerrero No. 9, Esquina con Avenida Hidalgo,
San Luis Huexotla, Texcoco 56220,
State of Mexico. MEXICO
Tel.: +52-595 92 84427

https://agrociencia-colpos.org/index.php/agrociencia

Cover: Dr. Jane Goodall. *In memoriam*.
1934-2025
English primatologist, anthropologist, and ethologist renowned for her pioneering, decades-long research on wild primates.

AGRICULTURA
SECRETARÍA DE AGRICULTURAY DESARROLLO RURAL

Contents

Volume 59, Number 8 | November 16 - December 31, 2025

Agrociencia

MODERN AGRICULTURE SYSTEMS: ENHANCING PRECISION FARMING THROUGH ADVANCED AERIAL TECHNIQUES

Mayuranathan **Mani**[1], Dhivya **Baskar**[2],
Sathish Kumar **Pakkarisamy Janakiraman**[3], Surendran **Rajendran**[4*]

[1]SRM Valliammai Engineering College. Department of Computer Science and Engineering. Kattankulathur, Tamil Nadu 603203, India.
[2]Karpaga Vinayaga College of Engineering and Technology. Department of Artificial Intelligence and Data Science. Chengalpattu, Tamil Nadu 603308, India.
[3]Panimalar Engineering College. Department of Computer Science and Engineering. Chennai, Tamil Nadu 600123, India.
[4]Saveetha Institute of Medical and Technical Sciences. Saveetha School of Engineering, Department of Computer Science and Engineering. Chennai, Tamil Nadu 602105, India.
* Author for correspondence: dr.surendran.cse@gmail.com

Citation: Mani M, Baskar D, Pakkarisamy Janakiraman SK, Rajendran S. 2025. Modern agriculture systems: Enhancing precision farming through advanced aerial techniques. **Agrociencia** 59(8): 1073-1087. https://doi.org/ 10.47163/agrociencia.v59i8.3551

Editor in Chief:
Dr. Fernando C. Gómez Merino

Received: July 09, 2025.
Approved: November 18, 2025.
Published in Agrociencia: November 20, 2025.

ABSTRACT

In modern agriculture, early detection and treatment of crop diseases and pests are necessary for increasing yields and ensuring food security. Traditional methods are labor-intensive and time-consuming, leading to inefficiencies and delayed responses. This research presents a solution using drones for continuous monitoring and automated spraying of fertilizers and pesticides. Drones equipped with multispectral, thermal, and red, green, and blue (RGB) cameras collect high-resolution images of fields, which are then processed using machine learning techniques such as YOLOv5 for disease detection and Random Forest for fertilizer classification. Data is transmitted to an Internet of Things (IoT) platform, where it i1s analyzed to generate vegetation indices such as the Normalized Difference Vegetation Index (NDVI) and Enhanced Vegetation Index (EVI), which offer information on crop health. Upon detecting a disease, the system automatically triggers the drone's spraying mechanism, ensuring targeted management. Field trials demonstrate the system's ability to accurately detect diseases and optimize resource usage, improving crop health and yield. The integration of IoT enables real-time monitoring and alerts, allowing farmers to make informed decisions promptly. This study demonstrates the potential for combining drone technology, machine learning, and IoT to revolutionize agriculture, providing a scalable and efficient solution to modern farming challenges.

Keywords: Agriculture, drone technology, fertilizer spraying, Internet of Things, machine learning, triggering, real-time monitoring.

INTRODUCTION

To address the rising need for nourishment and ensure food stability objectives, modern agriculture increasingly relies on polymer coverings such as agricultural plastic sheets

(Du *et al*., 2024). Pesticide and fertilizer use is a widespread agricultural practice that protects crops from pests and diseases while enhancing yield and productivity. However, the residues these chemicals leave on food can pose significant health risks to consumers. Severe exposure can lead to acute toxicity, and long-term accumulation has been associated with hormonal disruptions, neurotoxicity, and even cancer.

Inappropriate or excessive use of fertilizers and pesticides has a negative impact on crops over time, leading to nutrient imbalances in the soil and reducing crop yields. Pesticide overuse often results in pest resistance, requiring stronger chemicals that further harm plants (Chen *et al*., 2024). Environmental consequences include soil degradation, water pollution from runoff, and air pollution from chemical volatilization. Technologies available for the application of fertilizers and pesticides include tractor-mounted sprayers, manual sprayers, robotic sprayers, and drone sprayers.

The manufacturing sector is evolving with the incorporation of cutting-edge technologies, marking the shift from conventional methods to Industry 4.0 and beyond (Dalenogare *et al*., 2018; Ghobakhloo, 2020; Askerbekov *et al*., 2024). Technologies such as the Internet of Things (IoT), innovative analytics, radio-frequency identification (RFID), automated storage systems, and robotics tackle particular tasks, enhancing logistics and distribution coordination, stock management, and worker safety (Raj *et al*., 2020). Amid these innovations, Unmanned Aerial Vehicles (UAVs), usually referred to as drones, and their interconnected systems within the outline of the Internet of Drones (IoD), are notably transformative.

Several industries are progressively adapting drones for commercial applications to improve workflow optimization, enhance worker security, and optimize stock control (Maghazei and Netland, 2019; Ayamga *et al*., 2021). Drone adoption has expanded rapidly, with an increasing number of registered UAV units and certified pilots contributing to broader agricultural and industrial applications (The Drone Girl, 2024). The market for commercial drones was estimated at USD 19.89 billion in 2022, with forecasts indicating a compound annual growth rate of 13.9 % until 2030 (Grand View Research, 2024). Increased use in industries such as construction fuels this expansion, with drones reducing surveying durations by 85 %, thereby improving project efficiency and safety. Technological progressions and flexible regulatory frameworks worldwide, including those implemented by the US Federal Aviation Administration, have bolstered this upsurge, with more than 500 000 drones recorded for commercial purposes in the USA by 2021 (Choi *et al*., 2023).

Several recent innovations highlight the transformative potential of drones in agriculture. For example, Singh *et al*. (2024) developed an intelligent farming UAV equipped with IoT technologies that use machine learning methods, such as TensorFlow Lite with an EfficientDetLite1 model, to recognize objects from a specialized dataset trained on three crop types, including pineapple, papaya, and cabbage, achieving an inference time of 91 ms. Meesaragandla *et al*. (2024) proposed a cutting-edge strategy with increased adaptability and a more structured methodology compared to conventional techniques, leading to an impressive 60-fold boost in efficiency.

Detecting weed clusters can be achieved through image capture with drones, followed by processing and spraying. Rathore *et al*. (2024) introduced a Field Area Calculation (FAC) system using a drone, which captured images and calculated the area through image processing and Gauss's area formula (surveyor's formula). The results were compared to satellite images. The proposed method demonstrated improved performance and yielded results that closely matched expectations. Jonak *et al*. (2024) presented a technique combining a YOLOv5 classifier with high-resolution imaging using a full-frame Sony Alpha A7R IV sensor mounted on a DJI Matrice 600 drone. Their study also emphasized selecting an appropriate super-resolution method to enhance low-resolution aerial images, improving the accuracy of crop and weed detection.

Roma *et al*. (2024) used a DJI Mavic 2 Pro UAV to capture visible light images in an area characterized by complex terrain features, such as peaks and valleys. A dataset of plastic film samples was constructed, and the parameters of the U-Net deep learning model, integrated into ArcGIS Pro, were continuously adjusted and optimized to achieve accurate plastic film identification. Meanwhile, Trappey *et al*. (2023) proposed a method that employs Object-Based Image Analysis (OBIA) and Digital Elevation Models (DEM) to segment and classify images and orthomosaics, enabling the extraction of key plant metrics such as canopy area, height, volume, and NDVI.

Through an in-depth literature review, Song *et al*. (2023) analyzed both patent and non-patent literature in the field of agricultural drones and established a knowledge framework for UAV technologies. Additionally, extensive macro- and micro-level patent evaluations were performed to assess patenting trends and identify leading technologies in the agricultural drone sector. In line with ongoing drone applications, Subramaniam *et al*. (2023) designed a device featuring a circular storage system with a hammer-driven release mechanism. The release outlet is positioned 50 cm below the drone's frame within the airflow zone, and the storage unit comprises eight cylindrical compartments, each 38 mm in diameter, enabling the deployment of up to 56 balls in a single operation.

Automation and precision technologies have focused on improving efficiency, accuracy, and resource management in crop management practices. Goodrich *et al*. (2023) aimed to enhance and optimize crop-dusting with agricultural drones by developing an advanced reservoir design and a stabilized release mechanism to improve the precision and efficiency of the application. Ghafar *et al*. (2023) introduced a novel approach that utilizes a progressive gap-minimization algorithm to reduce sensor redundancy and determine optimal sensor placement across four types of agricultural fields. In addition, a genetic algorithm was applied to optimize multi-agent flight trajectories for sensor scanning within a simulated agricultural environment using a robust agent-based model.

Recent innovations in agricultural automation and precision spraying have focused on improving efficiency, reducing chemical use, and enhancing crop monitoring. Moradi *et al*. (2024) developed a two-wheeled agricultural robot equipped with a

camera, wireless controller, and mobile app, enabling precise spraying of fertilizers and pesticides, automated robot movement, and continuous monitoring of crop health and growth. Similarly, Zhou *et al*. (2023) designed a dynamic fertilization management system for liquid fertilizers, combining accurate variable-rate application with deep fertilization technology using a fuzzy Proportional-Integral-Derivative (PID) algorithm. Honrao and Awadhani (2023) proposed an oscillating nozzle agriculture sprayer, which applies pesticides directly to plant spoilage and fruits, reducing waste and minimizing chemical usage.

Advances in informatics facilitate decision-making and promote sustainable farming. Deepa *et al*. (2024) proposed Agri-Ontology, a framework for structuring heterogeneous agricultural data through Natural Language Processing (NLP) techniques and ontology construction. Using BERT and Jaccard similarity, they extracted relationships from the Agrovoc dataset and used a BiGAN framework for performance evaluation, achieving an accuracy of 94.64 % and outperforming existing approaches. Building on this work, Deepa *et al*. (2025) introduced Agricultural Advancement using NLP (AA-NLP), an ontology-based framework that combines NLP techniques to process unstructured agricultural data. The system integrates named entity recognition, sentiment analysis, and semantic similarity to transform textual inputs into structured ontological knowledge, enhancing information retrieval, classification, and decision-making.

Bhargavi *et al*. (2024) proposed Smart Agriculture Computing using Quantum Natural Language Processing (SAC-QNLP) to improve decision-making and resource management. By integrating quantum computing with NLP, the framework processes large agricultural datasets more efficiently than classical methods. Simulation results showed higher forecasting accuracy and scalability, highlighting its potential to enhance productivity and sustainability. Selvaraj *et al*. (2025) developed a hybrid model combining Vision Transformer (ViT) and Convolutional Neural Network (CNN) for multi-disease detection in coffee plants. The approach integrates a counterfactual recommendation system to suggest suitable management and preventive measures. Their model achieved 98.81 % accuracy on 1056 images and was deployed in the Affogato app to support small-scale farmers with sustainable crop management.

From the reviewed literature, it is clear that although drones and machine learning are applied for crop monitoring, weed detection, and spraying, several limitations remain. Many models are dataset-specific and fail to generalize across different crops and environments. Approaches like U-Net or OBIA need large datasets and high computational power, limiting real-time use. Furthermore, some studies focus solely on detection without providing management recommendations or enabling automated spraying, and manual calibration of sensors and spraying systems can further reduce accuracy. These gaps remark the need for an integrated, IoT-enabled framework capable of real-time detection, classification, and precise spraying. In response, this work proposes a novel technology that combines drones and robots for continuous crop health monitoring and the targeted application of fertilizers and pesticides.

MATERIALS AND METHODS

This study proposes the use of advanced agricultural drones for the continuous monitoring of crops. High-resolution cameras capture crop images, which are then transmitted via Wi-Fi to an IoT-based cloud platform for storage and preprocessing using cloud computing services. The preprocessed data are analyzed using machine learning techniques such as YOLOv5, which trains and validates models to detect the presence of diseases or pests. Once identified, relevant features are extracted and classified using a Random Forest algorithm, allowing the system to recommend suitable management. Based on these recommendations, the drone autonomously applies the appropriate fertilizers or pesticides in precise quantities.

Crop image dataset

The proposed method allows pest and disease detection using cameras, followed by the application of appropriate management via drones. Images of maize and tomato crops, collected at different time intervals to capture variability in growth stages and environmental conditions, are included in the dataset provided by Kwabena *et al*. (2023) for crop pest and disease detection. The dataset was divided into two categories: (i) raw images, comprising 10 734 samples, including 5389 maize (*Zea mays* L.) and 5435 tomato (*Solanum lycopersicum* L.) images; and (ii) augmented images, which were further split into training and testing sets containing 50 835 images (23 657 maize and 27 178 tomato samples) and classified into 12 categories according to pest and disease symptoms: seven for maize (healthy, fall armyworm, leaf blight, maize streak virus, leaf spot, grasshopper, and leaf beetle) and five for tomato (healthy, tomato leaf curl virus, leaf blight, *Septoria* leaf spot, and *Verticillium* wilt). All images were stored in .jpg format, with dimensions of either 3024 × 4032 or 4032 × 3024 pixels. Images were captured under diverse background conditions, including white, illuminated, dark, and natural settings.

IoT cloud integration

Collected crop data were transmitted to the IoT cloud using wireless communication technology. The Wi-Fi module established a TCP/IP connection with the cloud and transmitted images through a Representational State Transfer Application Programming Interface (REST API) web service. To ensure data reliability, image files were sent in chunks. Upon reaching the cloud server, the data were securely stored in Google Cloud Storage for subsequent processing and analysis.

In the proposed system, the Internet of Things (IoT) plays a central role in enabling real-time connectivity, data management, and decision-making. The IoT framework functions as an intermediary between the agricultural field and the cloud platform by collecting images from drones and transmitting them securely via Wi-Fi 6 and REST API protocols. Once uploaded, the IoT infrastructure enables seamless integration with machine learning models (YOLOv5 and Random Forest) for automated disease detection and management recommendation. Furthermore, IoT provides real-

time alerts and feedback through connected devices, allowing remote monitoring of crop health. This integration ensures continuous surveillance, low-latency data transmission, and automated drone activation for spraying operations, thereby increasing the efficiency of pest and disease management while providing actionable, cloud-based insights for precision agriculture.

Machine learning algorithm

You Only Look Once version 5 (YOLOv5) is an advanced one-stage object detection algorithm widely recognized for its speed and accuracy in real-time applications. It consists of three major components: the backbone, neck, and detector. The backbone extracts and processes image features using Convolutional Neural Networks (CNNs), while the neck bridges the backbone and detector by generating multi-scale feature maps through a Feature Pyramid Network (FPN), enhancing detection of objects of varying sizes. The detector then predicts bounding boxes and class probabilities to identify the target objects.

In this study, YOLOv5 was used to analyze drone-captured images of crops and accurately detect symptoms of pest infestation and plant diseases in real time. Its lightweight architecture enables low-latency processing on edge devices, making it ideal for agricultural drones that must handle large image datasets during flight. Once the affected regions are detected, a Random Forest algorithm classifies the identified diseases or pests and recommends appropriate fertilizers and pesticides based on learned patterns from the training dataset.

By integrating detection and recommendation, the proposed machine learning framework minimizes human error, accelerates decision-making, and supports precision agriculture by ensuring that each crop receives timely and targeted management. YOLOv5 was selected for its superior performance compared to traditional two-stage models such as Faster R-CNN, achieving an overall accuracy of 96 %, with 95 % precision and 93 % recall in this work. These results are consistent with previous findings (Jonak *et al*., 2024; Singh *et al*., 2024), confirming YOLOv5's suitability for high-performance, real-time detection of crop pests and diseases in dynamic agricultural environments.

The detector used sophisticated feature maps to identify the bounding boxes and class possibilities of each identified object. YOLO segments the input image into a grid, with each cell responsible for detecting multiple bounding boxes and assigning confidence scores. Class labels are then allocated to the boxes with the highest scores, enabling real-time detection and classification of multiple objects simultaneously. The overall workflow of the proposed system is illustrated (Figure 1).

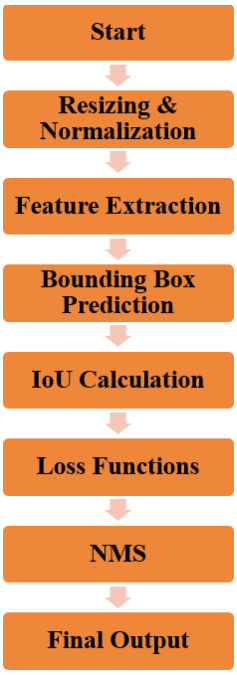

Figure 1. Schematic representation of the proposed disease detection process.

Training and testing

In this study, a dataset of 50 835 images was utilized and divided into two subsets: 80 % (40 668 images) for training and 20 % (10 167 images) for testing. All images were resized to a uniform resolution of 256 × 256 pixels to ensure consistency across the dataset. This approach enabled the machine learning model to learn from a wide range of conditions and visual features. The training subset was used to develop a robust detection model, while the testing subset served to evaluate its accuracy and overall performance.

Management recommendation

After the detection of diseases and pests, the Random Forest algorithm was used to recommend suitable fertilizers and pesticides. As a robust ensemble learning method widely applied in classification and regression tasks, Random Forest was trained using datasets encompassing major maize and tomato diseases and pests, along with their corresponding treatments (Table 1). These combinations, derived from established agronomic practices and prior research, allowed the model to generate precise, data-driven, and condition-specific treatment recommendations.

Following the detection of crop diseases and pests, the Random Forest algorithm was used to recommend appropriate fertilizers and pesticides. Gini impurity measures the degree of impurity at a node within a decision tree, representing the probability that a randomly chosen element would be incorrectly classified:

Table 1. Pest and disease management recommendations of maize (*Zea mays* L.) and tomato (*Solanum lycopersicum* L.) provided by the Random Forest algorithm.

Crop	Disease	Suitable fertilizer	Suitable pesticide
Maize	Northern leaf blight (*Exserohilum turcicum*)	Nitrogen-rich fertilizer	Mancozeb, Azoxystrobin
	Gray leaf spot (*Cercospora* sp.)	Potassium-rich fertilizer	Propiconazole, Tebuconazole
	Common rust (*Puccinia* sp.)	Phosphorus-rich fertilizer	Chlorothalonil, Mancozeb
	Corn borer (*Ostrinia nubilalis*)	Nitrogen-rich fertilizer	Permethrin, *Bacillus thuriniensis*
	Armyworm (*Spodoptera frugiperda*)	Potassium-rich fertilizer	Spinosad, Lambda-cyhalothrin
	Corn rootworm (*Diabrotica* sp.)	Phosphorus-rich fertilizer	Bifenthrin, Clothianidin
Tomato	Early blight (*Alternaria* sp.)	Nitrogen-rich fertilizer	Chlorothalonil, Mancozeb
	Late blight (*Phytophthora infestans*)	Potassium-rich fertilizer	Copper fungicides, Mancozeb
	Septoria leaf spot (*Septoria lycopersici*)	Phosphorus-rich fertilizer	Chlorothalonil, copper fungicides
	Tomato hornworm (*Manduca quinquemaculata*)	Nitrogen-rich fertilizer	*Bacillus thuringiensis*, Spinosad
	Whiteflies (*Bemisia* sp.)	Potassium-rich fertilizer	Imidacloprid, Neem oil
	Aphids (*Aphis* sp.)	Phosphorus-rich fertilizer	Pyrethrin

$$Gini = 1 - \sum_{i=1}^{n} (p_i)^2$$

where p_i represents the probability of class i at a particular node.

Entropy quantifies the amount of uncertainty or randomness in a dataset:

$$Entropy = -\sum_{i=1}^{n} p_i log_2(p_i)$$

Information Gain (IG) measures the effectiveness of a split in a decision tree by measuring the reduction in entropy achieved after the split:

$$IG = Entropy(parent) - \sum_{j} \frac{N_j}{N} Entropy(child_j)$$

where N_j represents the number of samples in child node j and N is the total number of nodes.

The Out-of-Bag (OOB) error is used to estimate the generalization performance. It is calculated as the average error for each training instance, using only the trees that excluded that instance in their bootstrap samples.

$$OOB\ Error = \frac{1}{N}\sum_{i=1}^{N} I(y_i \neq \hat{y}OOB, i)$$

where N denotes the total number of training instances, y_i is the actual label, and $\hat{y}OOB, i$ is the predicted label from the OOB samples.

Feature importance measures the contribution of each feature in predicting the target variable. It is computed as the average decrease in impurity across all trees in the forest whenever a feature is used for splitting:

$$Feature\ Importance = \frac{1}{T}\sum_{t=1}^{T}(\frac{\Delta\ Impurity(t)}{Number\ of\ splits}$$

where T is the total number of trees, and $\Delta\ Impurity(t)$ is the decrease in impurity for tree t.

Implementation of the UAV-based precision spraying

The spraying process in the proposed system was implemented using the onboard mechanism of the Yamaha RMAX drone. This robust and versatile UAV is widely used in agricultural and industrial applications. It was introduced in the 1990s and has become a leading platform for precision spraying, crop monitoring, and data acquisition. It features a two-stroke liquid-cooled engine that ensures stability and endurance during flight and a 28 L payload tank connected to a multi-nozzle spraying system for uniform and efficient distribution of liquid fertilizers and pesticides (Figure 2).

Once the algorithms detect and classify crop diseases or pests, the corresponding treatment recommendations are transmitted to the drone controller via an IoT-based communication platform. The variable-rate control unit automatically adjusts nozzle flow according to the severity and spatial extent of the detected infection. This precision-targeted spraying approach minimizes over-application, reduces chemical wastage, and limits environmental exposure. The RMAX operates at a flight altitude of 2–3 m above the crop canopy and applies treatments in optimized swath patterns with overlap correction to ensure even coverage. Compared with manual spraying,

Figure 2. Schematic representation of the Yamaha RMAX- Unmanned Aerial Vehicle (UAV) spraying mechanism used in the proposed system.

this system provides higher accuracy, lower environmental impact, and greater efficiency in large-scale agricultural operations. The technical specifications of the Yamaha RMAX are summarized (Table 2).

Performance metrics such as accuracy, precision, recall (sensitivity), and F1-score are essential for evaluating the effectiveness of machine learning models. Accuracy measures the proportion of correctly predicted instances out of the total number of instances. Precision evaluates the proportion of correctly predicted positive cases among all predicted positives, while recall (or sensitivity) measures the proportion of actual positive cases that are correctly identified by the model. The F1-score represents the harmonic mean of precision and recall, providing a balanced measure of both. These metrics are computed based on the values of true positives (TP), true negatives (TN), false positives (FP), and false negatives (FN).

Table 2. Technical specifications of the Yamaha RMAX-Unmanned Aerial Vehicle (UAV) used in the proposed spraying system.

Specifications		Details
Dimensions	Length	3.63 m
	Width	0.72 m
	Height	1.08 m
Weight	Empty weight	64 kg
	Maximum takeoff weight	94 kg
	Payload Capacity	28–31 kg
Power and Performance	Powerplant	Water-cooled, two-cylinder, two-stroke engine
	Main rotor diameter	3.115 m
	Endurance	Approximately 1 h per flight
Usage and Approvals	Countries used	Japan, Australia, South Korea, United States
	US Federal Aviation Administration approval	Approved for agriculture operations including pesticides and fertilizers spraying
	Flight condition	Flight below 60 m, within visual line of sight

RESULTS AND DISCUSSION

The confusion matrix (Figure 3) illustrates the classification performance of the model across three classes (0, 1, and 2). The model accurately predicted Class 0 in 68 instances, while 13 instances of Class 0 were misclassified as Class 2.

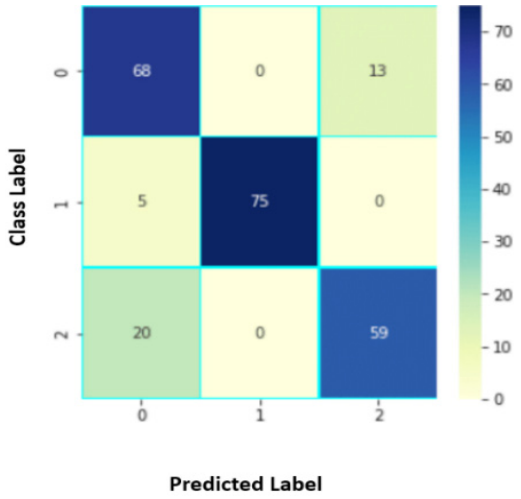

Figure 3. Confusion matrix illustrating the classification performance of the model across three classes (0, 1, and 2).

For Class 1, the model demonstrated high accuracy, correctly predicting 75 instances with only five misclassifications in Class 0. For Class 2, the model correctly identified 59 instances but misclassified 20 instances as Class 0. These results indicate that the model performs well for Class 1 with minimal error, whereas Class 2 has the highest misclassification rate, particularly with Class 0. Overall, the model maintains good classification accuracy but shows variability across classes, which indicates that it requires refinement in distinguishing between Classes 0 and 2.

The performance of YOLOv5 and Random Forest classifiers for crop disease detection and treatment recommendation demonstrated superior performance (Table 3). Both models achieve high accuracy, but Random Forest consistently outperformed

Table 3. Performance metrics of YOLOv5 and Random Forest for crop disease detection and treatment recommendation.

	Accuracy (%)	Precision (%)	Recall (%)	F1-Score (%)
YOLOv5	96	95	93	94
Random Forest	97	96	95	95.5

YOLOv5 across all metrics, with slightly higher precision, recall, and F1-score. This demonstrates that Random Forest provides more reliable and consistent predictions for the dataset, supporting accurate treatment recommendations.

Drone-based spraying offers several advantages over traditional manual spraying in agriculture. By reducing direct contact with chemical fertilizers and pesticides, drones minimize health risks to human workers. Additionally, drones cover larger areas in less time, whereas manual spraying is more labor-intensive and time-consuming. Over the long term, drones prove to be cost-effective by lowering labor expenses and optimizing the use of fertilizers and pesticides, while human spraying incurs higher labor and equipment costs. Drones provide real-time monitoring and dynamic adjustments during application. Overall, drone-based spraying is safer, more efficient, and more economically advantageous compared to conventional human spraying techniques.

The comparison of agricultural drones (Table 4) highlights differences in payload capacity, flight duration, coverage area, and spraying efficiency. The DJI Agras T20 and Yamaha RMAX each support payloads of up to 20 kg, making them suitable for large-scale field operations (Yamaha Motor Co., 2017; DJI, 2020). The Yamaha RMAX further demonstrates the longest reported operational endurance (60–90 min), a spray width of approximately 7 m, and a control range of up to 10 km, enabling wider coverage per mission (Zhang and Kovacs, 2012; Yamaha Motor Co., 2017). The DJI Agras T20, while operating with a slightly shorter flight time, can spray up to 30 ha per deployment (DJI, 2020).

Other platforms, such as the DJI Agras MG-1S and Yuneec H520E, offer lower payload capacity and shorter endurance, making them more appropriate for medium- or small-scale fields (Tsouros *et al*., 2019). Lightweight fixed-wing models like the Parrot Bluegrass and SenseFly eBee X provide longer flight times but are limited in

Table 4. Comparative specifications of agricultural drones for crop spraying applications.

Drone Model	Payload Capacity	Maximum Flight time	Coverage area per flight	Spray width	Spray system	Control range
DJI Agras T20	20 kg	15–20 min	Up to 30 ha	5 m	Four-nozzle system	5 km
DJI Agras MG-1S	10 kg	10–15 min	Up to 10 ha	5 m	Four-nozzle system	2 km
Yuneec H520E	5 kg	30 min	Up to 5 ha	4 m	Two-nozzle system	1.6 km
Parrot Bluegrass	1.8 kg	25–30 min	Up to 7 ha	2 m	One-nozzle system	2 km
SenseFly eBee X	1.6 kg	50–60 min	Up to 20 ha	3 m	Variable	5 km
Yamaha RMAX	20 kg	60–90 min	Up to 10 ha	7 m	Six-nozzle system	10 km

payload and spray volume, reducing their utility for dense crop coverage (Radoglou-Grammatikis *et al*., 2020). Overall, based on payload capability, flight endurance, and spray coverage, the Yamaha RMAX remains well-suited for large-scale fertilizer and pesticide applications.

CONCLUSION

This study established a precision spraying system for crops that applies suitable fertilizers and pesticides based on real-time detection of diseases and pests. The framework integrates the YOLOv5 model for accurate identification of multiple crop diseases and pests, while the Random Forest algorithm processes this information to recommend the appropriate fertilizers and pesticides. The Yamaha RMAX drone, equipped with a multi-nozzle spraying system, was employed to execute precise chemical application. By combining detection, recommendation, and automated spraying, the system reduces chemical wastage, minimizes environmental impact, and enhances overall crop management efficiency. This integrated approach not only improves precision in crop protection but also supports sustainable farming by optimizing the use of agricultural inputs.

The framework can be further advanced through improvements in sensor technology, autonomous drone navigation, and predictive modeling for crop management. Incorporating blockchain technology could enhance data security and traceability, while assessing environmental impacts would strengthen sustainability. Additionally, addressing socio-economic factors, such as making the technology accessible to small-scale farmers, could maximize its benefits, contributing to food security, rural economic growth, and broader adoption of precision agriculture practices.

REFERENCES

Askerbekov D, Garza-Reyes JA, Ghatak RR, Joshi R, Kandasamy J, Nascimento DLM. 2024. Embracing drones and the Internet of drones systems in manufacturing–An exploration of obstacles. Technology in Society 78: 102648. https://doi.org/10.1016/j.techsoc.2024.102648

Ayamga M, Akaba S, Nyaaba AA. 2021. Multifaceted applicability of drones: A review. Technological Forecasting and Social Change 167: 120677. https://doi.org/10.1016/j.techfore.2021.120677

Bhargavi G, Das M, Banumathi S, Malarvizhi E, Surendran R. 2024. Leveraging NLP and quantum computing for advanced agricultural solutions. *In* 8th International Conference on Electronics, Communication and Aerospace Technology (ICECA). Institute of Electrical and Electronics Engineers. Coimbatore, India, pp: 900–906. https://doi.org/10.1109/iceca63461.2024.10800767

Chen C, Hussain Z, Liu J, Zaman M, Akhlaq M. 2024. Innovative technologies in sprinkler irrigation: An overview. Agrociencia 58 (7): 1–18. https://doi.org/10.47163/agrociencia.v58i7.3191

Choi U, Moon C, Ahn J. 2023. Energy minimization of dynamic multi-UAV communication network for cooperative multihop data gathering. IEEE Transactions on Aerospace and Electronic Systems 59 (3): 3082–3099. https://doi.org/10.1109/taes.2022.3221031

Dalenogare LS, Benitez GB, Ayala NF, Frank AG. 2018. The expected contribution of Industry 4.0 technologies for industrial performance. International Journal of Production Economics 204: 383–394. https://doi.org/10.1016/j.ijpe.2018.08.019

Deepa R, Das M, Thilakavathy P, Prabhu AB, Surendran R. 2024. Harvesting knowledge: An innovative ontology framework for agricultural advancement using NLP methodologies. *In* 2024 Third International Conference on Electrical, Electronics, Information and Communication Technologies (ICEEICT). Institute of Electrical and Electronics Engineers. Tiruchirappalli, India, pp: 1–7. https://doi.org/10.1109/iceeict61591.2024.10718542

Deepa R, Jayaraman V, Srinivasulu S, Umamageswari B, Surendran R. 2025. Agri-ontology: A novel ontology framework for agricultural domain. *In* 2025 International Conference on Electronics and Renewable Systems (ICEARS). Institute of Electrical and Electronics Engineers. Tuticorin, India, pp. 1151–1157. https://doi.org/10.1109/icears64219.2025.10941477

DJI (Da Jiang Innovations). 2020. DJI AGRAS T20 support. Shenzhen DJI Sciences and Technologies Ltd. Shenzhen, China. https://www.dji.com/mx/support/product/t20 (Retrieved: October 2025).

Du X, Huang D, Dai L, Du X. 2024. Recognition of plastic film in terrain-fragmented areas based on drone visible light images. Agriculture 14 (5): 736. https://doi.org/10.3390/agriculture14050736

Ghafar AS, Hajjaj SSH, Gsangaya KR, Sultan MTH, Mail MF, Hua LS. 2023. Design and development of a robot for spraying fertilizers and pesticides for agriculture. Materials Today: Proceedings 81: 242–248. https://doi.org/10.1016/j.matpr.2021.03.174

Ghobakhloo M. 2020. Industry 4.0, digitization, and opportunities for sustainability. Journal of Cleaner Production 252: 119869. https://doi.org/10.1016/j.jclepro.2019.119869

Goodrich P, Betancourt O, Arias AC, Zohdi T. 2023. Placement and drone flight path mapping of agricultural soil sensors using machine learning. Computers and Electronics in Agriculture 205: 107591. https://doi.org/10.1016/j.compag.2022.107591

Grand View Research. 2024. Commercial drone market size, share and trends report 2030. Grand View Research. San Francisco, CA, USA. https://www.grandviewresearch.com/industry-analysis/global-commercial-drones-market (Retrieved: October 2025).

Honrao DV, Awadhani LV. 2023. Design and development of agricultural spraying system. Materials Today: Proceedings 77: 734–738. https://doi.org/10.1016/j.matpr.2022.11.417

Jonak M, Mucha J, Jezek S, Kovac D, Cziria K. 2024. SPAGRI-AI: Smart precision agriculture dataset of aerial images at different heights for crop and weed detection using super-resolution. Agricultural Systems 216: 103876. https://doi.org/10.1016/j.agsy.2024.103876

Kwabena MP, Akoto-Adjepong V, Adu K, Ayidzoe MA, Bediako E, Nyarko-Boateng O, Boateng S, Donkor FE, Bawah FU, Awarayi S, *et al*. 2023. Dataset for crop pest and disease detection. Mendeley Data V1. https://doi.org/10.17632/bwh3zbpkpv.1

Maghazei O, Netland T. 2019. Drones in manufacturing: Exploring opportunities for research and practice. Journal of Manufacturing Technology Management 31 (6): 1237–1259. https://doi.org/10.1108/jmtm-03-2019-0099

Meesaragandla S, Jagtap MP, Khatri N, Madan H, Vadduri AA. 2024. Herbicide spraying and weed identification using drone technology in modern farms: A comprehensive review. Results in Engineering 21: 101870. https://doi.org/10.1016/j.rineng.2024.101870

Moradi S, Babapoor A, Ghanbarlou S, Kalashgarani MY, Salahshoori I, Seyfaee A. 2024. Toward a new generation of fertilizers with the approach of controlled-release fertilizers: A review. Journal of Coatings Technology and Research 21 (1): 31–54. https://doi.org/10.1007/s11998-023-00817-z

Radoglou-Grammatikis P, Sarigiannidis P, Lagkas T, Moscholios I. 2020. A compilation of UAV applications for precision agriculture. Computer Networks 172: 107148. https://doi.org/10.1016/j.comnet.2020.107148

Raj A, Dwivedi G, Sharma A, Lopes De Sousa Jabbour AB, Rajak S. 2020. Barriers to the adoption of industry 4.0 technologies in the manufacturing sector: An inter-country comparative perspective. International Journal of Production Economics 224: 107546. https://doi.org/10.1016/j.ijpe.2019.107546

Rathore R, Ahamad S, Soni A, Dewangan AK, Jain A. 2024. Agriculture field area calculation using drone camera: Method and framework design. SN Computer Science 5 (2). https://doi.org/10.1007/s42979-023-02577-4

Roma E, Catania P, Vallone M, Orlando S. 2024. Assessing the effectiveness of pruning in an olive orchard using a drone and a multispectral camera: A three-year study. Agronomy 14 (5): 1023. https://doi.org/10.3390/agronomy14051023

Selvaraj K, Selvanarayanan R, Venkatesan SKG, Rajendran S. 2025. Future-proof coffee plant disease detection based on counter-factual recommendation with a hybrid vision transformer and convolutional neural network model. Agrociencia 59 (4): 1–24. https://doi.org/10.47163/agrociencia.v59i4.3385

Singh E, Pratap A, Mehta U, Azid SI. 2024. Smart agriculture drone for crop spraying using image-processing and machine learning techniques: Experimental validation. IoT, 5 (2): 250–270. https://doi.org/10.3390/iot5020013

Song C, Wang Q, Wang G, Liu L, Zhang T, Han J, Lan Y. 2023. Study on the design and experiment of Trichogramma ball delivery system based on agricultural drone. Drones 7 (10): 632. https://doi.org/10.3390/drones7100632

Subramaniam R, Hajjaj SSH, Gsangaya KR, Sultan MTH, Mail MF, Hua LS. 2023. Redesigning dispenser component to enhance performance crop-dusting agriculture drones. Materials Today: Proceedings 81: 166–172. https://doi.org/10.1016/j.matpr.2021.03.015

The Drone Girl. 2024. The state of drones in 2024: How many drones are registered in the U.S., and how many pilots are certified? San Francisco, CA, USA. https://www.thedronegirl.com/2024/04/01/drones-in-2024 (Retrieved: October 2024).

Trappey AJC, Lin GB, Chen HK, Chen MC. 2023. A comprehensive analysis of global patent landscape for recent R&D in agricultural drone technologies. World Patent Information 74: 102216. https://doi.org/10.1016/j.wpi.2023.102216

Tsouros DC, Bibi S, Sarigiannidis PG. 2019. A review on UAV-based applications for precision agriculture. Information 10 (11): 349. https://doi.org/10.3390/info10110349

Yamaha Motor Co. 2017. RMAX industrial unmanned helicopter: Product specifications. Yamaha Motor Corporation. Iwata, Japan.

Zhang C, Kovacs JM. 2012. The application of small unmanned aerial systems for precision agriculture: A review. Precision Agriculture 13 (6): 693–712. https://doi.org/10.1007/s11119-012-9274-5

Zhou W, An T, Wang J, Fu Q, Wen N, Sun X, Wang Q, Liu Z. 2023. Design and experiment of a targeted variable fertilization control system for deep application of liquid fertilizer. Agronomy 13 (7): 1687. https://doi.org/10.3390/agronomy13071687

Agrociencia

PROTECTING CROPS FROM WILDLIFE ANIMALS IN SMART AGRICULTURE WITH REAL-TIME OBJECT DETECTION USING YOLOV5 ALGORITHM

Suresh **Maruthai**[1], Mageshwari **Munusamy**[2], Prabakaran **Narayanaswamy**[3], Surendran **Rajendran**[4*]

[1]St Joseph's College of Engineering. Department of Electronics and Communication Engineering. Chennai, Tamil Nadu 600119, India.
[2]Vel Tech Rangarajan Dr.Sagunthala R&D Institute of Science and Technology. Department of Artificial Intelligence and Data Science. Chennai, Tamil Nadu 600055, India.
[3]Koneru Lakshmaiah Education Foundation, Department of Electronics and communication Engineering. Vaddeswaram, Andhra Pradesh 522501, India.
[4]Saveetha Institute of Medical and Technical Sciences. Saveetha School of Engineering, Department of Computer Science and Engineering. Chennai, Tamil Nadu 602105, India.
* Author for correspondence: surendran.phd.it@gmail.com

Citation: Maruthai S, Munusamy M, Narayanaswamy P, Rajendran S. 2025. Protecting crops from wildlife animals in smart agriculture with real-time object detection using YOLOv5 algorithm. **Agrociencia** 59(8): 1088-1100. https://doi.org/ 10.47163/agrociencia.v59i8.3552

Editor in Chief:
Dr. Fernando C. Gómez Merino

Received: July 09, 2025.
Approved: December 01, 2025.
Published in Agrociencia: December 09, 2025.

ABSTRACT

Agriculture is essential for human survival, as it provides food, employment, economic growth, livelihood, and rural development, while also maintaining environmental balance and food security. However, due to the damage caused by wild animals, many farmers are abandoning cultivation. Existing techniques for deterring animals from agricultural fields are limited to their detection and the use of ultrasonic sounds. The proposed approach utilizes the YOLO machine learning algorithm to identify animals in the fields, generate ultrasonic sounds based on the detected species, activate Light-Emitting Diodes (LEDs) to simulate fire, and send an alert message to an authorized individual upon detection. The results obtained from this method surpass current approaches in reliability, precision, recall, and F1-score, achieving values ranging from 94 to 96 %.

Keywords: machine learning, animal deterrence, crop protection, food security.

INTRODUCTION

Agriculture is the science, skill, and practice of cultivating plants and rearing animals for food, energy, and other essential products that sustain human life. It encompasses a wide range of activities, from sowing and harvesting crops to managing livestock. Among the many challenges faced by agricultural systems, animal intrusion is a major source of losses. Wildlife such as deer, rabbits, and birds can damage crops by feeding on them, while larger animals, including cattle, horses, and even elephants, may trample plants and compact the soil. In addition, pests and diseases caused by insects, fungi, bacteria, viruses, and other pathogens can severely affect crops, leading to substantial yield losses (Mahaveerakannan, 2025). Extreme weather conditions,

such as floods, frost, and hailstorms, further exacerbate these problems by destroying crops and disrupting agricultural cycles. Crop losses due to these combined factors represent a major challenge in agriculture, leading to significant financial setbacks and posing a serious threat to food security.

Over time, farmers have used a wide range of methods to protect their crops from animal damage, including electric fencing, scare tactics, chemical repellents, traps, and other deterrents. However, these traditional approaches present significant challenges. Electric fencing, although commonly used, can kill animals attempting to enter a field, raising ethical and ecological concerns. Chemical repellents, such as commercial sprays, urea, or homemade solutions, discourage animals through unpleasant tastes, odors, or irritation, but they may also pose health risks to humans who inhale contaminated air or consume treated produce, in severe cases leading to fatal outcomes. These limitations show the need for a smart, cost-effective, and eco-friendly solution capable of safeguarding crops without harming wildlife (Surendran *et al*., 2025).

In Bangladesh, rodents represent a major agricultural threat. While chemical rodent repellents are available, they can create health hazards for consumers. To address this, Awal *et al*. (2024) proposed an electronic rodent-repelling system that generates ultrasonic sounds when an intrusion is detected. For larger wildlife, such as deer, deterrence becomes more complex. Landform fluctuations can weaken echo signals, reducing the effectiveness of acoustic deterrence. To overcome this, Asada *et al*. (2024) developed a deer-repellent system using acoustic ray tracking and mountaineering algorithms, supported by OpenStreetMap data to better estimate deer locations.

Animal intrusion is not limited to agricultural fields, affecting roads, base camps, and rural communities as well. Despite the variety of available techniques, major advancements have been slow due to individual limitations of each method. As a result, recent studies have increasingly turned to artificial intelligence and image processing. Sajithra Varun and Nagarajan (2023) introduced deep learning techniques for early animal detection, using image prediction, classification, and feature extraction. Similarly, Fernando *et al*. (2023) applied deep learning algorithms to improve detection accuracy, while Dave *et al*. (2023) implemented YOLOv8 technology to enhance data extraction and precision, achieving superior results compared to earlier approaches. Arulprakash *et al*. (2025) contributed with a system validated at the field level using specific animal datasets, noting that future developments could scale the technology to larger farms, incorporate drone-based aerial monitoring, and adapt it to a broader range of species and environmental conditions.

Other researchers have examined species-specific challenges. Robertson *et al*. (2023) reviewed agricultural conflicts involving elephants across Asia and Africa and evaluated the effectiveness of semi-captive versus wild elephants. They also introduced a new repellent technology aimed at reducing crop damage. Raveena and Surendran (2024) addressed a different threat by studying *Amblyomma sculptum*, a South American tick species capable of transmitting pathogens, and proposed repellent strategies to reduce mosquito-borne disease transmission.

The escalating conflict between people and wildlife in agricultural landscapes has increased the need for advanced detection systems. Simla *et al*. (2023) introduced a deep learning algorithm combined with sensor monitoring to detect animals and send alerts to farmers and forest officers. Krishnamoorthy *et al*. (2024) showed that animals pose risks not only to crops but also to human safety; for example, snake bites cause approximately 120 000 deaths annually. To mitigate this, Punetha and Vuppu (2023) developed a snake-repellent model. Deforestation is another key driver of human-animal conflict that increases animal movement into farmlands. To address this, Natikar and Dayananda (2023) proposed an animal-recognition framework using Convolutional Neural Networks (CNNs) with TensorFlow Object Detection.

More recent work has advanced real-time intrusion detection. Delwar *et al*. (2025) evaluated several deep learning models and identified YOLOv8 as the most effective, reaching over 99 % accuracy. Their system was deployed on an ESP32-CAM IoT device to deliver real-time alerts. Likewise, Balakrishnan *et al*. (2025) developed a wildlife intrusion detection system using VGG16 with transfer learning and deep-SORT for real-time multi-animal tracking, achieving 92.19 % accuracy and automated alert delivery to support both crop protection and biodiversity conservation. Sonowal *et al*. (2025) proposed a low-cost Passive Infrared Sensor (PIR) classification method capable of distinguishing between humans and animals with 95 % accuracy, also providing estimates of intruder distance and movement direction.

Building on these advancements, the present work focuses on real-time image detection and deterrence of common wild and domestic animals. The proposed system integrates the You Only Look Once version 5 (YOLOv5) algorithm with Internet of Things (IoT) components, including Node Microcontroller Units (NodeMCU), Global System for Mobile Communication (GSM) modules, ultrasonic sensors, and LED indicators. The objectives were to (i) develop a real-time animal detection framework using image processing and deep learning; (ii) integrate deterrent mechanisms such as ultrasonic signals, LED lights, and GSM alerts; and (iii) evaluate system performance through experimental validation. It is hypothesized that combining YOLOv5-based detection with IoT-enabled deterrents will significantly improve crop protection, outperforming traditional classifiers such as Random Forest, CNNs, Support Vector Machines (SVMs), and Recurrent Neural Network (RNN) models in accuracy, precision, recall, and F1-score, offering a more effective and sustainable solution for preventing animal intrusions.

MATERIALS AND METHODS

Existing systems utilize an ARM Cortex microprocessor with edge Artificial Intelligence (AI) to detect animals through a camera and deter them accordingly. However, its functionality is limited to the deterrence of small animals. The proposed repellent system employs a NodeMCU (ESP8266) integrated with the YOLOv5 machine learning algorithm (Figure 1). In this system, animals are detected using a webcam.

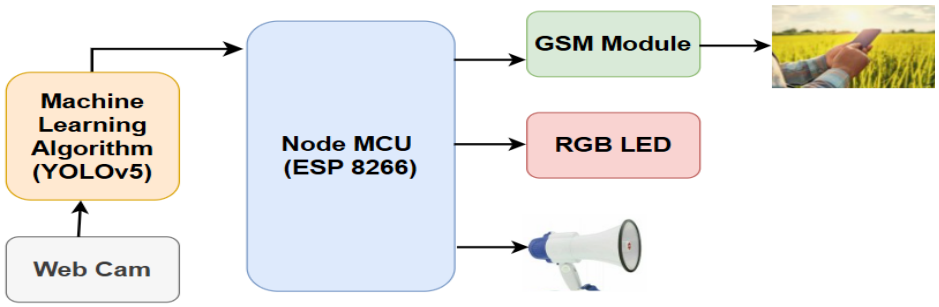

Figure 1. Proposed architecture of the smart animal repellent system with the YOLOv5 algorithm integrated with Node Microcontroller Units (NodeMCU), Global System for Mobile Communication (GSM) modules, ultrasonic sensors, and Light-Emitting Diodes (LEDs).

The camera captures images triggered by a PIR sensor with a detection range of 15–25 m. The captured images are then processed using the YOLOv5 algorithm for animal identification and deterrence.

Image dataset

In this study, a model was trained using a dataset comprising 5400 images of animals. These images were categorized into 90 different classes, including species such as bears, cattle, bulls, deer, butterflies, and peacocks. The dataset was obtained from Kaggle (https://www.kaggle.com/datasets/antoreepjana/animals-detection-images-dataset), providing a diverse range of animal images essential for the effective performance of the system. The dataset was divided into 70 % for training, 15 % for validation, and 15 % for testing. To enhance model robustness, data augmentation techniques such as flipping, rotation, and brightness adjustment were applied.

Image preprocessing

Implementing strategic landscaping practices, such as the cultivation of repellent plants, can alter the surrounding environment, making it less hospitable to wildlife and reducing the likelihood of animal intrusion. By integrating these diverse preprocessing and preventive methods, farmers can effectively mitigate crop damage and promote sustainable agricultural practices that prioritize the harmonious coexistence of humans and wildlife within shared ecosystems.

Before feeding images into the network, several preprocessing steps were used to enhance the performance and accuracy of the model. These include resizing the input images to a fixed size compatible with the network architecture and normalizing pixel values. Images were resized to a uniform dimension compatible with the model architecture (640 × 640 pixels for YOLOv5) to ensure consistent input representation and optimal model performance. The resizing operation is defined as:

$$I' = resize\big(I, (H, W)\big)$$

where, I is the original image, I' is the resized image, and H and W are the desired height and width, respectively.

Pixel values are normalized to a range that facilitates stable and efficient model training. Common normalization ranges include [0, 1] or [-1, 1]. The normalization operation can be expressed as:

$$p' = \frac{p}{255}$$

where p represents the original pixel intensity in the range [0,255]. This operation scales the pixel values to the range [0,1], standardizing the input data for the neural network.

YOLOv5 Algorithm

YOLOv5 is a state-of-the-art object detection algorithm that divides an input image into a grid and predicts bounding boxes along with class probabilities for objects within each grid cell. The algorithm is trained on annotated datasets containing images of animals with corresponding bounding boxes and class labels, and learns to recognize and differentiate animal species based on visual features such as shape, texture, and color.

YOLOv5 predicts bounding boxes using a grid-based structure, where each grid cell is responsible for predicting a fixed number of bounding boxes. The bounding box parameters are computed as follows:

$$b_x = \sigma(t_x) + c_x$$
$$b_y = \sigma\big(t_y\big) + c_y$$
$$b_w = p_w e^{t_w}$$
$$b_h = \ p_h e^{t_h}$$

where t_x and t_y represent the predicted center coordinates relative to the grid cell, while t_w and t_h denote the predicted width and height of the bounding box; (c_x, c_y) are the top-left coordinates of the corresponding grid cell, and p_w and p_h represent the anchor box dimensions. The sigmoid function σ constrains t_x and t_y to the range [0, 1], ensuring that the predicted center remains within the grid cell boundaries.

The YOLOv5 model was implemented using the PyTorch framework and trained for 200 epochs with a batch size of 16. The Adam optimizer was employed with a learning

rate of 0.001. Training was performed on an NVIDIA RTX 2080 Ti GPU with 12 GB of memory and a system equipped with 32 GB of RAM. To accelerate convergence and enhance detection accuracy, pretrained YOLOv5 weights were utilized for transfer learning.

Each bounding box includes an objectness score, indicating the likelihood of containing an object. The objectness score is calculated as:

$$P_{object} = \sigma(t_0)$$

where t_0 is the raw objectness score predicted by the network.

YOLOv5 predicts the probability of each class for each bounding box. The class probabilities are determined as:

$$P_{class|object} = softmax(t_{class})$$

YOLOv5 utilizes a function that includes localization loss, confidence loss, and classification loss. The localization loss, which measures the error between predicted and actual bounding box coordinates, is defined as:

$$L_{loc} = \sum_{i=0}^{S^2} \sum_{j=0}^{B} 1_{ij}^{obj} [(b_x - \hat{b}_x)^2 + (b_y - \hat{b}_y)^2 + \left((b_w - \hat{b}_w)^2 + (b_h - \hat{b}_h)^2\right]$$

The confidence loss, which evaluates the accuracy of objectness predictions, is expressed as:

$$L_{conf} = \sum_{i=0}^{S^2} \sum_{j=0}^{B} 1_{ij}^{obj} (C - \hat{C})^2 + \sum_{i=0}^{S^2} \sum_{j=0}^{B} 1_{ij}^{noobj} (C - \hat{C})^2$$

The classification loss, which quantifies the error in predicting object classes, is defined as:

$$L_{class} = \sum_{i=0}^{S^2} 1_i^{obj} \sum_{c \in classes} \left(p(c) - \hat{p}(c)\right)^2$$

The total YOLOv5 loss function, which combines the above components, is represented as:

$$L_{total} = \lambda_{coord} L_{loc} + L_{conf} + \lambda_{class} L_{class}$$

where 1_{ij}^{obj} is the indicator function for the presence of an object, 1_{ij}^{noobj} is the indicator function for the absence of an object, *S* represents the grid size, *B* represents the number of bounding boxes per grid cell, and λ_{coord} and λ_{class} are hyperparameters to balance loss components, which collectively enable YOLOv5 to detect objects efficiently and accurately in real-time.

YOLOv5 identifies and classifies objects within images, as demonstrated by the bounding boxes around the animals (Figure 2). Each detected object is labeled with its corresponding class and confidence score, such as "monkey_0.53," "elephant_0.98," and "cattle_0.6, 0.88, 0.93, and 0.92," with the final classification determined by the highest confidence value. YOLOv5 is recognized for its speed and accuracy, making it suitable for diverse applications, including autonomous driving and security surveillance.

Figure 2. Example of object recognition and confidence labeling using YOLOv5.

The hearing frequency ranges of various animals were used for training (Table 1). Based on these frequency ranges, the system generates ultrasonic sounds for effective deterrence.

Table 1. Hearing frequency ranges of different animal species.

Animal	Frequency range (kHz)
Monkey	10–65
Elephant	12–16
Buffalo	3–40
Pig	40.5–42
Horse	33.5–55
Cattle	23–35

Experimental setup

After detecting and analyzing animals, the system executes three automated actions to deter intrusions (Figure 3). First, it emits ultrasonic sounds at species-specific frequencies to repel the detected animal. Second, it sends a Short Message Service (SMS) alert to the field owner through GSM module, which operates independently of internet connectivity. Third, it activates LED lights that flash with varying intensity to provide visual deterrence. The system integrates the YOLOv5 algorithm with the NodeMCU (ESP8266) microcontroller for a low-cost and efficient operation. The NodeMCU was programmed using Arduino Integrated Development Environment (IDE), while the machine learning model was developed in Python. The GSM module (SIM800) handled alert communication, and deterrent mechanisms were automatically triggered in real time based on the detection results.

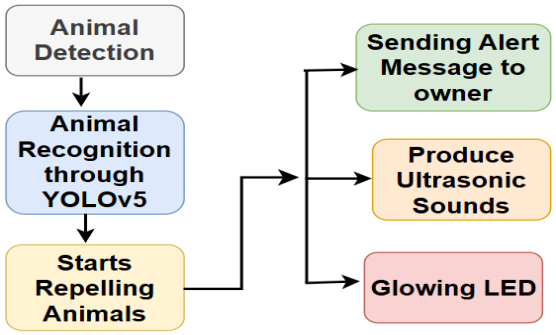

Figure 3. Process flow of the proposed animal detection and deterrence system.

In this study, the system utilized various hardware components, including the GSM module, ultrasonic sensors, LEDs, and the NodeMCU microcontroller, as well as software tools such as the Machine Learning Classifier, Python, and Arduino IDE (Table 2).

Evaluation metrics

Evaluation metrics play an important role in determining model performance through mathematical formulas. By analyzing these metrics, stakeholders can identify and select the most efficient system for wildlife deterrence. Accuracy is calculated as the ratio of the sum of True Positives (TP) and True Negatives (TN) to the total number of instances, including True Positives, True Negatives, False Positives (FP), and False Negatives (FN):

$$Accuracy = \frac{TP + TN}{TP + TN + FP + FN}$$

Table 2. Hardware and Software requirements of proposed system.

Hardware requirements	
Components	Specifications
Node microcontroller unit (ESP 8266)	-
Battery	5 V
Light-Emitting Diodes (LEDs)	2–3 V, 20 mA
Ultrasonic sensor (HC-SR04)	5 V; sensing distance of 2–400 cm
Global System for Mobile Communication (GSM) module (SIM800)	3.4–4.4 V; quad-band frequency
Passive Infrared Sensor (PIR)	5 V; sensing distance of 15–25 m
Software requirements	
Requirements	Purpose
Arduino Integrated Development Environment (IDE)	Developing and uploading the control logic for the system.
Python	Developing the machine learning model for animal detection and behavior prediction.
YOLOv5	Building and training models for recognizing animal patterns.
Global System for Mobile Communication (GSM) communication libraries	Used to manage Short Message Service (SMS) sending and receiving functions.

Precision is defined as the ratio of true positives to the sum of true positives and false positives:

$$Precision = \frac{TP}{TP + FP}$$

Recall is defined as the ratio of true positives to the sum of true positives and false negatives:

$$Recall = \frac{TP}{TP + FN}$$

The F1-score represents the harmonic mean of precision and recall, combining both metrics into a single performance measure:

$$F1 - score = \frac{2 \times (precision \times Recall)}{(precision + recall)}$$

RESULTS AND DISCUSSION

The YOLOv5 algorithm demonstrated high accuracy and efficiency in identifying animals within both images and video streams. It recognizes animals quickly and precisely using cutting-edge object detection techniques, allowing for seamless integration into applications such as wildlife monitoring, livestock management, and animal research. The algorithm's ability to process images in real time improves the system's functionality and usability in numerous settings. Overall, these findings demonstrate the potential to transform animal detection and monitoring practices, making it a valuable tool for researchers, conservationists, and agricultural professionals alike.

When an animal enters the agricultural field, the camera detects its presence and sends the image to the processor. The processor analyzes the input and immediately sends an alert message, "Alert: Animal detected in the field," to the authorized person via GSM technology, without requiring an internet connection. The performance of the animal repellent system was evaluated using a confusion matrix, comprising true negative, true positive, false negative, and false positive values (Figure 4). The matrix contains few false positive and false negative recognitions.

Figure 4. Confusion matrix illustrating the performance of the YOLOv5-based animal repellent system.

The performance metrics for the model (Table 3) showed high effectiveness. The system achieved an accuracy of 97 %, demonstrating its capability to correctly identify instances of animals in the test dataset. The precision value of 95 % signifies that the system accurately identifies true positives with minimal false positives. Furthermore, a recall rate of 96 % reflects the system's proficiency in detecting a significant proportion of actual animal instances, indicating few false negatives. The F1-score, which balances precision and recall, is 94 %, underscoring the system's robust overall performance in accurately and consistently detecting animals. Collectively, these metrics confirm that the YOLOv5 algorithm is highly effective for the proposed animal repellent system.

Table 3. Performance evaluation of the proposed YOLOv5-based animal repellent system.

Performance metrics	YOLOv5
Accuracy	97 %
Precision	95 %
Recall	96 %
F1-Score	94 %

The performance evaluation of various classifiers for the proposed animal repellent system shows notable differences in accuracy (Table 4). The proposed method using the YOLOv5 algorithm outperformed all other classifiers, achieving an accuracy of 97 %, being the most effective of the tested classifiers at accurately detecting animals in the system. These comparative results provide strong evidence that the proposed approach is reliable, validating the model's robustness and effectiveness in real-world crop protection scenarios.

Table 4. Accuracy comparison of YOLOv5 and traditional classifiers in animal detection.

Classifier	Accuracy
Random Forest	89.6 %
Convolution Neural Networks (CNNs)	91.8 %
Support Vector Machine (SVM)	93.6 %
Recurrent Neural Network (RNN)	88.6 %
Proposed method (YOLOv5)	97.0 %

Despite its promising performance, the proposed system has certain limitations. First, detection accuracy may decrease under low-light conditions or adverse weather, such as heavy rain or fog, since the camera-based approach is sensitive to illumination. Second, although the dataset is diverse, it may not fully represent rare or region-specific species, potentially affecting generalization in real-world deployments. Third, the system relies on GSM modules to send alerts, which may be unreliable in areas with poor network coverage. Finally, while ultrasonic deterrents are generally effective, some animals may adapt to repeated exposure, reducing long-term efficiency.

While the proposed YOLOv5-based system demonstrates strong performance in real-time animal detection and deterrence, several avenues remain open for future research. First, the system could be expanded to cover larger agricultural areas by incorporating drone-based surveillance for broader monitoring. Second, augmenting the dataset with region-specific animal species would further improve detection accuracy and adaptability. Third, exploring advanced machine learning approaches, such as

YOLOv8 or hybrid deep learning models, could enhance precision under diverse weather and lighting conditions. Finally, integrating renewable energy sources, such as solar-powered modules, would promote sustainability and scalability of the system in rural farming communities.

CONCLUSION

In this work, we proposed an animal repellent system for crop protection using the YOLOv5 algorithm. The system demonstrated high accuracy, precision, recall, and F1-score, outperforming traditional classifiers. These results highlight the superiority of the YOLOv5 framework for real-time animal detection and deterrence in agricultural fields.

REFERENCES

Arulprakash M, Thangadurai K, Mohammed ZA, Venkatesh J, Kumar BH, Muthulekshmi M. 2025. CNN-based autonomous smart drones for precision agriculture and crop monitoring. *In* 2025 5th International Conference on Intelligent Technologies. Institute of Electrical and Electronics Engineers. Hubbali, India. https://doi.org/10.1109/conit65521.2025.11167427

Asada S, Nagai Y, Wakabayashi K, Yukawa C, Oda T, Barolli L. 2024. Optimization of deer repellent devices placement based on hill climbing and acoustic ray tracing. *In* Barolli L. (ed.), Advances in Internet, Data and Web Technologies. Lecture Notes on Data Engineering and Communications Technologies. Springer: Cham, Switzerland. https://doi.org/10.1007/978-3-031-53555-0_52

Awal MA, Partha PKP, Islam MR. 2024. Design and development of a variable ultrasonic frequency generator for rodents repellent. Smart Agricultural Technology 7: 100414. https://doi.org/10.1016/j.atech.2024.100414

Balakrishnan P, Anny Leema A, Kiruba GGB, Gupta A, Aryan R. 2025. Deep-track: A real-time animal detection and monitoring system for mitigating human-wildlife conflict in fringe areas. Journal for Nature Conservation 88: 127063. https://doi.org/10.1016/j.jnc.2025.127063

Dave B, Mori M, Bathani A, Goel P. 2023. Wild animal detection using YOLOv8. Procedia Computer Science 230: 100–111. https://doi.org/10.1016/j.procs.2023.12.065

Delwar TS, Mukhopadhyay S, Kumar A, Singh M, Lee Y, Ryu JY, Hosen ASMS. 2025. Real-Time farm surveillance using IoT and YOLOv8 for animal intrusion detection. Future Internet 17 (2): 70. https://doi.org/10.3390/fi17020070

Fernando WPS, Madhubhashana IK, Gunasekara DNBA, Gogerly YD, Karunasena A, Supunya R. 2023. Image processing-based solution to repel crop-damaging wild animals. *In* Raj JS, Perikos I, Balas VE. (eds.), Intelligent Sustainable Systems. Lecture Notes in Networks and Systems. Springer, Singapore. https://doi.org/10.1007/978-981-99-1726-6_1

Krishnamoorthy K, Malarvizhi C, Kanniammal S, Kamalakannan R, Dinesh M. 2024. Revolutionizing Agriculture empirical impact of intelligent agri-field monitoring systems based on Internet of Things association. *In* 2024 International Conference on Innovative Computing, Intelligent Communication and Smart Electrical Systems. Institute of Electrical and Electronics Engineers. Chennai, India. https://doi.org/10.1109/icses63760.2024.10910289

Mahaveerakannan R. 2025. Rice yield prediction using hybrid quantum deep learning framework: Comparison study of using optical remote sensing, UAV-based multispectral imagery, and weather data. *In* 2025 7th International Conference on Inventive Material Science and Applications. Institute of Electrical and Electronics Engineers. Namakkal, India, pp: 1521–1525. https://doi.org/10.1109/icima64861.2025.11073876

Natikar K, Dayananda RB. 2023. Addressing crop damage from animals with faster R-CNN and YOLO Models. *In* Joby PP, Alencar MS, Falkowski-Gilski P. (eds.), IoT Based Control Networks and Intelligent Systems. Lecture Notes in Networks and Systems. Springer: Singapore. https://doi.org/10.1007/978-981-99-6586-1_44

Punetha S, Vuppu S. 2023. The sustainable conversion of floral waste into natural snake repellent and docking studies for antiophidic activity. Toxicon 233: 107254. https://doi.org/10.1016/j.toxicon.2023.107254

Raveena S, Surendran R. 2024. Detectron2 powered-image segmentation and object detection for smart weed control program in coffee plantation. *In* 2024 International Conference on Innovation and Intelligence for Informatics, Computing, and Technologies. Institute of Electrical and Electronics Engineers. Sakhir, Bahrain, pp: 812–819. https://doi.org/10.1109/3ict64318.2024.10824261

Robertson MR, Olivier LJ, Roberts J, Yonthantham L, Banda C, N'gombwa IB, Dale R, Tiller LN. 2023. Testing the effectiveness of the "smelly" elephant repellent in controlled experiments in semi-captive Asian and African savanna elephants. Animals 13 (21): 3334. https://doi.org/10.3390/ani13213334

Sajithra Varun S, Nagarajan G. 2023. DeepAID: A design of smart animal intrusion detection and classification using deep hybrid neural networks. Soft Computing https://doi.org/10.1007/s00500-023-08270-1

Simla AJ, Chakravarthi R, Leo LM. 2023. Agricultural intrusion detection (AID) based on the internet of things and deep learning with the enhanced lightweight M2M protocol. Soft Computing. https://doi.org/10.1007/s00500-023-07935-1

Sonowal D, Sharma A, Chetia B, Dutta N, Mazumdar R, Bonjyotsna A, Dehingia K. 2025. PIR sensor based intruder detection with direction and distance estimation supported by SVM. Sensing and Imaging 26 (1). https://doi.org/10.1007/s11220-025-00566-w

Surendran R, Uma SM, Rambabu B, Narayanan L, Kalyani G. 2025. Precision livestock management: Real-time monitoring and health assessment of livestock using IoT and RFID tag technology for enhanced agricultural productivity and animal welfare. *In* Seventh International Conference on Intelligent Sustainable Systems. Institute of Electrical and Electronics Engineers. Tirunelveli, India, pp: 231–235. https://doi.org/10.1109/iciss63372.2025.11076572

Agrociencia

SEEDLING AND ADULT PLANT RESISTANCE TO *Uromyces viciae-fabae* (Pers.) J. Schröt. IN MEXICAN FABA BEAN (*Vicia faba* L.) GENOTYPES

Jorge **Pérez-Cárcamo**[1], José Sergio **Sandoval-Islas**[1], María Florencia **Rodríguez-García**[3], Cristian **Nava-Díaz**[1], Olga **Gómez-Rodríguez**[1], Serafín **Cruz-Izquierdo**[2*]

[1]Colegio de Postgraduados Campus Montecillo. Posgrado en Fitosanidad. Carretera México-Texcoco km 36.5, Montecillo, Texcoco, State of Mexico, Mexico. C. P. 56264.
[2]Colegio de Postgraduados Campus Montecillo. Posgrado en Recursos Genéticos y Productividad-Genética. Carretera México-Texcoco km 36.5, Montecillo, Texcoco, State of Mexico, Mexico. C. P. 56264.
[3]Instituto Nacional de Investigaciones Forestales, Agrícolas y Pecuarias. Campo Experimental Valle de México. Carretera Los Reyes-Texcoco km 13.5, Coatlinchán, Texcoco, State of Mexico, Mexico. C. P. 56250.
* Author for correspondence: sercruz@colpos.mx

Citation: Pérez-Cárcamo J, Sandoval-Islas JS, Rodríguez-García MF, Nava-Díaz C, Gómez-Rodríguez O, Cruz-Izquierdo S. 2025. Seedling and adult plant resistance to *Uromyces viciae-fabae* (Pers.) J. Schröt. in Mexican faba bean (*Vicia faba* L.) genotypes. **Agrociencia** 59(8): 1101-1115. https://doi.org/ 10.47163/agrociencia.v59i8.3334

Editor in Chief:
Dr. Fernando C. Gómez Merino

Received: March 23, 2025.
Approved: November 21, 2025.
Published in Agrociencia: November 28, 2025.

ABSTRACT

Faba bean rust (*Vicia faba* L.) is a globally significant disease caused by *Uromyces viciae-fabae* (Pers.) J. Schröt, resulting in yield losses of up to 70 %. Genetic resistance, whether specific or non-specific, is viable for reducing losses caused by this fungus. In faba bean, genotypes with specific resistance to *U. viciae-fabae* have been found, although most genotypes allow for some levels of pathogen reproduction. Therefore, the objective was to evaluate the resistance to *U. viciae-fabae* in faba bean lines at the seedling and adult plant stages. Thirty faba bean genotypes were examined as part of two breeding initiatives at Postgraduate College and the Agricultural, Aquaculture, and Forestry Research and Training Institute of the State of Mexico. Adult plants were evaluated in the field at two locations: 1) Palmillas, Texcaltitlán, State of Mexico, and 2) Postgraduate College Montecillo Campus, Texcoco, State of Mexico. A two-factor factorial model was used in the design, which included a generalized randomized block design and four replicates. The variables evaluated were the percentage of disease severity, final severity, and grain yield. Seedlings were inoculated with a concentration of 3×10^6 urediniospores mL^{-1}, incubated in a growth chamber at 18 ± 2 °C and 100 % relative humidity for 24 h, and transferred to a temperature-controlled greenhouse at 18 ± 2 °C. The variables evaluated included the number of pustules per leaf, the severity percentage, pustule size, latency period (LP1, LP50, and LP100), and the type of infection. Approximately 95 % of the lines tested in seedlings were susceptible to faba bean rust, with line 20CP showing moderate resistance. Incomplete non-hypersensitive resistance was identified in the bean-*U. viciae-fabae* pathosystem.

Keywords: incomplete genetic resistance, hypersensitivity reaction, faba bean rust.

INTRODUCTION

Faba bean rust is a disease of global importance caused by the biotrophic fungus *U. viciae-fabae* (Pers.) J. Schröt (syn. *U. fabae*) (Ijaz *et al*., 2017; Rubiales and Khazaei, 2022). It is a macrocyclic and autoecious rust with sexual and asexual phases, but its sexual phase is rarely observed in temperate regions (Rubiales and Khazaei, 2022). This fungus can cause yield losses of up to 70 % when it attacks at early stages and up to 30 % if the infection occurs in adult plants (Terefe *et al*., 2016).

Genetic resistance is viable to reduce the losses caused by *U. viciae-fabae*. It can be specific (vertical, complete) or non-specific (horizontal, incomplete, partial) (Niks *et al*., 2011). Specific resistance only confers protection for a short period of time, since it is given only by a major gene. When a fungus acquires a virulence gene, the resistance is broken; therefore, efforts have been made to generate varieties with non-specific resistance that is durable over several crop cycles. In faba bean (*Vicia faba* L.), complete resistance to this pathogen has not been found, but non-specific or incomplete resistance to *U. viciae-fabae* has been observed, since most faba bean genotypes allow certain levels of pathogen reproduction (Sillero *et al*., 2000; Ijaz *et al*., 2021).

Sillero *et al*. (2000) first reported the hypersensitivity reaction in the faba bean crop. They observed late-onset necrotic reactions, resulting in small pustules with macroscopically visible necrosis. This hypersensitivity reaction is considered incomplete resistance because it is associated with a longer latency period, a reduction in pustule size, and a lower frequency of infection, with the difference that it presents macroscopically visible necrosis. This hypersensitive response in faba bean is controlled by dominant genes (Ávila *et al*., 2003; Adhikari *et al*., 2016).

Non-specific resistance reduces epidemic development despite a high degree of compatibility between the pathogen and the host (Parlevliet, 1975). Several sources of resistance that delay rust disease in faba bean have been detected (Torres *et al*., 2006). This reduces the potential of reinfections, allowing the plant to overcome the disease with minimal impact on yield. Genetic resistance is a viable strategy to generate rust-resistant or tolerant faba bean genotypes. According to Ávila *et al*. (2017), there are no studies or published information on this subject in Mexico. The resistance of Mexican faba bean genotypes to this pathogen is unknown. Therefore, the hypothesis to be tested in this study is that there are faba bean lines with resistance in both adult plants and seedlings from two improvement programs in Mexico. The objective of this study was to evaluate 30 faba bean lines for their resistance to *U. viciae-fabae*, both at the seedling and adult plant stages, and to understand the behavior of the genotypes to the disease in two environments.

MATERIALS AND METHODS

Germplasm

Thirty lines of faba bean (*Vicia faba* L.) were evaluated as part of the Postgraduate College (CP) Montecillo Campus and the Agricultural, Aquaculture, and Forestry

Research and Training Institute of the State of Mexico (ICAMEX) improvement program (Table 1).

Table 1. Faba bean (*Vicia faba* L.) genotypes used in the evaluation of resistance in seedlings and adult plants to *Uromyces viciae-fabae*.

Name	Subspecies	Name	Subspecies
1 ICAMEX	*major*	16 ICAMEX	*major*
2 ICAMEX	*major*	17 ICAMEX	*major*
3 ICAMEX	*major*	18 ICAMEX	*major*
4 ICAMEX	*major*	19 ICAMEX	*major*
5 ICAMEX	*major*	20 ICAMEX	*major*
6 ICAMEX	*major*	1 CP	*minor*
7 ICAMEX	*major*	5 CP	*minor*
8 ICAMEX	*major*	9 CP	*minor*
9 ICAMEX	*major*	13 CP	*minor*
10 ICAMEX	*major*	16 CP	*minor*
11 ICAMEX	*major*	17 CP	*minor*
12 ICAMEX	*major*	20 CP	*minor*
13 ICAMEX	*major*	22 CP	*minor*
14 ICAMEX	*major*	46 CP	*minor*
15 ICAMEX	*major*	47 CP	*minor*

ICAMEX: Agricultural, Aquaculture, and Forestry Research and Training Institute of the State of Mexico; CP: Postgraduate College.

Resistance evaluation in adult plants

The experiment was repeated each year under field conditions, in two locations and over two years: 1) Palmillas, in the municipality of Texcaltitlán, State of Mexico (23° 15′ 00″ N and 99° 34′ 00″ W), at an altitude of 2824 m, in 2020, under rainfed conditions in the autumn-winter agricultural cycle; and 2) Colegio de Postgraduados Campus Montecillo, in the municipality of Texcoco, State of Mexico (19° 27′ 51″ N and 98° 54′ 15″ W), at an altitude of 2250 m in 2021, under rainfed conditions in the spring-summer agricultural cycle. In both locations, the same faba bean genotypes were planted (Table 1) under a factorial model of two factors with a generalized randomized block experimental design with four replications.

The experimental unit consisted of four 2.8-m-long furrows spaced 40 cm apart. Two weedings were performed at 30 and 50 d after emergence (DAE). Fertilization was carried out with a 60-80-40 formula with urea fertilizers (Fertilizante del campo®), triple calcium superphosphate (Agrocolmex®), and potassium chloride (Agrocolmex®). To ensure the presence of the disease in the central part of each plot, a plant was inoculated with *U. viciae-fabae* pathotype CP21, which was morphologically identified using the keys of Cummins and Hiratsuka (2003). Temperature and relative humidity were recorded with the data logger Onset HOBO U23 Pro v2, which was placed 20

DAE. The average temperature in Texcaltitlán during the 130 DAE was 11.68 °C, with a minimum of -1 °C and a maximum of 31.1 °C, and an average relative humidity of 83.76 %, with a minimum of 26.1 % and a maximum of 100 %. In Texcoco, the minimum temperature was 5.4 °C, with an average of 17.14 °C and a maximum of 33.5 °C, and the minimum relative humidity was 29.11 %, with an average of 78.67 % and a maximum of 100 %.

Recorded variables

Disease severity was assessed as the percentage of the total plant surface covered with pustules, following Villegas-Fernández *et al*. (2011). Evaluations were conducted every 10 d beginning with the appearance of the first pustules, using the severity relative to the entire plant as the reference. A total of six readings were taken. Final severity was defined as the disease severity recorded at the last evaluation (sixth reading).

In addition, the Area Under the Disease Progress Curve (AUDPC) was calculated to quantify the cumulative disease pressure over time, using the equation described by Bjarko and Line (1988):

$$AUDPC = \sum_{i} \frac{Y_i + Y_{i+1}}{2} * (t_{i+1} - t_1)$$

where Y is the percentage of leaves with pustules at each reading, and t represents the corresponding time.

Grain yield was recorded as the total grain weight of all plants per plot (g plot^{-1}) and subsequently converted to kg ha^{-1}. Data from both locations were analyzed using SAS 9.3 (SAS Institute, 2013), and mean comparisons were performed using the DMS test ($p \leq 0.05$).

Resistance evaluation in seedlings

The seedling response of the 30 faba bean genotypes was tested at the National Laboratory of Rusts and Other Cereal Diseases (LANAREC) of the National Institute of Forestry, Agriculture, and Livestock Research (INIFAP), Valley of Mexico Experimental Field (CEVAMEX), located at 19° 29′ 88″ N and 98° 54′ 22″ W, at an altitude of 2260 m. Seeds of each genotype were sown in 295 cm3 Styrofoam cups with Promix® brand peat substrate. The experimental unit was one seedling, with ten replicates used in total. Eight days after sowing, the seedlings were inoculated with fresh urediniospores of the *U. viciae-fabae* isolate CP21 from the faba bean rust collection at the Genetic Resistance Laboratory of the Plant Pathology Program of the Postgraduate College, with a concentration of 3×10^6 urediniospores mL^{-1}. Mineral oil (Sotrol® 170) was used as a diluent vehicle. Inoculation was carried out with a sprinkler adapted to a FELISA® brand vacuum pump, model 1500. Once inoculated, all seedlings were transferred to

a bioclimatic chamber with a temperature of 18 ± 2 °C, white light, and 100 % relative humidity for 24 h. After incubation, the seedlings were moved to a greenhouse with a controlled temperature of 18 ± 2 °C.

Recorded variables

The total number of pustules per leaf (calculated as the average from three leaves taken from the central part of each plant), the percentage of severity according to Villegas-Fernández *et al*. (2011), and the average pustule size (also based on three central leaves) were all recorded 20 d after inoculation. The latency period (LP) was monitored beginning 10 d after inoculation, evaluating LP1, LP50, and LP100, which correspond to the appearance of the first pustule, 50 % of erumpent pustules, and 100 % of erumpent pustules, respectively. The LP50 was estimated as the number of days from inoculation to the time when 50 % of the final number of urediniospores became visible (Niks *et al*.,2011).

Infection type (IT) was measured using the scale of Stakman *et al*. (1962), adapted for faba bean by Sillero *et al*. (2000). In this scale, IT0 corresponds to asymptomatic reactions, where IT denotes necrotic spots; IT1 indicates tiny pustules with minimal sporulation; IT2 reflects necrosis surrounding small pustules; IT3 represents pustules that sporulate in the presence of chlorosis; and IT4 corresponds to well-formed pustules without chlorosis or necrosis. Data for all evaluated variables were analyzed using SAS 9.3 (SAS Institute, 2013), and mean comparisons were performed using the Tukey test ($p \leq 0.05$).

RESULTS AND DISCUSSION

Adult plant resistance

Urediniospores of *U. viciae-fabae* germinate at temperatures ranging from 5 to 26 °C, with an optimum of 20 °C (Joseph and Hering, 1997). Emeran *et al*. (2011) report that a humidity of 80 % is adequate for the development of the disease. Although the temperature was not optimal in field experiments, it was within the ranges of temperature and relative humidity reported for urediniospore germination. Therefore, field conditions were adequate for the development of the disease.

The first pustules were observed at 32 DAE in the Texcaltitlán area, at an early stage of the crop, while in Texcoco they were observed at 61 DAE (Figure 1). Since 30 genotypes were evaluated, only three genotypes were used as models, as the other materials exhibited similar behavior. Significant differences ($p \leq 0.05$) were observed for the genotype factor in the final severity and yield variables, while there was no significant difference in the AUDPC variable. Regarding the environment, there were highly significant differences ($p \leq 0.01$) in the three measured variables. There was a significant difference ($p \leq 0.05$) in the genotype × environment interaction in the final severity and yield variables. The differences for all sources of variation are attributed to the different environmental conditions and genotypes (Table 2).

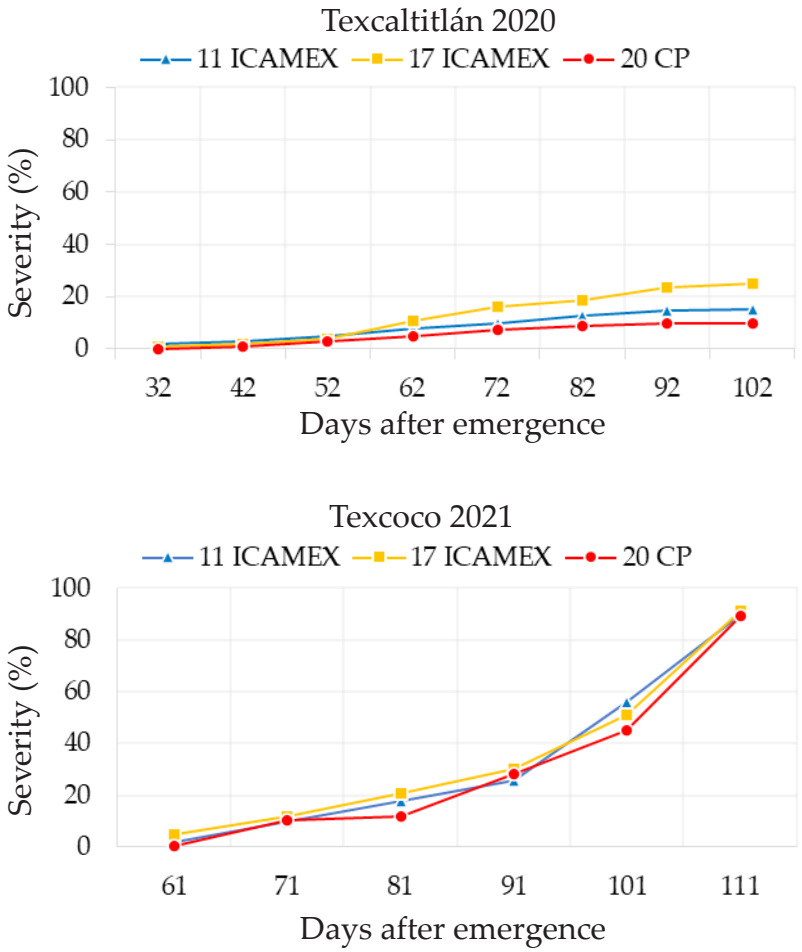

Figure 1. Comparative progression of faba bean rust severity in Texcaltitlán and Texcoco, Mexico.

Table 2. Analysis of variance (ANOVA) for final severity, area under the disease progress curve (AUDPC), and yield in 30 faba bean (*Vicia faba* L.) lines evaluated across two locations.

Source of variation	DF	Final severity (%)	AUDPC	Yield (kg ha^{-1})
Genotype	1	23.92 *	845.47 ns	1 438 616.40 **
Environment	29	252 900.05 **	2 419 064.93 **	82 059 756.81 **
Genotype × environment interaction	29	19.01 *	633.376 ns	1 274 390.39 **
Experimental error		11.80	730.66	187 361.2
Mean		53.09	190.97	1498.61
Coefficient of variation (%)		6.46	14.15	28.88

*, **: significant at $p \leq 0.05$ and $p \leq 0.01$, respectively. DF: degrees of freedom; ns: not significant.

There were statistical differences found between environments, with the adult plant (Table 3) having the lowest final severity and AUDPC, and higher yield in Texcaltitlán compared to Texcoco. The average yield of all genotypes in Texcaltitlán was 35 % higher than the national average of 1360 kg ha^{-1} (SIAP, 2024). Meanwhile, the average yield for all genotypes in Texcoco was 40 % lower than the national average. Texcoco had a higher final rust severity, which limited the grain yield of the genotypes.

Table 3. Environmental comparison of mean final severity, area under the disease progress curve (AUDPC), and yield for 30 faba bean (*Vicia faba* L.) genotypes under *Uromyces viciae-fabae* infection.

Environments	Final severity (%)	AUDPC	Yield (kg ha^{-1})
Texcaltitlán	15.61 b	75.04 b	2174.00 a
Texcoco	90.58 a	307.24 a	827.50 b
Mean	53.09	191.14	1500.75

Values with the same letter are significantly equal (Tukey, $p \leq 0.05$).

All genotypes were susceptible in the field, presenting a final severity greater than 49 %, with line 17 ICAMEX being the most susceptible. This is consistent with the findings of Ijaz *et al*. (2021), who reported a severity of 80 to 90 % for the Fiord cultivar that was considered susceptible. Of the 30 genotypes evaluated, materials 17 CP, 20 CP, 1 CP, and 46 CP presented a lower susceptibility according to the statistical differences, but this does not provide evidence that they have a level of resistance in adult plants that can be used for the generation of varieties resistant to rust, at least to the CP21 pathotype.

Regarding yield, the genotypes 17 ICAMEX and 20 ICAMEX had the best performance, both exceeding 2150 kg ha^{-1}, while 13 CP and 47 CP showed the lowest yield, which did not exceed 750 kg ha^{-1}. It should be noted that the CP genotype belongs to the *minor* subspecies, having a low yield compared to the ICAMEX genotypes of the *major* species (Table 4).

All genotypes evaluated in Texcoco showed a final severity greater than 80 % and lower yields compared to Texcaltitlán (Table 5). For example, genotype 8 ICAMEX had a better yield in Texcaltitlán, while its yield was lower in Texcoco with 86 % severity. While the genotypes exhibited some level of horizontal resistance in Texcaltitlán, they demonstrated susceptibility in Texcoco. This behavior could be due to the fact that the climatic conditions in Texcoco were close to the optimal range of temperature and relative humidity conditions for the development of the disease, allowing a greater number of polycycles.

Sillero *et al*. (2000) mention that susceptibility is very common in faba bean cultivation and that resistance genes have been found in few genotypes. Some can express their

Table 4. Mean final severity and yield of 30 adult-plant faba bean (*Vicia faba* L.) genotypes evaluated across two environments in 2020–2021 affected by *Uromyces viciae-fabae*.

Genotype	Final severity %	Yield (kg ha^{-1})
17 ICAMEX	58.33 a	2172.17 a
20 ICAMEX	56.33 ab	2213.33 a
16 ICAMEX	55.00 ab	2009.83 ab
14 ICAMEX	55.50 ab	1635.17 abcde
9 ICAMEX	55.00 ab	1756.83 abc
13 ICAMEX	54.66 ab	2061.83 ab
2 ICAMEX	54.50 ab	1980.50 ab
12 ICAMEX	54.50 ab	1848.17 abc
3 ICAMEX	54.16 ab	1684.83 abcd
10 ICAMEX	53.83 ab	1845.50 abc
5 ICAMEX	53.83 ab	1647.50 abcde
6 ICAMEX	53.66 ab	1668.67 abcd
19 ICAMEX	53.33 ab	1888.50 abc
7 ICAMEX	53.33 ab	1354.83 abcdef
15 ICAMEX	53.33 ab	1183.50 bcdef
4 ICAMEX	53.33 ab	1635.33 abcde
47 CP	53.16 ab	702.00 ef
16 CP	53.00 ab	1002.83 cdef
8 ICAMEX	52.50 ab	2067.50 ab
11 ICAMEX	52.50 ab	1571.67 abcdef
1 ICAMEX	52.50 ab	1177.83 bcdef
18 ICAMEX	52.16 ab	2055.00 ab
13 CP	52.00 ab	639.50 f
5 CP	51.66 ab	1572.83 abcdef
22 CP	50.83ab	972.00 cdef
9 CP	50.83 ab	1112.50 bcdef
17 CP	50.33 b	735.33 def
20 CP	50.00 b	794.17 def
1 CP	50.00 b	791.67 def
46 CP	49.16 b	1177.17 bcdef

Values with the same letter are significantly equal (Tukey, $p \leq 0.05$).

resistance at high or low temperatures depending on the genetic information. The same authors mention that genotype V-313 showed horizontal resistance with 12 and 22 % severity at 10 and 20 °C, respectively, but at 25 ° C it had a severity of 70 %, showing susceptibility, while V-1335 showed a severity of 10–17 % at the three temperatures evaluated. According to our results, the genotypes could have resistance genes that interact with temperatures. On the other hand, locations play a fundamental role in the expression and behavior of bean genotypes (González-González *et al*., 2016). However, to determine whether genotype 20 CP exhibits this type of interaction, it is necessary to study it at different controlled temperatures to observe its response.

Table 5. Mean comparison of final severity and yield for 30 adult-plant faba bean (*Vicia faba* L.) genotypes based on the genotype × environment interaction under *Uromyces viciae-fabae* infection.

Genotype	Texcoco		Texcaltitlán	
	Final severity %	Yield (kg ha^{-1})	Final severity %	Yield (kg ha^{-1})
16 CP	95.00 a	851.00 jklmno	11.00 c	1154.67 ghijklmno
13 ICAMEX	93.33 a	997.33 ijklmno	16.00 bc	3126.33 abcd
16 ICAMEX	93.33 a	1011.00 ijklmno	16.66 bc	3008.67 abcd
20 ICAMEX	91.66 a	767.67 lmno	21.00 bc	3659 a
6 ICAMEX	91.66 a	770.67 jklmno	15.66 bc	2566.67 abcdefg
5 CP	91.66 a	1445.00 efghijklmno	11.66 c	1700.67 defghijklmno
19 ICAMEX	91.66 a	1092.67 hijklmno	15.00 bc	2684.33 abcdef
3 ICAMEX	91.66 a	475.67 no	16.66 bc	2894.00 abcde
10 ICAMEX	91.66 a	723.67 mno	16.00 bc	2967.33 abcd
14 ICAMEX	91.66 a	864.33 jklmno	18.33 bc	2406.00 abcdefghi
17 ICAMEX	91.66 a	607.67 lmno	25.00 bc	3736.67 a
47 CP	90.66 a	701.67 lmno	15.66 bc	702.33 lmno
18 ICAMEX	90.00 a	1123.33 ghijklmno	14.33 bc	2986.67 abcd
2 ICAMEX	90.00 a	1022.33 hijklmno	19.00 bc	2938.67 abcd
15 ICAMEX	90.00 a	511.67 no	16.66 bc	1855.33 defghijklmno
11 ICAMEX	90.00 a	1124.00 ghijklmno	15.00 bc	2019.33 cdefghijklm
20 CP	90.00 a	576.67 mno	10.00 c	1011.67 ijklmno
22 CP	90.00 a	843.00 jklmno	11.66 c	1101.00 ghijklmno
5 ICAMEX	90.00 a	1031.67 hijklmno	17.66 bc	2263.33 abcdefghij
7 ICAMEX	90.00 a	604.00 mno	16.66 bc	2105.67 cdefghijkl
12 ICAMEX	90.00 a	794.67 klmno	19.00 bc	2901.67 abcde
9 ICAMEX	90.00 a	1020.00 hijklmno	20.00 bc	2493.67 abcdefg
4 ICAMEX	90.00 a	1035.67 hijklmno	16.66 bc	2235 bcdefghijk
9 CP	90.00 a	955.67 ijklmno	11.66 c	1269.33 fghijklmno
1 ICAMEX	88.33 a	419.67 o	15.00 bc	1936.00 defghijklmn
17 CP	90.00 a	652.67 lmno	10.66 c	818.00 jklmno
8 ICAMEX	88.33 a	711.00 lmno	16.66 bc	3424.00 abc
13 CP	88.33 a	578.67 mno	15.66 bc	700.33 lmno
1 CP	86.66 a	773.67 klmno	11.66 c	809.67 klmno
46 CP	86.66 a	494.33 no	11.66 c	1860.00 defghijlkkmno

Values with the same letter are significantly equal (Least significant difference, $p \leq 0.05$).

Seedling resistance

There was a highly significant difference between the lines evaluated in the seedling stage in all variables (Table 6). For the variable infection type, all genotypes presented infection type III except for 20 CP, which showed infection type I and a longer LP50 and LP100 compared to the other faba bean lines, up to 3 d. In addition, this genotype had a lower number and size of pustules, which was reflected in the severity, and showed incomplete, non-hypersensitive resistance.

Table 6. Response of 30 faba bean bean (*Vicia faba* L.) genotypes to *Uromyces viciae-fabae* at the seedling stage under controlled conditions.

Genotype	Type of infection[†]	LP1[Þ]	LP50[Þ]	LP100[Þ]	Number of pustules[¶]	Severity[¶Þ]	Size of pustules[¶§]
1 ICAMEX	3 a	13 a	14.6 bc	16.7 bcdefg	8.1 abc	10.1 abc	1.2 abcd
1 CP	3 a	11 c	14.7 b	16.6 cdefg	12.3 abc	13.2 abc	1.1 abcdefg
18 ICAMEX	3 a	11.6 b	14.5 bcd	16.6 cdefg	11.6 abc	14.7 abc	0.9 efgh
19 ICAMEX	3 a	11 c	14.3 bcd	17.3 bcd	9.4 abc	11.6 abc	1.2 abcde
5 ICAMEX	3 a	11 c	13.5 defg	16 fg	11.9 abc	14.2 abc	1.3 abc
9 CP	2.7 a	10.8 c	14.3 bcd	17.6 bc	6.9 bc	6.7 c	0.9 gh
13 ICAMEX	3 a	11.1 c	13.8 bcdfg	16 fg	8.1 bc	11 abc	1.3 abc
10 ICAMEX	3 a	11 c	13.7 bcdefg	15.8 g	9.3 abc	12 abc	1.1 bcdef
14 ICAMEX	3 a	11 c	14 bcdef	16 fg	10 abc	12.7 abc	1.4 a
22 CP	3 a	11 c	14.2 bcde	16.6 cdefg	9.7 abc	10.2 abc	1.0 cdefg
8 ICAMEX	3 a	11 c	14.1 bcdef	16.5 defg	15.5 a	18.6 a	1.2 abcd
47 CP	3 a	11 c	14.7 b	17.7 b	7.9 abc	9.6 abc	1.1 cdefg
15 ICAMEX	3 a	11 c	13.7 bcdefg	16.1 fg	13.6 abc	19.3 a	1.3 abc
11 ICAMEX	3 a	11 c	14 bcdefg	16 fg	12.5 abc	17.1 ab	1.4 ab
5 CP	3 a	11 c	14.1 bcdef	16.5 defg	12.7 abc	18 a	0.9 fgh
3 ICAMEX	3 a	11.2 bc	13 g	16f g	10.8 abc	15.1 abc	1.2 abcde
4 ICAMEX	3 a	11 c	13.2 efg	16.2 efg	8.6 abc	12.6 abc	1.2 abcdef
13 CP	3 a	11 c	13.1 fg	16.7 bcdefg	11.9 abc	15 abc	0.9 gh
2 ICAMEX	3 a	11.1 c	13.6 defg	16.2 efg	11.4 abc	15.1 abc	1.2 abcd
7 ICAMEX	2.7 a	11 c	13.5 efg	16.7 bcdefg	10.0 abc	13.7 abc	1.0 cdefg
6 ICAMEX	3 a	11.1 c	13 g	16 fg	11.8 abc	15.2 abc	1.1 cdefg
17 CP	3 a	11 c	14.2 bcde	17 bcdef	9.3 abc	14.3 abc	0.9 defgh
12 ICAMEX	3 a	11 c	14 bcdefg	16 fg	10.2 abc	16.5 abc	1.1 abcdefg
16 CP	3 a	11 c	14 bcdefg	16.7 bcdefg	10.0 abc	13.6 abc	0.9 fgh
17 ICAMEX	3 a	11 c	13.8 cdefg	16 fg	14.6 a	17.1 ab	1.0 cdefg
16 ICAMEX	3 a	11 c	13.2 efg	16 fg	8.7 abc	13.2 abc	1.2 abcdef
20 CP	1.1 b	11.1 c	17.3 a	20 a	8 abc	7.8 bc	0.7 h
9 ICAMEX	3 a	11 c	13.6 cdefg	16.5 defg	6.8 c	11.2 abc	1.1 cdefg
46 CP	3 a	11.2 bc	14.2 bcde	17.2 bcde	7.7 abc	12.4 abc	0.9 efgh
20 ICAMEX	3 a	11 c	13.5 edfg	16.2 efg	8.6 abc	13.2 abc	1.21 abcdfg
p	≤ .0001	≤ .0001	≤ .0001	≤ .0001	≤ 0.0005	≤ .0001	≤ .0001

[†]: qualitative scale according to Stakman *et al*. (1962), adapted to faba bean by Sillero *et al*. (2000); ¶: average of three leaves from the central part of the plant; [§]: diameter in millimeters; [Þ]: LP: Latency Period. Values with the same letter are significantly equal (Tukey, $p \leq 0.05$).

According to Parlevliet (1979), an incomplete non-hypersensitive response should be considered partial resistance. The behavior of the 20 CP line can be incorporated into genetic improvement programs aimed at developing varieties with vertical resistance, where the gene-to-gene relationship is applied. For each host resistance gene, there is a corresponding pathogenicity gene in the pathogen (Flor, 1942). Resistance genes are designated as R, and their counterparts in the pathogen are known as avirulence

genes (Avr). When an R gene recognizes an Avr gene in the pathogen, it activates a cell death process in the infected cell, known as the hypersensitive response. This reaction stops infection and colonization entirely, thereby conferring resistance to the plant (Burbano-Figueroa, 2020).

Line 9 CP also had similar behavior in the final severity, AUDPC, and yield variables but presented infection type III, with 97 % of the genotypes exhibiting a susceptible infection type (IT3). Infection type IV was not observed, nor was infection type 0. This aligns with Ijaz *et al*. (2021), who evaluated 40 Australian genotypes used as parents in the faba bean improvement program at the IA Watson Grains Research Center in Narrabri and did not identify any genotypes with infection type 0. In contrast, Sillero *et al*. (2000) reported that several faba bean cultivars exhibited infection type IV in their seedling evaluation, using the same infection type scale applied in this study. According to Stakman *et al*. (1962), Sillero *et al*. (2000), and Ijaz *et al*. (2021), IT0 is classified as resistant, IT1 as somewhat resistant, IT2 as moderately resistant, IT3 as moderately susceptible, and IT4 as very susceptible.

The data obtained show that all cultivars have a degree of resistance in seedlings to the CP21 pathotype. The high percentage of cultivars with a susceptible type of infection in seedlings and high percentages of severity of these cultivars in adult plants (Tables 3 and 4) show that the germplasm that was evaluated presented a low quantitative resistance to faba bean rust. The same results were obtained by Sillero *et al*. (2000), which show that a faba evaluation must be carried out on varieties, lines, and non-advanced materials from the different improvement programs, as well as collections in search of a greater number of materials with incomplete resistance given by major genes and quantitative resistance. Quantitative resistance in varieties allows for a durable resistance to the different existing pathotypes (Vanderplank, 1963; Robinson, 1987). It is also confirmed that incomplete non-hypersensitive resistance exists in the bean-*U. viciae-fabae* pathosystem.

Incomplete resistance is common in faba beans and has been reported by several authors, including Sillero *et al*. (2000) and Herath *et al*. (2001). Hypersensitive resistance was only identified by Sillero *et al*. (2000); however, the necrotic reaction occurs late, resulting in a limited infection size rather than complete resistance (Sillero *et al*., 2010). Both types of resistance are associated with a longer latency period, a reduction in pustule size, and a lower infection frequency. They only differ in the presence or absence of macroscopically visible necrosis (Sillero *et al*., 2000); therefore, hypersensitive resistance was not found in the present study.

It was also observed that line 17 ICAMEX was very susceptible both as an adult plant and as a seedling. This is important since it can be used as a susceptibility reference for the development of monopustular strains, inoculum production, plant-pathogen interaction studies, and as a susceptible border to achieve infection in the field in the evaluation of genotypes. It is necessary to continue studying the reaction of faba bean germplasm at the national level, focusing on quantitative and incomplete non-hypersensitive resistance to faba bean rust, in order to use it in genetic improvement

programs, since information on the genetic basis of resistance in faba beans is still scarce, both in Mexico and worldwide.

For the multivariate analysis of all evaluated variables, distinct groups were identified, with line 20CP standing out due to its incomplete resistance (Figure 2). This line clusters with line 9CP, which also shows quantitative resistance characteristics by limiting rust development. This is reflected in its longer LP1, LP50, and LP100 values relative to the other materials (Table 6), as well as its lower number of pustules, reduced severity, and a pustule size of 0.9 mm. Although it did not exhibit a hypersensitive reaction, its infection type was 2.7.

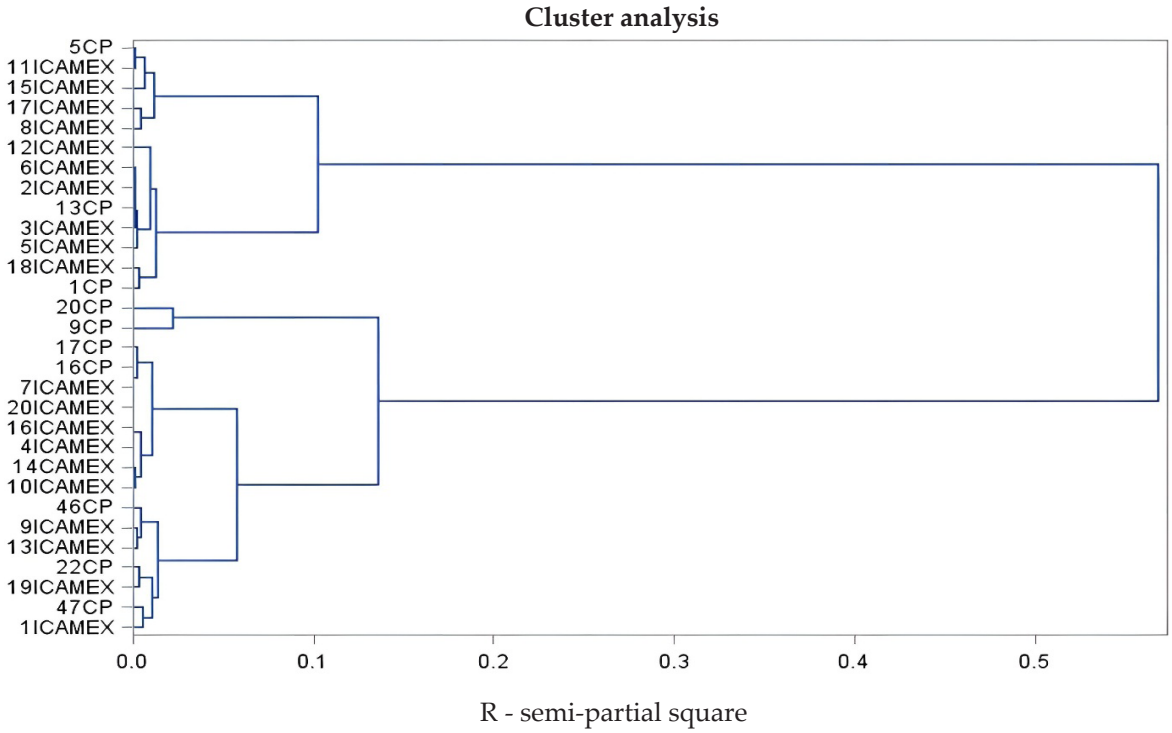

Figure 2. Multivariate characterization of genotypes using infection type, latency periods, pustule traits, and disease severity.

Ijaz *et al*. (2021) conducted a plant histology study in which they described the infection process of *U. viciae-fabae* in susceptible genotypes with infection type III. Urediniospores germinate on the leaf surface and form appressoria over the stomata, from which the germ tube penetrates into the leaf apoplast. Within the apoplast, substomatal vesicles are produced, giving rise to intercellular infection hyphae. These hyphae branch throughout the intercellular spaces of the leaf and generate haustorial mother cells, from which haustoria are formed to infect the mesophyll cells.

After 4–5 d, substantial hyphal growth with numerous haustoria is observed, without compromising the integrity of the host cell membrane. Infection sites continue expanding and subsequently form pustules at 7 d postinoculation. Resistant genotypes with infection type I also show notable hyphal growth and haustoria formation on host cells; however, tissue darkening with callose deposition appears at infection sites 4 d postinoculation. Pustules are detected at 11 d and display variable size, remaining smaller than those formed in the susceptible genotype.

CONCLUSIONS

There is at least one genotype with incomplete hypersensitive resistance among the Mexican faba bean genotypes evaluated. Line 20CP behaved as moderately resistant in seedlings. In the bean-*U. viciae-fabae* pathosystem, incomplete hypersensitive resistance was identified. No complete hypersensitive resistance was observed. Ten genotypes possess quantitative resistance components.

ACKNOWLEDGEMENTS

We thank the Secretariat of Science, Humanities, Technology, and Innovation (SECIHTI) and Postgraduate College Montecillo Campus for the financial support allocated through participation in the 2023-03 Call to support research projects; the Agricultural, Aquaculture, and Forestry Research and Training Institute of the State of Mexico (ICAMEX) for the germplasm provided for this study; and the National Institute of Forestry, Agricultural, and Livestock Research (INIFAP) for the support provided and the use of its facilities.

REFERENCES

Adhikari KN, Zhang P, Sadeque A, Hoxha, S, Trethowan R. 2016. Single independent genes confer resistance to faba bean rust (*Uromyces viciae-fabae*) in the current Australian cultivar Doza and a central European line Ac1655. Crop Pasture 67 (6): 649–654. https://doi.org/10.1071/CP15333

Ávila CM, Ruiz-Rodríguez MD, Cruz-Izquierdo S, Atienza SG, Cubero JI, Torres AM. 2017. Identification of plant architecture and yield-related QTL in *Vicia faba* L. Molecular Breeding 37 (7): 88. https://doi.org/10.1007/s11032-017-0688-7

Ávila CM, Sillero JC, Rubiales D, Moreno MT, Torres AM. 2003. Identification of RAPD markers linked to the Uvf-1 gene conferring hypersensitive resistance against rust (*Uromyces viciae-fabae*) in *Vicia faba* L. Theoretical and Applied Genetics 107 (2): 353–358. https://doi.org/10.1007/s00122-003-1254-8

Bjarko ME, Line RF. 1988. Heritability and number of genes controlling leaf rust resistance in four cultivars of wheat. Phytopathology 78 (4): 457–461.

Burbano-Figueroa O. 2020. Resistencia de plantas a patógenos: una revisión sobre los conceptos de resistencia vertical y horizontal. Revista Argentina de Microbiología 52 (3): 245–255. https://doi.org/10.1016/j.ram.2020.04.006

Cummins GB, Hiratsuka Y. 2003. Illustrated genera of rust fungi (Third edition). The American Phytopathological Society. St. Paul, MN, USA. 175 p.

Emeran AA, Sillero JC, Fernández-Aparicio M, Rubiales D. 2011. Chemical control of faba bean rust (*Uromyces viciae-fabae*). Crop Protection 30 (7): 907–912. https://doi.org/10.1016/j.cropro.2011.02.004

Flor H. 1942. Inheritance of pathogenicity in *Melampsora lini*. Phytopathology 32: 653–669.

González-González M, Zamora-Díaz M, Solano-Hernández S. 2016. Evaluación agronómica y física en líneas avanzadas de cebada maltera. Revista Mexicana de Ciencias Agrícolas 7 (1): 159–171.

Herath I, Stoddard F, Marshall D. 2001. Evaluating faba beans for rust resistance using detached leaves. Euphytica 117 (1): 47–57. https://doi.org/10.1023/a:1004071916288

Ijaz U, Adhikari K, Kimber R, Trethowan R, Bariana H, Bansal U. 2021. Pathogenic specialization in *Uromyces viciae-fabae* in Australia and rust resistance in faba bean. Plant Disease 105 (3): 636–642. https://doi.org/10.1094/pdis-06-20-1325-re

Ijaz U, Adhikari KN, Stoddard FL, Trethowan RM. 2017. Rust resistance in faba bean (*Vicia faba* L.): Status and strategies for improvement Australas. Plant Pathology 47 (1): 71–81. https://doi.org/10.1007/s13313-017-0528-6

Joseph ME, Hering TF. 1997. Effects of environment on spore germination and infection by faba bean rust (*Uromyces viciae-fabae*). The Journal of Agricultural Science 128 (1): 73–78. https://doi.org/10.1017/s0021859696003930

Niks RE, Parlevliet JE, Lindhout P, Bai Y. 2011. Breeding crops with resistance to diseases and pests. Wageningen University the Netherlands: Gelderland, Netherlands. 200 p. https://doi.org/10.3920/978-90-8686-171-2

Parlevliet JE. 1975. Partial resistance of barley to leaf rust, *Puccinia hordei*. I. Effect of cultivar and development stage on latent period. Euphytica 24 (1): 21–27. https://doi.org/10.1007/BF00147164

Parlevliet JE. 1979. Components of resistance that reduce the rate of epidemic development. Annual Review of Phytopathology 17 (1): 203–222. https://doi.org/10.1146/annurev.py.17.090179.001223

Robinson R. 1987. Host management in crop pathosystems. McMillan Publishing Company: New York, NY, USA. 263 p.

Rubiales D, Khazaei H. 2022. Advances in disease and pest resistance in faba bean. Theoretical and Applied Genetics 135 (11): 3735–3756. https://doi.org/10.1007/s00122-021-04022-7

SAS Institute. 2013. Base SAS® 9.4 Procedures Guide: Statistical Procedures (Second edition). SAS Institute Inc. Cary, NC, USA.

SIAP (Servicio de Información Agroalimentaria y Pesquera). 2024. Anuario estadístico de la producción agrícola. Gobierno de México. Servicio de Información Agroalimentaria y Pesquera. Ciudad de México, México. https://nube.siap.gob.mx/cierreagricola/ (Retrieved: January 2024).

Sillero JC, Moreno M, Rubiales D. 2000. Characterization of new sources of resistance to *Uromyces viciae-fabae* in a germplasm collection of *Vicia faba* L. Plant Pathology 49: 389–395. DOI:10.1046/j.1365-3059.2000.00459.x

Sillero JC, Villegas-Fernández AM, Thomas J, Rojas-Molina MM, Emeran AA, Fernández-Aparicio M, Rubiales D. 2010. Faba bean breeding for disease resistance. Field Crops Research 115: 297–307. https://doi.org/10.1016/j.fcr.2009.09.012

Stakman EC, Stewart DM, Loegering WQ. 1962. Identification of physiologic races of *Puccinia graminis* var. *tritici*. United States Department of Agriculture. USDA Agricultural Research Service. ARS. pp: 1–53. https://www.ars.usda.gov/ARSUserFiles/50620500/Cerealrusts/Pgt/Stakman_code_Pgt.pdf

Terefe H, Fininsa C, Sahile S, Tesfaye K. 2016. Effect of integrated climate change resilient cultural practices on faba bean rust (*Uromyces viciae-fabae*) epidemics in Hararghe Highlands. Ethiopia 7: 8. doi: 10.4172/2157-7471.1000373

Torres AM, Román B, Ávila CM, Satovic Z, Rubiales D, Sillero JC, Cubero JI, Moreno MT. 2006. Faba bean breeding for resistance against biotic stresses: towards application of marker technology. Euphytica 147: 67–80. DOI: 10.1007/s10681-006-4057-6

Vanderplank JE. 1963. Plant diseases: Epidemics and control. Academic Press: NY, USA & London. 349 p.

Villegas-Fernández AM, Sillero JC, Emeran AA, Flores F, Rubiales D. 2011. Multiple-disease resistance in *Vicia faba* L.: multi-environment field testing for identification of combined resistance to rust and chocolate spot. Field Crops Research 124 (1): 59–65. https://doi.org/10.1016/j.fcr.2011.06.004

Voegele RT. 2006. *Uromyces fabae*: development, metabolism, and interactions with its host *Vicia faba*. FEMS Microbiology Letters 259 (2): 165–173. https://doi.org/10.1111/j.1574-6968.2006.00248.x

Agrociencia

IONIC PROPORTIONS OF THE NUTRIENT SOLUTION AND THEIR EFFECT ON MACRONUTRIENT EXTRACTION IN HYDROPONICALLY GROWN LETTUCE

Rodolfo **de la Rosa-Rodríguez**[1], Ricardo David **Valdez-Cepeda**[2], Luis Octavio **Solís-Sánchez**[1], Alfredo **Lara-Herrera**[3*], Libia Iris **Trejo-Téllez**[4*]

[1]Universidad Autónoma de Zacatecas (UAZ). Unidad Académica de Ingeniería Eléctrica. Avenida Ramón López Velarde No. 801, Col. Centro, Zacatecas, Zacatecas, Mexico. C. P. 98000.
[2]Universidad Autónoma Chapingo. Zacatecas, Mexico. C. P. 98085.
[3]UAZ. Unidad Académica de Agronomía. Carretera Zacatecas-Guadalajara km 15.5, Cieneguillas, Zacatecas, Mexico. C. P. 98170.
[4]Colegio de Postgraduados. Programa de Edafología. Carretera México-Texcoco km 36.5 Montecillo, State of Mexico, Mexico. C. P. 56264.
* Authors for correspondence: alara204@hotmail.com; tlibia@colpos.mx

Citation: De la Rosa-Rodríguez R, Valdez-Cepeda RD, Solis-Sánchez LO, Lara-Herrera A, Trejo-Téllez LI. 2025. Ionic proportions of the nutrient solution and their effect on macronutrient extraction in hydroponically grown lettuce. **Agrociencia** 59(8): 1116-1133. https://doi.org/ 10.47163/agrociencia.v59i8.3444

Editor in Chief:
Dr. Fernando C. Gómez Merino

Received: May 02, 2025.
Approved: November 25, 2025.
Published in Agrociencia: December 10, 2025.

ABSTRACT

The nutrient solution (NS) consists of water with dissolved mineral ions, whose proportions depend on the species, cultivar, phenological stage, and environmental conditions, among other factors. This study aimed to evaluate the effect of variations in the proportions of NO_3^- and K^+ in the Steiner nutrient solution on the extraction of macronutrients in lettuce grown in a closed hydroponic system. The treatments were as follows: T1 (control): original Steiner NS, with proportions of 9.000:0.750:5.250 molc m^{-3} for the anions NO_3^-:$H_2PO_4^-$:SO_4^{2-} and 5.250:6.750:3.000 molc m^{-3} for the cations K^+:Ca^{2+}:Mg^{2+}; T2: 11.338:0.354:2.479 and 5.250:6.750:3.000 molc m^{-3}; T3: 6.371:1.194:8.362 and 5.250:6.750:3.000 molc m^{-3}; T4: 9.000:0.750:5.250 and 6.375:5.675:2.522 molc m^{-3}; and T5: 9.000:0.750:5.250 and 3.158:8.743:3.886 molc m^{-3}. Concentrations of N, P, K, Ca, and Mg were determined in leaves, buds, and roots, and together with dry biomass data, were used to estimate nutrient extraction per organ. The highest nutrient content was recorded in leaves (79 % of the total extracted). The greatest extractions corresponded to N and K, reaching 5.89 and 5.67 mg $plant^{-1}$, respectively, with T2 (high NO_3^- proportion). Increasing NO_3^- in the anionic proportion enhanced Ca and Mg uptake, whereas increasing K^+ reduced the extraction of these same cations. Treatments T2 and T4 showed the highest total extractions, mainly due to the greater values of N and K obtained compared with treatments in which the proportion of these ions was reduced. These results indicate that modifications in the anionic and cationic proportions of the nutrient solution significantly influence nutrient extraction in lettuce, with the treatment containing the highest NO_3^- proportion being the most efficient for the uptake of N, K, Ca, and Mg.

Keywords: nutrient extraction, ionic balance, anion interactions, cation interactions.

INTRODUCTION

Nutrient solution (NS) consists of water in which oxygen and mineral nutrients in ionic form are dissolved (Trejo-Téllez and Gómez-Merino, 2012). These nutrients contribute to biomass synthesis and influence multiple physiological and biochemical processes in plants, thus determining the quantity and quality of food produced (Engels *et al*., 2023). The amount of nutrients required by plants depends on the species, variety, phenological stage and environmental conditions, among other factors (Sambo *et al*., 2019).

Because various factors influence nutrient availability and concentration, each NS must be formulated with specific characteristics to achieve the expected yield and quality. Among the most important parameters are: a) pH, which affects nutrient availability, with the highest availability occurring within a pH range of 5.5 to 6.5 (Baca-Castillo *et al*., 2016); b) the NO_3^-:NH_4^+ ratio, which is relevant because both ionic forms of N are involved differently in biochemical, metabolic and physiological processes, potentially enhancing or limiting lettuce production (Wenceslau *et al*., 2021); c) the temperature of the NS, which directly influences the amount of dissolved oxygen available to roots (Ouyang *et al*., 2020); and d) electrical conductivity (EC), with an optimal range of 1.5 to 2 dS m^{-1} for lettuce (Adhikari *et al*., 2019). In addition, the mutual relationship among anions and among cations (ionic balance) is essential to prevent undesirable chemical reactions —such as nutrient precipitation— and to ensure an adequate nutrient supply that allows plants to reach their maximum yield (Baca-Castillo *et al*., 2016).

The composition of macro- and micronutrients in an NS directly influences plant growth, leaf number and area, yield, and crop quality, including mineral content (Ahmed *et al*., 2021). Therefore, the formulation of the NS must be adjusted to the specific requirements of each species and to the environmental conditions under which the crop is grown (Kumari *et al*., 2018).

Based on these considerations, Steiner (1961) proposed a methodology for formulating true nutrient solutions, characterized by maintaining the same osmotic pressure and pH, as well as constant mutual ionic relationships. These proportions, expressed as percentages, were: 60:5:35 for the anions NO_3^-:$H_2PO_4^-$:SO_4^{2-} and 35:45:20 for the cations K^+:Ca^{2+}:Mg^{2+}. However, in hydroponic systems it is possible to establish different ionic relationships and various total salt concentrations, as long as solubility limits that cause precipitation are not exceeded and imbalances, deficiencies or toxicities that affect plant physiological processes are avoided (Sambo *et al*., 2019).

Ionic proportions in the NS can alter cell membrane functionality and, consequently, the solute balance and the internal concentration of nutrients, causing symptoms similar to nutrient deficiencies (Coskun *et al*., 2017). Among essential elements, K and N are required in larger quantities (Oosterhuis *et al*., 2014). For this reason, changes in their concentrations and/or proportions in the NS can significantly affect the absorption and accumulation of one or more nutrients. For example, changes in NO_3^- within the anionic proportion cause notable variations in the concentration of N and K

more than in other ions (Al-Meselmani, 2022). Likewise, an 80:20 NO_3^-:NH_4^+ ratio may increase N concentration (Lara-Izaguirre *et al*., 2019), whereas reducing this ratio may induce ammonium toxicity (Ozores-Hampton *et al*., 2015).

It has also been documented that modifications in the proportion of K^+ within the cations can affect its concentration in lettuce shoots (Barickman *et al*., 2016). Furthermore, its proportion can influence the translocation of Ca, Mg, and P (Szczerba *et al*., 2009). Similarly, Malvi (2011) reported that an adequate proportion of NO_3^- contributes to optimal concentrations of K, Mg, Fe, Mn, and Zn.

A wide range of NS formulations exists for hydroponic plant production; however, the ionic proportions among them vary widely. Among these proportions, those corresponding to NO_3^- and K^+ are the most important, since N and K participate in most physiological processes in leafy vegetables (Riaño-Castillo *et al*., 2019). Nevertheless, further information is required regarding the response of plants grown in hydroponic systems to different nutrient relationships used in NS formulations (Al-Meselmani, 2022).

Considering the above, the present study was conducted to evaluate the effect of variations in the proportions of NO_3^- and K^+ in the Steiner nutrient solution on the extraction of macronutrients in lettuce grown under a closed hydroponic system. The working hypothesis states that increasing the proportion of NO_3^- to 80 % within the anionic mutual relationship and the proportion of K^+ to 43.8 % within the cationic mutual relationship of Steiner's NS will enhance macronutrient extraction in lettuce plants.

MATERIALS AND METHODS

Experimental site

This study was conducted from September 2 to October 31, 2022, in a 200 m² greenhouse equipped with a temperature and relative humidity control system, which operated by exchanging warm, dry internal air with fresh, humid external air. A closed floating root (FR) hydroponic system was established inside the greenhouse, in which the roots remained submerged in the nutrient solution (NS), while the aerial part of the plants was supported by a floating structure (Baca-Castillo *et al*., 2016). The greenhouse is located in Zacatecas, Zacatecas, Mexico, at coordinates 22° 43′ 42″ N and 102° 40′ 58″ W, at an elevation of 2236 m.

Treatments and experimental design

The treatments consisted of different macronutrient proportions in the NS. The reference solution was that proposed by Steiner (1961), along with four modified ionic proportion variants applied to a lettuce crop grown in a closed FR hydroponic system. The anionic proportions of NO_3^-:$H_2PO_4^-$:SO_4^{2-} evaluated were 60:5:35, 80:2.5:17.5, and 40:7.5:52.5, while the cationic proportions of K^+:Ca^{2+}:Mg^{2+} were 35:45:20, 43.8:38.9:17.3,

and 20:55.4:24.6. The five nutrient solution (NS) treatments evaluated are described in Table 1. All treatments were maintained at an electrical conductivity (EC) of 1.5 dS m^{-1} and the same osmotic potential (−0.0547 MPa) (Lara-Herrera *et al*., 2023).

Table 1. Macronutrient composition of the nutrient solutions evaluated.

Treatments	NO_3^-	$H_2PO_4^-$	SO_4^{2-}	K^+	Ca^{2+}	Mg^{2+}
			(mol_c m^{-3})			
T1	9.000	0.750	5.250	5.250	6.750	3.000
T2	11.338	0.354	2.479	5.250	6.750	3.000
T3	6.371	1.194	8.362	5.250	6.750	3.000
T4	9.000	0.750	5.250	6.375	5.675	2.522
T5	9.000	0.750	5.250	3.158	8.743	3.886

Water used in the treatments

The water used in the treatments was previously deionized by reverse osmosis (ROH22133BW, Water IXC®, Guadalajara, Mexico). The analysis showed the following concentrations (mg L^{-1}): 7.70 N, ND (not detected) P, 3.09 K, 19.12 Ca, 2.43 Mg, and 2.65 S as macronutrients, and the following micronutrients: Fe ND, Mn 0.004, B 0.121, Cu 0.013, Mo ND, and Ni 0.038. The water quality parameters were: pH 7.40, EC 0.036 dS m^{-1}, 167.7962 mg HCO_3^- L^{-1}, 34.86 mg Na L^{-1}, and 46.87 mg Cl L^{-1}.

Plant material and production system

Lettuce (*Lactuca sativa* L.) cv. "Toscana RZ (45-08)" from Rijk Zwaan was used. This iceberg-type lettuce is vigorous, dark green, and produces round heads. Seeds were sown in 297-cell polystyrene trays filled with peat as substrate and irrigated for 28 days after sowing. Subsequently, seedlings were removed from the trays, and roots were washed to remove substrate before being placed in sterile, low-salt water for 5 days to allow plant adaptation.

Management of the nutrient solution during the experiment

In addition to the macronutrients corresponding to each treatment, all nutrient solutions received a uniform concentration of micronutrients (mg L^{-1}): 2.25 Fe, 1.11 Mn, 0.18 Zn, 0.09 Cu, 0.21 B, and 0.06 Mo. Electrical conductivity (EC) and pH were measured daily before replenishing the water consumed the previous day. The volume lost was restored, and pH was adjusted to 5.5. These procedures ensured EC and pH remained within suitable ranges for lettuce development at each phenological stage (Baca-Castillo *et al*., 2016).

The variables were evaluated in three crop stages:
Stage 1: 20 days after transplanting (DAT), corresponding to rosette formation.

Stage 2: 40 DAT, at the onset of bud formation.
Stage 3: 60 DAT, corresponding to completion of bud formation in early-maturing cultivars (cycle of 60–70 DAT). Maximum growth under hydroponic conditions occurs between 55 and 60 days (Sánchez-Alegría *et al*., 2015).

Macronutrient sources used for preparing the solutions were: $Ca(NO_3)_2{\cdot}4H_2O$, KNO_3, K_2SO_4, $MgSO_4{\cdot}7H_2O$, KH_2PO_4, and H_2SO_4. Micronutrients were supplied through a commercial mixture containing the concentrations listed above, in which Fe, Mn, Zn, and Cu were chelated with EDTA.

Measured variables

Macronutrient concentration in lettuce leaf, bud, and root tissues. Plant material was processed, and N, P, K, Ca, and Mg concentrations were determined following the methodology described by Lara-Herrera *et al*. (2023).

Dry weight of lettuce plant organs. Lettuce plants were separated into leaves, buds, and roots. Samples were dried in an oven (Thermo Fisher Scientific 51028118, USA) at 68 ± 2 °C, and dry mass was recorded using a digital scale (Kern AES 200-4N, Germany).

Macronutrient extraction. This parameter was determined based on the percentage obtained for each of the five macronutrients in the three plant organs, together with the dry weight of each corresponding organ. It is expressed using the following formula:

$$Ex = \frac{\text{DWo x Cm}}{100}$$

Where:
Ex = Macronutrient extraction (mg)
DWo = Dry weight of the organ (mg)
Cm = Macronutrient concentration in tissue (%)

Experimental design and statistical analysis

A randomized complete block design was used, with five treatments and six replicates per treatment, for a total of 30 experimental units. Each unit contained three plants (one for each phenological stage), resulting in a total of 90 plants evaluated throughout the experiment. Data were analyzed using ANOVA, and mean comparisons were performed with Tukey's test at a 5 % significance level ($p \leq 0.05$). All analyses were conducted using SAS software version 9.4.

RESULTS AND DISCUSSION

Macronutrient concentration in lettuce leaves

Nitrogen and phosphorus. In stages 2 and 3, treatment T2 showed the highest leaf N concentration (Table 2). This result agrees with Lara-Herrera *et al.* (2023), who reported that this proportion of NO_3^- in the nutrient solution increases yield, fresh weight, and leaf area index in hydroponically grown lettuce. The increase in leaf N concentration is associated with the greater availability of NO_3^- in the nutrient solution (Combrink and Kempen, 2019). Similarly, Djidonou and Leskovar (2019) observed that an increase in N supply enhanced N concentration in the leaves of hydroponic lettuce between 28 and 35 DAT.

In contrast, leaf P concentration in treatment T2 showed lower values than in the other treatments in both stages (Table 3). This behavior is explained by the lower

Table 2. Nitrogen concentration (g kg^{-1} dry matter) in leaves, buds, and roots at three developmental stages of lettuce plants as affected by macronutrient ratios in the nutrient solution.

Organ	Treatments	Stage 1	Stage 2	Stage 3
Leaves	T1	40.250 ± 4.194 a	30.683 ± 7.075 b	25.783 ± 4.073 bc
	T2	41.008 ± 4.912 a	45.033 ± 4.583 a	36.158 ± 2.618 a
	T3	38.983 ± 5.103 a	26.833 ± 7.353 b	24.091 ± 3.070 c
	T4	40.950 ± 3.541a	31.500 ± 6.369 b	28.816 ± 3.914 bc
	T5	37.333 ± 5.118a	32.083 ± 3.844 b	30.333. ± 1.8604 b
Organ	Treatments	Stage 1	Stage 2	Stage 3
Buds	T1	32.433 ± 4.923 a	26.950 ± 4.558 bc	22.691 ± 2.732 bc
	T2	34.035 ± 3.725 a	33.016 ± 2.779 ab	32.575 ± 6.110 a
	T3	22.400 ± 17.502 a	26.133 ± 4.145 c	17.908 ± 6.980 c
	T4	21.150 ± 12.540 a	31.908 ± 2.139 abc	22.400 ± 2.944 bc
	T5	29.071 ± 14.374 a	33.891 ± 4.418 a	28.816 ± 4.097 ab
Organ	Treatments	Stage 1	Stage 2	Stage 3
Roots	T1	37.333 ± 2.441 a	32.083 ± 6.402 a	22.400 ± 3.075 ab
	T2	23.800 ± 18.561 a	37.233 ± 9.125 a	19.308 ± 5.286 b
	T3	24.791 ± 19.981 a	23.800 ± 13.544 a	26.658 ± 9.480 ab
	T4	24.081 ± 18.918 a	43.983 ± 26.191 a	30.041 ± 5.117 a
	T5	36.096 ± 4.881 a	29.633 ± 9.047 a	30.450 ± 2.894 a

T1 = Ionic proportions in the nutrient solution: NO_3^- = 9.000, $H_2PO_4^-$ = 0.750, SO_4^{2-} = 5.250, K^+ = 5.250, Ca^{2+} = 6.750, Mg^{2+} = 3.000 $mol_c\ m^{-3}$. T2 = 11.338, 0.354, 2.479, 5.250, 6.750, 3.000. T3 = 6.371, 1.194, 8.362, 5.250, 6.750, 3.000. T4 = 9.000, 0.750, 5.250, 6.375, 5.675, 2.522. T5 = 9.000, 0.750, 5.250, 3.158, 8.743, 3.886. Stage 1 = 20 days after transplanting (rosette formation), Stage 2 = 40 days after transplanting (onset of bud formation), and Stage 3 = 60 days after transplanting (completion of bud formation). Values expressed as mean ± standard deviation. Different letters within each stage and organ indicate significant differences (Tukey, $p \leq 0.05$).

Table 3. Phosphorus concentration (g kg^{-1} dry matter) in leaves, buds, and roots at three developmental stages of lettuce plants, as affected by the proportions of macronutrients in the nutrient solution.

Organ	Treatments	Stage 1	Stage 2	Stage 3
Leaves	T1	5.322 ± 0.576 a	5.271 ± 1.217 a	4.047.83 ± 0.423 a
	T2	4.782 ± 0.746 a	3.608 ± 0.329 b	2.550.32 ± 0.517 b
	T3	4.639 ± 0.616 a	5.182 ± 0.818 a	4.204.39 ± 0.497 a
	T4	5.384 ± 0.921 a	4.512 ± 0.769 ab	4.659.01 ± 0.724 a
	T5	5.397 ± 0.846 a	4.701 ± 0.187 ab	4.324.64 ± 0.197 a
Organ	Treatments	Stage 1	Stage 2	Stage 3
Buds	T1	6.582 ± 0.989 a	8.017 ± 1.092 a	6.153 ± 1.034 a
	T2	5.956 ± 2.089 a	6.002 ± 0.246 b	3.584 ± 0.714 b
	T3	5.046 ± 3.930 a	7.985 ± 1.322 a	5.864 ± 2.091 a
	T4	4.146 ± 2.907 a	8.027 ± 1.104 a	7.244 ± 1.146 a
	T5	4.900 ± 4.131 a	8.959 ± 0.956 a	7.509 ± 0.672 a
Organ	Treatments	Stage 1	Stage 2	Stage 3
Roots	T1	10.132 ± 0.840 a	7.353 ± 1.452 bc	6.128 ± 2.586 bc
	T2	6.826 ± 5.422 a	3.979 ± 0.604 d	2.293 ± 0.340 c
	T3	7.588 ± 5.938 a	12.639 ± 2.686 a	11.653 ± 4.377 a
	T4	6.252 ± 5.739 a	6.834 ± 1.804 c	8.691 ± 3.676 ab
	T5	9.617 ± 2.562 a	9.667 ± 0.710 b	9.456 ± 0.912 ab

T1 = Ionic proportions in the nutrient solution: NO_3^- = 9.000, $H_2PO_4^-$ = 0.750, SO_4^{2-} = 5.250, K^+ = 5.250, Ca^{2+} = 6.750, Mg^{2+} = 3.000 mol_c m^{-3}. T2 = 11.338, 0.354, 2.479, 5.250, 6.750, 3.000. T3 = 6.371, 1.194, 8.362, 5.250, 6.750, 3.000. T4 = 9.000, 0.750, 5.250, 6.375, 5.675, 2.522. T5 = 9.000, 0.750, 5.250, 3.158, 8.743, 3.886. Stage 1 = 20 days after transplanting (rosette formation), Stage 2 = 40 days after transplanting (onset of bud formation), and Stage 3 = 60 days after transplanting (completion of bud formation). Values expressed as mean ± standard deviation. Different letters within each stage and organ indicate significant differences (Tukey, $p \leq 0.05$).

proportion of phosphate in the nutrient solution and by the increase in biomass under this treatment, which results in a dilution effect of P in plant tissue. A similar effect was reported by Parra-Terraza (2016) when modifying the N:K ratio in the nutrient solution for tomato seedlings. Additionally, ionic balance also influences this response, as an increase in NO_3^- concentration requires proportional adjustments in the concentrations of $H_2PO_4^-$ and SO_4^{2-} (Al-Meselmani, 2022).

Potassium, calcium, and magnesium. Across the three growth stages, the control treatment (T1) showed a higher K concentration than treatment T5 (Table 4). This behavior of K in leaves supplied with the control solution was likely due to a balanced ionic proportion that favored the accumulation of this cation (Kempen *et al*., 2016). In the case of foliar Ca and Mg concentrations, during the first growth stage the lower

Table 4. Potassium concentration (g kg^{-1} dry matter) in leaves, buds, and roots at three developmental stages of lettuce plants, as affected by macronutrient proportions in the nutrient solution.

Organ	Treatments	Stage 1	Stage 2	Stage 3
Leaves	T1	37.153 ± 2.810 a	31.694 ± 6.110 a	30.919 ± 4.665 a
	T2	31.109 ± 3.225 ab	28.165 ± 3.116 ab	24.852 ± 3.673 ab
	T3	30.341 ± 4.039 ab	30.59 ± 4.654 a	26.459 ± 3.988 ab
	T4	32.474 ± 5.059 ab	29.471 ± 4.231 ab	29.677 ± 3.054 a
	T5	29.428 ± 3.816 b	22.218 ± 3.559 b	21.926 ± 4.823 b
Organ	Treatments	Stage 1	Stage 2	Stage 3
Buds	T1	23.229 ± 3.797 a	19.181 ± 1.132 b	24.311 ± 6.018 ab
	T2	16.725 ± 5.248 a	17.865 ± 1.483 b	12.057 ± 2.995 b
	T3	17.565 ± 13.672 a	21.817 ± 2.303 ab	20.502 ± 11.050 ab
	T4	15.276 ± 10.019 a	23.556.56 ± 2.336 a	29.171 ± 10.012 a
	T5	15.476 ± 13.334 a	11.054.30 ± 3.106 c	15.910 ± 10.856 ab
Organ	Treatments	Stage 1	Stage 2	Stage 3
Roots	T1	31.710 ± 3.172 a	14.211 ± 5.771 b	7.485 ± 4.201 c
	T2	19.840 ± 15.457 a	8.324 ± 3.175 bc	2.819 ± 0.512 c
	T3	22.461 ± 17.978 a	25.049 ± 5.258 a	16.983 ± 2.515 ab
	T4	19.044 ± 17.158 a	23.803 ± 4.295 a	22.139 ± 5.148 a
	T5	27.211 ± 7.697 a	4.524 ± 1.468 c	8.229 ± 8.593 bc

T1 = Ionic proportions in the nutrient solution: NO_3^- = 9.000, $H_2PO_4^-$ = 0.750, SO_4^{2-} = 5.250, K^+ = 5.250, Ca^{2+} = 6.750, Mg^{2+} = 3.000 $mol_c\ m^{-3}$. T2 = 11.338, 0.354, 2.479, 5.250, 6.750, 3.000. T3 = 6.371, 1.194, 8.362, 5.250, 6.750, 3.000. T4 = 9.000, 0.750, 5.250, 6.375, 5.675, 2.522. T5 = 9.000, 0.750, 5.250, 3.158, 8.743, 3.886. Stage 1 = 20 days after transplanting (rosette formation), Stage 2 = 40 days after transplanting (onset of bud formation), and Stage 3 = 60 days after transplanting (completion of bud formation). Values expressed as mean ± standard deviation. Different letters within each stage and organ indicate significant differences (Tukey, $p \leq 0.05$).

K concentration in the nutrient solution (T5) resulted in higher concentrations of both elements in the leaves (Tables 5 and 6). This response may be attributed to the greater availability of calcium and to the antagonism that Ca and Mg can exert on K when the proportion of the latter in the nutrient solution is low (Mitra, 2017; Combrink and Kempen, 2019). In the last two stages, differences were observed only for Mg concentration (Table 6), with the highest values occurring under T5 (the treatment with the lowest K proportion in the nutrient solution). These patterns are attributed to modifications in the cationic balance of the nutrient solution (Mitra, 2017; Kamboj, 2019).

Macronutrient concentration in lettuce buds

Nitrogen and phosphorus. In Stage 2, only T5 exceeded the control (T1) in N concentration; however, in Stage 3, the increase in N proportion in the nutrient

solution allowed this treatment to surpass the control (Table 2). An adequate supply of N in the nutrient solution is essential to meet crop demand; otherwise, plants cannot achieve appropriate foliar N concentrations (Kempen *et al*., 2016). Moreover, although T2 increased N concentration, it simultaneously showed a decrease in P concentration during Stages 2 and 3 (Table 3). This behavior is related to ionic adjustment within the nutrient solution: increasing the proportion of NO_3^- in the anionic fraction reduces the relative concentrations of $H_2PO_4^-$ and SO_4^{2-}, thereby decreasing P availability to the bud (Al-Meselmani, 2022).

Potassium, calcium, and magnesium. In Stage 2, increasing the proportion of K in the nutrient solution (T4) resulted in the highest K concentration in the bud, while decreasing K (T5) produced the lowest concentration (Table 4). In contrast, Mg exhibited the opposite trend: its concentration decreased when K in the nutrient solution increased and rose when K decreased (Table 6). In Stage 3, a similar trend was observed: reducing K in the nutrient solution was associated with higher Mg concentration in the bud. This pattern is consistent with ionic competition among cations, as high K concentrations in the nutrient solution can limit the uptake of other cations such as Ca and Mg due to their lower availability (Parra-Terraza, 2016). In the case of Ca, no significant effects were observed across the three stages (Table 5). This outcome differs from Parra-Terraza (2016), who reported an increase in Ca concentration when the proportion of NO_3^- was raised in a nutrient solution for tomato seedlings.

Macronutrient concentration in lettuce roots

Nitrogen and phosphorus. In Stage 3, increasing the proportion of NO_3^- in the nutrient solution resulted in the lowest N concentration in roots, while variations in K concentration—either increasing or decreasing—were associated with the highest root N values (Table 2). The fact that a higher proportion of NO_3^- leads to lower root N concentrations may be explained by two factors: (1) NO_3^- uptake depends largely on N demand in the aerial part, so under high demand, NO_3^- flow is preferentially directed to the shoots (Kempen *et al*., 2016); and (2) nitrate tends to accumulate mainly in aboveground tissues rather than in the roots (Sosa *et al*., 2017).
Regarding P, significant effects were observed in Stages 2 and 3, with T2 showing the lowest concentrations in roots (Table 3). This behavior in the intermediate and final stages is attributed to the imbalance between N and P in the nutrient solution, since increasing nitrate requires proportional reductions in phosphate and sulfate (Al-Meselmani, 2022).

Potassium, calcium, and magnesium. In Stages 2 and 3, increasing the proportion of K (T4) in the nutrient solution produced the highest K concentration in roots. A similar effect occurred with the reduction of NO_3^- (T3), which also surpassed the other

Table 5. Calcium concentration (g kg^{-1} dry matter) in leaves, buds, and roots at three developmental stages of lettuce plants, as affected by macronutrient proportions in the nutrient solution.

Organ	Treatments	Stage 1	Stage 2	Stage 3
	T1	9.777 ± 0.823 ab	8.182 ± 2.602 a	8.706 ± 1.504 a
	T2	9.663 ± 0.994 ab	8.556 ± 1.291 a	8.818 ± 0.803 a
Leaves	T3	8.384 ± 1.198 b	7.819 ± 1.560 a	7.466 ± 2.273 a
	T4	9.429 ± 1.030 ab	7.467 ± 0.861 a	7.802 ± 2.226 a
	T5	10.143 ± 1.358 a	8.286 ± 0.505 a	8.995 ± 1.681 a
Organ	Treatments	Stage 1	Stage 2	Stage 3
	T1	3.634 ± 0.570 a	4.327 ± 0.719 a	2.599 ± 0.467 a
	T2	4.862 ± 2.209 a	4.070 ± 0.244 a	2.768 ± 0.252 a
Buds	T3	2.752 ± 2.183 a	4.182 ± 0.601 a	3.424 ± 1.369 a
	T4	2.775 ± 1.607 a	4.053 ± 0.343 a	4.151 ± 1.185 a
	T5	2.594 ± 1.731 a	4.572 ± 0.398 a	4.298 ± 1.231 a
Organ	Treatments	Stage 1	Stage 2	Stage 3
	T1	5.787 ± 0.677 a	13.789 ± 4.212 bc	29.091 ± 5.486 ab
	T2	3.902 ± 3.089 a	21.921 ± 6.016 ab	35.948 ± 0.115.82 a
Roots	T3	4.053 ± 3.157 a	12.645 ± 4.242 c	23.015 ± 4.296 ab
	T4	3.217 ± 2.709 a	15.621 ± 3.844 abc	19.095 ± 6.478 b
	T5	6.952 ± 1.593 a	23.452 ± 8.428 a	32.265 ± 16.158 ab

T1 = Ionic proportions in the nutrient solution: NO_3^- = 9.000, $H_2PO_4^-$ = 0.750, SO_4^{2-} = 5.250, K^+ = 5.250, Ca^{2+} = 6.750, Mg^{2+} = 3.000 $mol_c\ m^{-3}$. T2 = 11.338, 0.354, 2.479, 5.250, 6.750, 3.000. T3 = 6.371, 1.194, 8.362, 5.250, 6.750, 3.000. T4 = 9.000, 0.750, 5.250, 6.375, 5.675, 2.522. T5 = 9.000, 0.750, 5.250, 3.158, 8.743, 3.886. Stage 1 = 20 days after transplanting (rosette formation), Stage 2 = 40 days after transplanting (onset of bud formation), and Stage 3 = 60 days after transplanting (completion of bud formation). Values expressed as mean ± standard deviation. Different letters within each stage and organ indicate significant differences (Tukey, $p \leq 0.05$).

treatments in K concentration (Table 4). This can be attributed to the fact that a lower proportion of NO_3^- may reduce aerial biomass (Kempen *et al.*, 2016), thereby lowering nutrient demand and favoring K accumulation in the root. However, Tsouvaltzis *et al*. (2020) reported the opposite response in red lettuce, suggesting that plant genotype and production system influence this behavior.

For Ca concentration in roots, T4 surpassed the control in Stage 2 (Table 5). Additionally, a clear antagonism with K was observed in Stage 1, where increased K (T4) produced the lowest Mg concentrations in roots. Conversely, reduced K (T5) led to the highest Mg concentrations in roots in Stages 2 and 3 (Table 6). The proportion of NO_3^- also influenced Mg concentration in roots: T3 (lowest NO_3^-) reduced Mg, while T2 (highest NO_3^-) increased it in Stages 2 and 3—both relative to T5. This pattern occurs because NO_3^- interacts synergistically with Mg uptake (Malvi, 2011; Kamboj, 2019).

Table 6. Magnesium concentration (g kg^{-1} dry matter) in leaves, buds, and roots at three developmental stages of lettuce plants, as affected by macronutrient proportions in the nutrient solution.

Organ	Treatments	Stage 1	Stage 2	Stage 3
Leaves	T1	2.204 ± 0.135 ab	1.836 ± 0.309 bc	1.987 ± 0.268 ab
	T2	1.924 ± 0.287 b	1.912 ± 0.162 b	2.035 ± 0.253 ab
	T3	1.963 ± 0.329 ab	1.634 ± 0.224 bc	1.632 ± 0.326 b
	T4	2.198 ± 0.420 ab	1.594 ± 0.186 c	1.689 ± 0.429 b
	T5	2.515 ± 0.383 a	2.359 ± 0.152 a	2.386 ± 0.580 a
Organ	Treatments	Stage 1	Stage 2	Stage 3
Buds	T1	1.031 ± 0.181 a	1.411 ± 0.206 b	1.258 ± 0.162 ab
	T2	0.894 ± 0.206 a	1.555 ± 0.128 b	1.097 ± 0.133 b
	T3	0.788 ± 0.618 a	1.300 ± 0.201 b	0.924 ± 0.289 b
	T4	0.738 ± 0.467 a	1.264 ± 0.127 b	1.055 ± 0.213 b
	T5	0.798 ± 0.559 a	2.577 ± 0.271 a	1.610 ± 0.276 a
Organ	Treatments	Stage 1	Stage 2	Stage 3
Roots	T1	1.185 ± 0.089 a	2.541 ± 0.559 b	4.493 ± 1.019 ab
	T2	0.762 ± 0.593 a	3.094 ± 0.337 ab	5.027 ± 0.475 a
	T3	0.878 ± 0.685 a	2.232 ± 0.470 b	2.605 ± 0.849 b
	T4	0.671 ± 0.568 a	2.654 ± 0.526 b	2.521 ± 1.056 b
	T5	1.173 ± 0.168 a	3.693 ± 0.848 a	5.136 ± 2.801 a

T1 = Ionic proportions in the nutrient solution: NO_3^- = 9.000, $H_2PO_4^-$ = 0.750, SO_4^{2-} = 5.250, K^+ = 5.250, Ca^{2+} = 6.750, Mg^{2+} = 3.000 mol_c m^{-3}. T2 = 11.338, 0.354, 2.479, 5.250, 6.750, 3.000. T3 = 6.371, 1.194, 8.362, 5.250, 6.750, 3.000. T4 = 9.000, 0.750, 5.250, 6.375, 5.675, 2.522. T5 = 9.000, 0.750, 5.250, 3.158, 8.743, 3.886. Stage 1 = 20 days after transplanting (rosette formation), Stage 2 = 40 days after transplanting (onset of bud formation), and Stage 3 = 60 days after transplanting (completion of bud formation). Values expressed as mean ± standard deviation. Different letters within each stage and organ indicate significant differences (Tukey, $p \leq 0.05$).

Nutrient extraction by developmental stage

In Stage 1, no significant differences among treatments were observed regarding macronutrient extraction in any of the three plant organs (Tables 7–9). This is consistent with Sosa *et al*. (2017), who reported that in the early stages of lettuce development, nutrient demand is still low, and consequently, tissue concentrations remain limited.

Leaves. In Stage 2, P extraction showed no differences among treatments (Table 7). This is attributed to the fact that P concentration is higher in the roots than in the aboveground organs (Table 3), a result consistent with Sosa *et al*. (2017), who reported that in lettuce (65-day production cycle), P concentration in roots was 2–3 % higher than in the other organs. In the present study, P extraction increased by 25 % from Stage 1 to Stage 2 and by 7 % from Stage 2 to Stage 3. This trend agrees with the aforementioned authors, who observed the highest P concentration in aboveground tissue between 17 and 43 days after emergence.

Table 7. Nutrient extraction (mg) in lettuce leaves at three developmental stages, grown in a closed hydroponic system with five nutrient proportions in the nutrient solution.

Treatments	N	P	K	Ca	Mg
			Stage 1		
T1	404.8 ± 182.9 a	57.7 ± 24.3 a	530.2 ± 249.9 a	88.8 ± 37.2 a	23.0 ± 10.4 a
T2	648.5 ± 184.1 a	90.0 ± 31.3 a	580.3 ± 212.9 a	119.0 ± 45.0 a	28.2 ± 10.9 a
T3	513.3 ± 212. a	71.3 ± 28.7 a	596.1 ± 229.5 a	102.4 ± 42.5 a	27.2 ± 11.2 a
T4	559.1 ± 212.7 a	79.7 ± 31.6 a	570.6 ± 306.2 a	131.1 ± 61.9 a	32.2 ± 13.6 a
T5	586.2 ± 238.9 a	76.5 ± 27.9 a	662.1 ± 278.3 a	144.8 ± 64.9 a	34.3 ± 14.5 a
			Stage 2		
Treatments	N	P	K	Ca	Mg
T1	1498.8 ± 357.0 ab	229.2 ± 57.0 a	1700.9 ± 300.1 bc	407.9 ± 97.5 b	79.5 ± 21.3 b
T2	1960.9 ± 540.7 a	213.4 ± 53.2 a	2369.3 ± 654.6 a	672.8 ± 236.5 a	127.4 ± 45.9 a
T3	1013.9 ± 160.5 b	200.6 ± 6.1 a	1577.1 ± 135.7 bc	396.9 ± 99.5 b	71.6 ± 10.8 b
T4	1418.2 ± 110.7 ab	233.1 ± 26.7 a	1931.6 ± 210.4 ab	450.0 ± 65.0 b	82.2 ± 9.9 ab
T5	1302.0 ± 324.3 b	216.8 ± 53.0 a	1159.6 ± 199.2 c	482.2 ± 134.4 ab	114.2 ± 36.7 ab
			Stage 3		
Treatments	N	P	K	Ca	Mg
T1	1944.5 ± 530.5 ab	325.8 ± 53.5 a	2608.8 ± 709.4 a	852.5 ± 352.2 ab	149. 8 ± 53.8 a
T2	2111.6 ± 414.7 a	225.0 ± 58.5 a	2126.1 ± 567.3 a	938.1 ± 318.4 a	169.4 ± 41.8 a
T3	1034.9 ± 297.3 b	264.2 ± 80.4 a	1745.8 ± 447.9 ab	541.4 ± 138.2 ab	99.8 ± 29.6 a
T4	1240.5 ± 638.5 ab	277.5 ± 144.8 a	2189.1 ± 1130.3 a	725.7 ± 380.9 ab	110.6 ± 55.0 a
T5	1090.8 ± 673.5 b	209.3 ± 118.9 a	916.8 ± 517.5 b	492.6 ± 356.7 b	118.9 ± 86.3 a

T1 = Ionic proportions in the nutrient solution: NO_3^- = 9.000, $H_2PO_4^-$ = 0.750, SO_4^{2-} = 5.250, K^+ = 5.250, Ca^{2+} = 6.750, Mg^{2+} = 3.000 $mol_c\ m^{-3}$. T2 = 11.338, 0.354, 2.479, 5.250, 6.750, 3.000. T3 = 6.371, 1.194, 8.362, 5.250, 6.750, 3.000. T4 = 9.000, 0.750, 5.250, 6.375, 5.675, 2.522. T5 = 9.000, 0.750, 5.250, 3.158, 8.743, 3.886. Stage 1 = 20 days after transplanting (rosette formation), Stage 2 = 40 days after transplanting (onset of bud formation), and Stage 3 = 60 days after transplanting (completion of bud formation). Values expressed as mean ± standard deviation. Different letters within each element and stage indicate significant differences (Tukey, $p \leq 0.05$).

The remaining macronutrients exhibited a similar pattern. In Stage 2, the treatment with the highest proportion of NO_3^- (T2) showed the greatest extraction of K, Ca, and Mg compared with T1 (Table 7). In Stage 3, the results were similar, which can be attributed to the fact that a higher proportion of NO_3^- leads to greater N accumulation in leaves (Combrink and Kempen, 2019). Lettuce also has a high capacity to accumulate NO_3^- in foliar tissue (Karthika *et al.*, 2018; Djidonou and Leskovar, 2019).

Furthermore, synergistic effects between NO_3^- and K^+ (Coskun *et al.*, 2017), as well as with Mg^{2+} (Njira and Nabwami, 2015), were observed, since increasing NO_3^- in the nutrient solution enhanced the extraction of these cations in leaves.

Buds. In stages 1 and 3, the contents of the five macronutrients in the bud did not differ among treatments (Table 8). In stage 2, the extraction of N, Ca and Mg also showed no differences among treatments. The K contents in T4 (high K) and T5 (low K) were statistically different, with the higher K supply resulting in the highest mean value; however, it did not surpass the control (T1) (Table 8). This behavior agrees with Kempen *et al.* (2016) and Combrink and Kempen (2019), who reported that plants grown hydroponically can increase nutrient extraction when the nutrient is more available in the solution. Phosphorus extraction was only different between T2 (high NO_3^-) and T4 (high K), with the former being lower than the latter (Table 8).

Table 8. Nutrient extraction (mg) in lettuce buds at three growth stages, grown in a closed hydroponic system under five nutrient-solution ionic proportion treatments.

			Stage 1		
Treatments	N	P	K	Ca	Mg
T1	17.0 ± 6.8 a	4.1 ± 1.6 a	16.1 ± 7.6 a	2.2 ± 0.6 a	0.6 ± 0.2 a
T2	29.6 ± 13.8 a	6.3 ± 2.8 a	24.2 ± 12.4 a	3.6 ± 1.6 a	1.0 ± 0.5 a
T3	21.3 ± 8.5 a	4.6 ± 2.0 a	18.3 ± 9.0 a	2.8 ± 1.2 a	0.8 ± 0.4 a
T4	22.5 ± 8.7 a	5.3 ± 2.5 a	19.2 ± 9.5 a	2.8 ± 1.2 a	0.8 ± 0.4 a
T5	24.6 ± 11.6 a	5.6 ± 2.5 a	19.5 ± 8.0 a	3.0 ± 1.4 a	0.9 ± 0.4 a
			Stage 2		
Treatments	N	P	K	Ca	Mg
T1	103.7 ± 50.6 a	27.8 ± 8.6 ab	75.6 ± 17.8 abc	16.4 ± 5.9 a	5.6 ± 2.3 a
T2	110.4 ± 52.4 a	16.7 ± 7.3 b	64.7 ± 19.9 bc	13.8 ± 6.3 a	4.6 ± 2.5 a
T3	96.3 ± 34.2 a	25.3 ± 6.1 ab	87.3 ± 19.1 ab	15.3 ± 5.8 a	4.8 ± 1.4 a
T4	139.4 ± 41.2 a	33.2 ± 10.3 a	104.4 ± 31.4 a	18.1 ± 6.1 a	5.5 ± 1.8 a
T5	129.2 ± 53.7 a	27.4 ± 9.6 ab	43.7 ± 9.2 c	17.2 ± 7.3 a	7.8 ± 3.6 a
			Stage 3		
Treatments	N	P	K	Ca	Mg
T1	318.9 ± 43.9 a	78.4 ± 8.1 a	178.1 ± 27.1 a	47.9 ± 3.7 a	14.6 ± 4.1 a
T2	328.4 ± 56.4 a	44.8 ± 10.5 a	141.6 ± 27.6 a	49.1 ± 11.1 a	16.5 ± 4.0 a
T3	177.3 ± 67.9 a	58.6 ± 16.7 a	146.5 ± 38.3 a	42.0 ± 14.3 a	9.9 ± 2.9 a
T4	323.3 ± 265.2 a	79.8 ± 60.0 a	159.4 ± 87.7 a	43.1 ± 32.4 a	16.1 ± 19.3 a
T5	164.3 ± 151.5 a	47.3 ± 39.1 a	119.0 ± 113.3 a	30.9 ± 25.4 a	11.3 ± 10.2 a

T1 = Ionic proportions in the nutrient solution: NO_3^- = 9.000, $H_2PO_4^-$ = 0.750, SO_4^{2-} = 5.250, K^+ = 5.250, Ca^{2+} = 6.750, Mg^{2+} = 3.000 $mol_c\ m^{-3}$. T2 = 11.338, 0.354, 2.479, 5.250, 6.750, 3.000. T3 = 6.371, 1.194, 8.362, 5.250, 6.750, 3.000. T4 = 9.000, 0.750, 5.250, 6.375, 5.675, 2.522. T5 = 9.000, 0.750, 5.250, 3.158, 8.743, 3.886. Stage 1 = 20 days after transplanting (rosette formation), Stage 2 = 40 days after transplanting (onset of bud formation), and Stage 3 = 60 days after transplanting (completion of bud formation). Values expressed as mean ± standard deviation. Different letters within each element and stage indicate significant differences (Tukey, $p \leq 0.05$).

Roots. In this organ, the extraction of N, Ca, and Mg was not affected by the different nutrient solutions (NSs) in stages 1 and 2; the same occurred for Ca in stage 3 (Table 9). Conversely, in stage 2, K extraction was higher in T3 compared with T5. In stage 3, P extraction in T3 was higher than that recorded in the other treatments. The greater P extraction in T3 is attributed to the ionic balance that must be maintained in the NS; when the proportion of NO_3^- decreases, the relative proportions of phosphate and sulfate increase, enhancing P uptake (Kempen *et al*., 2016). This result contrasts with the findings of Kumari *et al.* (2018), who reported synergistic interactions between N and P.

Table 9. Nutrient extraction (mg) in lettuce roots at three developmental stages, grown in a closed hydroponic system with five nutrient proportions in the nutrient solution.

			Stage 1		
Treatments	N	P	K	Ca	Mg
T1	83.8 ± 46.1 a	27.4 ± 17.1 a	160.7 ± 105.0 a	7.9 ± 4.2 a	3.0 ± 1.7 a
T2	114.7 ± 45.2 a	27.9 ± 11.8 a	148.3 ± 60.6 a	15.8 ± 7.0 a	4.0 ± 1.7 a
T3	77.4 ± 38.6 a	22.8 ± 11.3 a	95.8 ± 49.0 a	14.5 ± 6.5 a	2.8 ± 1.4 a
T4	90.4 ± 42.8 a	28.2 ± 12.4 a	104.0 ± 48.4 a	12.2 ± 5.7 a	2.9 ± 1.3 a
T5	86.8 ± 36.8 a	24.7 ± 9.8 a	92.6 ± 40.4 a	14.4 ± 6.9 a	2.9 ± 2.0 a
			Stage 2		
Treatments	N	P	K	Ca	Mg
T1	236.3 ± 45.0 a	68.5 ± 14.4 a	208.8 ± 83.6 a	57.0± 27.0 a	15.9 ± 9.8 a
T2	217.7 ± 66.3 a	33.1 ± 16.0 b	150.7 ± 98.8 ab	59.7 ± 41.1 a	16.7 ± 10.7 a
T3	181.0 ± 88.2 a	79.0 ± 25.0 a	240.2 ± 82.5 a	53.3 ± 16.1 a	14.5 ± 6.7 a
T4	176.5 ± 48.4 a	50.1 ± 16.6 ab	169.3 ± 57.2 ab	51.3 ± 20.3 a	11.2 ± 4.7 a
T5	210.2 ± 76.6 a	55.6 ± 11.8 ab	57.8 ± 45.2 b	87.8 ± 42.5 a	24.7 ± 12.6 a
			Stage 3		
Treatments	N	P	K	Ca	Mg
T1	214.1 ± 57.1 ab	81.7 ± 20.1 b	116.6 ± 93.4 ab	85.8 ± 29.0 a	18.7 ± 9.5 b
T2	371.7 ± 87.1 a	31.5 ± 4.0 b	65.7 ± 31.2 b	148.6 ± 58.0 a	45.5 ± 10.2 a
T3	221.3 ± 118.7 ab	154.7 ± 53.9 a	192.4 ± 20.5 a	63.6 ± 30.7 a	20.4 ± 9.7 b
T4	192.5 ± 100.4 b	80.4 ± 44.8 b	117.4 ± 75.1 ab	78.0 ± 47.2 a	17.0 ± 10.1 b
T5	166.6 ± 113.2 b	37.1 ± 20.3 b	34.4 ± 27.8 b	85.1 ± 82.8 a	15.7 ± 13.3 b

T1 = Ionic proportions in the nutrient solution: NO_3^- = 9.000, $H_2PO_4^-$ = 0.750, SO_4^{2-} = 5.250, K^+ = 5.250, Ca^{2+} = 6.750, Mg^{2+} = 3.000 $mol_c\ m^{-3}$. T2 = 11.338, 0.354, 2.479, 5.250, 6.750, 3.000. T3 = 6.371, 1.194, 8.362, 5.250, 6.750, 3.000. T4 = 9.000, 0.750, 5.250, 6.375, 5.675, 2.522. T5 = 9.000, 0.750, 5.250, 3.158, 8.743, 3.886. Stage 1 = 20 days after transplanting (rosette formation), Stage 2 = 40 days after transplanting (onset of bud formation), and Stage 3 = 60 days after transplanting (completion of bud formation). Values expressed as mean ± standard deviation. Different letters within each element and stage indicate significant differences (Tukey, $p \leq 0.05$).

Interestingly, in stage 3, Mg extraction was not higher in the treatment with reduced NO_3^- (T3), but rather in T2, which had the highest proportion of this anion. This suggests that, in this developmental stage, greater NO_3^- availability favored Mg uptake, which aligns with the interaction reported between anion and cation absorption in hydroponic systems (Kempen *et al*., 2016). Finally, the increased extraction of K under a low NO_3^- proportion agrees with Weil *et al*. (2020), who indicate that elevated concentrations of NO_3^- can reduce K uptake in roots.

Total nutrient extraction. Total macronutrient extraction showed that the largest proportion accumulated in the aerial part of the plant, particularly in the leaves, which accounted for nearly 80 % of the total extracted by the plant (Figure 1). This value is slightly lower than that reported by Sosa *et al.* (2017), who found 88.9 % foliar extraction in 'Coolguard' lettuce at 65 days after transplanting. Among the macronutrients evaluated, K exhibited the highest total extraction, followed by N, whereas Mg was the least extracted nutrient, as shown in Figure 1. This pattern agrees with Weil *et al*. (2020) and Hong *et al.* (2022), who indicate that both K and N tend to accumulate preferentially in leaves due to their high mobility.

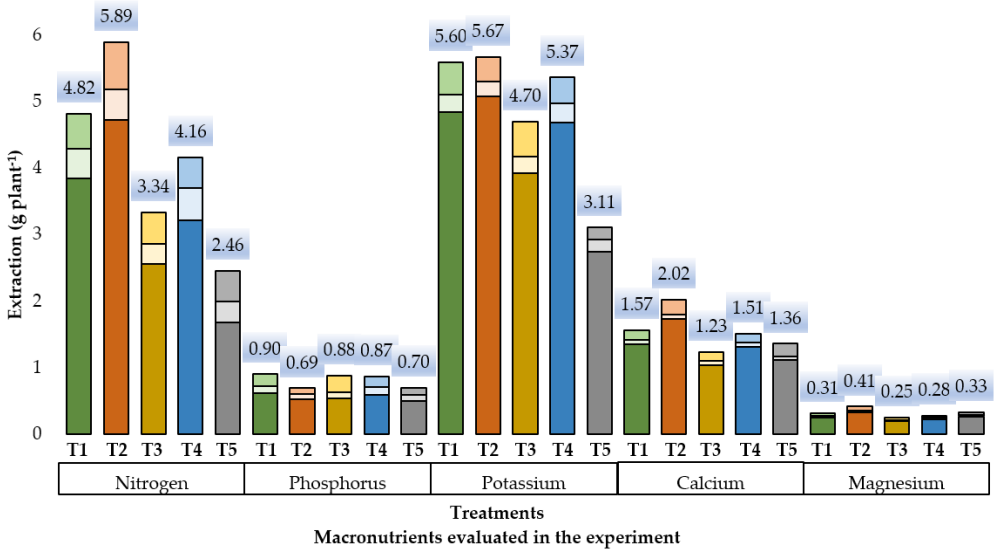

Figure 1. Total macronutrient extraction per treatment in lettuce leaves (basal section of each bar), buds (middle section of the bar), and roots (upper section of the bar) grown in a closed hydroponic system, as affected by five proportions of anions and cations in the nutrient solution. T1 = Ionic proportions in the nutrient solution: NO_3^- = 9.000, $H_2PO_4^-$ = 0.750, SO_4^{2-} = 5.250, K^+ = 5.250, Ca^{2+} = 6.750, Mg^{2+} = 3.000 $mol_c\ m^{-3}$. T2 = 11.338, 0.354, 2.479, 5.250, 6.750, 3.000. T3 = 6.371, 1.194, 8.362, 5.250, 6.750, 3.000. T4 = 9.000, 0.750, 5.250, 6.375, 5.675, 2.522. T5 = 9.000, 0.750, 5.250, 3.158, 8.743, 3.886.

In this study, P extraction was also highest in leaves, which contrasts with the findings of Hong *et al.* (2022), who reported greater P concentrations in the bud. Finally, the bud was the organ with the lowest overall extraction, contributing an average of 7 % of total nutrients, and showed significant differences only in Stage 2 for K, when its proportion in the nutrient solution was increased (Table 8).

CONCLUSIONS

The largest proportion of nutrients accumulated in the leaves, which accounted for approximately 79.5 % of the total extracted during the crop cycle; roots ranked second, with more than 13 %. The highest extractions corresponded to N and P, reaching 5.89 and 5.67 g plant^{-1}, respectively, under treatment T2 (highest proportion of NO_3^-). Treatments T2 and T4 showed the greatest extraction of N and K compared with the treatments in which the proportion of these ions was reduced. Increasing K^+ in the cationic proportion decreased the concentration of Ca^{2+} and Mg^{2+} in all three organs evaluated. Similarly, increasing NO_3^- in the anionic proportion reduced P extraction but enhanced the uptake of Ca^{2+} and Mg^{2+}.

REFERENCES

Adhikari ND, Simko I, Mou B. 2019. Phenomic and physiological analysis of salinity effects on lettuce. Sensors 19 (21): 4814. https://doi.org/10.3390/s19214814

Ahmed ZF, Alnuaimi AK, Askri A, Tzortzakis N. 2021. Evaluation of lettuce (*Lactuca sativa* L.) production under hydroponic system: Nutrient solution derived from fish waste vs. inorganic nutrient solution. Horticulturae 7 (9): 1–12. https://doi.org/10.3390/horticulturae7090292

Al-Meselmani AM. 2022. Nutrient Solution for hydroponics. In Turan M, Argin S, Yildirim E, Güneş A. (eds.), Recent research and advances in soilless culture. IntechOpen: Istambul, Türkiye, pp: 1–25. http://doi: 10.5772/intechopen.96844

Baca-Castillo GAJ, Rodríguez CE, Quevedo NA. 2016. La solución nutritiva en hidroponía. Colegio de Postgraduados. Texcoco, Estado de México, México. 208 p.

Barickman TC, Horgan TE, Wheeler JR, Sams CE. 2016. Elevated levels of potassium in greenhouse-grown red romaine lettuce impacts mineral nutrient and soluble sugar concentrations. HortScience 51 (5): 504–509. https://doi.org/10.21273/HORTSCI.51.5.504

Combrink NJJ, Kempen E. 2019. Nutrient solution management. Department of Agronomy Stellenbosch University. Stellenbosch, South Africa. 77 p.

Coskun D, Britto DT, Kronzucker HJ. 2017. The nitrogen–potassium intersection: membranes, metabolism, and mechanism. Plant, Cell & Environment 40 (10): 2029–2041. https://doi.org/10.1111/pce.12671

Djidonou D, Leskovar DI. 2019. Seasonal changes in growth, nitrogen nutrition, and yield of hydroponic lettuce. HortScience 54 (1): 76–85. https://doi.org/10.21273/HORTSCI13567-18

Engels C, Kirkby EA, White PJ, Xu G. 2023. Mineral nutrition, yield, and source–sink relationships. In Rengel Z, Cakmak I, White PJ. (eds.), Marschner's Mineral Nutrition of Plants (fourth edition). Academic Press: London, UK, pp: 85–133. http://dx.doi.org/10.1016/B978-0-12-384905-2.00005-4

Hong J, Xu F, Chen G, Huang X, Wang S, Du L, Ding G. 2022. Evaluation of the effects of nitrogen, phosphorus, and potassium applications on the growth, yield, and quality of lettuce (*Lactuca sativa* L.). Agronomy 12 (10): 2477. https://doi.org/10.3390/agronomy12102477

Kamboj N. 2019. Mineral Nutrients and Their Interaction in Plants. In Naresh RK (ed.), Research Trends in Agriculture Sciences, Chapter-8. AkiNik Publications: Uttar Pradesh, India, pp: 131–144. https://doi.org/10.22271/ed.book18

Karthika KS, Rashmi I, Parvathi MS. 2018. Biological functions, uptake and transport of essential nutrients in relation to plant growth. In Hasanuzzaman M, Fujita M, Oku H, Nahar K, Hawrylak-Nowak B. (eds.), Plant Nutrients and Abiotic Stress Tolerance. Springer: Singapore. pp: 1–49. https://doi.org/10.1007/978-981-10-9044-8_1

Kempen E, Agenbag A, Deckers S. 2016. Variations in water and macronutrient uptake of soilless tomato as affected by the nutrient solution composition. South African Journal of Plant & Soil 34 (2): 139–148. https://doi.org/10.1080/02571862.2016.1213321

Kumari S, Pradhan P, Yadav R, Kumar S. 2018. Hydroponic techniques: A soilless cultivation in agriculture. Journal of Pharmacognosy and Phytochemistry 7 (1): 1886–1891.

Lara-Herrera A, De la Rosa-Rodríguez R, Trejo-Téllez LI. 2023. Producción de lechuga (*Lactuca sativa* L.) con cinco proporciones de macronutrientes en solución nutritiva. Bioagro 35 (2): 113–122. http://www.doi.org/10.51372/bioagro352.4

Lara-Izaguirre A, Rojas-Velázquez AN, Romero-Méndez MJ, Ramírez-Tobías HM, Cruz-Crespo E, Alcalá-Jáuregui JA, Loredo-Osti C. 2019. Crecimiento y acumulación de NO_3^- en lechuga hidropónica con relaciones nitrato/amonio en dos estaciones de cultivo. Revista Fitotecnia Mexicana 42(1): 21–29.

Malvi U. 2011. Interaction of micronutrients with major nutrients with special reference to potassium. Karnataka Journal of Agricultural Sciences 24 (1): 106–109.

Mitra G. 2017. Essential plant nutrients and recent concepts about their uptake. In Naeem M, Ansari A, Gill S (eds.), Essential Plant Nutrient nutrients: Uptake, use efficiency, and management. Springer: Cham, Switzerland, pp: 3–36. https://doi.org/10.1007/978-3-319-58841-4

Njira KO, Nabwami J. 2015. A review of effects of nutrient elements on crop quality. African Journal of Food, Agriculture, Nutrition and Development 15 (1): 9777–9793. https://doi.org/10.18697/ajfand.68.13750

Oosterhuis DM, Loka D, Kawakami EM, Pettigrew WT. 2014. The physiology of potassium in crop production. Advances in Agronomy 126: 203–233. https://10.1016/B978-0-12-800132-5.00003-1.

Ouyang Z, Tian J, Yan X, Shen H. 2020. Effects of different concentrations of dissolved oxygen on the growth, photosynthesis, yield and quality of greenhouse tomatoes and changes in soil microorganisms. Agricultural Water Management 245: 106579. https://doi.org/10.1016/j.agwat.2020.106579

Ozores-Hampton M, Di Gioia F, Sato S, Simonne E, Morgan K. 2015. Effects of nitrogen rates on nitrogen, phosphorous, and potassium partitioning, accumulation, and use efficiency in seepage-irrigated fresh market tomatoes. HortScience 50 (11): 1636–1643. https://doi.org/10.21273/HORTSCI.50.11.1636

Parra-Terraza S. 2016. Relaciones NO_3^-/aniones y K^+/cationes en la solución nutritiva para el crecimiento de plántulas de tomate. Revista Mexicana de Ciencias Agrícolas 7 (7): 1527–1538. https://doi.org/10.29312/remexca.v7i7.147

Riaño-Castillo ER, Caicedo-Gegén L, Torres-Mesa A, Hurtado-Giraldo H, Gómez-Ramírez E. 2019. Cambios en los niveles de nutrientes en solución hidropónica de espinaca baby (*Spinacia oleracea* L.), para su futura aplicación en acuaponia. Orinoquia 23 (1): 73–84. https://doi.org/10.22579/20112629.544

Sambo P, Nicoletto C, Giro A, Pii Y, Valentinuzzi F, Mimmo T, Lugli P, Orzes G, Mazzetto F, Astolfi S, Terzano R, Cesco S. 2019. Hydroponic solutions for soilless production systems: issues and opportunities in a smart agriculture perspective. Frontiers in Plant Science 10: 923. https://doi.org/10.3389/fpls.2019.00923

Sánchez-Alegría A, Pérez-Patricio M, Camas-Anzueto JL, Gutiérrez-Miceli F, Aguilar-González A, Velázquez-Trujillo S. 2015. Análisis del porcentaje de crecimiento en plantaciones de lechuga hidropónica para detectar la falta de nutrimentos por medio de imágenes digitales. Aplicación del Saber: Casos y Experiencias 11 (12): 2144–2149.

Sosa A, Ruíz G, Padilla J, Etchevers J, Castellanos J, Robles R. 2017. Curvas de acumulación de nitrógeno, fósforo y potasio en lechuga (*Lactuca sativa* L.) cv. Coolward cultivada en invernadero en México. Informaciones Agronómicas de Hispanoamérica 25: 23–28.

Steiner AA. 1961. A universal method for preparing nutrient solutions of a certain desired composition. Plant and Soil 2 (15): 134–154. https://doi.org/10.1007/BF01347224

Szczerba MW, Britto DT, Kronzucker HJ. 2009. K^+ transport in plants: physiology and molecular biology. Journal of Plant Physiology 166 (5): 447–466. https://doi:10.1016/j.jplph.2008.12.009

Tsouvaltzis P, Kasampalis DS, Aktsoglou DC, Barbayiannis N, Siomos AS. 2020. Effect of reduced nitrogen and supplemented amino acids nutrient solution on the nutritional quality of baby green and red lettuce grown in a floating system. Agronomy 10 (7): 922. https://doi.org/10.3390/agronomy10070922

Trejo-Téllez LI, Gómez-Merino FC. 2012. Nutrient solutions for hydroponic systems. In Asao T (ed.), A Standard Methodology for Plant Biological Researches. IntechOpen: Rijeka, Croatia, pp: 1–17. http://dx.doi.org/10.5772/2215

Weil S, Barker AV, Zandvakili OR, Etemadi F. 2020. Plant growth and calcium and potassium accumulation in lettuce under different nitrogen regimes of ammonium and nitrate nutrition. Journal of Plant Nutrition 44 (2): 270–281. https://doi.org/10.1080/01904167.2020.1806313

Wenceslau DDSL, De Oliveira DF, De Oliveira Rabelo H, Ferbonink GF, Gomes LAA, Leonel ÉCA, Caione G. 2021. Nitrate concentration and nitrate/ammonium ratio on lettuce grown in hydroponics in Southern Amazon. African Journal of Agricultural Research 17 (6): 862–868. https://doi.org/10.5897/AJAR2020.15087

Agrociencia

SPATIAL-TEMPORAL ANALYSIS OF SCIENTIFIC PRODUCTION ON AGROBIODIVERSITY OF CROPS WITH FOOD VALUE

Victor Manuel **Toribio-Solis**[1], Mario **Rocandio-Rodríguez**[1], Alberto **Santillán-Fernández**[2*], Yolanda del Rocio **Moreno-Ramírez**[1], Julio César **Chacón-Hernández**[1], Efraín **Neri-Ramírez**[1], Rafael **Delgado-Martínez**[1]

[1]Universidad Autónoma de Tamaulipas. Facultad de Ingeniería y Ciencias. Mariano Matamoros s/n, Zona Centro, Ciudad Victoria, Tamaulipas. Mexico. C.P. 87000.
[2]Colegio de Postgraduados Campus Campeche. Investigador por Mexico SECIHTI. Carretera Haltunchén-Edzná, km 17.5, Sihochac, Champotón, Campeche, Mexico. C. P. 24450.
* Author for correspondence: santillan.alberto@colpos.mx

Citation: Toribio-Solis VM, Rocandio-Rodríguez M, Santillán-Fernández A, Moreno-Ramírez Y del R, Chacón-Hernández JC, Neri-Ramírez E, Delgado-Martínez R. 2025. Spatial-Temporal analysis of scientific production on agrobiodiversity of crops with food value. **Agrociencia** 59(8): 1134-1154. https://doi.org/ 10.47163/agrociencia.v59i8.3458

Editor in Chief:
Dr. Fernando C. Gómez Merino

Received: March 27, 2025.
Approved: December 01, 2025.
Published in Agrociencia: December 9, 2025.

ABSTRACT

The analysis of agrobiodiversity helps to understand the traditional and agroecological production systems that communities have developed to produce their food and conserve the diversity of their species. However, there are still few studies that examine research advances in the spatial-temporal scale of agrobiodiversity. The objective of this study was to conduct a bibliometric analysis of scientific production related to the agrobiodiversity of crops of food interest. Furthermore, the analysis methodologies used, the main findings reported, and areas of opportunity for generating new knowledge were identified. The literature search was conducted using the keywords "agrobiodiversidad" and "agrobiodiversity" in academic publishers (Elsevier, Scopus, Frontiers, MDPI, and Springer), open access databases (Scielo, Redalyc, Latindex, Clarivate Analytics, PeerJ, and DOAJ), and the Google Scholar web search engine. Between 2000 and 2023, 445 publications were identified, whose frequency showed a linear growth trend ($R^2 = 0.77$; $p < 0.0001$). The countries with the highest publication frequency were the United States (36 publications), Mexico (34), India (31), Brazil (29), Colombia (25), and Ecuador (25). The crops most frequently analyzed in Asian countries were rice and sugarcane; in North America, corn and beans; in South America, potatoes and coffee; and in Europe, wheat, grapes, and tomatoes. The most commonly used methodologies included diversity indices (Shannon-Wiener, Margalef, and Simpson) and statistical techniques: descriptive analysis (frequencies), inference (Pearson and Spearman correlations, analysis of variance, mean tests such as Tukey and Duncan), and multivariate analysis (clustering and principal components). Sixty-seven point eight six percent of the articles were limited to describing agrobiodiversity, leaving room for opportunity to develop research on genetic diversity aimed at productivity and conservation.

Keywords: Agroecology, content analysis, bibliometrics, family gardens, Mayan milpa.

INTRODUCTION

The genetic diversity of agricultural species and their wild relatives constitute an economic, agricultural, biological, and cultural heritage that is fundamental to food security and the well-being of local communities (Dzib-Aguilar *et al*., 2016). Agrobiodiversity is based on the variety of plants cultivated and harvested for food (Pérez-García, 2023). The concept of agrobiodiversity is not limited to cultivated species, but rather to the interaction of biological, social, and cultural components that converge in agricultural and food practices (Dyer y Taylor, 2008; Wood *et al*., 2015).

Agricultural activities are fundamental to the identity, relationships, history, and culture of many communities, especially in rural areas. Agriculture not only provides food and livelihoods, but is also deeply intertwined with people's traditions, customs, and ways of life, so that crops and agricultural practices can reflect a region's history, ancestral knowledge, and connection to the land (Poot-Pool *et al.,* 2015).

The influence of ethnic groups has been crucial for the domestication of wild species, as they have preserved the diversity of their germplasm over time (Santillán-Fernández *et al*., 2021a). Agrobiodiversity analysis helps to understand the traditional and agroecological production systems that communities have developed to produce their food and conserve the diversity of their species. (Dzib-Aguilar *et al*., 2016).

In agrobiodiversity analyses, seed selection, agronomic management, and ethnocultural factors influence crop heterogeneity, which in turn enhances their resilience and conservation in the face of external factors that are difficult to control, such as pests, diseases, and climate variations (Orozco-Ramírez *et al*., 2017). It is therefore essential to preserve ancestral agricultural systems, which integrate agroecological principles aimed at sustainable production and the responsible use of plant genetic resources (Ford-Lloyd *et al.,* 2008).

In agrobiodiversity analyses, it is essential to assess biological and cultural diversity and understand the spatial-temporal nature of agroecosystems as mechanisms for food security and ecological services (Jahrl *et al*., 2021). However, despite the importance of agrobiodiversity for food sovereignty (Ramírez-Juárez, 2022), resilience to climate change (de Sadeleer, 2024), and cultural identity (Isakson, 2009), there is little research evaluating the scope of what has been developed around the agrobiodiversity of crops with nutritional value.

Bibliometric analyses are useful tools for evaluating scientific research, as they examine published scientific articles and apply quantitative and qualitative methods to generate indicators and mathematical models that enable the development and evolution of a specific topic to be determined (Peng, 2017). They also enable areas of opportunity to be identified in order to generate new knowledge and thereby improve the quality of research (Martínez-Santiago *et al.,* 2017).

There are bibliometric analyses in the agricultural sector for specific crops such as corn (Santillán-Fernández *et al*., 2021b), wheat (Giraldo *et al*., 2019), and rice (Sun and Yuan, 2020), in sustainable agricultural systems (Rocchi *et al*., 2020), and environmental services of agroecosystems (Liu *et al*., 2019). However, few studies

analyze agrobiodiversity as a component of sustainable agricultural production that affects food security (Liu *et al.*, 2022).

In this context, the objective of this study was to conduct a bibliometric analysis of the agrobiodiversity of crops with nutritional value. Furthermore, the analysis methodologies used, and the main results obtained were identified, as well as areas of opportunity for generating new knowledge were detected. The study was based on the hypothesis that agrobiodiversity has been analyzed on a spatial-temporal scale according to the nutritional importance of crops.

MATERIALS AND METHODS

Source of information and data preparation

From January to May 2024, scientific articles were collected whose object of study were the analysis of agrobiodiversity in crops with nutritional value. Articles from January 2000 to December 2023 available from major publishers (Elsevier, Scopus, Frontiers, MDPI, and Springer), open-access journal article databases (Conricyt, Scielo, Redalyc, Latindex, Clarivate Analytics, PeerJ, and DOAJ), and the free-access web search engine Google Scholar were considered. The keywords used to search for articles were "agrobiodiversity" and "agrobiodiversidad," associated with sustainable agricultural production and food security.

Following the methodology of Santillán-Fernández *et al*. (2021b and 2023), through a content analysis of each publication, those studies whose main object of study was not the agrobiodiversity of crops with nutritional value were discarded. This analysis made it possible to identify the authors, year of publication, keywords, journal, title, bibliographic citations, language, institution of origin of the first author, country of origin of the first author, crops analyzed, data collection techniques, and analysis methodologies for each article.

To capture all variables, a spreadsheet was used, and the original language of each article was respected. To facilitate analysis, special characters such as ñ (replaced by n), accents, superscripts, subscripts, ® and ©, among others, were removed or changed. This information served as the basis for developing a spatial-temporal analysis, frequencies of research topics, impact of publications, bibliometric indicators, frequency of crops with greater relevance in the analysis of agrobiodiversity and author networks, keywords, data collection techniques, and analysis methodologies (Figure 1).

Spatial-time analysis

A graph of scientific production over time was constructed using the variables year of publication and number of citations. For the variable frequency of scientific articles per year, an ordinary least squares regression model was estimated to determine the trend in publication frequency (Fiallos, 2021). Furthermore, the countries of origin of the first author were spatially located to determine where research on the agrobiodiversity of crops with nutritional value has been conducted from 2000 to 2023. The ARGIS® geographic package was used for spatial representation (ESRI, 2015).

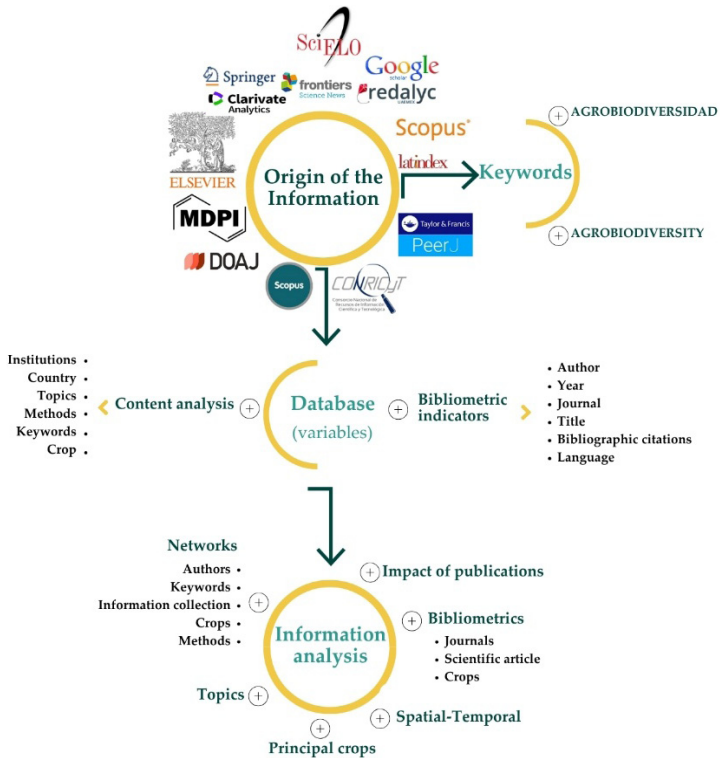

Figure 1. Flowchart of activities for the spatial-temporal analysis of scientific production on agrobiodiversity of crops with nutritional value from 2000 to 2023.

Research topics

Based on the titles of scientific articles, their abstracts, keywords, and with the help of specialists from the Autonomous University of Chapingo and the College of Postgraduates, Montecillo Campus, the subject matter addressed in each article was determined. Six categories were defined: 1) agronomy (articles related to crop productivity, backyard crops, family gardens, and crop management, including pests, diseases, nutrition, and irrigation), 2) ecology (articles associated with conservation, sustainable production, and use of plant genetic resources), 3) anthropology (works associated with cultural and social aspects of farmer-crop interaction), 4) health (articles focusing on crop production for curative purposes and/or alternative medicine for communities), 5) botany (works that described and/or identified plant species associated with crops), and 6) others (climate, genetics, geography, economics, biotechnology, rural development, and agroforestry). Once the articles were classified by topic, a graph of the topics was constructed according to the country of origin of the first author.

Impact of publications

With the help of variables such as bibliographic citations, scientific articles, and the country of origin of the first author, the number of publications and bibliographic citations per country was determined. Based on this information, a graph was constructed to associate them. Countries were grouped heuristically according to the number of publications and their impact, determined by the sum of their bibliographic citations.

Bibliometric indicators

Bibliometric indicators were generated, including: the journals with the highest publication frequency, the articles with the highest number of bibliographic citations, and the most relevant species in the analysis of agrobiodiversity for each continent.

Network analysis

Using Gephi software (Bastian *et al*., 2009), networks were constructed of co-authorship (to identify the main researchers), keywords (to identify the most recurrent concepts in the analysis of agrobiodiversity of crops with nutritional value), and networks of the crops studied, information collection methodologies, and information analysis techniques.

Prospects in Mexico

Finally, to identify new areas of research on the analysis of agrobiodiversity of crops with nutritional value in Mexico, the institutions affiliated with the first author were spatially located. Furthermore, networks of co-authorship, keywords, crops, methodologies for information gathering, and analysis techniques documented in scientific articles compiled from Mexican authors were constructed.

RESULTS AND DISCUSSION

Spatial-temporal analysis

From 2000 to 2023, 445 scientific articles were collected, which gave rise to 6,565 bibliographic citations. The annual frequency of publications showed an upward trend ($R^2 = 0.77$, $p < 0.0001$), with 83.59% of publications (372) concentrated in the period from 2010 to 2023 (Figure 2). This trend is consistent with reforms in international agricultural policies aimed at sustainable agricultural practices, conservation of genetic resources, and crop diversification, promoting the agrobiodiversity of local resources as a measure of adaptation to climate change (de Sadeleer, 2024).

Bibliographic citations showed a downward trend from 2016 to 2023. According to Santillán-Fernández *et al*. (2021b), when the highest productivity of articles is concentrated in current periods, and the highest number of citations is grouped in the oldest works, it is because the research topics analyzed are emerging, with ample room for the generation of new knowledge.

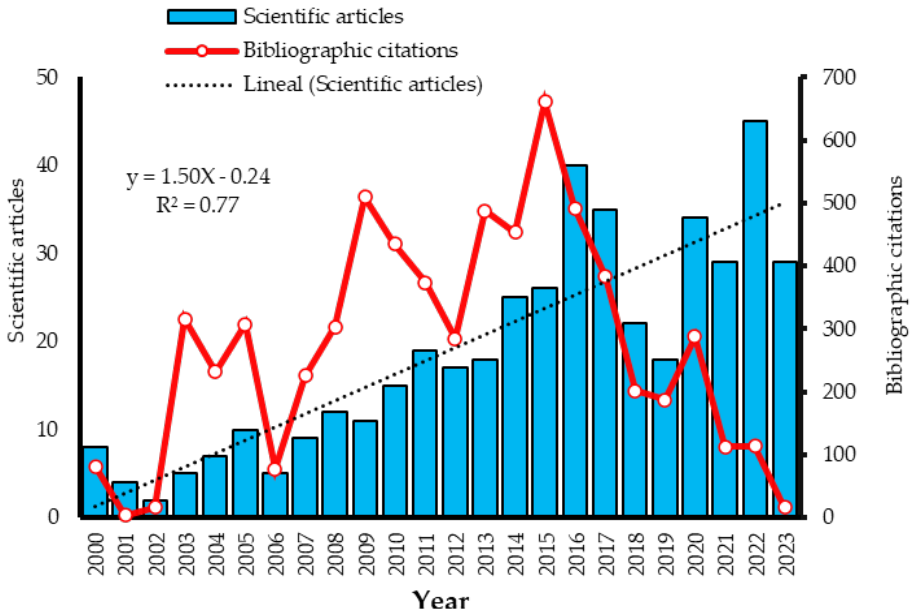

Figure 2. Temporal evolution of scientific production and bibliographic citations on agrobiodiversity issues of food crops from 2000 to 2023.

The 445 scientific articles originated in 73 countries; however, 344 articles (77.3%) of the total were concentrated in 17 of them (Figure 3). The countries with the highest frequency of publication were the United States (36), Mexico (34), India (31), Brazil

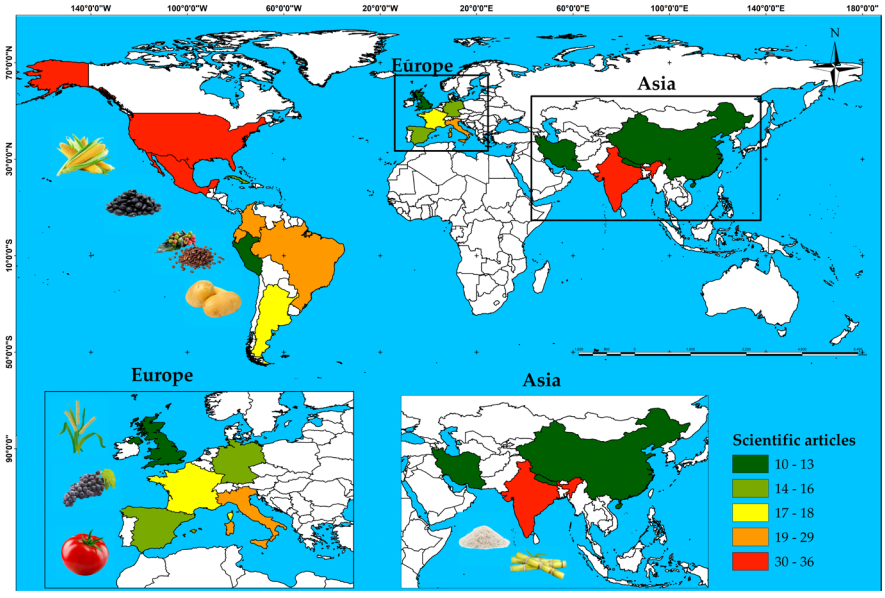

Figure 3: Spatial relationship of scientific production on agrobiodiversity topics related to crops with nutritional value from 2000 to 2023.

(29), Colombia (25), Ecuador (25), Italy (23), France (18), and Argentina (17). The most studied crops in Asian countries were rice and sugarcane; in North America, corn and beans; in South America, potatoes and coffee; and in Europe, wheat, grapes, and tomatoes. According to FAOSTAT (2025), these crops are the basis of human nutrition in each of the identified regions, which results in greater research on them, taking into account the economic context, food security, and food sovereignty (Ramírez-Juárez, 2022).

Research topics

In the main countries that recorded scientific production on agrobiodiversity of crops with nutritional value from 2000 to 2023, the most recurrent research topics were those associated with the analysis of agronomic factors that influence production systems (266 articles, 59.78%), ecology (62, 13.93%), anthropology (51, 11.46%), health (30, 6.74%), and botany (23, 5.17%) (Figure 4). In Latin American countries such as Mexico, Brazil, Colombia, and Ecuador, research was documented on the influence of agrobiodiversity on the lifestyle of indigenous peoples (anthropology).

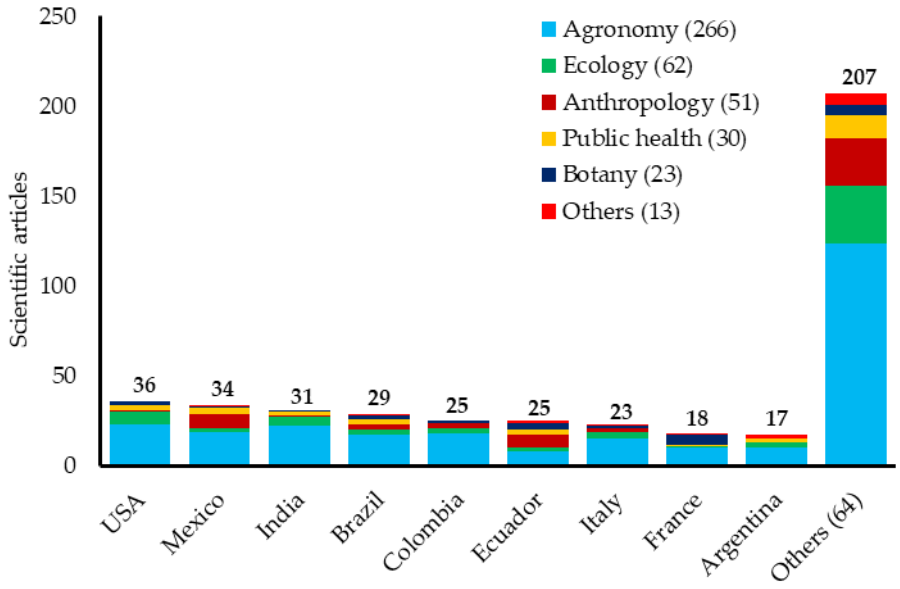

Figure 4. Main nations and research topics, according to the country of origin of the first author of scientific articles on the agrobiodiversity of crops with nutritional value from 2000 to 2023.

Isakson (2009) documented a strong influence of the milpa agricultural production system (combining corn with beans and squash) on the geopolitical customs of the indigenous peoples of Guatemala and Mexico, in their quest to guarantee food sovereignty and conserve their plant genetic resources. This is common in Latin

American countries where there is a wide variety of ethnic groups (Ortega-Ortega *et al*., 2017). Similarly, Narloch *et al*. (2013) found that issues related to ecology are increasingly frequent in the analysis of crop agrobiodiversity because agrobiodiversity allows for the conservation of genetic resources and promotes more sustainable production systems.

Impact of publications

The analysis of the impact of publications (measured by the number of citations) differentiated four groups (Figure 5). The first group consisted of countries that conducted research sporadically. In group two, publications were more consistent, but without high impact. In group three, publications were consistent and had medium impact, and this was the group where Latin American countries with a long agricultural tradition were concentrated (FAOSTAT, 2025). Group four (made up of the United States) had the highest number of research projects and bibliographic citations. According to Santillán-Fernández *et al*. (2021b), the agricultural policy adopted by the US, which promotes technological innovations to improve productivity in conjunction with research and development, has enabled it to become a global benchmark in the analysis of the agrobiodiversity of crops with nutritional value. However, much of this research has focused on demonstrating the competitiveness of monoculture versus polyculture systems (agrobiodiversity). Conversely, studies conducted in Latin American countries have prioritized agrobiodiversity as a mechanism for food sovereignty and resilience to climate change.

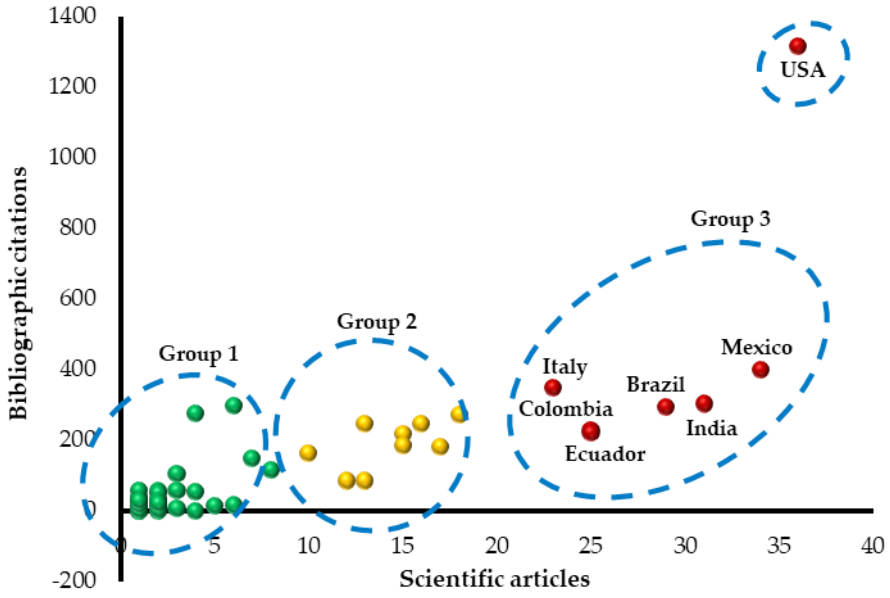

Figure 5. Impact of publications by country of origin of the first author on agrobiodiversity of crops with nutritional value from 2000 to 2023.

Another factor that helps explain the impact of US publications is the fact that they are published in English, which increases their likelihood of dissemination among the scientific community, as it is the most popular language in this community (Santillán-Fernández *et al*., 2023). Research carried out in Latin American countries is usually published in Spanish and in institutional journals, which limits constructive criticism and the impact of publications (Santillán-Fernández *et al*., 2021b). Publishing in English presents an opportunity for Spanish-speaking countries, where agrobiodiversity is often an ethnocultural issue (Oyarzun *et al*., 2013).

Bibliometric indicators

The 445 scientific articles analyzed were published in 296 journals, with an average of 1.5 articles, which implies that, apparently, there is no specialized journal for the topic analyzed. Ten journals accounted for 13.93% of the publications (62 articles) (Table 1), specializing in agriculture, agroecology, and genetic resources. The journals with the

Table 1. Bibliometric indicators of the main journals that published scientific articles on agrobiodiversity of crops with nutritional value from 2000 to 2023.

Journal	Country	Publisher	Impact factor¶	Subject	Articles	Citations
Indian Journal of Plant Genetic Resources	India	Indian Society of Plant Genetic Resources	--	Genetic resources	10	23
Agriculture and Human Values	.	Springer	4.2	Agriculture	7	162
Cultivos Tropicales	Cuba†	Instituto Nacional de Ciencias Agrícolas	--	Agriculture	7	105
Genetic Resources and Crop Evolution	Netherlands	Springer	1.7	Genetic resources	6	138
Journal of Agroecology	Iran	Universidad Ferdowsi de Mashhad	--	Agroecology	6	22
LEISA Revista de Agroecología	Peru †	Asociación Ecología, Tecnología y Cultura en los Andes	--	Agroecology	6	72
Agroecology and Sustainable Food Systems	United Kingdom	Taylor and Francis	3.3	Agroecology	5	47
Agroforestry Systems	Netherlands	Springer	2.5	Agroforestry	5	122
Sustainability	Switzerland	MDPI	3.3	Natural Sciences	5	39
Tropical and Subtropical Agroecosystems	Mexico†	Universidad Autónoma de Yucatán	--	Agroecosystems	5	27
Otras (286)					383	5808
Total					445	6565

†Journals published in Spanish.

¶According to the journals indexed in the Journal Citation Reports (WoS, 2022).

highest number of bibliographic citations were those published in English and with impact factors, indexed in the Journal Citation Reports (WoS, 2022). The impact factor plays a crucial role in deciding where to publish, as journals with a high impact factor increase the chances of reaching a wider audience (Santillán-Fernández *et al.*, 2021b). Of the 10 most cited articles on agrobiodiversity of crops with nutritional value, five belong to a first author whose affiliated institution is located in the US, and only one paper corresponds to a researcher in Latin America (Ecuador). All have been published in English and in Anglo-Saxon journals (Table 2). Gersbach and Schneider (2015) documented that consolidated economies such as those of the US, Canada, Australia, Spain, and the United Kingdom invest more in their research centers, which allows them greater technological and economic development, unlike Latin American economies.

Table 2. Bibliometric indicators of the main scientific articles on agrobiodiversity of crops with nutritional value from 2000 to 2023, ranked according to the number of bibliographic citations.

Author		Journal		Scientific article				
Name	Country	Name	Citations	Subject	Crop	Region	Methods	Results
Isakson (2009)	Canada	The Journal of Peasant Studies	255	Economy	Milpa	Guatemala	Surveys	Conservation, genetic resources
Kerr (2014)	USA	Annals of the Association of American Geographers	151	Productivity	African Millet Sorghum	Malawi	Surveys *in situ* assesment	Margalef index, Shannon index
Zimmerer (2003)	USA	Society and Natural Resources	148	Rural development	Ulluco potato	Peru	Surveys	Seed flow, production, conservation
Perreault (2005)	USA	Human Organization	131	Productivity	Family garden	Ecuador	Surveys Ethnographic	Food safety
Oyarzun *et al.* (2013)	Ecuador	Ecology of Food and Nutrition	129	Anthropology	Local resources	Ecuador	Ethnographic	Margalef index, Shannon index
Zimmerer (2004)	USA	Progress in Human Geography	124	Agroforestry	Local resources	USA	Surveys Snowball	Geographic information system, remote sensing
Calvet *et al.* (2012)	Spain	Ecology and Society	116	Rural development	Family garden	Spain	Surveys *in situ* assessment	Producer network, *in situ* conservation
Gunn *et al.* (2010)	Australia	American Journal of Botany	108	Genetics	Walnut tree	China	Markers Molecular	Morphometry, genotypic variation
Zimmerer *et al.* (2015)	USA	Current Opinion in Environmental Sustainability	107	Rural development	Local resources	USA	Surveys *in situ* assessment	Producer network, *in situ* conservation
Narloch *et al.* (2013)	United Kingdom	Land Use Policy	94	Economy	Local resources	Bolivia Peru	Surveys	Payment for ecosystem services

Among countries with established economies that invest in research, it is common for them to conduct research outside their borders in order to generate new knowledge that will help improve their quality of life (Gersbach and Schneider, 2015). This explains why researchers from Canada, the US, and the UK focused their studies on Latin American countries such as Ecuador, Peru, Bolivia, and Guatemala. Among the 10 most cited articles, interviews, surveys, and *in situ* assessments were the most frequently used data collection techniques, which enabled them to generate diversity indices to promote the conservation of agrobiodiversity. This trend was no different in the total number of articles analyzed, as surveys, interviews, and *in situ* assessments were recurrent in 61.57% of the articles (274). Diversity indices such as Shannon-Wiener, Margalef, and Simpson were common in 119 publications (26.74%).

Other common analysis methodologies were frequency counting (14.15%, 63 articles), Pearson and Spearman correlation (11.46%, 51), analysis of variance and Tukey and Duncan mean tests (9.67%, 43), and multivariate cluster and principal component methods (4.27%, 19). Sixty-seven point eight six percent of the articles (302) limited themselves to describing agrobiodiversity as a mechanism for food production and resilience to climate change, leaving room for opportunity to develop research on crop genetic diversity aimed at productivity and conservation.

Species of greatest relevance in the analysis of agrobiodiversity

In Europe, studies focused on wheat, grapes, and tomatoes; in America, corn and potatoes; in Asia, rice; in Africa, sugarcane; and in Oceania, wheat (Table 3). In most cases, the areas of study were the regions described by Vavilov as centers of origin (Boege, 2009). America, Asia, and Europe accounted for 94.61% of publications (421 articles). Hummer and Hancock (2015) explain that these continents are home to a large number of research centers, as they are the geographical regions with the highest concentration of the world's population.

Backyard production (family gardens) was the most analyzed system (23.37%, 104 articles). The sustainable food production systems promoted by governments have increased the establishment of family farming, as they contribute to food sovereignty (Saediman *et al*., 2021), allow families to save on expenses, and guarantee access to quality and safe products (Jahrl *et al*., 2021). Backyard farming favors the cultivation of seeds, vegetables, and fruits in small outdoor spaces, usually for self-consumption and continuously throughout the year, by combining two or more crops in the same space and time. In this way, it rewards agrobiodiversity and contributes to adaptation to climate change (Tomatis *et al.*, 2023).

Table 3. Main crops with nutritional value by continent, documented in scientific articles compiled from 2000 to 2023.

Continent	Crop		Frequency		Authors
	General	Scientific	Number	%	
Africa (15, 3.37 %)	Family garden		4	0.90	Semu (2018)
	Sugarcane	*Saccharum officinarum* L.	2	0.45	Netondo *et al.* (2010)
	Rice	*Oryza sativa* L.	2	0.45	Bathe *et al.* (2019)
	Others		7	1.57	
America (214, 48.09 %)	Family garden		40	8.99	Poot-Pool *et al.* (2015)
	Corn	*Zea mays* L.	31	6.97	Ortega-Ortega *et al.* (2017)
	Potato	*Solanum tuberosum* L.	25	5.62	de Haan *et al.* (2010)
	Coffee	*Coffea arabica* L.	9	2.02	Méndez *et al.* (2013)
	Bean	*Phaseolus vulgaris* L.	8	1.80	Abbott (2005)
	Squash	*Cucurbita* spp.	8	1.80	dos Santos *et al.* (2012)
	Rice	*Oryza sativa* L.	6	1.35	Schoenly *et al.* (2003)
	Chili	*Capsicum annuum* L.	6	1.35	Castillo-Aguilar *et al.* (2021)
	Sorghum	*Sorghum* spp.	5	1.12	Kerr (2014)
	Tomato	*Solanum lycopersicon* L.	5	1.12	Moya-López *et al.* (2016)
	Prickly pear cactus	*Opuntia* spp.	4	0.90	Reyes-Agüero y Aguirre-Rivera (2011)
	Otros		67	15.05	
Asia (93, 20.90 %)	Family garden		26	5.84	Gopi *et al.* (2016)
	Rice	*Oryza sativa* L.	17	3.82	Na *et al.* (2014)
	Sugarcane	*Saccharum officinarum* L.	10	2.24	Trinh *et al.* (2003)
	Squash	*Cucurbita* spp.	5	1.12	Nassiri *et al.* (2017)
	Potato	*Solanum tuberosum* L.	4	0.90	Singha y Ullah (2020)
	Others		31	6.98	
Europe (114, 25.62 %)	Family garden		34	7.64	Signore *et al.* (2019)
	Wheat	*Triticum* spp.	16	3.60	Costanzo y Bàrberi (2016)
	Grapevine	*Vitis vinifera* L.	14	3.15	Bonhomme *et al.* (2021)
	Tomatos	*Solanum lycopersicum* L.	11	2.47	Socies-Fiol y Cuéllar-Padilla (2017)
	Apple	*Malus domestica* Borkh	7	1.57	Pfiffner *et al.* (2019)
	Chestnuts	*Castanea* spp.	7	1.57	Beccaro *et al.* (2020)
	Rice	*Oryza sativa* L.	4	0.90	Ford-Lloyd *et al.* (2008)
	Corn	*Zea mays* L.	4	0.90	Stagnati *et al.* (2022)
	Others		17	3.82	
Oceania (9, 2.02 %)	Wheat	*Triticum* spp.	4	0.90	Bardsley y Thomas (2005)
	Walnut tree	*Juglans regia* L.	2	0.45	Gunn *et al.* (2010)
	Others		3	0.67	
Total			445	100.00	

Author network

The 445 scientific articles were written by 393 lead authors and 841 co-authors, with a total of 1,234 different authors (Figure 6). The main authors were: Gauchan_D (seven articles) from the Bioversity International Research Center in Kathmandu, Nepal, who developed topics on the conservation of grains and seeds from local breeds through agrobiodiversity; Zimmerer_KS (six) from Pennsylvania State University (USA), a specialist in environmental geography, whose studies have focused on sustainable food

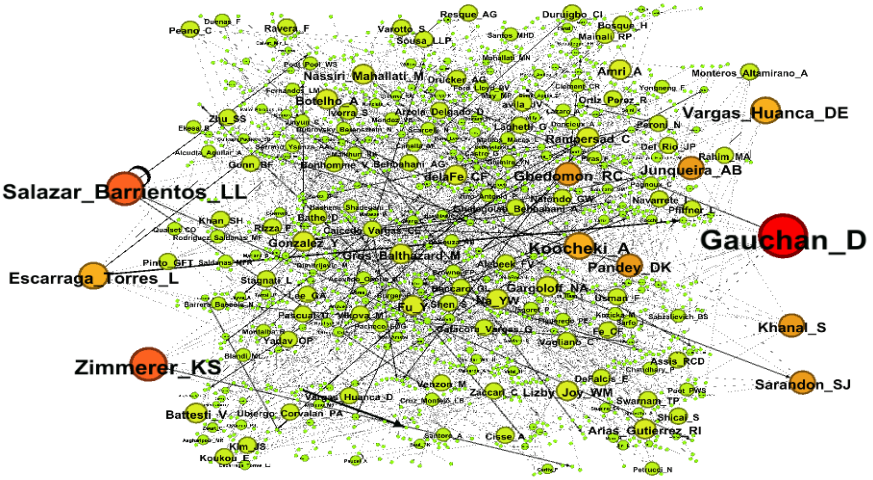

Figure 6. International network of authors who published scientific articles on agrobiodiversity of crops with nutritional value from 2000 to 2023.

production as a mechanism for resilience to climate change through agrobiodiversity; and Salazar-Barrientos_LL (four) from the Conkal Institute of Technology (Mexico), who has conducted research on agrobiodiversity in backyard production systems (family gardens) and Mayan milpa.

In bibliometric analyses, author networks provide information about leading researchers in the topic in question, enabling the planning of research synergies (Santillán-Fernández *et al*., 2021b). However, author network analysis does not usually analyze the number of links between authors or the density of the network (Santillán-Fernández *et al*., 2023). Links are important for authors because they provide ideas, knowledge, and information from geographically distant locations, while density is an indicator of how much the nodes interact with each other. Mathematically, it is a value within the range [0 to 1]; the closer to one, the greater the interaction in the network (Aguilar-Gallegos *et al*., 2016). In the case of this study, the network was composed of 1,234 nodes (authors) with 1,108 links and a density of 0.0001, which opens up an area of opportunity to develop synergies with other national and international researchers, which tends to improve the quality of research by rewarding constructive criticism (Santillán-Fernández *et al*., 2021b).

Prospects in Mexico

Thirty-four scientific articles on the subject were published in Mexico. The spatial distribution of institutions (Figure 7) showed that agrobiodiversity studies are concentrated in the center and south of the country. According to Santillán-Fernández *et al*. (2021a), this trend coincides with the greater wealth of ethnic groups in the region, which have influenced the domestication of species and maintain agrobiodiversity as the basis of their subsistence systems, mainly with crops such as corn, beans, chili

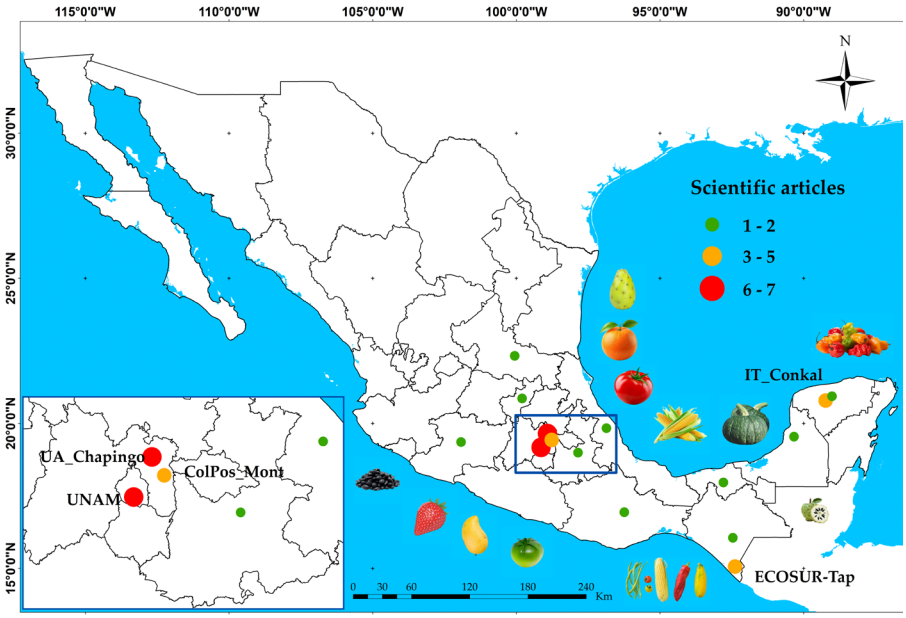

Figure 7. Spatial location of institutions in Mexico with productivity of scientific articles on agrobiodiversity of crops with food value from 2000 to 2023.

peppers, tomatoes, squash, and fruit trees (mango and citrus). In contrast, the highest agricultural productivity is located in central and northern Mexico, in intensive systems geared toward the competitiveness of monocultures (SIAP, 2025).

The highest number of publications was concentrated in institutions in the center of the country: Chapingo Autonomous University (UA_Chapingo), National Autonomous University of Mexico (UNAM), and Montecillo Campus Graduate School (ColPos_Mont). The centralization of research in Mexico has been described by Santillán-Fernández *et al*. (2021b, 2023), who found that the territorial gap between production areas and research centers limits technology transfer, which in turn affects national agricultural productivity. However, researchers were registered in the south of the country, where the greatest diversity of population and cultivated species is concentrated, such as Salazar-Barrientos_LL from the Conkal Institute of Technology, Ubiergo-Corvalan_PA and Cruz-Montejo_LB from the Autonomous University of Chiapas, and Alcudia-Aguilar_A, Poot-Pool_WS, and Serrano-Ysunza_AA from the Tabasco campus of the Colegio de la Frontera Sur (Figure 8).

Authors tend to form research synergies among researchers from the same institution (77 nodes, 77 links, density of 0.1) (Figure 8), which limits constructive criticism of research and affects its quality. Furthermore, no researcher with consistent output was found during the period analyzed. According to Santillán-Fernández *et al*. (2021b), agricultural research in Mexico responds to scientific trends based on national agricultural policy. In the context of food sovereignty and climate change, the

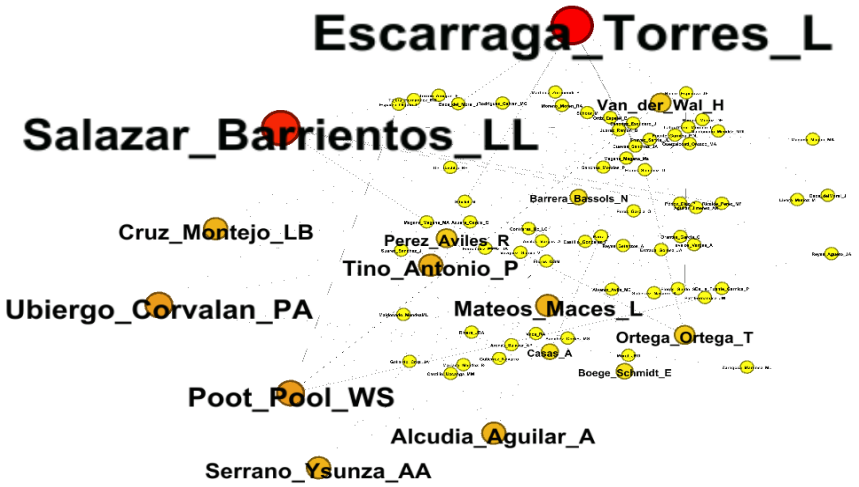

Figure 8. Network of authors in Mexico who published scientific articles on agrobiodiversity of crops with nutritional value from 2000 to 2023.

analysis of agrobiodiversity of crops with nutritional value presents itself as an area of opportunity to develop research and synergies with researchers from other national and international institutions.

Finally, in the analysis of keyword networks, main crops, information collection methodologies, and information analysis techniques (Figure 9), it was found that the

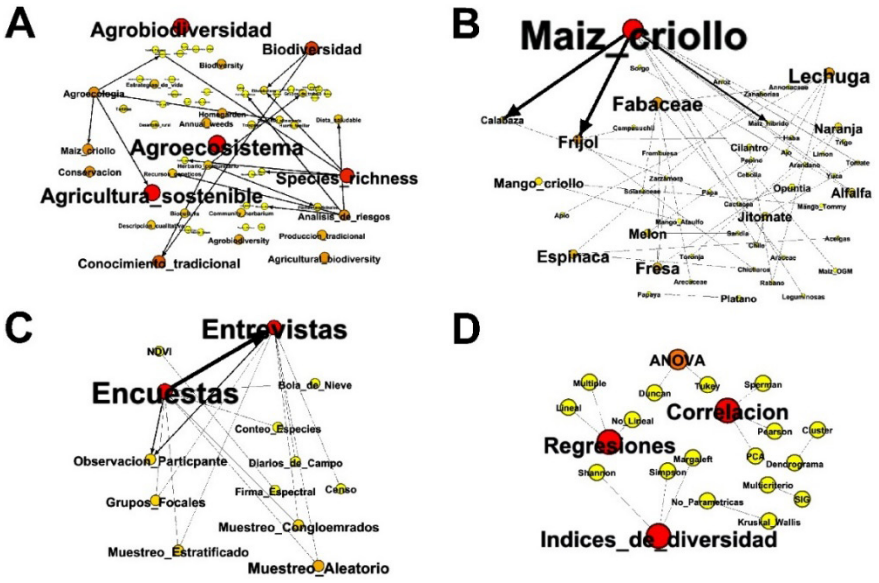

Figure 9. Keyword networks (A), main crops (B), information collection methodologies (C), and information analysis techniques (D) documented in scientific articles compiled from 2000 to 2023.

most used concepts to describe the agrobiodiversity of crops with nutritional value were agroecosystem, sustainable agriculture, agrobiodiversity, and species richness (Figure 9A). Leyva-Galán and Lores-Pérez (2012) found that agrobiodiversity analysis is based on the principles of agroecology and is often understood as a mechanism for resilience in the face of environmental crisis.

The crops most frequently analyzed were corn in association with squash, beans, and some species of domestic chili peppers (Figure 9B). This association is traditionally known in south-central Mexico as milpa Maya (Isakson, 2009), and it constitutes the food base for the indigenous peoples in these regions of the country (Santillán-Fernández *et al*., 2021a). Some vegetable species (lettuce, spinach, cilantro, and tomato), cyclical fruit trees (melon and strawberry), and perennial fruit trees (mango and orange) are beginning to be the subject of study in agrobiodiversity analyses, which is why agroforestry systems are presented as an opportunity for research (Corella-Saborío, 2016).

In terms of data collection methodologies, the most commonly used were surveys and interviews with producers (Figure 9C). Qualitative techniques that integrate social perceptions were also applied, such as participant observation, focus groups, and field diaries, as well as quantitative methods, including sampling (random, stratified, and cluster), species counting, and morphometric analysis of germplasm in situ. Together, these tools made it possible to calculate diversity indices (Simpson, Margalef, and Shannon), apply regression models (linear and nonlinear), perform correlations (Pearson and Spearman), and carry out variance analyses with mean tests such as Tukey and Duncan (Figure 9D).

The use of new technologies such as remote sensing, geographic information systems, and satellite imagery in the analysis of agrobiodiversity in Mexico was not documented, nor were multivariate techniques such as principal component and cluster analysis, even though they allow for a reduction in the number of variables analyzed, which is usually large in agrobiodiversity studies. According to Santillán-Fernández *et al*. (2023), new technologies improve the quality of research, so the use of geostatistical models to assess agrobiodiversity would allow the addition of territorial and social components that have been little explored until now.

Bibliometric techniques proved to be an effective tool for identifying areas of opportunity in the development of knowledge about the agrobiodiversity of crops with nutritional value. However, the theoretical nature of the findings should be considered as a way of expanding the state of the art. Therefore, it is recommended that future research delve deeper into the practical application of scientific results, incorporating a greater diversity of crops and considering their interaction with ethnic groups in relation to the territory. It is also pertinent to explore the use of new technologies, such as remote sensing, to determine agrobiodiversity parameters aimed at both productivity and conservation.

CONCLUSIONS

Agrobiodiversity has been studied on a spatial-temporal scale, considering the nutritional relevance of crops. However, much of the research has been limited to its description, which opens up an area of opportunity to delve deeper into genetic diversity for productivity and conservation purposes. The southeast of Mexico is identified as a strategic region for this type of study, since it concentrates the greatest diversity of crops and ethnic groups. Although corn and beans have been the most analyzed crops, it is possible to expand the knowledge frontier to species such as chili peppers, squash, fruit trees, and vegetables.

REFERENCES

Abbott JA. 2005. Counting beans: Agrobiodiversity, indigeneity, and agrarian reform. The Professional Geographer 57 (2): 198–212. https://doi.org/10.1111/j.0033-0124.2005.00472.x

Aguilar-Gallegos N, Martínez-González EG, Aguilar-Ávila J, Santoyo-Cortés H, Muñoz-Rodríguez M, García-Sánchez EI. 2016. Análisis de redes sociales para catalizar la innovación agrícola: de los vínculos directos a la integración y radialidad. Estudios Gerenciales 32: 197–207. https://doi.org/10.1016/j.estger.2016.06.006

Bardsley D, Thomas I. 2005. Valuing local wheat landraces for agrobiodiversity conservation in Northeast Turkey. Agriculture, Ecosystems and Environment 106 (4): 407–412. https://doi.org/10.1016/j.agee.2004.08.011

Bastian M, Heymann S, Jacomy M. 2009. Gephi: An open source software for exploring and manipulating networks. Proceedings of the International AAAI Conference on Web and Social Media 3 (1): 361–362. https://doi.org/10.1609/icwsm.v3i1.13937

Bathe D, Manzelli M, Bamba B, Tendeng E, Djiba S, Fofana A, Drame KN. 2019. Agrobiodiversity in Middle Casamance (South Senegal): Collection and agro-morphological assessment of traditional rice landraces. Journal of Agriculture and Environment for International Development 113 (2): 229–251. https://doi.org/10.12895/jaeid.20192.1144

Beccaro GL, Donno D, Lione GG, de Biaggi M, Gamba G, Rapalino S, Riondato I, Gonthier P, Mellano MG. 2020. *Castanea* spp. agrobiodiversity conservation: Genotype influence on chemical and sensorial traits of cultivars grown on the same clonal rootstock. Foods 9 (8): 1062. https://doi.org/10.3390/foods9081062

Boege E. 2009. Centros de origen, pueblos indígenas y diversificación del maíz. Ciencias 92: 18–28.

Bonhomme V, Terral JF, Zech-Matterne V, Ivorra S, Lacombe T, Deborde G, Kuchler P, Limier B, Pastor T, Rollet P, Bouby L. 2021. Seed morphology uncovers 1500 years of vine agrobiodiversity before the advent of the Champagne wine. Scientific Reports 11 (1): 2305. https://doi.org/10.1038/s41598-021-81787-3

Calvet L, Calvet-Mir M, Molina JL, Reyes-García V. 2012. Seed exchange as an agrobiodiversity conservation mechanism. A case study in Vall Fosca, Catalan Pyrenees, Iberian Peninsula. Ecology and Society 17 (1): 29. https://doi.org/10.5751/es-04682-170129

Castillo-Aguilar CC, López-Castilla LC, Pacheco N, Cuevas-Bernardino JC, Garruña R, Andueza-Noh RH. 2021. Phenotypic diversity and capsaicinoid content of chilli pepper landraces (*Capsicum* spp.) from the Yucatan Peninsula. Plant Genetic Resources 19 (2): 159–166. https://doi.org/10.1017/S1479262121000204

Corella-Saborío MF. 2016. Agroforestería y biodiversidad: La importancia de los sistemas agroforestales en la conservación de especies. Biocenosis 30 (1–2).

Costanzo A, Bàrberi P. 2016. Field scale functional agrobiodiversity in organic wheat: Effects on weed reduction, disease susceptibility and yield. European Journal of Agronomy 76: 1–16. https://doi.org/10.1016/j.eja.2016.01.012

de Haan S, Núñez J, Bonierbale M, Ghislain M. 2010. Multilevel agrobiodiversity and conservation of Andean potatoes in central Peru. Mountain Research and Development 30 (3): 222–231. https://doi.org/10.1659/mrd-journal-d-10-00020.1

de Sadeleer N. 2024. La nueva Política Agrícola Común al rescate del medio ambiente ¿está justificada la revuelta agraria? Unión Europea Aranzadi 4 (6): 89–128.

dos Santos MH, Rodríguez R, Gonçalves LSA, Sudré CP, Pereira MG. 2012. Agrobiodiversity in *Cucurbita* spp. landraces collected in Rio de Janeiro assessed by molecular markers. Crop Breeding and Applied Biotechnology 12 (2): 96–103. https://doi.org/10.1590/S1984-70332012000200001

Dyer GA, Taylor JE. 2008. A crop population perspective on maize seed systems in Mexico. Proceedings of the National Academy of Sciences 105 (2): 470–475. https://doi.org/10.1073/pnas.0706321105

Dzib-Aguilar LA, Ortega-Paczka R, Segura-Correa JC. 2016. Conservación *in situ* y mejoramiento participativo de maíces criollos en la Península de Yucatán. Tropical and Subtropical Agroecosystems 19 (1): 51–59.

ESRI (Environmental Systems Research Institute. ArcGIS Versión 10.3). 2015. Software de procesamiento digital de imágenes satelitales. California, USA. http://www.esri.com/software/arcgis/arcgis-for-desktop (Recuperado: agosto 2024).

FAO (Organización de las Naciones Unidas para la Alimentación y la Agricultura). 2025. FAOSTAT. Cultivos y productos de ganadería. Roma, Italia. https://www.fao.org/faostat/es/#data (Recuperado: febrero 2025)

Fiallos G. 2021. La correlación de Pearson y el proceso de regresión por el método de mínimos cuadrados. Ciencia Latina Revista Científica Multidisciplinar 5 (3): 2491–2509. https://doi.org/10.37811/cl_rcm.v5i3.466

Ford-Lloyd BV, Brar D, Khush GS, Jackson MT, Virk PS. 2008. Genetic erosion over time of rice landrace agrobiodiversity. Plant Genetic Resources 7 (2): 163–168. https://doi.org/10.1017/S1479262108137935

Gersbach H, Schneider MT. 2015. On the global supply of basic research. Journal of Monetary Economics 75: 123–137. https://doi.org/10.1016/j.jmoneco.2015.02.004

Giraldo P, Benavente E, Manzano-Agugliaro F, Gimenez E. 2019. Worldwide research trends on wheat and barley: A bibliometric comparative analysis. Agronomy 9 (7): 352. https://doi.org/10.3390/agronomy9070352

Gopi G, Arunraj R, Rajees PC. 2016. Impacts of home gardening in agrobiodiversity hotspots among small and marginal farm households. Madras Agricultural Journal 103: 187–191. https://doi.org/10.29321/MAJ.10.001017

Gunn BF, Aradhya M, Salick JM, Miller A, Yongping Y, Lin L, Xian H. 2010. Genetic variation in walnuts *(Juglans regia* and J. *sigillata*; Juglandaceae): Species distinctions, human impacts, and the conservation of agrobiodiversity in Yunnan, China. American Journal of Botany 97 (4): 660–671. https://doi.org/10.3732/ajb.0900114

Hummer KE, Hancock JF. 2015. Vavilovian centers of plant diversity: Implications and impacts. HortScience 50 (6): 780–783. https://doi.org/10.21273/hortsci.50.6.780

Isakson SR. 2009. No hay ganancia en la milpa: The agrarian question, food sovereignty, and the on-farm conservation of agrobiodiversity in the Guatemalan highlands. The Journal of Peasant Studies 36 (4): 725–759. https://doi.org/10.1080/03066150903353876

Jahrl I, Moschitz H, Cavin JS. 2021. The role of food gardening in addressing urban sustainability – A new framework for analysing policy approaches. Land Use Policy 108: 105564. https://doi.org/10.1016/j.landusepol.2021.105564

Kerr RB. 2014. Lost and found crops: Agrobiodiversity, indigenous knowledge, and a feminist political ecology of sorghum and finger millet in northern Malawi. Annals of the Association of American Geographers 104 (3): 577–593. https://doi.org/10.1080/00045608.2014.892346

Leyva-Galán Á, Lores-Pérez A. 2012. Nuevos índices para evaluar la agrobiodiversidad. Agroecología 7 (1): 109–115.

Liu W, Wang J, Li C, Chen B, Sun Y. 2019. Using bibliometric analysis to understand the recent progress in agroecosystem services research. Ecological Economics 156: 293–305. https://doi.org/10.1016/j.ecolecon.2018.09.001

Liu Y, Ren X, Lu F. 2022. Research status and trends of agrobiodiversity and traditional knowledge based on bibliometric analysis (1992–Mid-2022). Diversity 14 (11): 950. https://doi.org/10.3390/d14110950

Martínez-Santiago SY, Alvarado-Segura AA, Zamudio-Sánchez FJ, Cristóbal-Acevedo D. 2017. Análisis espacio-temporal de la modelación forestal en México. Revista Chapingo Serie Ciencias Forestales y del Ambiente 23 (1): 5–22. https://doi.org/10.5154/r.rchscfa.2016.01.003

Méndez VE, Bacon CM, Olson MB, Morris KS, Shattuck A. 2013. Conservación de agrobiodiversidad y medios de vida en cooperativas de café bajo sombra en Centroamérica: Ecosistemas 22 (1): 16–24.

Moya-López CC, Orozco-Crespo E, Mesa-Fleitas ME. 2016. Ferias de agro-biodiversidad cubanas: vía para la selección de variedades de tomate. Agronomía Mesoamericana 27 (2): 301–310. https://doi.org/10.15517/am.v27i2.24362

Na YW, Choi YM, Baek HJ, Lee SY, Kang JH, Kim SH. 2014. Seed longevity of rice germplasm in the national agrobiodiversity center. Korean Journal of Crop Science 59 (3): 216–222. https://doi.org/10.7740/kjcs.2014.59.3.216

Narloch U, Pascual U, Drucker AG. 2013. How to achieve fairness in payments for ecosystem services? Insights from agrobiodiversity conservation auctions. Land Use Policy 35: 107–118. https://doi.org/10.1016/j.landusepol.2013.05.002

Nassiri MM, Koocheki A, Tavakoli-Kakhki HR, Soltani M. 2017. Agrobiodiversity indices for three cucurbit species in Khorasan-Razavi Province. Journal of Agroecology 9 (1): 1–14. https://doi.org/10.22067/jag.v9i1.22431

Netondo GW, Waswa F, Maina L, Naisiko T, Masayi N, Ngaira JK. 2010. Agrobiodiversity endangered by sugarcane farming in Mumias and Nzoia Sugarbelts of Western Kenya. African Journal of Environmental Science and Technology 4 (7): 437–445.

Orozco-Ramírez Q, Odenthal J, Astier M. 2017. Diversidad de maíces en Pátzcuaro, Michoacán, México, y su relación con factores ambientales y sociales. Agrociencia 51 (8): 867–884.

Ortega-Ortega T, Vázquez-García V, Flores-Sánchez D, Núñez-Espinoza JF. 2017. Agrobiodiversidad, género y soberanía alimentaria en Tlaxiaco. Revista Mexicana de Ciencias Agrícolas 8 (18): 3673–3682. https://doi.org/10.29312/remexca.v8i18.213

Oyarzun PJ, Borja RM, Sherwood S, Parra V. 2013. Making sense of agrobiodiversity, diet, and intensification of smallholder family farming in the highland Andes of Ecuador. Ecology of food and nutrition 52 (6): 515–541. https://doi.org/10.1080/03670244.2013.769099

Peng SB. 2017. Booming research on rice physiology and management in China: A bibliometric analysis based on three major agronomic journals. Journal of Integrative Agriculture 16 (12): 2726–2735. https://doi.org/10.1016/S2095-3119(17)61804-5

Pérez-García O. 2023. Diversidad biocultural ligada a maíces nativos del estado de Puebla, México. Ecosistemas y Recursos Agropecuarios 10 (2): e3430. https://doi.org/10.19136/era.a10n2.3430

Perreault T. 2005. Why chacras (swidden gardens) persist: Agrobiodiversity, food security, and cultural identity in the Ecuadorian Amazon. Human Organization 64 (4): 327–339. https://doi.org/10.17730/humo.64.4.e6tymmka388rmybt

Pfiffner L, Cahenzli F, Steinemann B, Jamar L, Bjørn MC, Porcel M, Tasin M, Telfser J, Kelderer M, Lisek J, Sigsgaard L. 2019. Design, implementation and management of perennial flower strips to promote functional agrobiodiversity in organic apple orchards: A pan-European study. Agriculture, Ecosystems and Environment 278: 61–71. https://doi.org/10.1016/j.agee.2019.03.005

Poot-Pool WS, van der Wal H, Flores-Guido S, Pat-Fernández JM, Esparza-Olguín L. 2015. Home garden agrobiodiversity differentiates along a rural—peri–urban gradient in Campeche, México. Economic Botany 69 (3): 203–217. https://doi.org/10.1007/s12231-015-9313-z

Ramírez-Juárez J. 2022. Seguridad alimentaria y la agricultura familiar en México. Revista Mexicana de Ciencias Agrícolas 13 (3): 553–565. https://doi.org/10.29312/remexca.v13i3.2854

Reyes-Agüero JA, Aguirre-Rivera JR. 2011. Agrobiodiversity of cactus pear (*Opuntia*, Cactaceae) in the meridional highlands plateau of Mexico. Journal of Natural Resources and Development 1: 1–9. https://doi.org/10.5027/jnrd.v1i0.01

Rocchi L, Boggia A, Paolotti L. 2020. Sustainable agricultural systems: A bibliometrics analysis of ecological modernization approach. Sustainability 12 (22): 9635. https://doi.org/10.3390/su12229635

Saediman H, Gafaruddin A, Hidrawati H, Salam I, Ulimaz A, Rianse IS, Sarinah S, Taridala S. 2021. The contribution of home food gardening program to household food security in Indonesia: A review. WSEAS Transactions on Environment and Development 17 (1): 795–809. https://doi.org/10.37394/232015.2021.17.75

Santillán-Fernández A, Salinas-Moreno Y, Valdez-Lazalde JR, Bautista-Ortega J, Pereira-Lorenzo S. 2021a. Spatial delimitation of genetic diversity of native maize and its relationship with ethnic groups in Mexico. Agronomy 11 (4): 672. https://doi.org/10.3390/agronomy11040672

Santillán-Fernández A, Salinas-Moreno Y, Valdez-Lazalde JR, Pereira-Lorenzo S. 2021b. Spatial-temporal evolution of scientific production about genetically modified maize. Agriculture 11 (3): 246. https://doi.org/10.3390/agriculture11030246

Santillán-Fernández A, Vásquez-Bautista N, Pelcastre-Ruiz LM, Ortigoza-García CA Padilla-Herrera E, Tadeo-Noble AE, Carrillo-Ávila E, Juárez-López JF, Vera-López JE, Bautista-Ortega J. 2023. Bibliometric analysis of forestry research in Mexico published by Mexican journals. Forests 14 (3): 648. https://doi.org/10.3390/f14030648

Schoenly KG, Domingo IT, Barrion AT. 2003. Determining optimal quadrat sizes for invertebrate communities in agrobiodiversity studies: A case study from tropical irrigated rice. Environmental Entomology 32 (5): 929–938. https://doi.org/10.1603/0046-225X-32.5.929

Semu AA. 2018. The Study of homegarden agrobiodiversity, practices of homegardening and its role for *in-situ* conservation of plant biodiversity in Eastern Hararghe, Kombolcha Town Oromia regional state Ethiopia. Open Journal of Forestry 8 (2): 229–246. https://doi.org/10.4236/ojf.2018.82016

SIAP (Sistema de Información Agroalimentaria y Pesquera). 2025. Cierre de la producción agrícola). Gobierno de México. Sistema de Información Agroalimentaria y Pesquera. Ciudad de México, México. https://www.gob.mx/siap/acciones-y-programas/produccion-agricola-33119 (Recuperado: diciembre 2024).

Signore A, Renna M, Santamaria P. 2019. Agrobiodiversity of vegetable crops: Aspect, needs, and future perspectives. Annual Plant Reviews Online 2 (1): 41–64. https://doi.org/10.1002/9781119312994.apr0687

Singha L, Ullah Z. 2020. Genetic variability studies for yield and its attributing traits in potato (*Solanum tuberosum* L.). International Journal of Current Microbiology and Applied Sciences 9 (2): 1974–1983. https://doi.org/10.20546/ijcmas.2020.902.225

Socies-Fiol A, Cuéllar-Padilla M. 2017. ¿Quién mantiene la memoria biocultural y la agrobiodiversidad en la isla de Mallorca? Algunos aprendizajes desde las variedades locales de tomate. Disparidades. Revista de Antropología 72 (2): 477–503. https://doi.org/10.3989/rdtp.2017.02.008

Stagnati L, Soffritti G, Desiderio F, Lanubile A, Zambianchi S, Marocco A, Rossi G, Busconi M. 2022. The rediscovery of traditional maize agrobiodiversity: A study case from Northern Italy. Sustainability 14 (9): 12110. https://doi.org/10.3390/su141912110

Sun J, Yuan BZ. 2020. A bibliometric analysis of research on rice and irrigation from the 'Agronomy' category based on the Web of Science. Current Science 119 (3): 438–446. https://doi.org/10.18520/cs/v119/i3/438-446

Tomatis F, Egerer M, Correa-Guimaraes A, Navas-Gracia LM. 2023. Urban gardening in a changing climate: A review of effects, responses and adaptation capacities for cities. Agriculture 13 (2): 502. https://doi.org/10.3390/agriculture13020502

Trinh LN, Watson JW, Hue NN, De NN, Minh NV, Chu P, Sthapit BR, Eyzaguirre PB. 2003. Agrobiodiversity conservation and development in Vietnamese home gardens. Agriculture, Ecosystems and Environment 97 (1–3): 317–344. https://doi.org/10.1016/S0167-8809(02)00228-1

Wood SA, Karp DS, DeClerck F, Kremen C, Naeem S, Palm CA. 2015. Functional traits in agriculture: Agrobiodiversity and ecosystem services. Trends in Ecology and Evolution 30 (9): 531–539. https://doi.org/10.1016/j.tree.2015.06.013

WoS (Web of Science). 2022. Journal Citation Reports. London, UK. https://clarivate.com/academia-government/scientific-and-academic-research/research-funding-analytics/journal-citation-reports/ (Recuperado: diciembre 2024).

Zimmerer KS, Carney JA, Vanek SJ. 2015. Sustainable smallholder intensification in global change? Pivotal spatial interactions, gendered livelihoods, and agrobiodiversity. Current Opinion in Environmental Sustainability 14: 49–60. https://doi.org/10.1016/j.cosust.2015.03.004

Zimmerer KS. 2003. Geographies of seed networks for food plants (potato, ulluco) and approaches to agrobiodiversity conservation in the Andean countries. Society & Natural Resources 16 (7): 583–601. https://doi.org/10.1080/08941920309185

Zimmerer KS. 2004. Cultural ecology: Placing households in human-environment studies-the cases of tropical forest transitions and agrobiodiversity change. Progress in Human Geography 28 (6): 795–806. https://doi.org/10.1191/0309132504ph520pr

Agrociencia

ASSESSING THE IMPACT OF ECONOMIC CHANGES ON WHEAT PRODUCTION IN SAUDI ARABIA: AN APPLICATION OF THE INTERRUPTED TIME SERIES MODEL

Yosef **Alamri**[1]

[1]King Saud University. Department of Agricultural Economics, Collage of Food and Agricultural Sciences. Riyadh 12372, Saudi Arabia.
* Author for correspondence: yosef@ksu.edu.sa

Citation: Alamri Y. 2025. Assessing the impact of economic changes on wheat production in Saudi Arabia: An application of the interrupted time series model. **Agrociencia** 59(8): 1155-1163. https://doi.org/ 10.47163/ agrociencia.v59i8.3500

Editor in Chief:
Dr. Fernando C. Gómez Merino

Received: Mayo 19, 2025.
Approved: November 20, 2025.
Published in Agrociencia: November 25, 2025.

ABSTRACT

This research examines how Policy 335, which reduced governmental subsidies for wheat cultivation, affected wheat production patterns in Saudi Arabia. The Interrupted Time Series (ITS) methodology was used to assess both the immediate and long-term effects of this policy from 1990 to 2023. The analysis shows an instant reduction in wheat output following policy enactment, although this effect was not statistically significant at the 5 % threshold. In subsequent years, a substantial long-term production decline was documented, with the reduction in governmental assistance identified as the principal driver of this downward trend. Additional economic variables, including producer pricing and pesticide expenditures, showed no meaningful impact on wheat output. In contrast, increased fertilizer utilization helped offset the policy's adverse effects, emphasizing the importance of resource optimization. The outcomes indicate that governmental assistance plays a vital role in maintaining stability in agricultural production. The evidence highlights the necessity for effective resource management and environmentally sustainable farming approaches, especially in resource-limited settings such as Saudi Arabia, to reduce dependence on wheat imports. Continuous assessment and flexible policy adjustments are essential for ensuring long-term viability and food security amid evolving economic and environmental conditions.

Keywords: Policy 335, fertilizer consumption, government support.

INTRODUCTION

Wheat (*Triticum aestivum* L.) has historically served as a fundamental component of Saudi Arabia's food security framework, with grain output totaling 1.75 million Mg in 2023, of which wheat constitutes a substantial share. Nevertheless, the nation faces difficulties in sustaining long-term wheat production independence due to the area's dry climate conditions, scarce water availability, and depletion of finite groundwater reserves. These obstacles, together with ongoing economic and environmental transformations, have progressively increased the country's dependence on wheat imports.

By 2023, wheat imports represented 69 % of total agricultural imports, indicating a transition from a self-reliant producer to one of the globe's leading wheat-importing nations. This transformation mainly results from reduced governmental assistance for wheat cultivation, particularly emphasized by Policy No. 335, implemented in 2008, which gradually phased out domestic wheat farming. This policy, together with groundwater resource depletion, has fundamentally reshaped Saudi Arabia's wheat production environment.

The Interrupted Time Series (ITS) model has been widely used to assess the impact of policy changes and external shocks on agricultural production. Cariappa *et al*. (2022) highlighted the role of government interventions in mitigating the disruptions caused by external shocks such as the COVID-19 pandemic in India. While market disruptions were temporary, state interventions provided resilience. Similarly, Praveen *et al*. (2020) demonstrated the long-term effects of fertilizer policies in India, which mirrors the role of fertilizers in mitigating the impacts of Policy 335 in Saudi Arabia. These studies, together with Hyndman and Rostami-Tabar (2025), who addressed forecasting challenges during disruptions, provide a solid methodological foundation for examining the impact of Policy 335.

Alamri and Tyler (2018) determined that governmental policies directly affected Saudi Arabia's wheat supply and demand dynamics, with Resolution 335 notably decreasing production levels. Ghanem *et al*. (2018) examined the economic drawbacks of using desalinated water for agricultural irrigation, reinforcing the justification for reducing wheat cultivation to preserve water resources. Likewise, Alrwis *et al*. (2016) highlighted the extended consequences of diminished wheat production on food security, representing a vital issue for Saudi Arabia. Alamri and Al-Duwais (2019) projected that policies such as Resolution 335 heightened the nation's dependence on wheat imports, remarking on the necessity to reassess these policies for enhanced food security outcomes.

This study evaluates the impact of Policy 335 on Saudi wheat production dynamics by employing the ITS model to examine both immediate and long-term effects. The model allows for a comparison of pre- and post-policy periods, shedding light on the influence of reduced government support on wheat production trends. Additionally, the study considers regional production variations, sustainability challenges due to water scarcity, and the potential for policy adjustments in improving resource efficiency, particularly in sustainable agricultural practices.

Considering the escalating dependence on imports and mounting challenges from climate change and water scarcity, this study's findings are essential for Saudi Arabia's food security planning. The research evaluates the impact of Policy 335 on wheat production dynamics from 1990 to 2023, with the objective of assessing both immediate and long-term effects using the ITS model, analyzing the influence of economic and environmental variables such as fertilizer consumption, rainfall, and temperature, and providing policy implications to support sustainable wheat production, improve resource efficiency, and reduce reliance on imports. Additionally, the study contributes

to broader discussions on agricultural policy effectiveness in arid regions and offers guidance for strengthening food security in countries facing similar constraints.

MATERIALS AND METHODS

This study employs a quantitative time-series design covering the period 1990–2023, utilizing secondary data collected from the General Authority for Statistics (GASTAT, 2025) of Saudi Arabia, the Food and Agriculture Organization of the United Nations (FAO, 2025), and the World Development Indicators (WDI) (World Bank, 2025). The dataset includes key annual variables relevant to wheat production, such as area harvested, total production, yield (Mg ha^{-1}), producer prices, import prices, fertilizer consumption, pesticide use, average temperature, and total annual rainfall.

The main intervention variable is "Policy 335," representing the government's decision to phase out wheat production support starting in 2008. To capture the effect of this policy intervention, the data are structured into two distinct periods: the pre-policy phase (1990–2008) and the post-policy phase (2009–2023). This temporal segmentation allows the econometric model to isolate and measure both the immediate and sustained effects of the policy on wheat production dynamics in Saudi Arabia.

Experimental design

The study utilizes an Interrupted Time Series (ITS) design to analyze the impact of Policy 335 on wheat production. The ITS model is well-suited for national-level data, particularly when regional control groups are unavailable, as it compares production trends before and after the policy intervention while controlling for covariates. The model incorporates three components: the baseline trend, which reflects the pre-policy trajectory of wheat production and represents the counterfactual scenario without policy change; the immediate effect, which denotes a discrete shift in production levels following the introduction of Policy 335; and the post-policy trend, which captures long-term changes in production patterns after the policy.

The ITS model is expressed as:

$$Y_{it} = \alpha + \beta_1 Time_t + \beta_2 Post_t + \beta_3 (Time_t \times Post_t) + \gamma X_t + \in_{it}$$

where Y_{it} represents wheat production at time t, $Time_t$ is the continuous variable representing the year, $Post_t$ is the binary indicator for the post-policy period (1 if $t \geq 2009$, 0 otherwise), $Time_t \times Post_t$ is the interaction term capturing changes in the production trend post-policy, X_t is control variables (e.g., producer prices, rainfall, temperature), and $\in$ is the error term. The econometric model incorporates covariates such as producer prices, import prices, pesticide use, and climatic variables to account for potential confounding factors.

Conceptually, the ITS framework used in this study is equivalent to a piecewise linear regression model, where the year 2008 serves as a structural break or "knot." This

specification allows separate estimation of pre- and post-policy slopes and intercepts, thereby capturing both the immediate level shift and the long-term trend change associated with the policy intervention.

Advanced analyses

In addition to the baseline analysis, several advanced analyses were conducted to improve the robustness and depth of the findings:

Interaction examination. Potential relationships among critical variables, including producer pricing, pesticide application, and climate conditions (such as precipitation and temperature), were investigated to determine whether policy effects on wheat production differ based on these elements.

Temporal period assessment. The data were segmented into shorter timeframes (such as five-year intervals), both preceding and following policy implementation. This methodology enables the detection of delayed policy consequences on wheat production and helps determine whether the policy's influence changes over time.

Price impact evaluation. The research additionally examines whether wheat price variations, especially following policy intervention, correlate with production level changes, thereby assessing the wider economic environment and its influence on wheat production patterns.

Validation and sensitivity testing. To guarantee result reliability and accuracy, validation procedures were conducted, including assessments for autocorrelation, heteroscedasticity, and model design. Sensitivity evaluations examined delayed policy effects and the influence of exceptional years, such as determining whether severe weather conditions or market irregularities (like global price spikes) affected production trends and policy consequences.

Agricultural sustainability assessment. The study extends its examination to encompass a long-term sustainability evaluation of wheat cultivation in Saudi Arabia, accounting for environmental modifications (including decreased precipitation and rising temperatures) and analyzing whether policy modifications can address these challenges.

Statistical procedures

The study employs non-parametric statistics where necessary, particularly for robustness checks in the presence of non-normality in the residuals. In addition, to account for autocorrelation and heteroscedasticity, Newey-West standard errors were used to adjust the coefficients and provide more reliable estimates. In cases of temporal dependence, Autoregressive Integrated Moving Average (ARIMA) models were applied to model the time-series data more accurately and address any autocorrelation issues. The software used for data analysis includes R (version 4.0 or

later), with the "auto.arima" function from the forecast package, and the "lmtest" and "sandwich" packages for regression analysis and heteroscedasticity adjustments. All tests were conducted at a significance level of 5 %.

RESULTS AND DISCUSSION

The findings from this research offer significant perspectives on Saudi Arabia's wheat production across both immediate and extended timeframes, explaining how Policy 335 resulted in a considerable reduction in wheat output. This outcome aligns with earlier studies, which emphasized how external disruptions generated disturbances in agricultural production (Cariappa *et al*., 2022). Likewise, policy-driven interruptions can produce enduring effects, with the decrease in production persisting over an extended period and reflecting a fundamental transformation in the nation's wheat production framework.

The post-policy impact variable in the ITS model indicated an immediate reduction in production following the policy change, with a coefficient of -531 283 (Table 1).

Table 1. Estimates and significance of key variables assessing wheat production analysis in Saudi Arabia using Interrupted Time Series (ITS), Autoregressive Integrated Moving Average (ARIMA), and Newey-West adjusted models.

Variable	ITS model estimate (in thousands)	ITS model standard error (in thousands)	ARIMA model estimate (in thousands)	ARIMA model standard error (in thousands)	Newey-West model estimate (in thousand)	Newey-West model standard error (in thousands)	*p*-value (Newey-West)
Intercept	-29.61	49.63	3.01	0.60	-20.53	41.74	0.63
Time (years)	-	-	-	-	9.68	20.69	0.64
Post-policy impact	-531.28	358.05	-	-	-536.53	324.47	0.11
Post-policy trend	-211.66	63.24	-	-	-202.60	73.96	<0.01 *
Producer price (USD Mg^{-1})	1.60	1.23	-1.04	0.82	1.53	1.95	0.44
Pesticide import price (USD Mg^{-1})	60.73	127.82	-162.56	66.21	65.05	76.72	0.40
Fertilizer consumption (kg ha^{-1})	28.31	5.32	-	-	27.99	5.91	<0.01 *
R-squared	-	-	-	-	0.90	-	-
Adjusted R-squared	-	-	-	-	0.88	-	-
Akaike information criterion (AIC)	-	-	968.96	-	937.8	-	-
Bayesian information criterion (BIC)	-	-	978.12	-	968.96	-	-
Log-likelihood	-478.48	-	-	-	-	-	-

*Significant variables ($p < 0.05$).

Although this decline was not statistically significant at the 5 % level (p = 0.11), it remains noteworthy and aligns with Mulwa *et al*. (2025), who observed that agricultural policy shifts often lead to immediate production drops. Despite the lack of statistical significance, the reduction in wheat output immediately after the policy is consistent with literature showing that abrupt policy changes tend to disrupt agricultural sectors, particularly wheat production, which is highly sensitive to such interventions. Overall, the results indicate that the policy triggered an immediate downturn in wheat production.

After the initial decline, the post-policy trend revealed a significant and sustained long-term reduction in wheat production, with a coefficient of -211 664 (p = <0.01), confirming that the policy's effects persisted over time. This pattern aligns with Plewis (2019), who found that agricultural policy changes frequently lead to long-lasting structural shifts after early disruptions. In Saudi Arabia's case, the continued decrease in production following Policy 335 demonstrates the enduring consequences of reduced governmental support, reinforcing the findings of Chitikela *et al*. (2025), who showed that policy interventions commonly reshape agricultural output trajectories. These results highlight that, although the immediate impact was not statistically significant, the long-term effects were substantial and indicative of a structural shift in wheat production trends.

In contrast, the fertilizer consumption variable showed a statistically significant positive effect on wheat production (coefficient = 28 308, p = <0.01), indicating that increased fertilizer use played a critical role in mitigating the negative impacts of the policy shift. This significant positive relationship confirms the importance of fertilizers in sustaining agricultural productivity even when government support is reduced. The finding aligns with Praveen *et al*. (2020), who reported that greater fertilizer use in India helped offset the adverse effects of declining subsidies and enhanced overall productivity. Similarly, in Saudi Arabia, the expanded reliance on fertilizers appears to have supported wheat production despite diminished governmental assistance, underscoring the relevance of resource inputs during periods of policy transition.

External factors such as producer price, pesticide import price, and annual mean precipitation did not show significant effects on wheat production, indicating that these variables did not meaningfully influence output during the study period. This finding aligns with Kumar *et al*. (2024), who noted that when major policy changes occur, their influence on agricultural production can outweigh the effects of other economic variables. In this case, the policy shift had a more pronounced impact on wheat production, a conclusion supported by the model's strong performance, with an R-squared of 0.9 and an adjusted R-squared of 0.88. The complete model demonstrates robust explanatory power, accounting for a substantial proportion of the variation in wheat production, and the F-statistic of 35.14 and a p-value of 1.108×10^{-11} confirm its overall statistical significance.

The visual representation of the results, which shows a clear shift in the production trend before and after the policy change, provides additional support for the conclusions

derived from the statistical analysis (Figure 1). The marked change in the production slope in 2009 remarks that Policy 335 produced both an immediate and sustained impact on wheat production in Saudi Arabia. This graphical depiction, contrasting pre- and post-policy trends, strengthens the hypothesis that policy adjustments can generate significant changes in agricultural production, aligning with the findings reported by Praveen *et al*. (2020) and Chitikela *et al*. (2025) on the long-term effects of policies.

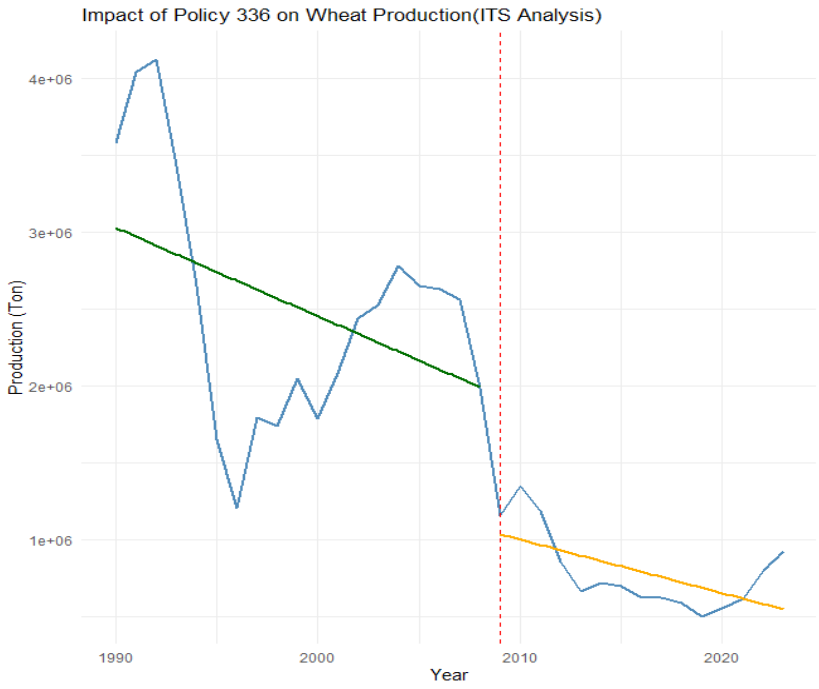

Figure 1. Shift in wheat production following Policy 335 in Saudi Arabia (Interrupted Time Series analysis).

In summary, the findings confirm that the reduction of governmental support for wheat cultivation under Policy 335 had immediate and sustained negative effects on wheat production. This aligns with Mulwa *et al*. (2025) and Cariappa *et al*. (2022), who found that major policy shifts can destabilize agricultural systems. This shows the importance of maintaining governmental support to ensure long-term stability and productivity in the sector. Furthermore, the beneficial impact of fertilizers in offsetting the policy transition's negative consequences emphasizes the significance of optimizing resource utilization and implementing environmentally sustainable farming methods.

These results carry substantial policy ramifications for Saudi Arabia, where constraints such as water scarcity and climate change increasingly threaten wheat production.

Improving resource efficiency, particularly through optimized fertilizer use, and adopting sustainable agricultural practices could help reduce dependence on wheat imports. This study contributes to the broader discussion on agricultural policy in resource-limited contexts by offering insights for policymakers seeking to strengthen food security and mitigate the long-term effects of policy shifts on production. Future research should examine regional variability and climate-related pressures to develop a more comprehensive understanding of the enduring impacts of policy changes on wheat cultivation.

CONCLUSIONS

This study found that Policy 335 had a significant impact on wheat production in Saudi Arabia, resulting in both immediate and long-term declines due to reduced government support. Increased fertilizer consumption helped to mitigate some of these negative effects, highlighting its critical role in maintaining productivity during policy transitions. Variables such as producer prices, pesticide costs, and annual mean precipitation had no significant influence, indicating that the policy shift was the primary cause of changes in wheat output.

Overall, the findings emphasize the importance of government support in stabilizing agricultural systems, particularly in resource-constrained settings like Saudi Arabia. Because long-term effects of policy changes tend to outweigh short-term disruptions, targeted assistance for strategic crops, efficient fertilizer use, and adaptive strategies addressing water scarcity and climate stress are recommended. These measures are vital for strengthening food security and improving the resilience of the country's agricultural sector.

REFERENCES

Alamri Y, Al-Duwais A. 2019. Food security in Saudi Arabia (Case study: Wheat, barley, and poultry). Journal of Food Security 7 (2): 36–39.

Alamri Y, Tyler M. 2018. Functions of wheat supply and demand in Saudi Arabia. Journal of Agricultural Economics and Rural Development 4 (2): 461–468.

Alrwis KN, Ghanem AM, Ahamad SB, Aldawdahi NM. 2016. The impact of the loss of wheat to agricultural resources and food security of the Kingdom of Saudi Arabia. Egyptian Journal of Agricultural Economics 26 (2): 866–873. https://doi.org/10.21608/meae.2016.121133

Cariappa AA, Acharya KK, Adhav CA, Sendhil R, Ramasundaram P, Kumar A, Singh S, Singh GP. 2022. COVID-19 induced lockdown effect on wheat supply chain and prices in India – Insights from state interventions led resilience. Socio-Economic Planning Sciences 84: 101366. https://doi.org/10.1016/j.seps.2022.101366

Chitikela G, Rathod S, Vijayakumar S. 2025. Change point-driven interrupted time series and machine learning models for forecasting Indian food grain production. Discover Food 5 (1): 68. https://doi.org/10.1007/s44187-025-00350-5

FAO (Food and Agriculture Organization). 2025. FAOSTAT. FAO Database on food and agriculture. United Nations Food and Agriculture Organization. Rome, Italy. https://www.fao.org/faostat/es/#home (Retrieved: March 2025).

GASTAT (General Authority for Statistics). 2025. Economic statistics. Government of the Kingdom of Saudi Arabia. Riyadh, Saudi Arabia. https://www.stats.gov.sa/en/ (Retrieved: March 2025).

Ghanem AM, Al-Ruwais KN, Al-Qunaibet MH, Al-Nashwan OS, Al-Duwais ABM. 2025. Study of the current and proposed status of wheat cultivation and production in the Kingdom of Saudi Arabia. African Journal of Advanced Studies in Humanities and Social Sciences 4 (2): 10–19.

Ghanem AM, Alrwis KN, Alnashwan OS, Kamara SA, Ahmed SAB, Aldawdahi NM. 2018. Economic efficiency of desalinated water to be used in agricultural production in the Kingdom of Saudi Arabia. Desalination and Water Treatment 111, 101–110. https://doi.org/10.5004/dwt.2018.22239

Hyndman RJ, Rostami-Tabar B. 2025. Forecasting interrupted time series. Journal of the Operational Research Society 76 (4): 790–803. https://doi.org/10.1080/01605682.2024.2395315

Kumar A, Roy D, Tripathi G, Adhikari R. 2024. Contract farming, farmers' income and adoption of food safety practices: Evidence from remote areas of Nepal. Agricultural Economics Research Review 37 (1): 59–78. https://doi.org/10.5958/0974-0279.2024.00010.7

Mulwa D, Kazuzuru B, Misinzo G, Bett B. 2025. Impact of Rift Valley fever outbreaks on food price index in Burundi: An interrupted time series analysis. Food and Humanity 4: 100530. https://doi.org/10.1016/j.foohum.2025.100530

Plewis I. 2019. Adopting hybrid Bt cotton: Using interrupted time-series analysis to assess its effects on farmers in northern India. Review of Agrarian Studies 9 (2).

Praveen KV, Singh A, Kumar P, Jha GK, Kingsly I. 2020. Advancing with fertilizers in Indian agriculture: Trends, challenges, and research priorities. Agricultural Economics Research Review 33: 49–60. https://doi.org/10.5958/0974-0279.2020.00017.8

World Bank. 2025. World development indicators. Washington, DC, USA. https://datatopics.worldbank.org/world-development-indicators/ (Retrieved: March 2025).

Agrociencia

BLOCKCHAIN-BASED CROP MONITORING USING AN INTERPLANETARY FILE SYSTEM

Jananee **Vinayagam**[1], Dhivya **Baskar**[2], Tamilvizhi **Thanarajan**[3*] Mahendran **Rajamanickam**[4]

[1]SRM Institute of science and Technology, Department of Computer science and Engineering, Ramapuram, Chennai, 600089, India.
[2]Karpaga Vinayaga College of Engineering and Technology. Department of Computer Science and Engineering. Chengalpattu, Tamil Nadu 603308, India.
[3]Panimalar Engineering College. Department of Computer Science and Engineering. Chennai, Tamil Nadu 600123, India.
[4]Koneru Lakshmaiah Education Foundation. Computer Science and Engineering. Guntur, Andhra Pradesh 522502, India.
* Author for correspondence: tamilvizhi.phd.it@gmail.com

Citation: Vinayagam J, Baskar D, Thanarajan T, Rajamanickam M. 2025. Blockchain-Based crop monitoring using an interplanetary file system. **Agrociencia** 59(8): 1164-1178. https://doi.org/ 10.47163/ agrociencia.v59i8.3553

Editor in Chief:
Dr. Fernando C. Gómez Merino

Received: July 10, 2025.
Approved: November 27, 2025.
Published in Agrociencia: December 04, 2025.

ABSTRACT

Continuous monitoring of crops is essential for early issue detection and data-driven decision making, which supports improved yield, quality, and environmental sustainability in agriculture. Blockchain technology has been used for continuous monitoring of agricultural fields, although its adoption remains limited due to economic and technological constraints. This study proposes an enhanced crop-monitoring framework with InterPlanetary File System (IPFS) technology to overcome the limitations of existing models. Experimental evaluation showed that the proposed model achieved 98 % accuracy and a 99.8 % confidentiality rate. System throughput increased from 3 kb s^{-1} for 10 kb of data to 307 kb s^{-1} for 3000 kb, demonstrating strong scalability. By integrating decentralized IPFS storage with blockchain-based traceability, the system ensures data integrity, cost-efficiency, and reliable real-time monitoring, offering a practical solution for precision agriculture. These findings demonstrate the potential of the IPFS-enabled framework as an efficient alternative to conventional blockchain-dependent models.

Keywords: Agriculture, blockchain technology, machine learning.

INTRODUCTION

Crop monitoring has become essential in modern agriculture, with studies indicating yield increases of up to 25 % and water savings of up to 30 % (Panek-Chwastyk *et al*. (2024). By integrating technologies such as satellite imagery and drones, farmers can detect crop stressors, including pests and diseases, with accuracies approaching 90 %, allowing for timely and effective interventions Shammi *et al*., (2024). Precise monitoring also optimizes resource allocation, saving fertilizer by up to 50 % and reducing pesticide usage by 20–30 %, which reinforces economic gains while supporting ecological balance through reduced chemical leaching and soil deterioration Padmini and Kuzhalvaimozhi, (2024). Additionally, early detection of yield fluctuations

supports informed decision-making, saving up to 30 United States Dollars (USD) per acre through optimized harvesting and marketing strategies. Overall, the integration of robust monitoring systems can improve returns on investment by up to 300 %, reinforcing their role as a cornerstone of modern farming operations Padmini and Kuzhalvaimozhi, (2024).

Information and communication technologies (ICTs) are widely used in agriculture and are closely related to process regulation and farming efficiency. Internet of Things (IoT)-based agricultural monitoring systems collect crop data in real time, allowing for more informed decisions about planting, watering, and pest control. By delivering precise, up-to-date data, IoT-based observation devices help farmers optimize the use of agricultural inputs Mahalingam and Sharma, (2023). By limiting hazardous chemicals, reducing waste, and maximizing resource utilization, these systems help farmers reduce their environmental impact. Real-time data enables close observation and regulation of crop growth conditions, resulting in higher-quality harvests that are less susceptible to disease and pests. Farmers can also increase their earnings by lowering the costs of labor, nutrients, water, and other supplies using IoT-based agricultural monitoring systems Mahalingam and Sharma, (2023)..

The various functions performed by IoT in agriculture include continuous crop monitoring, tracking and tracing agricultural products from seeding to selling, farming using Unmanned Aerial Vehicles (UAVs), supply chain management, precision farming, and aquaponics farms. To support and enhance these capabilities, Panek-Chwastyk *et al*. (2024) examined the viability of acclimatizing the Earth Observation for Agricultural Statistics (EOstat) crop monitoring system, primarily implemented for continuous observation of crop growth in Poland. The system used data collected from satellites and agrometeorological information obtained through the Copernicus program and utilized a machine learning algorithm and the Extreme Gradient Boosting Regressor (XGBoost) for the identification of each unit.

Padmini and Kuzhalvaimozhi (2024) integrated IoT and Wireless Sensor Networks (WSNs) for real-time crop monitoring. To overcome the problem of hotspots and address load balancing, they introduced the Energy and Delay Aware Routing (EDAR) organization for direction finding in IoT applications. Wei and Fang (2024) targeted the implementation of a system for monitoring plant health in vertical farms by using multispectral LEDs with near-infrared (NIR) and ultraviolet A (UVA) light sources. IoT was responsible for controlling the LED spectrum, and a camera was connected to the IoT device with switchable filters and RGB CMOS sensors to estimate UV-NDVI and SI-NDVI.

Effective plant monitoring remains essential for enhancing and sustaining agricultural productivity and supporting informed agricultural management. Maity *et al*. (2024) developed a system that utilizes Passive Infrared (PIR) sensors to detect animal intrusion, smoke, and soil moisture levels in agricultural fields. This system integrates three core components: Arduino-based IoT devices, a web server application, and a smartphone interface for real-time monitoring and control. Similarly, Eisfelder *et*

al. (2024) introduced an approach that leverages Sentinel-1 (S1) and Sentinel-2 (S2) time-series data to classify crop types and cropland, evaluating the performance of 33 Random Forest models.

Several studies have incorporated intelligent technologies to improve crop monitoring. Stephen *et al*. (2023) applied deep learning methods using multiple Convolutional Neural Network (CNN) architectures, while Omia *et al*. (2023) evaluated remote sensing through spectral imagery. Kumar Pradhan *et al*. (2024) developed an Artificial Intelligence (AI) and IoT-based system for continuous monitoring and environmental detection, and Akilan and Baalamurugan (2024) created a sensor-based framework using an Adaptive Gaussian Filter (AGF) and ResNet50. Additional advances include IoT and deep learning models such as MobileNetV2, EfficientNetB0, and Mobile-UNet (Morellos *et al*., 2024), Model-Based Safety Analysis (MBSA) for identifying module failures (Abdulhamid *et al*., 2024), and CNN-based approaches including VGG16, DenseNet121, MobileNetV2, and ResNet50 for agricultural monitoring (Peng *et al*., 2024).

Crop monitoring can be significantly strengthened through the integration of advanced image recognition techniques. Shammi *et al*. (2024) focused on soybean growth assessment by employing multiple technologies for yield prediction. Li and Shi (2024) introduced an end-to-end Semi-Supervised Object Detection (SSOD) approach based on Detection Transformer (DETR) for monitoring the growth of *Brassica chinensis*, incorporating two additional strategies to address class imbalance and support multi-task optimization. Similarly, Nduku *et al*. (2024) used UAV imagery to estimate crop height in two winter wheat farms, analyzing the resulting datasets with machine learning models.

The growing reliance on IoT in agriculture introduces significant security risks, as interconnected devices are increasingly vulnerable to data breaches and malicious attacks. To address these concerns and overcome the limitations of existing techniques, an IoT-based crop monitoring system incorporating InterPlanetary File System (IPFS) technology was proposed.

Objectives and hypothesis

The primary objective of this study is to design and validate a secure, scalable crop-monitoring framework that integrates Internet of Things (IoT) sensing, cryptographic data protection, blockchain-based traceability, and InterPlanetary File System (IPFS) decentralized storage for efficient agricultural data management. Specifically, the study aims to (i) enhance data confidentiality and integrity using AES encryption and SHA-256 hashing mechanisms, (ii) improve system throughput and reduce execution time compared with conventional blockchain-based architectures, and (iii) assess the effectiveness of Support Vector Machine (SVM) models for crop monitoring and predictive analysis using preprocessed sensor and image data.

The hypothesis of this study is that the integration of IPFS-based decentralized storage with blockchain traceability and cryptographic security mechanisms will result in

significantly higher throughput, lower processing time, and improved confidentiality while maintaining data reliability when compared with traditional centralized or blockchain-only crop monitoring systems.

MATERIALS AND METHODS

A prediction system was proposed that integrates a security device with cloud infrastructure to safeguard data from attackers. Existing approaches suffer from limitations in their data-filtering mechanisms, as they often fail to adequately remove noise, irrelevant attributes, or corrupted sensor readings, leading to inaccurate analytical results. The proposed model addresses these issues by incorporating min-max scaling for preprocessing, the Advanced Encryption Standard (AES) for secure data acquisition, and a Support Vector Machine (SVM) for data analysis. This integrated approach enhances security, integrity, efficiency, accuracy, and traceability within IoT-based crop monitoring systems.

Data acquisition

Crop data is acquired from the cloud and analyzed using cloud computing infrastructure. This information includes soil moisture, humidity, temperature, crop growth stages, and satellite imagery. Cloud-based storage ensures secure, scalable, and continuous access to agricultural data, acting as the central repository for heterogeneous inputs from IoT devices, sensors, and remote sensing sources. It supports efficient storage and retrieval of large datasets, enables real-time synchronization between field devices, preprocessing modules, and machine learning workflows, and provides fault tolerance and backup to minimize data loss. Additionally, cloud storage integrates seamlessly with IPFS, enhancing security, traceability, and decentralized access.

Preprocessing

MIN-MAX scaling (minimum–maximum normalization) is used for data preprocessing. In crop monitoring, variables such as temperature, soil moisture, and sunlight intensity each have different measurement ranges. For example, soil moisture may vary from 0 to 100 %, while temperature may range from -20 to 40 °C. Scaling these values to a common range (such as 0 to 1) facilitates comparison, pattern detection, and correlation analysis across environmental factors. By standardizing and harmonizing heterogeneous inputs, MIN-MAX scaling plays a key role in improving the performance of crop monitoring systems. The preprocessing equation using MIN-MAX scaling is given in the following equation:

$$X' = \frac{(x - x_{min})}{X_{max} - X_{min}}$$

Cryptographic analysis

Modifications can be detected by comparing newly generated hashes of updated material with the hashes previously stored on IPFS. This process removes the need for decryption, which often requires exposing private keys and introduces security risks, so it is only required when recovering earlier data. Because integrity checks can be performed without revealing the underlying content, this method also helps maintain a clear separation of concerns.

The function CREATEDATAFORIPFS takes a list of records corresponding to database rows. For each row, it computes a hash of the content and produces tuples (*idi*, *H*(*recordi*)), where *H*() denotes the hashing function. The full content is then encrypted using the function *E*(), and both components are stored together on IPFS. The system uses the SHA-256 algorithm to generate fixed 256-bit cryptographic hashes, which uniquely represent the input data. Even minimal changes in the input cause substantial differences in the resulting hash, a property known as the avalanche effect.

Hashing

The hashing process can be represented as follows:

$$H\,(D) = SHA - 256\,(D)$$

where *H* denotes the hash function based on the SHA-256 technique and *D* indicates the data entry.

In the encryption stage, the Password-Based Key Derivation Function 2 (PBKDF2) is used as a key derivation function with an adjustable computational cost designed to prevent vulnerability to brute-force attacks. It generates a cryptographic key from a confidential secret, eliminating the need to store the encryption key in a central database and thus improving overall security.

Key derivation

The derived key *K*, used for both encryption and decryption, is obtained as follows:

$$K = KDF\,(P, S, N, L)$$

where the user-provided password is denoted by *P*, and the key derivation function by *KDF*.

This method does not save any encryption key. Instead, it encrypts a predefined string *S* using the key derived from the user password *P*, and the resulting ciphertext is stored on the IPFS. When a user later provides a password *P′*, a corresponding key *K′* is generated using the same KDF function. The stored ciphertext is then decrypted with *K′*. If the decrypted value matches the original string *S*, the password is validated and the verification succeeds; otherwise, access is denied. After successful verification, the derived key *K* is used for encryption operations.

Encryption

The encrypted data (*ED*) can be expressed as follows:

$$ED = E(K, D)$$

where *E* denotes the encryption function, *K* represents the secret key, and *D* refers to the data being encrypted.

The process begins with the generation of combined data, which is stored on IPFS, producing a unique Content Identifier (CID) that represents the encrypted and hashed content. Once this CID is generated, the blockchain stage is initiated. The CID is recorded on the blockchain through a smart contract, which maintains an immutable list of all CIDs associated with IPFS-stored data. This ensures permanent, tamper-proof tracking of data integrity and enables auditable traceability by Krishnan N *et al*. (2024).

The primary objectives of this smart contract are to store CIDs, retrieve them, and support verification of persisted data. The DATAVERIFICATION function (Algorithm 1) performs an integrity check by comparing the hashes of the current centralized database entries (Dapi) with those stored in IPFS (Db). It determines whether each row exists on the blockchain and whether its stored hash matches the current one. New records are uploaded to IPFS, and the resulting CIDs are added to the blockchain. Records with mismatched hashes are flagged as corrupted or irregular. Although homogeneity checks rely solely on hash comparison without requiring decryption, system policies may allow corrupted data to be restored by decrypting the corresponding encrypted content stored under the associated CID.

Algorithm 1: DATAVERIFICATION
Input: Current database records Dapi
Output: Verification result and blockchain update
For each record in Dapi do:
  Compute current hash Hcurrent = SHA-256(record)
  Retrieve stored hash Hstored from IPFS blockchain ledger
  If Hcurrent == Hstored then
    Mark record as verified
  Else
    Flag record as corrupted or altered
    Upload new encrypted data to IPFS
    Store new CID on blockchain
  End If
End For

Monitoring

Once the data is collected and preprocessed, Support Vector Machines (SVMs) are used for both regression and classification tasks in agriculture due to their strong mathematical foundations. These work by identifying the optimal hyperplane that separates classes or predicts continuous outcomes, with the closest data points (support vectors) defining this boundary. The optimization process seeks the hyperplane that maximizes the margin between support vectors, often solved using quadratic programming or gradient-based methods.

In agricultural applications, SVMs are trained on feature vectors extracted from satellite imagery and sensor data, including vegetation indices, temperature, and soil moisture. These features represent the input vectors (x) for the SVM:

The SVM classification and regression functions are defined as:

$f(x) = w \cdot x + b$

where *w* is the weight vector defining the separating hyperplane, *x* is the feature vector, and *b* is the bias term.

The optimal hyperplane is obtained by minimizing the objective function:

$\min (1/2 \, ||w||^2 + C \sum \xi i)$

subject to:

$yi \, (w \cdot xi + b) \geq 1 - \xi i$

where *C* is the regularization parameter that controls the trade-off between maximizing the margin and minimizing classification errors, *xi* is the input sample, *yi* is the class label, and *ξi* represents the slack variable allowing misclassifications. Through optimization of the parameters w and b, SVMs can classify crops, detect pests, predict yields, and evaluate crop health effectively. Additionally, the proposed method enhances data integrity, robustness, and secure retrieval by preventing third-party interference. System privacy is improved through hash-based comparisons, allowing verification without decrypting the stored data.

Experimental setup

The proposed system was implemented and evaluated in a controlled laboratory setting. The hardware setup included a workstation with an Intel Core i7 processor, 16 GB RAM, and a 1 TB SSD running Ubuntu 22.04 LTS. IoT data were simulated using Arduino Uno boards equipped with DHT11 temperature-humidity sensors and soil moisture sensors. A 2.4/5 GHz dual-band Wi-Fi 6 router was used for data transmission between the IoT devices and the cloud server.

The cloud environment was deployed on Google Cloud Platform (GCP), using Cloud Storage Buckets for data storage and virtual machines with 4 vCPUs and 8 GB RAM for computation. InterPlanetary File System (IPFS) version 0.21.0 was installed on the Ubuntu server (version 0.21.0), and SHA-256 hashing was integrated for data integrity verification. The software stack consisted of Python 3.10 for preprocessing (Min-

Max scaling), TensorFlow for SVM-based machine learning, and OpenSSL for AES encryption/decryption. Network performance was monitored with Wireshark, and MATLAB R2022a was used to generate comparative analysis graphs.

Performance enhancement

The performance of the proposed system was evaluated using two primary metrics: total processing time and throughput, with the goal of assessing how different data sizes influence encryption/decryption speed and overall system efficiency.

Throughput

The throughput (T) is defined as the volume of data (D) processed per unit time (t) during encryption or decryption. The relative throughput for encoded data (ED) and decoded data (DD) is defined as:

$$TE = \frac{size(ED)}{t}$$

$$TD = \frac{size(DD)}{t}$$

Total time

The total time is calculated as:

$$t = t_e - t_i$$

representing the difference between the start time *ti* and completion time *te* of a given operation. Measurements were taken for encoding, decoding, hashing, and storing encrypted data on IPFS across data sizes ranging from 10 to 3000 kb.

Scalability

System scalability was assessed by evaluating overall throughput across all processing stages, using the same data-size range (10–3000 kb). This analysis reflects the system's capacity to maintain performance as workload increases.

Data integrity

While AES and similar algorithms ensure confidentiality, they do not inherently protect data integrity. Encrypted data can still be modified without detection, potentially leading to corrupted but decryptable outputs. The proposed system addresses this limitation by incorporating hash-based integrity verification. A hash value (the data's unique electronic fingerprint) is computed before encoding. After decoding, the hash is recomputed and compared with the original. Matching hashes confirm that no tampering occurred during storage or transmission. This mechanism provides robust

protection against unauthorized modifications, strengthening the overall security of the system.

Performance metrics

The evaluation of the proposed system relied on several standard performance metrics. Accuracy measures the proportion of correctly classified instances among all instances, precision quantifies the proportion of true positive predictions among all predicted positives, and recall (or sensitivity) captures the proportion of true positives identified among all actual positive instances. The F1 score, defined as the harmonic mean of precision and recall, provides a balanced measure that accounts for both prediction correctness and completeness.

Accuracy was evaluated based on the classification output of the Support Vector Machine (SVM) model using a labeled dataset of crop health samples. The dataset was divided into training (70%) and testing (30%) subsets. Accuracy was calculated as the ratio of correctly predicted samples to the total number of evaluated samples, expressed as:

$$\text{Accuracy} = \frac{(TP+TN)}{(TP+TN+FP+FN)}$$

where TP represents true positives, TN true negatives, FP false positives, and FN false negatives.

The confidentiality rate was evaluated by measuring the proportion of successfully encrypted and securely verified data transmissions relative to the total number of data packets processed by the system. Data integrity verification was performed through SHA-256 hash matching between locally generated hashes and hashes stored in the IPFS ledger following encryption and decryption processes. The confidentiality rate was expressed as:

Confidentiality Rate = (Number of securely verified encrypted records / Total transmitted records) × 100%

Multiple transmission trials were conducted across varying data volumes to obtain stable average values for both accuracy and confidentiality evaluations.

RESULTS AND DISCUSSION

The use of IPFS allowed agricultural data to be stored and accessed in a decentralized manner, ensuring availability, integrity, and resilience across multiple nodes. This distributed architecture reduced vulnerability to attacks compared with traditional centralized storage systems. The integration of Min-Max scaling as a preprocessing step further enhanced machine learning performance by normalizing heterogeneous

feature values into a common range, resulting in more stable, accurate, and robust models. SVMs were also effective in the final analytical stage of crop monitoring tasks, such as crop classification, pest detection, and yield prediction, thanks to their strong regression capabilities and ability to capture complex nonlinear patterns via kernel functions.

The system incorporated the InterPlanetary File System (IPFS) and cloud infrastructure to achieve scalable and distributed data management. By distributing information across multiple nodes rather than relying on a single centralized server, the architecture minimizes performance bottlenecks and supports larger datasets and higher transaction volumes without degradation in speed. Cost efficiency was achieved by avoiding the computational and energy demands of traditional blockchain consensus mechanisms; instead, IPFS combined with AES-based encryption provided lightweight security and integrity verification. Additionally, the use of cloud resources on a pay-as-you-go model limits upfront investment and ensures that resources can be scaled according to demand.

A positive correlation was observed between system throughput and data size. Throughput measured approximately 3.07 kb s^{-1} for a 10 kb dataset but increased sharply to over 307.12 kb s^{-1} when processing 3000 kb. Lower throughput at small data sizes was primarily due to the disproportionate impact of initial encoding and decoding overhead, which becomes negligible as data volumes grow. As dataset size increases, the system operates more efficiently, highlighting the scalability of AES for large data workloads. These results demonstrate that AES supports secure, efficient encoding and decoding even when handling substantial quantities of information.

AES was selected for its strong security guarantees and its ability to efficiently process large datasets. As a block-cipher algorithm supporting 128-, 192-, and 256-bit keys, AES enables parallel processing of data blocks, minimizing computational overhead during both encryption and decryption. This efficiency is especially advantageous in agricultural applications, where continuous streams of sensor readings, satellite imagery, and IoT data produce substantial data volumes. Compared with older algorithms such as Data Encryption Standard (DES) and Triple-DES, AES offers significantly higher throughput while maintaining robust resistance to brute-force and cryptanalytic attacks. Its lightweight computational requirements ensure practical performance even with multi-megabyte inputs, making AES a scalable and secure choice for real-time crop monitoring and large-scale agricultural data management.

The results indicate that processing time increases with data size. For a 10 kb dataset, encryption, decryption, and hashing required approximately 2472, 2511, and 1 ms, respectively, while storing the data on IPFS took 720 ms. When the dataset size increased to 3000 kb, processing times rose to 3546 ms for encryption, 3490 ms for decryption, 190 ms for hashing, and 5295 ms for IPFS storage (Figure 1).

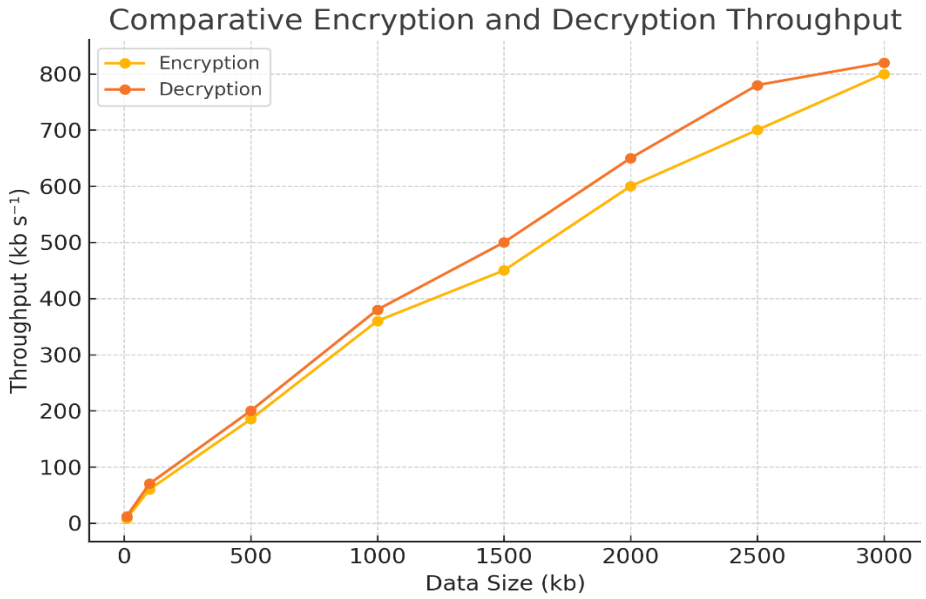

Figure 1. Comparative encryption and decryption throughput of the Advanced Encryption Standard (AES)-based module within the InterPlanetary File System (IPFS)-integrated crop monitoring system.

The consistent increase in computation time with larger datasets confirms the effectiveness of the AES and SHA-256 mechanisms. IPFS requires additional time for data storage due to network latency, data transfer, and processing overhead; however, this duration is acceptable in real-world scenarios since data preservation can be performed offline, unlike other systems.

The overall throughput of the model, including data encoding, hashing, and storage of encrypted IPFS data, was approximately 3 kb s^{-1} for a 10 kb dataset (Figure 2). As the dataset size increased to 3000 kb, throughput rose significantly to over 307 kb s^{-1}. These results demonstrate the model's ability to efficiently process large datasets, highlighting its scalability. The proposed model achieved 98 % accuracy, 99.8 % confidentiality rate, and reduced execution time to 9 ms. Compared to other systems, the model performed better across all evaluated metrics (Table 1 and Figure 3).

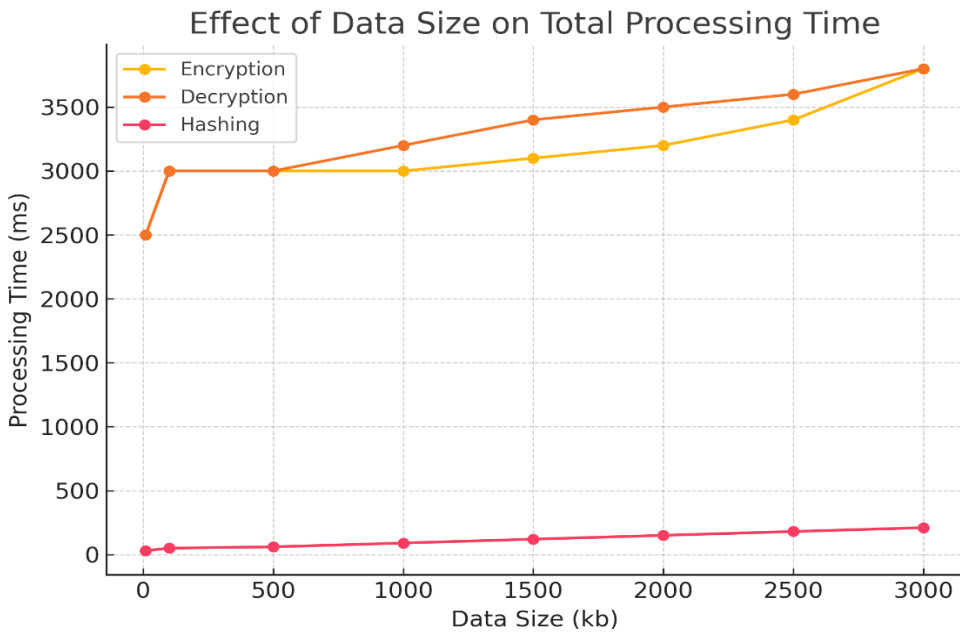

Figure 2. Effect of data size on total processing time for Advanced Encryption Standard (AES) and InterPlanetary File System (IPFS) operations.

Table 1. Comparative evaluation of various cryptographic techniques.

Technology	Encryption time (ms)	Decryption time (ms)	Execution time (ms)	Confidentiality rate (%)
Advanced Cipher Encryption-Blockchain (ACE-BC) (Alharbi, 2023)	-	-	-	97.54
Double Bilinear Diffie-Hellman (DBDH) (Goel and Neduncheliyan, 2023)	3.55	3.6	12	99.52
Secure Stream Encryption and Robust Block Algorithm (SSERBA) (Alotaibi Y 2024)	25	35	25	84
Elliptic Curve Integrated Encryption Algorithm (ECIEA) (Pourvahab and Ekbatanifard, 2019)	70	90	30	79
CLIENT (Ramamoorthi and Appathurai, 2023)	3.22	3.27	-	-
Elliptic Curve Cryptography-Secure Authentication Scheme (ECCSAS) (Velmurugadass *et al*., 2021)	50	53	50	76
Randomized Network Encryption for Cloud Blockchain (RNECB) (Mahalingam and Sharma, 2023)	2.7	2.6	11	98.89
Proposed model (InterPlanetary File System, IPFS)	2.5	2.4	9	99.8

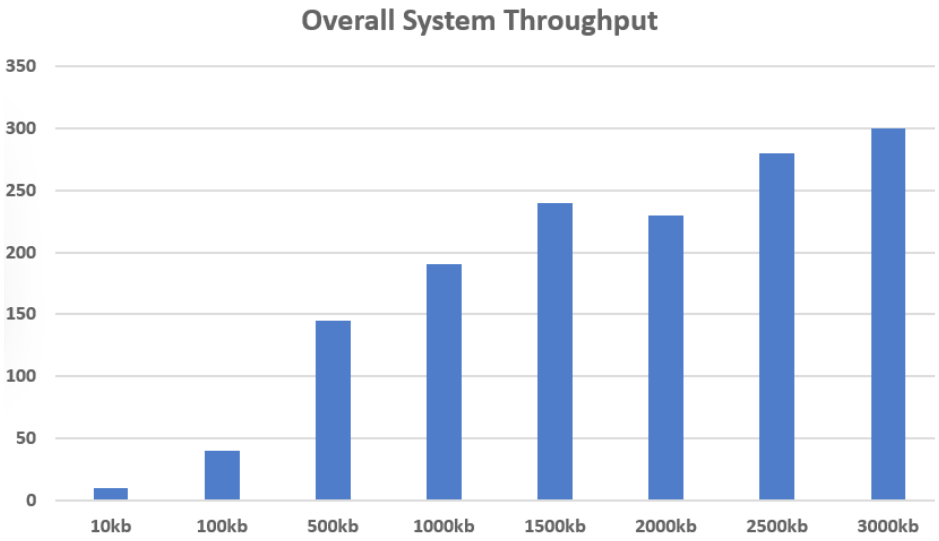

Figure 3. Overall throughput of the proposed crop monitoring system.

CONCLUSION

This study presented a blockchain-enabled crop monitoring framework that integrates the InterPlanetary File System (IPFS) to provide secure, scalable, and efficient management of agricultural data. The combination of decentralized storage with blockchain-based traceability strengthens data integrity, reduces costs, and supports reliable real-time monitoring. Although the results are promising, the proposed system has certain limitations. Its evaluation was conducted mainly with controlled datasets, and large-scale field validation using extensive IoT deployments is still required. Furthermore, while Advanced Encryption Standard (AES) offers strong security and scalability, computational delays may arise in resource-constrained devices when processing high-frequency sensor streams.

Future work will focus on incorporating advanced deep learning models for more robust multi-disease detection, integrating IoT sensors with mobile applications for real-time alerts, and applying federated learning to enhance privacy and collaborative training. Expanding the system with multilingual interfaces and region-specific datasets will further improve usability and promote broader adoption among small and marginal farmers, strengthening the inclusiveness and sustainability of the proposed framework.

FUTURE SCOPE

Future work will focus on extending the system to large-scale real-world field deployments, integrating advanced deep learning models for multi-disease detection,

and developing a mobile application interface for real-time farmer alerts. Additional enhancements will include the adoption of federated learning techniques to improve data privacy and collaborative model training across geographically distributed farms.

DATA AVAILABILITY

https://www.kaggle.com/datasets/osamajalilhassan/agriculture-crops-dataset

REFERENCES

Abdulhamid A, Rahman MM, Kabir S, Ghafir I. 2024. Enhancing safety in IoT systems: A model-based assessment of a smart irrigation system using fault tree analysis. Electronics 13 (6): 1156. https://doi.org/10.3390/electronics13061156

Akilan T, Baalamurugan KM. 2024. Automated weather forecasting and field monitoring using GRU-CNN model along with IoT to support precision agriculture. Expert Systems with Applications 249: 123468. https://doi.org/10.1016/j.eswa.2024.123468

Alharbi A. 2023. Applying access control enabled blockchain (ACE-BC) framework to manage data security in the CIS system. Sensors 23 (6): 3020. https://doi.org/10.3390/s23063020

Alotaibi, Y., Rajendran, B. and Rajendran, S., 2024. Dipper throated optimization with deep convolutional neural network-based crop classification for remote sensing image analysis. PeerJ Computer Science, 10, p.e1828. https://doi.org/10.7717/peerj-cs.1828

Eisfelder C, Boemke B, Gessner U, Sogno P, Alemu G, Hailu R, Mesmer C, Huth J. 2024. Cropland and crop type classification with Sentinel-1 and Sentinel-2 time series using Google Earth engine for agricultural monitoring in Ethiopia. Remote Sensing 16 (5): 866. https://doi.org/10.3390/rs16050866

Goel A, Neduncheliyan S. 2023. An intelligent blockchain strategy for decentralised healthcare framework. Peer-to-Peer Networking and Applications 16 (2): 846–857. 10.1007/s12083https://doi.org/-022-01429-x

Krishnan, N., Surendran, R. and Nathan, M., 2022, December. Crop tracker-A web application to sell or buy crops and predict crop price using machine learning. In 6th Smart Cities Symposium (SCS 2022), 2022: 152-156. IET. https://doi.org/10.1049/icp.2023.0386.

Kumar Pradhan A, Kumar D, Chaurasia H, Murmu S, Samal I, Kumar Bhoi T, Kumar GAK, Mondal B. 2024. Crop monitoring system integrating with Internet of Things and artificial intelligence. *In* Advances in Geographical and Environmental Sciences Springer Nature: Singapore, pp: 193–208. https://doi.org/10.1007/978-981-97-0341-8_10

Li H, Shi F. 2024. A DETR-like detector-based semi-supervised object detection method for *Brassica Chinensis* growth monitoring. Computers and Electronics in Agriculture 219: 108788. https://doi.org/10.1016/j.compag.2024.108788

Mahalingam N, Sharma P. 2023. An intelligent blockchain technology for securing an IoT-based agriculture monitoring system. Multimedia Tools and Applications 83 (4): 10297–10320. https://doi.org/10.1007/s11042-023-15985-8

Maity T, Paul S, Samanta J, Saha P. 2024. Design and development of IoT-based SmartTech-agri devices for smart agriculture crop field. Journal of The Institution of Engineers (India): Series B 105 (4): 753–762. https://doi.org/10.1007/s40031-024-01002-5

Morellos A, Dolaptsis K, Tziotzios G, Pantazi XE, Kateris D, Berruto R, Bochtis D. 2024. An IoT transfer learning-based service for the health status monitoring of grapevines. Applied Sciences 14 (3): 1049. https://doi.org/10.3390/app14031049

Nduku L, Munghemezulu C, Mashaba-Munghemezulu Z, Masiza W, Ratshiedana PE, Kalumba AM, Chirima JG. 2024. Field-Scale winter wheat growth prediction applying machine learning methods with unmanned aerial vehicle imagery and soil properties. Land 13 (3): 299. https://doi.org/10.3390/land13030299

Omia E, Bae H, Park E, Kim MS, Baek I, Kabenge I, Cho BK. 2023. Remote sensing in field crop monitoring: A comprehensive review of sensor systems, data analyses and recent advances. Remote Sensing 15 (2): 354. https://doi.org/10.3390/rs15020354

Padmini MS, Kuzhalvaimozhi S. 2024. Energy and delay aware routing model for smart crop monitoring application using internet of things. Computers and Electrical Engineering 116: 109207. https://doi.org/10.1016/j.compeleceng.2024.109207

Panek-Chwastyk E, Dąbrowska-Zielińska K, Kluczek M, Markowska A, Woźniak E, Bartold M, Ruciński M, Wojtkowski C, Aleksandrowicz S, Gromny E, *et al*. 2024. Estimates of crop yield anomalies for 2022 in Ukraine based on Copernicus Sentinel-1, Sentinel-3 Satellite Data, and ERA-5 agrometeorological indicators. Sensors 24 (7): 2257. https://doi.org/10.3390/s24072257

Peng M, Liu Y, Khan A, Ahmed B, Sarker SK, Ghadi YY, Bhatti UA, Al-Razgan M, Ali YA. 2024. Crop monitoring using remote sensing land use and land change data: Comparative analysis of deep learning methods using pre-trained CNN models. Big Data Research 36: 100448. https://doi.org/10.1016/j.bdr.2024.100448

Pourvahab M, Ekbatanifard G. 2019. Digital forensics architecture for evidence collection and provenance preservation in IaaS cloud environment using SDN and blockchain technology. IEEE Access 7: 153349–153364. https://doi.org/10.1109/access.2019.2946978

Ramamoorthi S, Appathurai A. 2023. Energy aware clustered blockchain data for IoT: An end-to-end lightweight secure and enroute filtering approach. Computer Communications 202: 166–182. https://doi.org/10.1016/j.comcom.2023.02.010

Reddy, P.S., Surendran, R., Divya, K., Raveena, S., Selvaperumal, S.K. and Lakshamanan, R., 2024, August. Accuracy analysis and comparison of crop yield prediction using NB algorithm and RNN. In AIP Conference Proceedings, 3161(1). p. 020363. AIP Publishing LLC. https://doi.org/10.1063/5.0229471.

Shammi SA, Huang Y, Feng G, Tewolde H, Zhang X, Jenkins J, Shankle M. 2024. Application of UAV multispectral imaging to monitor soybean growth with yield prediction through machine learning. Agronomy 14 (4): 672. https://doi.org/10.3390/agronomy14040672

Stephen A, Arumugam P, Arumugam C. 2023. An efficient deep learning with a big data-based cotton plant monitoring system. International Journal of Information Technology 16 (1): 145–151. https://doi.org/10.1007/s41870-023-01536-9

Velmurugadass P, Dhanasekaran S, Shasi Anand S, Vasudevan V. 2021. Enhancing blockchain security in cloud computing with IoT environment using ECIES and cryptography hash algorithm. Materials Today: Proceedings 37: 2653–2659. https://doi.org/10.1016/j.matpr.2020.08.519

Wei Z, Fang W. 2024. UV-NDVI for real-time crop health monitoring in vertical farms. Smart Agricultural Technology 8: 100462. https://doi.org/10.1016/j.atech.2024.100462

Agrociencia

ANTIOXIDANT ACTIVITY OF BOVINE MILK WHEY HYDROLYSATES OBTAINED BY ENZYMATIC ACTION

Arely **León-López**[1], Pinito **Saavedra-Suárez**[2], Adelfo **García-Ceja**[1], Antonio de Jesús **Cenobio-Galindo**[2], Gabriel **Aguirre-Álvarez**[2,3*]

[1]Tecnológico Nacional de México. Instituto Tecnológico Superior de Venustiano Carranza, Avenida Tecnológico S/N, Ciudad Lázaro Cárdenas, Venustiano Carranza, Puebla, Mexico. C. P. 73049.
[2]Universidad Autónoma del Estado de Hidalgo. Instituto de Ciencias Agropecuarias. Avenida Universidad km 1, Rancho Universitario, Tulancingo, Hidalgo. Mexico. C. P. 43600.
[3]Uni-Collagen S.A. de C.V. Arnulfo González 203, El Paraíso, Tulancingo, Hidalgo, Mexico. C. P. 43684.
* Author for correspondence: aguirre@uaeh.edu.mx

Citation: León-López A, Saavedra-Suárez P, García-Ceja A, Cenobio-Galindo AJ, Aguirre-Álvarez G. 2025. Antioxidant activity of bovine milk whey hydrolysates obtained by enzymatic action. **Agrociencia** 59(8): 1179-1193. https://doi.org/ 10.47163/agrociencia.v59i8.3146

Editor in Chief:
Dr. Fernando C. Gómez Merino

Received: March 01, 2025.
Approved: November 14, 2025.
Published in Agrociencia: November 20, 2025.

ABSTRACT

Bovine Milk Whey (MW) is the primary by-product of the dairy industry and possesses highly beneficial nutritional and biological properties, making it economically and technologically valuable. MW was obtained from panela cheese and hydrolyzed with two proteolytic enzymes, Heliozym and HT Proteolytic 200, at different times (0, 0.25, 0.5, 1, 2, 3, 4, 6 h). The resulting hydrolysates were characterized through physicochemical analyses, Fourier-transform infrared spectroscopy (FTIR), isoelectric point (IP), molecular weight, thermal properties assessment, and evaluation of antioxidant activity using 2,2′-azino-bis (3-ethylbenzothiazoline-6-sulfonic acid) (ABTS) and 2,2-diphenyl-1-picrylhydrazyl (DPPH) radical inhibition assays. The composition of native bovine MW was 0.15 % fat, 0.43 % protein, 5.19 % lactose, and 0.36 % minerals. Sodium dodecyl sulfate polyacrylamide gel electrophoresis (SDS-PAGE) analysis revealed characteristic bands corresponding to β-lactoglobulin (18 kDa), α-lactalbumin (14.0 kDa), bovine serum albumin (BSA) (66.4 kDa), lactoferrin (75 kDa), immunoglobulin G (IgG, ~160 kDa), and protease peptone (Pp) (25–30 kDa). The IP (isoelectric point) of native whey shifted from 4.58 to 3.97 after 3 h of treatment with Heliozym. Conversely, after 4 h, the HT Proteolytic 200 sample showed an IP of 8.94. Thermal analysis indicated that the endothermic curves of α-lactalbumin and β-lactoglobulin were not detected, suggesting complete protein degradation after 6 h. Luminosity values varied significantly ($p < 0.05$) during enzymatic treatment, with notable differences between hydrolysates resulting from Heliozym and HT Proteolytic 200 action. Antioxidant activity showed maximum ABTS radical inhibition at 6 h of treatment, with values of 97.98 ± 0.85 % for Heliozym and 79.74 ± 2.4 % for HT Proteolytic 200. For DPPH radical inhibition, peak values were 36.33 ± 1.61 % for HT Proteolytic 200 and 41.31 ± 3.17 % for Heliozym after 6 h. The final properties of whey hydrolysates were influenced by substrate pretreatment, hydrolysis conditions, temperature and pH, and the specific enzyme used.

Keywords: enzymatic hydrolysis, isoelectric point, antioxidant activity.

INTRODUCCTION

Milk whey (MW) is a yellowish to greenish clear liquid obtained after milk coagulation during the cheese-making process, represents 85–95 % of the volume of milk, and contains minerals, proteins, and lactose (Kaminarides *et al*., 2020; León-López *et al*., 2022). MW can be classified into sweet and acid whey. Sweet whey presents a pH > 5.6, a water content of 93–94 %, 6–10 g L^{-1} of protein, 2.5–4.7 g L^{-1} of mineral, and a lactose content of 46–52 g L^{-1}. It is produced through enzymatic action. Acid whey presents a pH < 5.6, a water content of 94–98 %, 6–8 g L^{-1} of protein, 4.3–7.2 g L^{-1} of minerals, and a lactose content of 44–46 g L^{-1}, and is obtained by organic acid action. MW also contains lactic and citric acids, non-protein nitrogen compounds such as urea and uric acid, and B-group vitamins (Sarabandi *et al*., 2022).

MW is the most important waste in the dairy industry, as it presents highly beneficial nutritional and biological properties, making it economically and technologically valuable. MW proteins are a mix of different proteins such as β-lactoglobulin (2.9 g L^{-1}), α-lactoalbumin (0.6 g L^{-1}), immunoglobulin (0.3 g L^{-1}), serum albumin (0.6 g L^{-1}), lactoferrin (0.1 g L^{-1}), lactoperoxidase (0.03 g L^{-1}), protease-peptone (1 g L^{-1}), and glycomacropeptide (GMP) (0.9 g L^{-1}). MW proteins have the highest nutritional quality and biological value. They contain essential amino acids such as cysteine and branched-chain amino acids, described as leucine, isoleucine, and valine (Smithers, 2008). MW proteins also contain peptides with biological activity, such as antioxidant, antimicrobial, antihypertensive, anticancer, and immunomodulatory.

To release these peptides, it is necessary to apply enzymatic action, chemical treatment (acid or alkaline), microbial fermentation with proteolytic bacteria, ultrasound, thermal processes, and others (Nasri, 2017). MW protein hydrolysates have been considered one of the most important categories of raw material obtained from agro-food waste that can be used in different industries and are especially used as ingredients in food products such as meat products, dairies, bakeries, beverages, food supplements, or functional foods due to their nutritional and functional activities. The main objective of this research was the hydrolysis of bovine MW proteins by the enzymatic action of two different proteases under the same conditions of time and temperature, followed by the characterization of the resulting hydrolysates regarding their antioxidant activity and other parameters.

MATERIALS AND METHODS

Bovine milk whey was obtained from panela cheese production. A total of 40 L of skim milk was pasteurized (63 °C, 30 min), cooled to 40 ± 2 °C, and 7.5 g of $CaCl_2$ was added. Approximately 8.8 mL of rennet diluted in 5 mL of dH_2O was added to the milk, and after 30 min of waiting, the curd was formed, cut, and ripened for 20 min. The whey was then separated from the curd and used for the hydrolysates obtained.

Physicochemical composition

To evaluate fat, protein, lactose, total solids, and mineral salts of bovine MW (20 mL) at 4 °C from panela cheese elaboration, the infrared spectroscopy method was used with a FOSS Integrated Milk Testing Milkoscan FT 6000 (Foss Electric; Hillerød, Denmark).

Whey protein hydrolysis

Enzyme HT Proteolytic 200 was used at 0.1 % based on the weight of the protein substrate contained in whey, and 2 % w/v of Heliozym enzyme was used for 50 mL of whey. The hydrolysis was carried out at 50 °C for 6 h. Different samples were collected at 0, 0.25, 0.5, 1, 2, 3, 4, and 6 h. After hydrolysis, the samples were heated to 90 °C for 10 min to stop the hydrolysis treatment, and the samples were stored at 4 °C.

Determination of protein fractions

The sodium dodecyl sulfate gel electrophoresis (SDS-PAGE) method was used to determine protein fractions in whey hydrolysates. Gel concentrations of 15 % for the running gel and 4 % for the stacking gel were used. A volume of 1 mL of the sample was dissolved in 0.5 M Tris-HCl buffer pH 6.8 (1 % SDS, 10 % glycerol, and 0.01 % bromophenol blue) and heated to 90 °C for 5 min. The proteins were separated at 100 V for 2.5 h (ENDURO 300 V, USA). A molecular mass marker was used (BenchMark Protein Ladder, Thermo Scientific, MA, USA). The gels were stained with 0.05 % Coomassie Blue for 1 h (Schägger, 2006).

Isoelectric point determination

The isoelectric point of whey hydrolysates was measured according to Morand *et al*. (2011) with some modifications. Aqueous solutions of hydrolyzed whey were titrated with 1 M NaOH or 1 M HCl in a Zetasizer Malvern instrument (Zetasizer Nano ZS, UK). The test was performed at 25 °C with decreasing pH intervals of approximately 0.5 units. The isoelectric point of the sample was interpreted as the pH value at which the zeta potential value was zero.

Thermal properties of hydrolysates

The thermal measurements were carried out with a Q 2000 equipment with an RCS90 intracooler (TA Instruments; New Castle, DE, USA). It was calibrated with indium (Tm, onset = 1546.58 °C, ΔH = 28.45 J g^{-1}), and the detection conditions were 1.5 ± 0.1 mg of the sample. Prior to thermal analysis, the samples were stored in a hermetical container with P_2O_5 for 7 days to reach 0 % water content. The samples were packed and hermetically sealed in a stainless-steel pan, and an empty pan was used as a reference. Heating scan rates were performed from 16 °C to 150 °C at 5 °C min^{-1}. The TA 2000 analysis software (TA Instruments; New Castle, DE, USA) was used to determine the melting temperature (Tm) based on the endothermic changes recorded in the thermogram (Yang *et al*., 2013).

Color determination

A colorimeter CR-400/410 (Konica Minolta, Japan) was used to evaluate the color in the hydrolysates. The color measurement was expressed in luminosity (L*), + red, - green (a*) and + yellow, - blue (b*) parameters.

Antioxidant activity by radical inhibition

The radicals used to evaluate the antioxidant activity of the hydrolysates were 2,2'-azino-bis (3-ethylbenzothiazoline-6-sulfonic acid) (ABTS) and 2,2-diphenyl-1-picrylhydrazyl (DPPH). The ABTS radical solution was prepared according to Re *et al*. (1999). A solution of 2.45 mM potassium persulfate was mixed with 7 mM ABTS (Sigma-Aldrich; St. Louis, MI, USA). The mixture was stirred in the dark at room temperature for 16 h. The ABTS solution was stabilized to 0.7 ± 0.02 at 734 nm using ethanol. Then, 2 mL of the sample and 1 mL of the stabilized ABTS radical solution were mixed, and after 6 min the absorbance was measured at 734 nm in a spectrophotometer (Jenway Genova, Model 6705, Bibby Scientific; Staffordshire, UK).

For the DPPH scavenging reaction, 0.5 mL of the sample was mixed with 2.5 mL of 6.1 × 10^{-5} M DPPH radical (Sigma-Aldrich; St. Louis, MI, USA). The mixture was stored in darkness for 30 min and then read in a spectrophotometer (Jenway Genova, Model 6705, Bibby Scientific; Staffordshire, UK) at 515 nm (Brand-Williams *et al*., 1995). The antioxidant activity of both ABTS and DPPH radical scavenging was calculated according to the following equation:

$$\%\ inhibition = \frac{Initial\ absorbance - Final\ absorbance}{Initial\ absorbance} \times 100$$

Statistical analysis

The experiments were carried out in triplicate. The data obtained were evaluated by analysis of variance (ANOVA). All data were analyzed using the SPSS version 23 statistical program (IBM SPSS Statistics), with a significance level of $p < 0.05$ using (Tukey test).

RESULTS AND DISCUSSIONS

Bovine milk whey physicochemical composition

Fat present in MW was around 0.05 %, and it was composed of 66 % non-polar lipids (triacylglycerols and diacylglycerols) and 33 % polar lipids (phospholipids, phosphatidylethanolamine, phosphatidylcholine, sphingomyelins, phosphatidylinositol, and phosphatidylserine). The difference in fat concentration in MW and milk is related to the type of cheese and the source of the milk used for cheese production (Carter *et al*., 2018). MW from panela cheese showed 5.41 % total solids.

This result is similar to Barros *et al*. (2021), who reported 6.55 % total solids in whey from fresh cheese production. However, Cabral *et al*. (2019) obtained 17 % total solids in whey from fresh cheese production using cow milk.

The MW used in this research contained 4.8 g of mineral salts, representing a reduction of approximately 50 % from the initial milk content. Sweet whey can contain Ca, P, Na, K, and important trace minerals such as Fe, Zn, Cu, and Mg. In this research, the content of mineral salts was 0.36 % (Table 1), similar to the range reported by Suárez *et al*. (2009), who obtained values of 0.37–0.54 and 0.25–0.47 % of mineral salts in sweet whey.

Table 1. Physicochemical composition of bovine milk whey from panela cheese elaboration.

Sample	Fat (%)	Protein (%)	Lactose (%)	Total solids (%)	Mineral salts (%)
Milk whey	0.15	0.43	5.19	5.41	0.36

Lactose is a disaccharide composed of glucose and galactose, and it is the major carbohydrate present in sweet whey. This disaccharide promotes Ca, Mg, and P absorption in the intestines, favoring bone mineralization and the growth of beneficial bifidobacteria for colorectal health and the utilization of vitamin C (Karami and Akbari-Adergani, 2019). Lactose concentration in bovine MW was 5.19 %. However, Cabral *et al*. (2019) reported higher lactose concentrations (10–13.2 %). The concentration of lactose in whey can be related to the type of cheese and the source of milk used for its elaboration.

Protein concentrations in whey typically range from 20 to 25 %, with the predominant proteins being β-lactoglobulin (β-Lg), α-lactalbumin (α-La), bovine serum albumin (BSA), lactoferrin, and immunoglobulins (Ig) (Jauregi *et al*., 2021). In the present study, protein levels were considerably lower, ranging from 0.34 to 0.46 %. Such variation is largely attributable to cheese-making practices, including the type of cheese produced and the characteristics of the milk used, which generate whey with distinct sensory, nutritional, and technological properties.

Accurate determination of whey composition is essential for assessing its techno-functional and biological quality, thereby enabling the optimization of its technological performance and the adjustment of processing strategies (Mazorra-Manzano and Moreno-Hernández, 2019). Until now, most of the research on sweet whey valorization has focused on the recovery of components such as whey proteins, lactose, and minerals. Another major focus has been applying fermentation techniques to generate valuable outputs such as organic acids and oligosaccharides.

Electrophoretic profile of whey protein hydrolysates

SDS-PAGE profiles of whey protein hydrolysates obtained at different reaction times using HT Proteolytic 200 (Figure 1A) and Heliozym (Figure 1B) revealed distinct band patterns. The band corresponding to β-lactoglobulin was consistently observed at approximately 18 kDa. β-Lactoglobulin is a small, soluble, globular protein composed of 162 amino acids in a single polypeptide chain and accounts for roughly 60 % of total whey proteins. The molecular weights observed here are comparable to those reported for bovine and goat whey proteins hydrolyzed with Alcalase, trypsin, and amylase under varying conditions of time (30–300 min), temperature (30–70 °C), and enzyme concentration (0.25–2 %) (García-Casas *et al*., 2022). α-Lactalbumin, which constitutes approximately 20 % of total whey proteins, was detected as a band near 14 kDa.

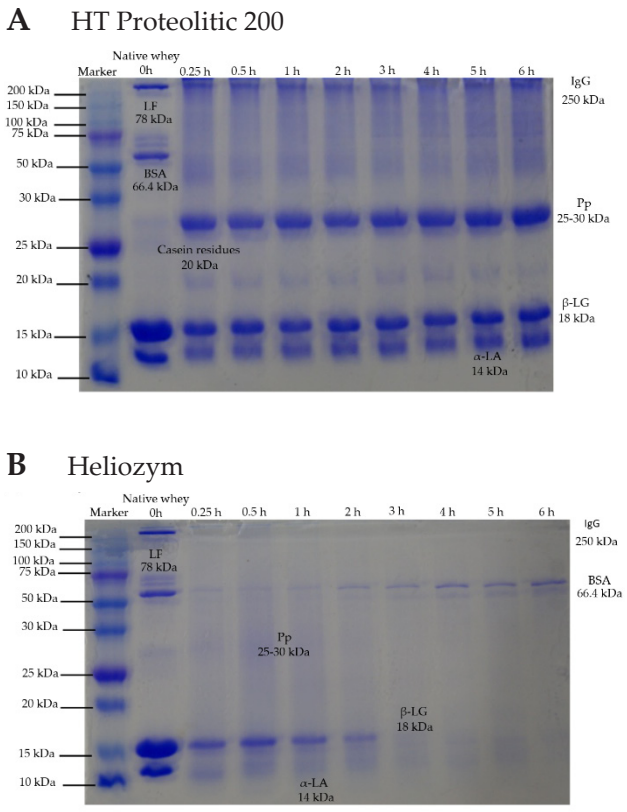

Figure 1. Electrophoretic profile of milk whey hydrolysates obtained by different proteases A: HT Proteolytic 200; B: Heliozym. The first column represents the marker (10–250 kDa). Columns 2–10 show the samples at different times of enzyme hydrolysis (0, 0.25, 0.5, 1, 2, 3, 4, 5, and 6 h).

Previous works observed similar results, reporting MW values of approximately 14.2, 14.17, and 14 kDa for this protein. BSA contains 17 cross-linked disulfide bonds formed by cysteine residues that stabilize its structure and represent about 3 % of the total protein. BSA consists of 583 amino acid residues arranged in a single polypeptide

chain. Its band was detected at approximately 66.4 kDa for both hydrolysis treatments. Previous studies have reported BSA bands within a similar molecular-weight range in bovine MW hydrolysates obtained by protease treatment and fermentation (Mazorra-Manzano and Moreno-Hernández, 2019).

Lactoferrin (LF) consists of a single polypeptide chain of 689 amino acids with a molecular weight of 78 kDa and represents 3 % of total whey proteins. The representative band for lactoferrin was observed around 75 kDa (Goulding *et al*., 2021). This band appears at 6 h of treatment with the HT Proteolytic 200 enzyme (Figure 1A); however, in the Heliozym treatment, the band is only observed in native whey. This result agrees well with previous works reporting lactoferrin bands around 70, 75, and 78 kDa (García-Casas *et al*., 2022).

The protein that represents 10 % of whey proteins is immunoglobulin (IgG), with a molecular weight of ~160 kDa and relatively stable to heat. The representative IgG bands are observed around 250 kDa (Figure 1A). A band was also observed around 25–30 kDa (Figure 1A) in the HT Proteolytic 200 enzyme treatment, corresponding to protease peptone (Pp), which is a mixture of proteins and peptides that results from casein proteolysis and has a molecular weight of ~28 kDa. The Pp band was only detected in native whey at approximately 25–30 kDa (Figure 1B). Bands representative of glycomacropeptide (GMP) were not observed in either figure, as this peptide contains 64 amino acids and has a molecular weight of 6.8 kDa (León-López *et al*., 2022).

Isoelectric point of whey hydrolysates

Proteins and hydrolysates exhibit an isoelectric point (IP), defined as the pH at which the net electric charge is zero; this property enables the identification and differentiation of specific hydrolysates and proteins. Native whey displayed three IP values: pH 4.58, associated with bovine serum albumin (BSA) and α-lactalbumin; pH 5.37, associated with β-lactoglobulin; and pH 8.66, associated with lactoferrin (Table 2). After 0.25 h

Table 2. PI in the kinetics of the hydrolysis by the action of different enzymes.

Hydrolysis time	Heliozym	HT Proteolytic 200
Native whey	4.58	4.58
	5.37	5.37
	8.66	8.66
0.25 h	5.90	5.70
0.5 h	5.90	6.50
1 h	6.10	6.50
2 h	8.90	7.00
3 h	3.70	8.02
4 h	----	8.94

Thermal properties of whey hydrolysates were determined using Differential Scanning Calorimetry (DSC).

of hydrolysis, the IP values were 5.7 and 5.9 for the treatments with Heliozym and HT Proteolytic 200, respectively. These findings indicate that the observed IP values correspond to β-LG peptides 92–101 and BSA peptides 490–495, considering that the enzyme used is of microbial origin and the treatments were conducted at pH 8 and 42–45 °C.

After 1 h of hydrolysis, the IP was 6.1 for Heliozym and 6.5 for HT Proteolytic 200. These values are associated with peptides β-LG 61–70 and BSA 29–39, respectively. Similar findings were reported in previous studies where trypsin and chymotrypsin were used for hydrolysate production (Wijayanti *et al*., 2014). The isoelectric points of 8.9 (Heliozym) and 7.0 (HT Proteolytic 200) correspond to β-LG 1–8, β-LG 78–83, β-LG, α-LA 105–108, and LF 18–35, respectively. These results align with those reported by Khajeh *et al.* (2021), who applied pepsin and heat treatment for whey hydrolysis.

At 3 h of treatment with the Heliozym enzyme, the IP of 3.7 corresponded to β-LG 33–39, β-LG 125–135, and β-LG 125–136 peptides. HT Proteolytic 200 showed an IP of 8.02, which is associated with the BSA 433–442 peptide (Power *et al*., 2014). However, for the Heliozym treatment after 4 h of hydrolysis, no values were recorded. For HT Proteolytic 200, the IP was 8.94, indicating the presence of LF 23–32, LF 47–53, and LF 49–55 peptides (Khajeh *et al*., 2021). No IP values were obtained for the samples at 5 and 6 h. Enzymatic hydrolysis and heating influence the IP value because the rate of hydrolysis increases as hydrolytic sites become exposed, raising the number of peptide bonds available for enzymatic attack (Wijayanti *et al*., 2014).

Thermal analysis provides information on transition temperatures, degree of crystallization, melting behavior, and heat capacity. Assessing the thermal properties of whey proteins and their hydrolysates is important because these properties are linked to stability and the thermodynamics of protein unfolding associated with the unfolding transition and temperature. Native whey exhibited three endothermic events: the first at approximately 65.5–70 °C, corresponding to the denaturation of α-lactalbumin; the second between 71 and 75.5 °C, related to β-lactoglobulin; and the third at 70–71 °C, associated with the denaturation of bovine serum albumin (BSA) (Figure 2).

Previous works reported denaturation temperatures for whey proteins β-lactoglobulin and α-lactalbumin around 78.7–87 °C, where the protein was hydrolyzed by thermal treatment at 80 °C for 15 min (Kumar *et al*., 2022). After 6 h of enzymatic hydrolysis, the endothermic curves of α-lactalbumin and β-lactoglobulin were not detected due to the complete hydrolysis of whey proteins. However, the BSA peak was still detected around 70–71.0 °C in the Heliozym treatment. When the temperature of whey proteins increases above 60 °C, their structure unfolds, exposing hydrophobic and thiol groups. At temperatures between 65–70 °C, the protein undergoes reversible conformational modifications, marking the denaturation temperature.

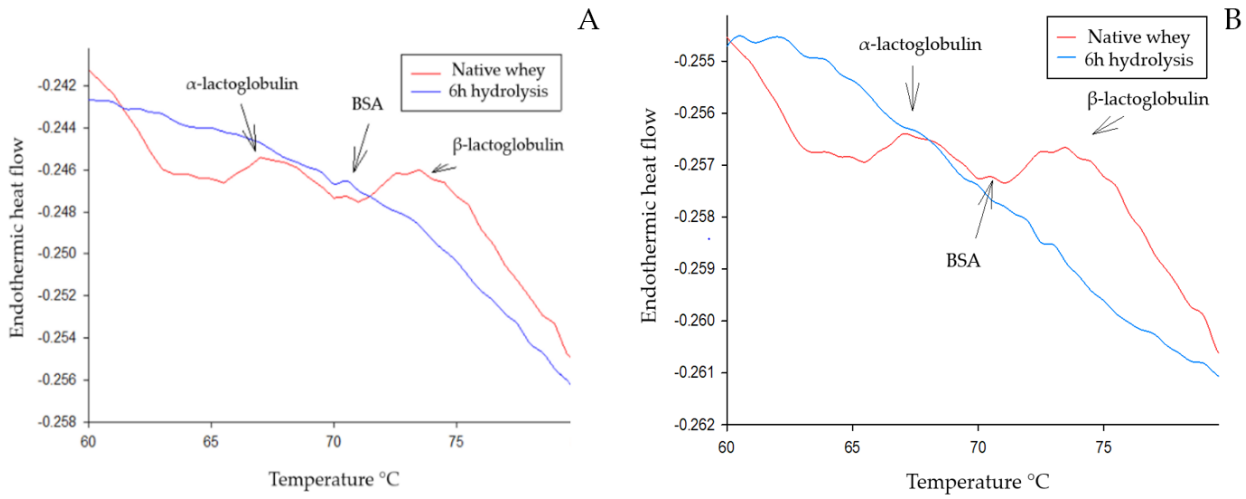

Figure 2. Comparison of native milk whey (0 h) and 6 h hydrolyzed whey thermograms. A: hydrolyzed with Heliozym; B: hydrolyzed with HT Proteolytic 200.

Color of the whey hydrolysates

Bovine MW is a yellow-green liquid. Luminosity (L) showed changes during enzymatic treatment; native whey presented significant differences ($p < 0.05$) compared with the other samples, with L values increasing to 49.62 ± 0.01 and 49.85 ± 0.08 for Heliozym and HT Proteolytic 200, respectively (Table 3). This change can be attributed to the loss of total solids in the hydrolyzed whey (Preci *et al*., 2021).

The a* parameter indicates greenish color. Bovine MW showed significant differences ($p < 0.05$) compared with hydrolysates (0.25, 0.5, and 1 h) obtained through Heliozym

Table 3. Color evaluation of whey hydrolysates during enzymatic action. Different letters represent the average of three replicates and indicate a significant difference at p<0.05.

	Heliozym			HT Proteolytic 200		
Hydrolysis time	L	a*	b*	L	a*	b*
Native	49.09 ± 0.10^{a}	-4.12 ± 0.01^{a}	10.22 ± 0.05^{a}	49.09 ± 0.10^{a}	-4.12 ± 0.01^{a}	10.22 ± 0.05^{a}
0.25 h	49.41 ± 0.05^{abc}	-3.27 ± 0.04^{bc}	7.64 ± 0.02^{bc}	49.15 ± 0.15^{ab}	-3.81 ± 0.04^{ab}	9.38 ± 0.10^{b}
0.5 h	49.42 ± 0.08^{abc}	-3.20 ± 0.02^{bc}	7.48 ± 0.02^{bc}	49.38 ± 0.25^{abc}	-3.80 ± 0.03^{ab}	9.33 ± 0.10^{b}
1 h	49.43 ± 0.17^{abc}	-3.15 ± 0.02^{bc}	7.17 ± 0.04^{c}	49.63 ± 0.13^{cd}	-3.75 ± 0.03^{abc}	9.03 ± 0.03^{b}
2 h	49.45 ± 0.11^{bc}	-3.08 ± 0.02^{cd}	7.06 ± 0.03^{cd}	49.66 ± 0.13^{cd}	-3.71 ± 0.04^{bc}	9.07 ± 0.03^{b}
3 h	49.47 ± 0.04^{bc}	-3.01 ± 0.03^{cd}	7.00 ± 0.06^{cd}	49.66 ± 0.06^{cd}	-3.65 ± 0.04^{bcd}	8.52 ± 0.40^{c}
4 h	49.60 ± 0.01^{cd}	-2.99 ± 0.03^{de}	6.99 ± 0.03^{cd}	49.70 ± 0.08^{cd}	-3.64 ± 0.02^{bcd}	8.39 ± 0.06^{c}
5 h	49.69 ± 0.01^{cd}	-2.95 ± 0.05^{de}	6.98 ± 0.02^{cd}	49.72 ± 0.09^{cd}	-3.63 ± 0.03^{bcd}	8.29 ± 0.12^{c}
6 h	49.62 ± 0.01^{cd}	-2.71 ± 0.52^{f}	6.77 ± 0.06^{d}	49.85 ± 0.08^{d}	-3.38 ± 0.01^{cd}	7.88 ± 0.05^{d}

Color expressed in luminosity (L*) and parameters + red, - green (a*), and + yellow, - blue (b*).

action. After 2 h of enzymatic treatment, no further changes in the a* value were observed. Similar results were obtained with the HT Proteolytic 200 enzyme, where native whey showed significant differences ($p < 0.05$) compared with treatments at different hydrolysis times (Rukluarh *et al*., 2019).

The b* parameter indicates yellow color in positive values. In the Heliozym treatment, MW showed significant differences ($p < 0.05$), reaching a b* value of 6.77 ± 0.06 after 6 h of hydrolysis. For hydrolysates obtained with HT Proteolytic 200, MW presented significant differences ($p < 0.05$) in samples at the early stages of hydrolysis (0.25, 0.5, 1, and 2 h). Other studies have reported that increasing hydrolysis time causes darkening in whey samples, particularly when hydrolysis occurs at different pH values ranging from 2.4 to 9 (Egerton *et al*., 2018).

Antioxidant activity of whey hydrolysates

Enzymatic hydrolysis is one of the most common methods used to generate bioactive peptides from native proteins. The most widely used enzymes are proteases, which are capable of promoting specific and selective protein modifications. During enzymatic digestion, peptides become exposed and exhibit functional properties such as antioxidant and antimicrobial activity. The enzymes Heliozym and HT Proteolytic 200 used in this study have high cleavage specificity and remain stable under different experimental conditions. Whey hydrolysates were evaluated for their antioxidant capacity through ABTS radical scavenging (Figure 3A) and DPPH inhibition (Figure 3B).

ABTS radical scavenging capacity is based on the ability of whey hydrolysates to neutralize the radical cation through decolorization generated by oxidation with potassium persulfate and its subsequent reduction by interaction with hydrogen-donor molecules. This method is widely used to evaluate both hydrophilic and

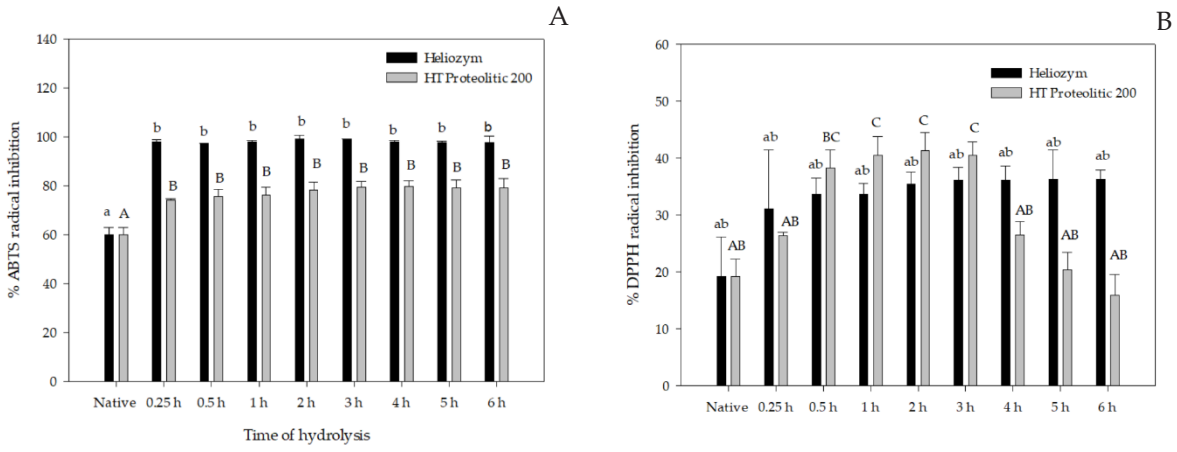

Figure 3. Antioxidant activity of whey hydrolysates from Heliozym and HT Proteolytic 200. A: 2,2′-azino-bis (3-ethylbenzothiazoline-6-sulfonic acid) (ABTS); B: 2,2-diphenyl-1-picrylhydrazyl (DPPH) radical scavenging. Different letters represent the mean of three replicates and indicate significant differences (Tukey, $p < 0.05$).

lipophilic antioxidants. For the sample without enzymatic treatment (native whey), ABTS radical inhibition was 59.8 ± 3.06 %, showing a significant difference ($p < 0.05$) compared with the other treatments. The hydrolysates obtained with both enzymes showed no significant differences ($p < 0.05$) among samples across different hydrolysis times. The highest radical inhibition values were 97.98 ± 0.85 % for Heliozym and 79.74 ± 2.4 % for HT Proteolytic 200. These results are higher than those previously reported: 65.18 % with pepsin (Zheng *et al*., 2022), 18 % with trypsin (Karami and Akbari-Adergani, 2019), 76.4 % with Alcalase, and 47 % with proteolytic enzyme at 4 h of hydrolysis and heat treatment.

DPPH is a free radical that accepts electrons or hydrogen from donor compounds. This assay is widely used to evaluate the antioxidant capacity of different compounds, including whey hydrolysates, to donate hydrogen atoms or electrons (Frezzini *et al*., 2019). The hydrolysates obtained through Heliozym treatment showed a significant difference ($p < 0.05$) between the native whey and the samples after 2 h of enzymatic treatment. The highest DPPH radical inhibition was 36.33 ± 1.61 % at 6 h of treatment. For HT Proteolytic 200, a significant difference ($p < 0.05$) was observed between the initial enzymatic treatment and the samples at 1, 2, and 3 h of hydrolysis. The highest inhibition was recorded at 3 h of treatment (41.31 ± 3.17 %).

Previous research has reported higher DPPH radical inhibition using different types of enzymes, such as Alcalase (63.54 %) and pepsin (66.97 %), as well as using other whey sources, including whey from mozzarella cheese (55.8 %) and donkey milk (68.43 %), and alternative processing methods, such as ultrasound (68.1 %). The variation in DPPH inhibition percentages is associated with the whey source, the type of enzyme, and the time and temperature conditions used during hydrolysis (León-López *et al*., 2022). The valorization of whey through enzymatic processes to obtain hydrolysates with low molecular weight and high functional activity, such as antioxidant, antimicrobial, and antiviral properties, offers a strategy for managing this by-product through the efficient and economical production of bioactive compounds with potential applications in the development of food and nutraceutical products, including beverages, meat, and dairy items.

Hydrolysis and antioxidant activity in bovine milk whey proteins

Most of the research on the valorization of bovine MW from cheese production focuses primarily on protein recovery (Kong *et al*., 2023). Whey proteins have a globular structure that includes disulfide bonds, which provide structural stability. The treatment and reuse of this type of whey are highly important, as it is one of the most environmentally polluting food by-products. Whey is considered a contaminant waste, making it a valuable source for obtaining added-value products such as whey hydrolysates (Du *et al*., 2022; León-López *et al*., 2022).

There are different methods to obtain hydrolysates from MW, including enzymatic action, fermentation, and chemical hydrolysis. However, enzymatic hydrolysis is widely recognized as an efficient, safe, and easy-to-control method due to its high

specificity, product safety, and mild production conditions. Proteases are the most commonly used enzymes in hydrolysis; nevertheless, it is essential to determine the appropriate treatment time and temperature, as the type of hydrolysates produced depends on these parameters (Muley *et al*., 2021).

The function of enzymes is to break peptide bonds when the denaturation of whey proteins occurs. In some cases, there are protein regions that remain inaccessible to the enzymes, where inactive peptides are present (da Cruz *et al*., 2020). The sensitivity of the enzyme can increase due to conditions such as the substrate/peptidase ratio, protein substrate pretreatment, temperature, pH of the hydrolysis conditions, reaction time, and type of protease, increasing the degree of hydrolysis (Shenana, 2019). The hydrolysates obtained from enzymatic treatment commonly present low molecular weight, around 6 kDa, with different charges, surface activity, improved solubility, and higher digestion and absorption rates, and they exhibit biological activities such as hypotensive, antimicrobial, antimutagenic, immunomodulating, and antioxidant effects.

Whey hydrolysates display diverse antioxidant functions, including free radical scavenging, hydrogen and electron donation, metal chelation, and inhibition of lipid oxidation, with activity increasing as hydrolysis releases more amino acids. These biological properties depend on peptide structure, amino acid sequence, and specific peptide composition (Du *et al*., 2022; León-López *et al*., 2022). Producing low-molecular-weight hydrolysates through controlled enzymatic hydrolysis of bovine MW is an effective strategy to obtain functional ingredients with strong antioxidant, antimicrobial, and other beneficial activities, suitable for incorporation into foods such as beverages, bread, and dairy products (Karami and Akbari-Adergani, 2019; Wei *et al*., 2024).

CONCLUSIONS

Bovine milk whey can be valorized when subjected to hydrolysis treatment by enzymatic action. The enzymatic treatment proved effective in generating hydrolysates with low molecular weight and greater antioxidant activity as the hydrolysis time increased. The final characteristics of bovine milk whey hydrolysates were influenced by specific conditions such as enzyme type, temperature, and treatment duration. This study provides useful information on the partial characterization of whey hydrolysates, and in future work, these products may be applied as ingredients in beverages and foods, dietary supplements, and other value-added applications.

ACKNOWLEDGEMENTS

The authors gratefully acknowledge Uni-Collagen S.A. de C.V. and the Secretariat of Science, Humanities, Technology and Innovation (SECIHTI) for their financial support, grant number 928897.

REFERENCES

Barros EL, da Silva CC, Canella MHM, Verruck S, Prestes AA, Vargas MO, Maran BM, Esmerino EA, Silva R, Balthazar CF, Calado VMA, Prudencio ES. 2021. Effect of replacement of milk by block freeze concentrated whey in physicochemical and rheological properties of ice cream. Food Science and Technology 42: e12521. https://doi.org/10.1590/fst.12521

Brand-Williams W, Cuvelier ME, Berset C. 1995. Use of a free radical method to evaluate antioxidant activity. LWT 28 (1): 25–30. https://doi.org/10.1016/S0023-6438(95)80008-5

Cabral SR, de Azevedo BB, da Silva MP, Figueiredo AS, Martins AL, de Pinho M. 2019. Optimization of cheese whey ultrafltration/diafltration for the production of beverage liquid protein concentrates with lactose partially removed. Journal of Membrane Science and Research 5 (2): 172–177. https://doi.org/10.22079/jmsr.2018.92367.1208

Carter B, Patel H, Barbano DM, Drake M. 2018. The effect of spray drying on the difference in flavor and functional properties of liquid and dried whey proteins, milk proteins, and micellar casein concentrates. Journal of Dairy Science 101 (5): 3900–3909. https://doi.org/10.3168/jds.2017-13780

da Cruz CZP, de Mendonça RJ, Guimaraes LHS, Ramos MAS, Garrido SS, de Paula AV, Monti R, Massolini G. 2020. Assessment of the bioactive potential of cheese whey protein hydrolysates using immobilized Alcalase. Food and Bioprocess Technology 13 (12): 2120–2130. https://doi.org/10.1007/s11947-020-02552-4

Du X, Jing H, Wang L, Huang X, Wang X, Wang H. 2022. Characterization of structure, physicochemical properties, and hypoglycemic activity of goat milk whey protein hydrolysate processed with different proteases. LWT 159: 113257. https://doi.org/10.1016/j.lwt.2022.113257

Egerton S, Culloty S, Whooley J, Stanton C, Ross R. 2018. Characterization of protein hydrolysates from blue whiting (*Micromesistius poutassou*) and their application in beverage fortification. Food Chemistry 245: 698–706. https://doi.org/10.1016/j.foodchem.2017.10.107

Frezzini MA, Castellani F, de Francesco N, Ristorini M, Canepari S. 2019. Application of DPPH assay for assessment of particulate matter reducing properties. Atmosphere 10 (12): 816. https://doi.org/10.3390/atmos10120816

García-Casas V, Seiquer I, Pardo Z, Haro A, Recio I, Olías R. 2022. Antioxidant potential of the sweet whey-based beverage colada after the digestive process and relationships with the lipid and protein fractions. Antioxidants 11 (9): 1827. https://doi.org/10.3390/antiox11091827

Goulding D, O'Regan J, Bovetto L, O'Brien N, O'Mahony J. 2021. Influence of thermal processing on the physicochemical properties of bovine lactoferrin. International Dairy Journal 119: 105001. https://doi.org/10.1016/j.idairyj.2021.105001

Jauregi P, Guo Y, Adeloye JB. 2021. Whey proteins-polyphenols interactions can be exploited to reduce astringency or increase solubility and stability of bioactives in foods. Food Research International 141: 110019. https://doi.org/10.1016/j.foodres.2020.110019

Kaminarides S, Zagari H, Zoidou E. 2020. Effect of whey fat content on the properties and yields of whey cheese and serum. Journal of the Hellenic Veterinary Medical Society 71 (2): 2149–2156. https://doi.org/10.12681/jhvms.23640

Karami Z, Akbari-Adergani B. 2019. Bioactive food derived peptides: A review on correlation between structure of bioactive peptides and their functional properties. Journal of Food Science and Technology 56 (2): 535–547. https://doi.org/10.1007/s13197-018-3549-4

Khajeh E, Jamshidian-Mojaver M, Naeemipour M, Farzin H. 2021. The identification of a novel peptide derived from lactoferrin isolated from camel milk with potential antimicrobial

activity. Iranian Journal of Medical Microbiology 15 (3): 302–316. https://doi.org/10.30699/ijmm.15.3.302

Kong L, Liu C, Tang H, Yu P, Wen R, Peng X, Yu X. 2023. Hygroscopicity and antioxidant activity of whey protein hydrolysate and its ability to improve the water holding capacity of pork patties during freeze–thaw cycles. LWT 182: 114784. https://doi.org/10.1016/j.lwt.2023.114784

Kumar L, Brennan M, Brennan C, Zheng H. 2022. Influence of whey protein isolate on pasting, thermal, and structural characteristics of oat starch. Journal of Dairy Science, 105 (1): 56–71. https://doi.org/10.3168/jds.2021-20711

León-López A, Pérez-Marroquín X, Estrada-Fernández A, Campos-Lozada G, Morales-Peñaloza A, Campos-Montiel R, Aguirre-Álvarez G. 2022. Milk whey hydrolysates as high value-added natural polymers: Functional properties and applications. Polymers 14 (6): 1258. https://doi.org/10.3390/polym14061258

Mazorra-Manzano M, Moreno-Hernández J. 2019. Propiedades y opciones para valorizar el lactosuero de la quesería artesanal. CienciaUAT 14 (1): 133–144. https://doi.org/10.29059/cienciauat.v14i1.1134

Morand M, Guyomarc'h F, Pezennec S, Famelart MH. 2011. On how κ-casein affects the interactions between the heat-induced whey protein/κ-casein complexes and the casein micelles during the acid gelation of skim milk. International Dairy Journal 21 (9): 670–678. https://doi.org/10.1016/j.idairyj.2011.01.012

Muley AB, Pandit AB, Singhal RS, Dalvi SG. 2021. Production of biologically active peptides by hydrolysis of whey protein isolates using hydrodynamic cavitation. Ultrasonics Sonochemistry 71: 105385. https://doi.org/10.1016/j.ultsonch.2020.105385

Nasri M. 2017. Protein hydrolysates and biopeptides: Production, biological activities, and applications in foods and health benefits. A review. Advances in Food and Nutrition Research 81: 109–159. https://doi.org/10.1016/bs.afnr.2016.10.003

Power O, Fernández A, Norris R, Riera FA, FitzGerald RJ. 2014. Selective enrichment of bioactive properties during ultrafiltration of a tryptic digest of β-lactoglobulin. Journal of Functional Foods 9: 38–47. https://doi.org/10.1016/j.jff.2014.04.002

Preci D, Fernandes I, Valduga E, Cansian RL, Steffens J, Steffens C, Brião V. 2021. Hidrólise de concentrado de soro de leite de ovelha por membrana e avaliação das propriedades antioxidantes e antimicrobianas. Scientia Plena 17 (2). https://doi.org/10.14808/sci.plena.2021.021501

Re R, Pellegrini N, Proteggente A, Pannala A, Yang M, Rice-Evans C. 1999. Antioxidant activity applying an improved ABTS radical cation decolorization assay. Free Radical Biology and Medicine 26 (9): 1231–1237. https://doi.org/10.1016/S0891-5849(98)00315-3

Rukluarh S, Kanjanapongkul K, Panchan N, Niumnuy C. 2019. Effect of inclusion conditions on characteristics of spray dried whey protein hydrolysate/γ-cyclodextrin complexes. Journal of Food Science and Agricultural Technology 5: 5–12.

Sarabandi K, Tamjidi F, Akbarbaglu Z, Samborska K, Gharehbeglou P, Kharazmi M, Jafari SM. 2022. Modification of whey proteins by sonication and hydrolysis for the emulsification and spray drying encapsulation of grape seed oil. Pharmaceutics, 14 (11): 2434. https://doi.org/10.3390/pharmaceutics14112434

Schägger H. 2006. Tricine–SDS-PAGE. Nature Protocols 1 (1): 16–22. https://doi.org/10.1038/nprot.2006.4

Shenana ME. 2021. Physico-chemical and functional properties of functional yoghurt made with different types of whey protein concentrates (Wpc). Annals of Agricultural Science, Moshtohor 59 (5): 455–462. http://doi:10.21608/assjm.2021.195014

Smithers GW. 2008. Whey and whey proteins—From 'gutter-to-gold'. International Dairy Journal 18 (7): 695–704. https://doi.org/10.1016/j.idairyj.2008.03.008

Suárez E, Lobo A, Álvarez S, Riera FA, Álvarez R. 2009. Demineralization of whey and milk ultrafiltration permeate by means of nanofiltration. Desalination 241 (1): 272–280. https://doi.org/10.1016/j.desal.2007.11.087

Wei M, Ning C, Ren Y, Hu F, Wang M, Li W. 2024. Characterisation and comparison of enzymatically prepared donkey milk whey protein hydrolysates. Food Chemistry: X 22: 101360. https://doi.org/10.1016/j.fochx.2024.101360

Wijayanti HB, Bansal N, Deeth HC. 2014. Stability of whey proteins during thermal processing: A review. Comprehensive Reviews in Food Science and Food Safety 13 (6): 1235–1251. https://doi.org/10.1111/1541-4337.12105

Yang N, Liu Y, Ashton J, Gorczyca E, Kasapis S. 2013. Phase behaviour and *in vitro* hydrolysis of wheat starch in mixture with whey protein. Food Chemistry 137 (4): 76–82. https://doi.org/10.1016/j.foodchem.2012.10.004

Zheng Y, Pang J, Liu Z. 2022. The purification and identification of antioxidants and dipeptidyl peptidase IV inhibitory peptides from whey protein hydrolysates. Food Bioengineering 1 (3–4): 298–306. https://doi.org/10.1002/fbe2.12027

Agrociencia

EXTRACTION OF SWEET POTATO (*Ipomoea batatas* L.) ANTHOCYANINS AND THEIR APPLICATION AS A NATURAL DYE IN YOGURT

Oscar **Reyes-Morales**[1], Keisy **Peralta-Matute**[1], Beatriz **Guerrero-León**[2], Juan **Maita-Chamba**[3], Dani **Ochoa-Cervantez**[4], Percy **García**[5], Jhunior Abrahan **Marcía-Fuentes**[1*]

[1]Universidad Nacional de Agricultura. Facultad de Ciencias Tecnológicas. Catacamas, Olancho, Honduras. C. P. 16101.
[2]Universidad Nacional de Loja. Centro de Investigación, Desarrollo e Innovación en Nutrición Animal (CIDiNA). Loja, Ecuador. C. P. 110101.
[3]Universidad Nacional de Loja. Centro de Investigaciones Tropicales del Ambiente y Biodiversidad. Loja, Ecuador. C. P. 110101.
[4]Universidad Nacional de Ciencias Forestales. Siguatepeque, Comayagua, Honduras.
[5]Fortalece Consultants Inc.
* Author for correspondence: jmarcia@unag.edu.hn

Citation: Reyes-Morales O, Guerrero-León, B, Maita-Chamba J, Ochoa-Cervantez D, García P, Marcía-Fuentes JA. 2025. Extraction of sweet potato (*Ipomoea batatas* L.) anthocyanins and their application as a natural dye in yogurt. **Agrociencia** 59(8): 1194-1209. https://doi.org/ 10.47163/agrociencia.v59i8.3424

Editor in Chief:
Dr. Fernando C. Gómez Merino

Received: February 04, 2025.
Approved: November 14, 2025.
Published in Agrociencia: November 25, 2025.

ABSTRACT

The aim of this investigation was to obtain a natural dye by ultrasound-assisted extraction from purple sweet potato (*Ipomoea batatas* L.) for its application in yogurt. The extraction parameters were optimized using a Box-Behnken design and response surface methodology in 15 treatments. Temperature, ethanol concentration, and sonication time were the variables studied in the extraction process, with anthocyanin concentration serving as the response variable, which was determined using the differential pH method. Treatment T11 was identified as the best treatment, with the following extraction conditions: a temperature of 60 °C, ethanol concentration of 60.16 %, and sonication time of 20 min. The concentration of anthocyanins fluctuated between 59.7 and 66.47 mg of cyanidin-3-glucoside L^{-1}. From T11, three yogurt samples were formulated with 0.6, 0.8, and 1 % of extract and a control without any addition (0 %). These samples were evaluated through sensory analysis with a hedonic scale of nine points with 50 panelists. The formulations with anthocyanins received favorable scores; the yogurt with 1 % dye stood out for having the highest acceptance in terms of color, although for the remaining attributes (flavor, aroma, and consistency), the yogurt with 0.8 % scored higher. In general, all samples with natural dye obtained an acceptable evaluation. Therefore, the extract can be used as a natural dye in yogurt without issue, making it a viable alternative to synthetic dyes and potentially leading to the development of functional foods due to its bioactive compound content.

Keywords: natural dye, ultrasound, sensory analysis.

INTRODUCTION

The growing interest in the intake of natural and healthy foods has driven many investigations for ingredients or bioactive compounds that benefit human health (Montero *et al*., 2020; Marcía-Fuentes *et al*., 2021; Maddela and García, 2021). In this context, the sweet potato (*Ipomoea batatas* L.) stands out for its high content of antioxidants such as anthocyanins and beta-carotene. The anthocyanins found in the skin of the purple sweet potato are known for their ability to be used as natural dyes, offering a healthy and sustainable alternative to the synthetic dyes used in the food industry (Coba-Carrera *et al*., 2019; Marcía-Fuentes *et al*., 2020; Saravia-Maldonado *et al*., 2020; Santos-Alemán *et al*., 2023a).

Anthocyanins have been shown in clinical and preclinical studies to have anti-inflammatory properties, reducing markers such as C-reactive protein, IL-6, or TNF-α, and improving endothelial function and vascular health. Additionally, they modulate the intestinal microbiota positively, stimulating beneficial bacteria such as *Bifidobacterium* and *Lactobacillus*, and favor the production of short-chain fatty acids, which are associated with better digestive and metabolic health (Fallah *et al*., 2020; Saini *et al*., 2024; Zhao *et al*., 2024).

Given the acknowledged health benefits associated with anthocyanins, the aim of this investigation was to extract anthocyanins from the purple sweet potato using ultrasound, optimizing the extraction parameters (temperature, time, and ethanol concentration) using a Box-Behnken design, for their subsequent application as a natural dye in yogurt and the evaluation of its sensory acceptability. It was proposed that the anthocyanin extract obtained with this technique can be used as a natural dye in yogurt, maintaining a favorable sensory acceptability. Its incorporation into yogurt not only provides natural color but can also improve its functional profile, favoring cardiovascular, immunological, and digestive health in consumers.

MATERIALS AND METHODS

The investigation was carried out between the months of February and September, 2024, in the facilities of the National University of Loja, in the province of Loja, Ecuador. The institution is located at an altitude of approximately 2060 m, with a mean annual temperature of 16 °C and an average rainfall of 1200 mm (INEC, 2023).

Sweet potato (*Ipomoea batatas* L.) of the purple variety was used as the raw material, which had previously been obtained from the Loja wholesale market from local crops. For the extraction of anthocyanins and the bromatological analyses, analytical grade reagents were used: ethanol (99 %, Hayman Kimia; Witham, UK), distilled water (Puritech; Guayaquil, Ecuador), citric acid (J.T. Baker; Phillipsburg, USA), sulfuric acid (Fisher Chemical; Fair Lawn, NJ, USA), hydrochloric acid (Fisher Chemical; Fair Lawn, NJ, USA), sodium hydroxide (Thermo Scientific; Illkirch, France), petroleum ether (Merck; Darmstadt, Germany), potassium chloride (ISOLAB; Eschau, Germany), sodium acetate (Merck; Darmstadt, Germany), and acetone (Merck; Darmstadt,

Germany). A mixed cross-sectional method was used, structured into four main phases, described below.

Sample preparing and conditioning (Phase I)

The raw material was selected manually, discarding roots with signs of rot or deterioration. Subsequently, it was washed with drinkable water and disinfected in a sodium hypochlorite-based solution (100 ppm, equivalent to 2.5 ml of 4 % commercial bleach in 1 L of water). The roots were carefully peeled with a surgical scalpel and a stainless-steel knife to extract the skin, avoiding the pulp, and obtaining a yield of approximately 154 g of skin for every 1000 g of purple sweet potato. The skins were weighed using a precision scale (Mettler Toledo ME204; Columbus, OH, USA) and lyophilized at -56 °C in a vacuum for 24 h (Labotec, model 01JLGGJ12; Midrand, South Africa). The lyophilized skins were ground using a two-speed blender with 700 W of power (Oster, model BLSTBESTE; Boca Raton, FL, USA) until a fine and homogenous powder was obtained. This powder was stored in sealed containers at room temperature in the dark until it was used.

Ultrasound-assisted extraction (Phase II)

Anthocyanins were extracted following the methodology proposed by Solórzano *et al*. (2023) and Mendoza *et al*. (2023) from the skin of purple sweet potato. A Box-Behnken design was implemented with three levels and three factors (temperature, time, and ethanol concentration) to optimize the extraction, following the response surface method (Mendoza *et al*., 2023). Every treatment had three repetitions, with a total of 45 experimental units. The independent variables were time of sonication, temperature, and solvent concentration. The dependent variable was the concentration of extracted anthocyanins.

For the extraction, 15 treatments were prepared with 0.25 g of homogenized sweet potato skin powder with 60 mL of ethanol solutions at 50, 60, and 70 %, acidified at 4 % with citric acid (J.T. Baker, Phillipsburg, NJ, USA). The samples were sonicated in an ultrasonic bath (MRC Laboratory Instruments; Harlow, UK) at a frequency of 40 kHz, at temperatures of 40, 50, and 60 °C, for periods of 20, 25, and 30 min. The extract obtained was filtered using 125 mm filter paper Whatman. No. 1 to remove residual solids.

The filtrates were concentrated using a rotavaporator (Yamato Scientific Co., Tokyo, Japan) equipped with a vacuum pump (Welch, modelo 2034, Mount Prospect, IL, EE. UU.) removing ethanol at a controlled temperature of 25-30 °C to prevent degradation of anthocyanins, following the procedure described by Zapata et al. (2014). During this process, the volume was reduced from 60 mL to approximately 5 mL. Subsequently, the extracts were centrifuged using a centrifuge (Unic, model C818, Dayton, NJ, USA) at 3400 rpm for 10 min. to promote sedimentation and clarification. Finally, the concentrates were stored at 4 °C for 24 h until application.

Proximal and bromatological analysis of the sweet potato

For proximal analyses, the roots of sweet potato in optimum conditions were washed, peeled, and split into skin and complete matrix. Both parts were dried at a controlled temperature and pulverized until a homogenous particle size was obtained. Bromatological analyses were carried out using the Thiex (2009) and Association of Official Analytical Chemists (AOAC, 2019) methods.

The analyses carried out included moisture (%) determined by kiln drying loss (Binder, model FD, Tuttlingen, Germany) at 95-100 °C to constant weight (AOAC 934.01), and dry matter (%) as a supplement to moisture; raw protein (%), quantified by Kjeldahl digestion with conversion factor 6.25 (AOAC 981.10); crude fat (%), by Soxhlet extraction with petroleum ether (AOAC 920.39); crude ash (%), by mufla incineration at 600 °C to white or grey mineral residue (AOAC 942.05). Raw fibre (%) was determined by acid and alkaline digestion according to Weende (AOAC 962.09), whereas neutral detergent fibre (NDF), acid detergent fibre (ADF) and acid detergent lignin (LDA) were determined using an ANKOM system (ANKOM Technology, Macedon, NY, USA)., with filter bags according to the standardised method of Van Soest et al. (1991), validated in AOAC (2019).

Total anthocyanins determination

Quantification was performed using the differential pH method (Marcía-Fuentes *et al*., 2021) from the corrected absorbances of each treatment in triplicate. Two buffer solutions were prepared: potassium chloride 0.025 M, pH 1.0 (ISOLAB; Eschau, Germany), and 0.4 M sodium acetate, pH 4.5 (Merck; Darmstadt, Germany), stored at 4 °C and protected from the light. The pH was adjusted with 37 % HCl (Fisher Chemical; Fair Lawn, NJ, USA). The concentrated extracts were diluted in each buffer, adjusting the dilution factor to keep absorbances within 0.2–1.2. Absorbances were measured in a spectrophotometer (Shimadzu, UV-1800; Kyoto, Japan) at 520 and 700 nm, in triplicate. The differential absorbance was calculated as follows:

$$A = (A\ 520\ nm - A\ 700\ nm)_{pH1.0} - (A\ 520\ nm - A\ 700\ nm)_{pH4.5}$$

The concentrations of monomeric anthocyanins were determined using the following equation:

$$Total\ anthocyanins\ (\text{mg L}^{-1}) = \frac{A \times MW \times DF \times 1000}{\in \times 1}$$

where MW is the molecular weight of cyanidin-3-glucoside (449.2 g mol^{-1}), $\in$ is the coefficient of molar extinction (26 900 L mol^{-1} cm^{-1}), DF is the dilution factor (5), and A is the differential absorbance. The results were expressed in equivalent terms of cyanidin-3-glucoside as a reference pigment.

Incorporating the natural dye into yogurt (Phase III)

The anthocyanin extract obtained under optimal conditions was added to artisanal yogurt made with Nutri brand milk (Lácteos San Antonio; Cuenca, Ecuador) and Toni brand natural sugar-free ferment (Industrias Lácteas Toni S.A.; Guayaquil, Ecuador). Fermentation was carried out by incubating the mixture for 6 h at 38–40 °C, with 6 % of sugar as a substrate for the lactic acid bacteria (Molina *et al*., 2024). Three treatments were formulated with different dye concentrations: 0.6 (T1), 0.8 (T2), and 1 % (T3), as well as a control without dye (T4).

Sensory evaluation (Phase IV)

A descriptive sensory test was applied on 50 untrained consumers (emotional judges), who evaluated attributes of color, aroma, flavor, and consistency using a nine-point hedonic scale (1 = I dislike it extremely; 9 = I like it extremely), according to the methodology proposed by Santos-Alemán *et al*. (2023b) and Mendoza *et al*. (2023).
The experimental design of the sensory evaluation was conducted using a completely balanced block design, with treatments T1 to T4 assigned to blocks A–D. Block A corresponded to treatment T1, with 0.6 % of extract in its formulation; block B to treatment T2, with 0.8 %; block C to treatment T3, with 1 % of extract; and block D to treatment T4, which worked as a control without the addition of pigment. The average scores for each attribute were recorded for analysis.

Statistical analysis

Extraction was optimized using a polynomial regression model validated with analysis of variance (ANOVA) within the methodology (response surface methodology) using Statgraphics Centurion 18 (version 18.1.13). The assumptions of normality (Shapiro-Wilk), homoscedasticity, and independence of residuals were verified. In case of a breach, the non-parametric Kruskal-Wallis test was applied to detect significant differences between treatments. In addition, Fisher's least significant difference (LSD) method was implemented to compare means with a 95 % confidence level.

RESULTS AND DISCUSSION

Proximal analysis of the sweet potato

Results of the bromatological analyses showed that the purple sweet potato presents a high humidity content (69.09 %) and low content of ash (0.9 %), raw fiber (0.84 %), raw fat (0.17 %), and protein (1.13 %). Additionally, a considerable amount of dry matter (30.9 %) and neutral detergent fiber (NDF) (11.95 %) was recorded, along with a low content of acid detergent fiber (ADF) (0.75 %) and undetectable levels of lignin (Table 1). These results are consistent with values reported by Vidal *et al*. (2018), which backs the stability and quality of purple sweet potato as a raw material for the extraction of natural dyes (Coba-Carrera *et al*., 2019).

Table 1. Results of the proximal analysis for the fractions of purple sweet potato (*Ipomoea batatas* L.) -complete matrix and shell- expressed on a wet basis (fresh weight).

Parameter	Sweet potato (complete matrix)	Sweet potato skin
Humidity (%)	69.09	76.99
Dry matter (%)	30.9	23.0
Raw protein (%)	1.13	0.897
Raw fat (%)	0.17	0.33
Raw ash (%)	0.9	2.67
Raw fiber (%)	0.84	3.33
Neutral detergent fiber (%)	11.95	10.98
Acidic detergent fiber (%)	0.75	4.70
Acidic detergent lignin (%)	Not detected	1.54

As for the skin of purple sweet potato (Table 1), a higher content of humidity (76.99 %), ash (2.67 %), raw fiber (3.33 %), and ADF (4.7 %) was observed in comparison to the complete matrix. These results coincide with earlier investigations that point out the skin of the sweet potato as an important source of insoluble dietary fiber, with beneficial effects in digestive health (Armijos *et al*., 2020). Likewise, lignin was found in low levels (1.54 %), yet it was not quantifiable in the complete matrix. This lower presence could be related to a better digestibility of the fiber in food applications (Guarner *et al*., 2011). These results indicate that the sweet potato skin has favorable chemical features, particularly due to its fiber content, which may add functional value to the dye made from this raw material.

Concentration of anthocyanins

The results displayed significant differences in the concentrations of anthocyanins among treatments (Table 2). The optimal treatments were T11, with 62.87 mg L^{-1} under conditions of 60 % ethanol, 60 °C, and 20 min of extraction; and T9, with 61.5 mg L^{-1}, under the same ethanol percentage and extraction time, but at a temperature of 40 °C. These results coincide with the recommendations by Stoica *et al*. (2022), who suggest that the extraction of anthocyanins from red onion skin must be carried out at an ethanol concentration of 60 % to favor the extraction of anthocyanins and balance the solubility of hydrophilic molecules.

By contrast, the least efficient treatment was T4, which only reached 3.2 mg L^{-1} with 70 % of ethanol, 60 °C, and 25 min of extraction. This yield suggests that high concentrations of ethanol combined with high temperatures may reduce the degradation of anthocyanins, as pointed out by Cacace and Mazza (2003).

These findings coincide with Sadilova *et al*. (2006), who showed that anthocyanins are sensitive to temperatures, pH, and solvents such as alcohol, and degrade easily. Likewise, Patras *et al*. (2010) indicate that high temperatures affect the color and

Table 2. Concentration of anthocyanins (mg of cyanidin-3-glucoside L-1) obtained from the ultrasound-assisted extraction of 0.25 g of purple sweet potato skin (*Ipomoea batatas* L.) using the Box-Behnken design, evaluated across 15 treatments in triplicate.

Treatment	Ethanol concentration (%)	Temperature (°C)	Time (min)	Anthocyanin concentration (mg L^{-1})
1	50	40	25	17.96 fg
2	70	40	25	28.13 e
3	50	60	25	11.85 h
4	70	60	25	3.20 i
5	50	50	20	15.08 g
6	70	50	20	21.09 f
7	50	50	30	26.76 e
8	70	50	30	22.59 f
9	60	40	20	61.50 a
10	60	40	30	39.75 cd
11	60	60	20	62.87 a
12	60	60	30	25.32 e
13	60	50	25	43.14 c
14	60	50	25	39.48 cd
15	60	50	25	54.73 b

Different letters in the same column indicate differences according to Tukey's test ($p \leq 0.005$).

functional activity of these molecules, whereas Zhang *et al*. (2015) report that high concentrations of ethanol may alter their molecular structure, reducing their stability and shelf life.

Analysis of variance and Pareto chart

The analysis of variance (ANOVA) of the quadratic model (Table 3) identified the time of extraction (B) and the quadratic term of ethanol (CC) as significant factors ($p = 0.0003$ and $p = 0.0000$, respectively), whereas the temperature (A) and the linear term of ethanol (C) were not significant ($p = 0.8625$ and $p = 0.1821$, respectively). The adjusted R^2 (74.69 %) indicates that the model adequately explains the variability of the experimental data. The results coincide with findings by Fernandes *et al*. (2020), who point out that the temperature, in some cases, does not have a significant influence on the efficiency of the extraction of anthocyanins when time and concentration of ethanol are controlled.

Results were verified in the Pareto chart, where time of extraction (B) and the quadratic term of the concentration of ethanol (CC) appear as the factors with the greatest influence on the concentration of anthocyanins, both of which surpass the line of reference (Figure 1A). The results of the means for time (Figure 1B) showed that short periods (20 min) maximize yield and prevent degradation caused by prolonged exposure, coinciding with reports by Tiwari *et al*. (2009). Regarding the concentration

Table 3. Analysis of variance (ANOVA) for the concentration of anthocyanins in the skin of purple sweet potato (*Ipomoea batatas* L.), considering linear and quadratic effects, as well as interactions of the independent variables.

Variables	*p*-value (concentration of anthocyanins)
Temperature	0.8625
Time	0.0003*
Ethanol concentration	0.1821
AA	0.3652
AB	0.2197
AC	0.7444
BB	0.6631
BC	0.7251
CC	0.0000*
R^2	74.69 %

*Significant to α = 0.05. AA: quadratic effect of the temperature; BB: quadratic effect of time; CC: quadratic effect of the concentration of ethanol; AB: temperature-time interaction; AC: temperature-ethanol concentration interaction; BC: time-ethanol concentration interaction.

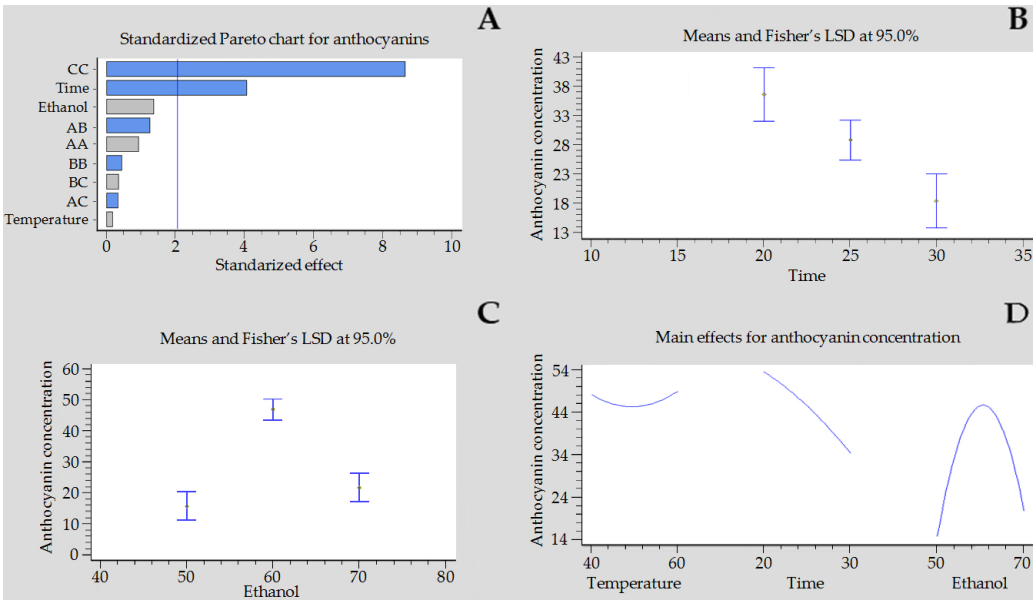

Figure 1. Graphic analysis of the factors that affect the concentration of anthocyanins (mg L^{-1}) obtained from 0.25 g of purple sweet potato (*Ipomoea batatas* L.) skin. A: Pareto chart of the concentration of anthocyanin; B: Means for time of extraction (min) + Fisher's least significant difference test (LSD); C: Means for the ethanol concentration (%) + Fisher's LSD test; D: behavior of the study variables against the concentration of anthocyanins. AA: quadratic effect of the temperature; BB: quadratic effect of time; CC: quadratic effect of the concentration of ethanol; AB: temperature-time interaction; AC: temperature-ethanol concentration interaction; BC: time-ethanol concentration interaction.

of ethanol (Figure 1C), 60 % provided the best balance between the polarity of the solvent and the stability of the anthocyanins, coinciding with descriptions by Cacace and Mazza (2003). The joint behavior of the variables (Figure 1D) indicated that the temperature keeps a stable effect in the interval between 40 and 60 °C, considered adequate to preserve the integrity of these compounds; however, prolonged exposure times may favor their degradation.

Optimization of the response variable (concentration of anthocyanins)

The optimization of the experimental design helped determine the ideal conditions to maximize the concentration of anthocyanins in the process of extraction (Table 4). The optimum treatment identified was T11, characterized by a short time, a high temperature, and an intermediate ethanol concentration. These conditions reflect the importance of a balance between time, temperature, and solvent for the efficient extraction of anthocyanins. These conditions coincide with Xue *et al*. (2021), who indicated that lower extraction times in ultrasound-assisted processes help obtain high yields, since they prevent the thermal degradation of anthocyanins.

Table 4. Optimal conditions of the anthocyanin extraction process from the skin of purple sweet potato (*Ipomoea batatas* L.), determined with the Box-Behnken design.

Variable	Optimum value
Temperature	60 °C
Time	20 min
Ethanol concentration	60.16 %
Anthocyanin concentration	60.72 mg L^{-1}

The optimal concentration obtained (60.72 mg L^{-1}), under the extraction conditions presented, validates the effectiveness of the quadratic model applied in the Box-Behnken design. This confirms its usefulness in the optimization of complex processes such as the ultrasound-assisted extraction, backing similar approaches by Tiwari *et al*. (2009) and Castañeda-Ovando *et al*. (2009) in studies on the extraction of phenolic compounds and anthocyanins.

Response surface of the Box-Behnken design

The Box-Behnken design proved to be efficient to optimize the extraction of anthocyanins from the skin of sweet potato by evaluating both the individual influence and the interactions between temperature, time, and the concentration of ethanol. This predictive tool helped identify optimal conditions, guiding potential industrial applications. Using the response surface methodology, the significance of adjusting and balancing critical parameters to promote efficient extraction was demonstrated. The most relevant response surfaces are shown and discussed below.

Surface at fixed ethanol concentration

With a constant percentage of ethanol (60 %), the concentration of anthocyanins increased considerably in combination with high temperatures (60 °C) and short times (20 min) (Figure 2). This behavior can be attributed to the greater solubility of the anthocyanins in ethanol at high temperatures, in which thermal energy facilitates the rupture of the cell walls (Castañeda-Ovando *et al*., 2009). However, prolonged times lead to a reduction in concentration, probably due to the thermal degradation of the compounds, which has also been reported by Tiwari *et al*. (2009).

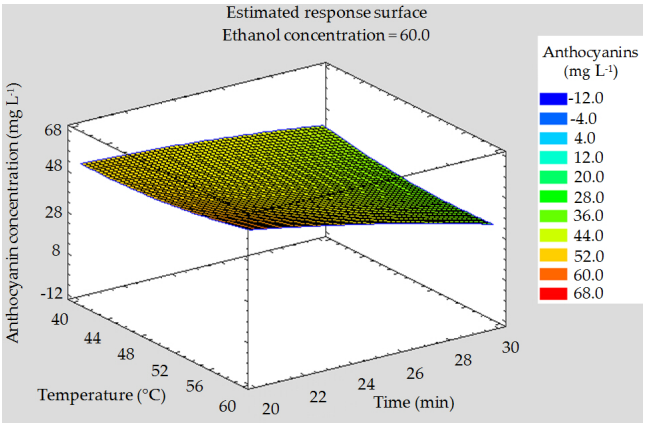

Figure 2. Response surface for the concentration of anthocyanins based on the temperature and the time of extraction with 60 % ethanol from 0.25 g of purple sweet potato (*Ipomoea batatas* L.) skin.

Surface at fixed sonication time

By keeping time constant (20 min), the concentration of anthocyanins displayed a direct dependence on the temperature and the ethanol concentration (Figure 3). The best results were obtained at 60 °C and 60 % of ethanol, thus confirming the need for a balance between temperature and solvent to avoid losses due to degradation or insufficient solvent. This finding is consistent with Cacace and Mazza (2003), who found that 60 % of ethanol offers the optimum balance between polarity and stability in the extraction of anthocyanins.

Surface at fixed temperature

When the temperature was fixed at 60 °C and the extraction time was short (20 min), the concentration of anthocyanin increased significantly (Figure 4). Slight deviations from these conditions reduced the efficiency of the process, which highlights the need for an accurate control of these variables. These findings are consistent with those reported by Xue *et al*. (2021), who also identified short time and controlled temperature as key factors in ultrasound-assisted extraction.

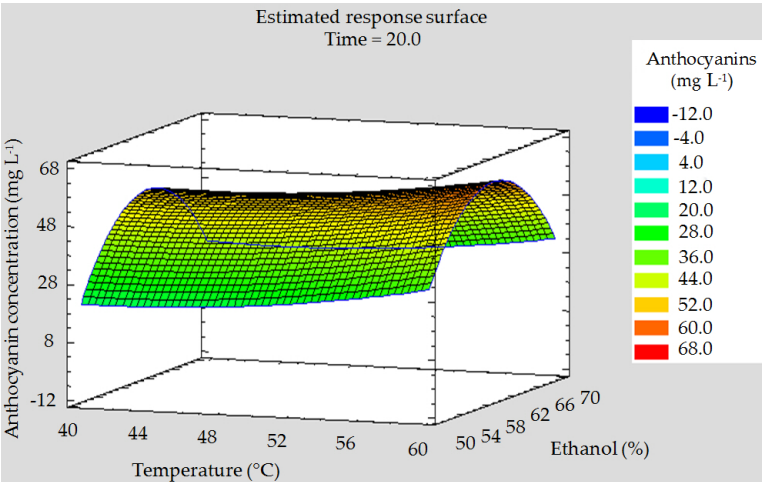

Figure 3. Response surface for the concentration of anthocyanins based on the temperature and ethanol concentration, with a fixed sonication time of 20 min from 0.25 g of purple sweet potato (*Ipomoea batatas* L.) skin.

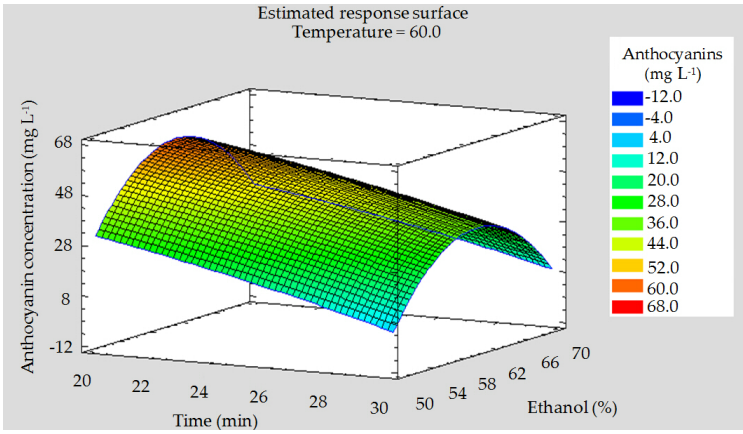

Figure 4. Response surface for the concentration of anthocyanins based on the time of extraction and concentration of ethanol, with a fixed temperature of 60 °C from 0.25 g of purple sweet potato (*Ipomoea batatas* L.) skin.

Path of steepest ascent

To further optimize the process, the path of steepest ascent was used, which projects the optimal combination of variables to maximize the concentration of anthocyanins (Table 5). A progressive increase in temperature from 50 to 70 °C favors the increase in the concentration, reaching an estimated maximum value of 87.86 mg L^{-1} at 70 °C. This behavior coincides with Chemat *et al*. (2012), who pointed out that moderate increases in temperature favor solubility and the diffusion of phenolic compounds in ultrasound-assisted extractions.

Table 5. Path of greatest ascent for the optimization of the concentration of anthocyanins in the extraction from 0.25 g of purple sweet potato (*Ipomoea batatas* L.) skin, depending on the projection of the evaluated variables.

Temperature (°C)	Time (min)	Ethanol (%)	Anthocyanin concentration prediction (mg L^{-1})
50.0	25.00	60.00	45.79
51.0	22.40	60.43	50.40
52.0	21.36	60.39	52.40
53.0	20.60	60.35	54.06
54.0	19.98	60.31	55.63
55.0	19.45	60.27	57.17
56.0	18.98	60.24	58.74
57.0	18.54	60.20	60.35
58.0	18.15	60.17	62.01
59.0	17.77	60.14	63.74
60.0	17.42	60.11	65.54
61.0	17.08	60.08	67.41
62.0	16.76	60.06	69.36
63.0	16.44	60.03	71.38
64.0	16.14	60.00	73.49
65.0	15.85	59.97	75.68
66.0	15.56	59.95	77.95
67.0	15.28	59.92	80.30
68.0	15.01	59.90	82.74
69.0	14.74	59.87	85.26
70.0	14.48	59.84	87.86

Likewise, a reduced extraction time (from 25 to 14 min) minimizes thermal degradation, allowing operation at relatively high temperatures without affecting the stability of the anthocyanins, as pointed out by Patras *et al*. (2010). During this process, the ethanol concentration was kept at around 60 %, validating the key role of this percentage to balance the solubility and stability of bioactive compounds, according to reports by Dai and Mumper (2010). The balance between a high temperature, a reduced time of extraction, and an intermediate concentration of ethanol is crucial to maximize the recovery of anthocyanins.

Sensory evaluation

The sensory evaluation helped obtain the means of the attributes evaluated, as well as the intent of purchase associated with each one of the yogurt samples, including those with natural dye and the control treatment (Table 6).

No significant differences were found in color (p = 0.5296), although T4 (yogurt without dye) had the highest score. This could be related to a preference for more natural tonalities or to samples with dye not presenting a sufficiently distinctive color.

Table 6. Results of the sensory evaluation and intent of purchase for different yogurt samples with and without natural dye, including a statistical analysis with the Kruskal-Wallis test.

Panel block	Color	Aroma	Flavor	Consistency	Intent of purchase (%)
A (T1)	6.18 ± 2.28	5.82 ± 2.30	6.02 ± 2.45	6.06 ± 2.45	60
B (T2)	6.27 ± 2.47	6.00 ± 2.32	6.43 ± 2.45	6.31 ± 2.43	60
C (T3)	6.35 ± 2.43	5.78 ± 2.21	6.18 ± 2.45	6.16 ± 2.46	66
D (T4)	6.59 ± 2.52	6.51 ± 2.16	6.94 ± 2.45	7.02 ± 2.39	82
Kruskal-Wallis test	0.5296	0.3282	0.0606	0.0526	-

*The values express a mean ± standard deviation on a hedonic nine-point scale evaluated by 50 panelists. The intent of purchase represents the percentage based on the total of the 50 evaluators willing to purchase the sample. No significant differences were observed (Kruskal-Wallis, $p > 0.05$).

Coello-García *et al*. (2000) pointed out that a greater chromatic intensity can influence the perception of the product.

The scores for aroma were similar between treatments ($p = 0.3282$). The lack of impact of the dye on aroma is consistent with studies that point out that the addition of natural pigments, such as anthocyanins, has no significant impact on the volatile compounds in charge of the aromatic profile of the product (Tian *et al*., 2022). In terms of the flavor, despite not being significant ($p = 0.0606$), T4 was the best valued, which suggests that the panelists perceived a better balance in the flavor of the yogurt without dye. According to Delwiche (2004), the perception of flavor can be influenced by visual stimuli and sensory expectations.

The values of consistency reflected a positive tendency for T4 ($p = 0.0526$). The dye did not perceptibly alter this attribute, indicating that it does not affect the physical structure of the yogurt. Regarding the purchase intent, the control treatment displayed the highest acceptance (82 %). Nevertheless, sample T3 (1 % dye) had a score of 66 %, which highlights an acceptable potential of the dye.

Jointly, the use of the dye displayed promising results. However, the preference for the control treatment highlights the need to adjust the concentration of the pigment in the yogurt to achieve an adequate balance between the intensity of the color and the sensory acceptance of the product. Adjustments in concentration can improve key attributes (Chemat *et al*., 2012).

CONCLUSIONS

The extraction of anthocyanins from the skin of sweet potato by ultrasound was efficient to obtain the pigment. The optimization of the process using a Box-Behnken surface response design determined that the best conditions are a temperature of 60

°C, an extraction time of 20 min, and an ethanol concentration of 60.16 %. The extract as a natural dye in yogurt displayed a good acceptance, although the control sample was the best valued. These results show the potential of the extract as a viable alternative to synthetic dyes, not only for its sensory acceptance but also for its possible health benefits thanks to its bioactive compounds.

REFERENCES

AOAC (Association of Official Analytical Chemists). 2019. Official methods of analysis of AOAC international (21st edition). Rockville, MD, USA. 700 p.

Armijos G, Villacrés E, Quelal MB, Cobeña G, Álvarez J. 2020. Evaluación físico-química y funcional de siete variedades de camote provenientes de Manabí-Ecuador. Revista Iberoamericana de Tecnología Postcosecha 21 (2).

Cacace JE, Mazza G. 2003. Optimization of extraction of anthocyanins from black currants with aqueous ethanol. Journal of Food Science 68 (1): 240–248. https://doi.org/10.1111/j.1365-2621.2003.tb14146.x

Castañeda-Ovando A, Pacheco-Hernández ML, Páez-Hernández ME, Rodríguez JA, Galán-Vidal CA. 2009. Chemical studies of anthocyanins: A review. Food Chemistry, 113 (4): 859–871. https://doi.org/10.1016/j.foodchem.2008.09.001

Chemat F, Vian MA, Cravotto G. 2012. Green extraction of natural products: Concept and principles. International Journal of Molecular Sciences 13 (7): 8615–8627. https://doi.org/10.3390/ijms13078615

Coba-Carrera RL, Apolo-Criollo LG, Segura-Mestanza JH, Brito-Moina HL. 2019. Obtención del colorante natural del Camote (*Ipomoea batatas*). Ciencia Digital 3 (3.2): 38–47. https://doi.org/10.33262/cienciadigital.v3i3.2.714

Coello-García MT, Díaz-Berciano C, Gómez-Pestaña NG. 2000. Efectos del color en la aceptabilidad, artificialidad, dulzor e intensidad del sabor de bebidas lácteas. Psicothema 12 (2): 140–144.

Dai J, Mumper RJ. 2010. Plant phenolics: Extraction, analysis and their antioxidant and anticancer properties. Molecules 15 (10): 7313–7352. https://doi.org/10.3390/molecules15107313

Delwiche J. 2004. The impact of perceptual interactions on perceived flavor. Food Quality and Preference 15 (2): 137–146. https://doi.org/10.1016/S0950-3293(03)00041-7

Fallah AA, Sarmast E, Fatehi P, Jafari T. 2020. Impact of dietary anthocyanins on systemic and vascular inflammation: Systematic review and meta-analysis on randomised clinical trials. Food and Chemical Toxicology 135: 110922. https://doi.org/10.1016/j.fct.2019.110922

Fernandes FA, Rodrigues S, de Brito ES, Tiwari BK. 2020. Ultrasound-assisted extraction of anthocyanins and phenolics from jabuticaba (*Myrciaria cauliflora*) peel: Kinetics and mathematical modeling. Journal of Food Science and Technology 57 (6): 2321–2328. https://doi.org/10.1007/s13197-020-04270-3

Guarner F, Sastre A, Requejo A, Ruíz-Roso B, Gómez-Martínez S, Esperanza-Díaz L. 2011. El libro blanco de la fibra dietética. Corporación Alimentaria Peñasanta: Siero, España.

INEC (Instituto Nacional de Estadística y Censos). 2023. Anuario meteorológico y climático del Ecuador. Quito, Ecuador. https://www.ecuadorencifras.gob.ec (Retrieved: August 2024).

Maddela NR, García LC. 2021. Innovations in biotechnology for a sustainable future. Springer: New York, NY, USA. 448 p.

Marcía-Fuentes JA, López-Salas L, Borrás-Linares I, Navarro-Alarcón M, Segura-Carretero A, Lozano-Sánchez J. 2021. Development of an innovative pressurized liquid extraction procedure by response surface methodology to recover bioactive compounds from carao tree seeds. Foods 10 (2): 398. https://doi.org/10.3390/foods10020398

Marcía-Fuentes JA, Montero-Fernández I, Zumbado-Fernández H, Lozano-Sánchez J, Santos-Alemán R, Navarro-Alarcón M, Borrás-Linares I, Saravia-Maldonado SA. 2020. Quantification of bioactive molecules, minerals and bromatological analysis in carao (*Cassia grandis*). Journal of Agricultural Science 12 (3): 88. https://doi.org/10.5539/jas.v12n3p88

Mendoza E, Marcía-Fuentes JA, Chuquilín-Goicochea RC, López J, Areche F, Ruiz J, Herrera A. 2023. Obtención de un colorante natural a partir *Tropaeolum tuberosum* Ruíz y Pavón para su aplicación en yogur. Revista Bionatura 8 (2): 38.

Molina C, Campos-García SK, Marcía-Fuentes JA, Ore-Areche F, Yadav A, Santos-Alemán R. 2024. Effects of capulin (*C. xalapensis*) on the microbiological, physicochemical and sensory properties of yogurt. Dairy 5 (3): 515–525. https://doi.org/10.3390/dairy5030039

Montero IF, Saravia SA, Santos RA, dos Santos RC, Marcía-Fuentes JA, da Costa HN. 2020. Nutrients in Amazonian fruit pulps with functional and pharmacological interest. African Journal of Pharmacy and Pharmacology 14 (5): 118–127. https://doi.org/10.5897/ajpp2020.5136

Patras A, Brunton NP, O'Donnell C, Tiwari BK. 2010. Effect of thermal processing on anthocyanin stability in foods; mechanisms and kinetics of degradation. Trends in Food Science and Technology 21 (1): 3–11. https://doi.org/10.1016/j.tifs.2009.07.004

Sadilova E, Stintzing FC, Carle R. 2006. Thermal degradation of acylated and nonacylated anthocyanins. Journal of Food Science 71 (8): C504–C512. https://doi.org/10.1111/j.1750-3841.2006.00148.x

Saini RK, Khan MI, Shang X, Kumar V, Kumari V, Kesarwani A, Ko EY. 2024. Dietary sources, stabilization, health benefits, and industrial application of anthocyanins—a review. Foods 13 (8). https://doi.org/10.3390/foods13081227

Santos-Alemán R, Marcía-Fuentes JA, Montero-Fernández I, King J, Pournaki S, Hoskin R, Moncada M. 2023b. Novel liquor-based hot sauce: Physicochemical attributes, volatile compounds, sensory evaluation, consumer perception, emotions, and purchase intent. Foods 12 (2): 369. https://doi.org/10.3390/foods12020369

Santos-Alemán R, Marcía-Fuentes JA, Page R, Kazemzadeh Pournaki S, Martín-Vertedor D, Manrique-Fernández V, Aryana K. 2023a. Effects of yogurt with carao (*Cassia grandis*) on intestinal barrier dysfunction, α-glycosidase activity, lipase activity, hypoglycemic effect, and antioxidant activity. Fermentation 9 (6): 566. https://doi.org/10.3390/fermentation9060566

Saravia-Maldonado SA, Santos-Alemán RS, Marcía-Fuentes JA, da Conceição MCF. 2020. Determination of total phenolic compounds, antioxidant activity and nutrients in Brazil nuts (*Bertholletia excelsa* H. B. K). Journal of Medicinal Plants Research 14 (8): 373–376. https://doi.org/10.5897/jmpr2020.6953

Solórzano L, Marcía-Fuentes JA, Chuquilín-Goicochea RC, Areche F, Herrera A, Ruíz-Cardona JM. 2023. Evaluación de la pulpa de macha macha (*Vaccinium floribundum* Kunth), en el desarrollo de una bebida isotónica. Revista Bionatura 8 (4): 38. https://doi.org/10.21931/rb/2023.08.04.38

Stoica F, Constantin OE, Stănciuc N, Aprodu I, Bahrim GE, Râpeanu G. 2022. Optimization of the parameters influencing the antioxidant activity and concentration of anthocyanins

extracted from red onion skins using a central composite design. Inventions 7 (4): 89. https://doi.org/10.3390/inventions7040089

Thiex N. 2009. Evaluation of analytical methods for the determination of moisture, crude protein, crude fat, and crude fiber in distillers dried grains with solubles. Journal of AOAC International 92 (1): 61–73. https://doi.org/10.1093/jaoac/92.1.61

Tian XZ, Wang X, Ban C, Luo QY, Li JX, Lu Q. 2022. Effect of purple corn anthocyanin on antioxidant activity, volatile compound and sensory property in milk during storage and light prevention. Frontiers in Nutrition 9: 862689. https://doi.org/10.3389/fnut.2022.862689

Tiwari BK, O'donnell CP, Patras A, Brunton N, Cullen PJ. 2009. Stability of anthocyanins and ascorbic acid in sonicated strawberry juice during storage. European Food Research and Technology 228 (5): 717–724. https://doi.org/10.1007/s00217-008-0982-z

van Soest PJ, Robertson JB, Lewis BA. 1991. Methods for dietary fiber, neutral detergent fiber, and nonstarch polysaccharides in relation to animal nutrition. Journal of Dairy Science 74 (10): 3583–3597. https://doi.org/10.3168/jds.S0022-0302(91)78551-2

Vidal AR, Zaucedo-Zuñiga AL, Ramos-García ML. 2018. Propiedades nutrimentales del camote (*Ipomoea batatas* L.) y sus beneficios en la salud humana. Revista Iberoamericana de Tecnología Postcosecha 19 (2).

Xue H, Tan J, Li Q, Cai X, Tang J. 2021. Optimization ultrasound-assisted extraction of anthocyanins from cranberry using response surface methodology coupled with genetic algorithm and identification anthocyanins with HPLC-MS2. Journal of Food Processing and Preservation 45 (7): e15378. https://doi.org/10.1111/jfpp.15378

Zapata LM, Heredia AM, Quinteros CF, Malleret AD, Clemente GC. 2014. Optimización de la extracción de antocianinas de arándanos. Ciencia, Docencia y Tecnología 25 (49): 166–192.

Zhang B, Liu R, He FZ, Duan CQ. 2015. Copigmentation of malvidin-3-O-glucoside with five hydroxybenzoic acids in red wine model solutions: Experimental and theoretical investigations. Food Chemistry 170: 226–233. https://doi.org/10.1016/j.foodchem.2014.08.026

Zhao Y, Wang L, Huang Y, Evans PC, Little PJ, Tian X, Weng J, Xu S. 2024. Anthocyanins in vascular health and disease: mechanisms of action and therapeutic potential. Journal of Cardiovascular Pharmacology 84 (3): 289–302. https://doi.org/10.1097/FJC.0000000000001602

Agrociencia

PROSPECT OF PHOTOVOLTAIC SOLAR SYSTEMS FOR AGRICULTURAL IRRIGATION IN THE STATE OF GUANAJUATO, MEXICO

Elmer Gabriel **Robles-Lecona**[1], Victor Javier **Gutierrez-Martinez**[1*], Enrique Arnoldo **Zamora-Cardenas**[1]

[1]Universidad de Guanajuato. Departamento de Ingeniería Eléctrica. Carretera Salamanca-Valle de Santiago km 3.5 + 1.8, Comunidad de Palo Blanco, Salamanca, Guanajuato, México. C. P. 36787.
* Author for correspondence: vj.gutierrez@ugto.mx

Citation: Robles-Lecona EG, Gutierrez-Martinez VJ, Zamora-Cardenas EA. 2025. Prospect of photovoltaic solar systems for agricultural irrigation in the state of Guanajuato, Mexico. **Agrociencia** 59(8): 1210-1225. https://doi.org/ 10.47163/ agrociencia.v59i8.3420

Editor in Chief:
Dr. Fernando C. Gómez Merino

Received: April 01, 2025.
Approved: November 30, 2025.
Published in Agrociencia: December 4, 2025.

ABSTRACT

This work analyzes the current situation of solar photovoltaic (SPV) systems for agricultural irrigation in the state of Guanajuato, Mexico, with an emphasis on their technical and economic challenges. It also describes the water resource management system in Mexico and in the state, its main uses, and the applicable regulations. Based on a summary of agricultural production statistics, Guanajuato is positioned as one of the country's main producers, and the prospects for SPV systems for irrigation are examined. It also provides an overview of their advantages, disadvantages, and drawbacks. As a result, it identifies poor management of both water resources and SPVs for irrigation, which is the main contribution of the study, given the scarce or inaccurate information available in the literature and at different levels of government on the development, implementation, and projections of this technology in the state.

Keywords: agricultural pumping, water resources.

INTRODUCTION

In the state of Guanajuato, agriculture depends heavily on the use of wells for irrigation due to the scarcity of surface water resources. Statistics on agricultural wells show intense activity in this sector, with more than 15,000 registered wells. Approximately 84% of the water extracted is used for agriculture, demonstrating its importance for production in the region (CONAGUA, 2024a). However, water resource management faces challenges such as overexploitation of aquifers, where extraction exceeds natural recharge and causes annual deficits. This situation has forced state and municipal authorities to implement restrictions and regulations on the use of wells to preserve water resources in the long term and ensure agricultural sustainability in the state.

The vast majority of wells used for agricultural irrigation use electricity from the general distribution networks, whose dealers have two rates subsidized by the government. The first rate, called "Low Voltage Agricultural Irrigation" (RABT, from the Spanish *Riego Agrícola en Baja Tensión*), applies exclusively to low voltage services

that use energy for pumping irrigation water to agricultural land and for lighting the premises where it is installed (CFE, 2024a). Basically, it establishes a rate similar to those called "Low Voltage Domestic 1 and 2" (DB1 and DB2, from the Spanish *Doméstica en Baja Tensión 1* and *2*) (CFE, 2024b). The second rate, "Medium Voltage Agricultural Irrigation" (RAMT, from the Spanish *Riego Agrícola en Media Tensión*), is similar to the RABT rate, with the difference that it applies to medium voltage services (CFE, 2024c).

On the other hand, the reduction in the cost of solar photovoltaic (SPV) system components has led the agricultural sector to increasingly focus its attention on this technology for pumping irrigation water, especially on farms without low- or medium-voltage electricity supply infrastructure (DNV, 2023). Negera *et al*. (2025) evaluated how SPVs impact the economy and food security of small producers in Ethiopia, obtaining promising results. For their part, Yusuf and Sanusi (2025) analyzed the reliability, availability, and profitability of small-scale SPVs.

In Mexico, Guevara *et al*. (2025) presented an economic and environmental analysis of the implementation of SPVs in approximately 3,500 chinampas in Xochimilco, Mexico City, demonstrating that it is possible to reduce operational costs by 60 to 70%. Molina *et al*. (2025) propose the "Parcelas 5.0" technology, which integrates photovoltaic energy, rainwater harvesting, precision agriculture, and vertical agriculture to optimize productivity and sustainability in small plots, representing one of the most innovative advances by integrating monitoring technologies. To date, no research or case studies have been reported for the state of Guanajuato, despite the presence of photovoltaic systems for agricultural irrigation, which represents a significant area of opportunity.

Among the main challenges to expanding the adoption of this technology are the training of farmers in its operation and maintenance, as well as ensuring the availability of components and repair services in rural areas. In addition, it is essential to develop cost-effective energy storage solutions that provide a continuous water supply for irrigation, even under conditions of low or no solar irradiation. Another important challenge concerns land use, since the installation of SPV modules can reduce the area available for cultivation. Therefore, proper integration into the agricultural environment, together with government policies that promote incentives to facilitate initial investment and address these challenges in a comprehensive manner, is required.

This article provides a documentary study of the current situation of agricultural irrigation from underground wells in the state of Guanajuato. The water resource management scheme and its associated regulations are briefly described. Moreover, aiming at highlighting the importance of irrigation systems, the state is positioned nationally according to its agricultural production, and the potential of SPV energy to transform the sector, increasing its efficiency and sustainability, is emphasized. This constitutes the main contribution of this work, given that, both in the literature and at different levels of government, there is little or no information on the development

and prospects of this technology in the state's agricultural sector, even though its promotion is already contemplated in public policies.

WATER RESOURCES MANAGEMENT, USE, AND REGULATIONS

Management systems

For stakeholders in the SPV sector applied to agricultural pumping, understanding the water resource management framework is essential, as project development requires fulfilling the administrative procedures necessary to demonstrate compliance with the main regulatory requirements. Water resource management in Mexico is organized into a hierarchical structure that includes various entities and agencies.

The National Water Commission (CONAGUA, from the Spanish *Comisión Nacional del Agua*) is the authority responsible for water administration and management at the national level, responsible for establishing water policies and coordinating actions at different levels. The Basin Organizations, under CONAGUA, operate in different river basins to implement policies at the regional level. In each basin, Basin Councils function as participatory and consultative bodies, composed of users, local governments, and civil organizations, which advise on decision-making. Irrigation Districts and Technified Rainfed Districts manage agricultural water use in specific areas under the supervision of the Basin Organizations. Finally, the Groundwater Technical Committees manage, protect, and monitor aquifers at the local level.

There are 13 river basin organizations that encompass the 37 hydrological regions of the country (Figure 1) (CONAGUA, 2018). The state of Guanajuato is located

Figure 1. Distribution of basin organizations and hydrological regions in Mexico (CONAGUA, 2018).

within the jurisdiction of the Lerma-Chapala River Basin Organization, which covers the Lerma River and Lake Chapala basins. The state also encompasses three main irrigation districts: District 011, known as "Alto Río Lerma"; District 085, "La Begoña"; and District 087, "Rosario-Mezquite." This organization and distribution aim to achieve more effective water management in a region where water resources are vital for agriculture.

In Mexico, as of 2020, 39% of the water volume allocated to consumptive uses (those in which the resource is not fully returned to its source or is discharged in a different form or location, such as in domestic, industrial, or livestock uses) was extracted from groundwater sources, while the remainder came from surface sources. During the period 2005–2020, groundwater withdrawals increased (Figure 2) from 36.3% to 39.4% (CONAGUA, 2024c). Of the total percentage withdrawn from groundwater sources, the state of Guanajuato is part of a group of six states that account for 45%.

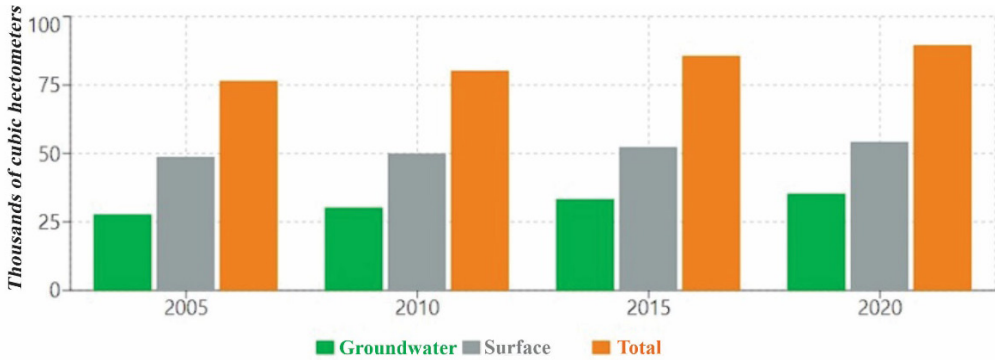

Figure 2. Volume of water used nationally by source type (CONAGUA, 2024c).

Water uses

Agricultural use is the most prevalent, accounting for 67.52% of the total national volume. During the period 2005–2020, its use for this sector increased by 11%, with national water use growing from 54.41 to 60.46 thousand hm^3 (cubic hectometers) (Figure 3). Of the total volume, 50.51% is concentrated in the states of Sinaloa, Sonora, Chihuahua, Michoacán, Tamaulipas, and Guanajuato (CONAGUA, 2024c). In particular, in the state of Guanajuato (Table 1), there are more underground concessions than surface concessions (CONAGUA, 2024d, 2024e).

When comparing the volume granted (Table 1) and the volume of water consumed (Table 2), clear overexploitation of aquifers can be observed, putting the availability of this resource at risk for future years. Hence, the importance of strengthening public policies for more effective management and monitoring. On the other hand, given the increase in groundwater extraction, the potential for development that SPVs can achieve for agricultural pumping can be visualized.

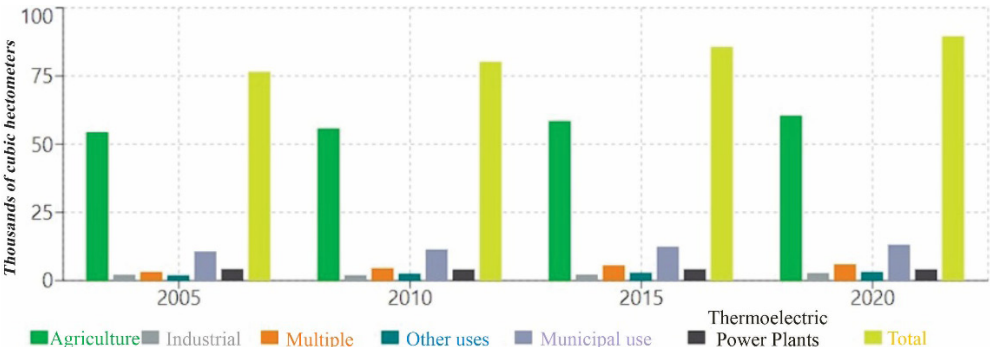

Figure 3. Evolution of water use volume by sector in Mexico (2005–2020) (CONAGUA, 2024c).

Table 1. Water concessions registered in the state of Guanajuato by type and volume (CONAGUA, 2024d, 2024e).

Type of concession	Number of concessions	Authorized Volume (hm^3 $year^{-1}$)	Observations
Groundwater	6412	1960	High dependence on groundwater; several overexploited aquifers.
Surface	1734	510	They depend heavily on annual availability, with variability depending on the climate.

Table 2. Annual consumptive water use for agriculture in Guanajuato, Mexico (2019-2023) (CONAGUA, 2022; IEE, 2024).

Year	Consumptive water use (hm^3)
2019	3850.5
2020	3910.7
2021	3965.2
2022	4010.3
2023	4050.6

Regulations for the use and management of water

Mexican legislation has established a comprehensive regulatory framework aimed at ensuring the sustainability and efficiency of water resource use, which must be considered and complied with by developers of SPV pumping projects, regardless of client requirements. The National Water Law constitutes the cornerstone of this framework, as it establishes the guidelines related to the exploration and exploitation

of the nation's water resources (Chamber of Deputies, 2023). It also defines the mechanisms through which both the public and private sectors can request the use and exploitation of water.

In this context, the law distinguishes between allocation and concession: the allocation corresponds to the entitlement granted by the Federal Executive Power, through CONAGUA or the respective Basin Organization, to municipalities and states for the exploitation, use, or management of water resources; whereas the concession refers to the same type of entitlement, but granted to individuals or legal entities, whether public or private. According to Article 20, "concessions and allocations shall be granted after considering the parties involved and the economic and environmental cost of the planned works." The validity of these entitlements is established for a period ranging from 5 to 30 years, with the possibility of extensions for equivalent terms under similar conditions.

The law stipulates that the granting of a concession or allocation shall take into account the average annual water availability, which is reviewed at least every three years by CONAGUA and published through the National Water Information System (CONAGUA, 2024b). Once an allocation or concession has been granted, it will not be possible to dispose of greater volumes of water, and to permanently increase or modify water extraction in terms of volume, flow, or specific use, the issuance of the respective concession or allocation title must invariably be processed.

Moreover, the law also specifies the cases in which CONAGUA shall impose administrative sanctions on the responsible parties, highlighting the following: (a) exploiting, using, or managing national waters without the corresponding entitlement; and (b) exploiting, using, or managing national waters in volumes greater than those authorized. In both cases, fines are established ranging from 1,950 to 26,000 Units of Measurement and Update (UMAs, from the Spanish *Unidad de Medida y Actualización*), a general economic reference unit in Mexico used instead of the minimum wage for various legal and administrative purposes, which at the time this documentary research was conducted, corresponded to between 89,095 and 1,187,940 MXN.

It was found that various public agencies lack information or do not possess updated and accurate data, particularly regarding the number of concessions, the volume of water granted under concession, and current consumption levels. However, the data presented result from the consultation of several sources, which show an adequate degree of consistency among them. Therefore, it is imperative that the applicable regulations be refined and that the institutions responsible for their enforcement carry out field investigations to generate and/or update their databases, thereby enabling the implementation of appropriate management actions.

SUMMARY OF AGRICULTURAL PRODUCTION STATISTICS

According to data consulted from 2024, the state of Guanajuato ranks among the leading agricultural producers nationwide (FAO, 2024; USDA, 2024). The cultivated

area has reached 966,000 ha, of which 473,000 ha are under irrigation conditions, representing 48% of the total (Guzmán-Soria *et al*., 2009; SADER, 2024; SIAP, 2024). In terms of agricultural production, values of 9,189,000 Mg have been reached by 2023, of which 8,061,000 Mg were obtained under irrigation conditions, representing 87.72% of total production, which highlights the importance of pumping systems for irrigation. In the state, various crops such as wheat, alfalfa, asparagus, and strawberries have seen significant increases in their yield per hectare (Figure 4). In recent years, the area planted in Guanajuato has shown a downward trend, but with an increase in productivity, especially under irrigation conditions, reflecting the technification of the sector.

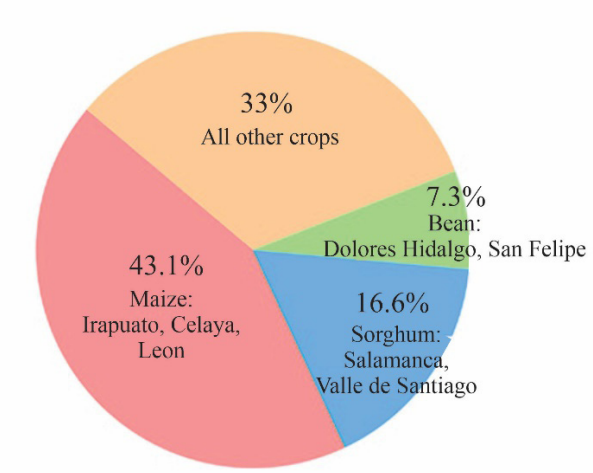

Figure 4. Percentage distribution of land area planted by crop in Guanajuato, Mexico, in 2023 (SIAP, 2024).

SOLAR PHOTOVOLTAIC SYSTEMS IN AGRICULTURE

The use of these systems in agricultural irrigation pumping has gained relevance due to their potential to reduce energy costs and promote sustainability (Cota-Espericueta *et al*., 2004; Walston *et al*., 2022; Carrausse and de Sartre, 2023). The state of Guanajuato has intense agricultural activity and is positioned advantageously in terms of solar radiation compared to other states in the country. Although no minimum average solar radiation values have been established for the development of an SPV (Matsumoto *et al*., 2014), Mexico has recorded a minimum average value of 4.14 kWh m^{-2}.

However, variability in solar energy availability poses a significant challenge. In Guanajuato, average irradiation is between 5 and 6 kWh m^{-2}, placing it in a competitive range nationally for solar energy projects (NASA, 2024). The efficiency of SPVs depends directly on the available sunlight, so days with low irradiation can affect farmers' ability to ensure a constant and sufficient supply of water, especially for crops that require continuous and uniform irrigation.

When applied to agricultural pumping, the high initial investment in solar modules, controllers, and pumps limits their adoption by small and medium-sized farmers without access to financing or subsidies, especially in rural communities where economic resources are scarce. Although the costs of SPV modules have decreased in recent years, the initial investment remains a barrier.

Although these systems require less maintenance than traditional fossil fuel-powered pumps, regular inspections and maintenance are still necessary to ensure optimal performance. The durability of components such as solar modules and pumps can be compromised by extreme environmental conditions, including high temperatures. This can result in the need for more frequent repairs or replacements, adding additional costs and complications for farmers.

Another challenge lies in the lack of technical knowledge and training among farmers on how to operate and maintain solar pumping systems. The successful adoption of this technology requires a level of technical skill and understanding that many farmers do not possess. The lack of training programs and technical assistance can limit the effectiveness and sustainability of the systems. Farmers need to be equipped with technology and knowledge to troubleshoot when necessary. Moreover, integrating these systems into traditional agricultural practices requires changes in farmers' habits and mindset, which can be a slow and challenging process.

Grid-connected systems

SPVs are classified as grid-connected or off-grid systems. The former allows farmers to continue operating on cloudy days or at night, as the grid provides a constant source of energy. However, despite government incentives, the initial installation of a grid-connected system can be costly, significantly affecting its profitability and return on investment times.

In most of the references consulted, it is mentioned that it is possible to sell surplus energy generated to the grid, which can result in a significant reduction in energy costs (Sarr *et al*., 2023). However, given the operating paradigm of the electricity market in Mexico, this is not possible, as the prices set for the purchase of surpluses are far from competitive, being based on the average value of the local marginal price and therefore do not represent a significant income for systems under 0.5 MW (DOF, 2017). Dependence on the grid means that, in the event of grid failures, supply may be interrupted.

Off-grid systems

Off-grid SPVs are particularly useful in rural areas of the state where grid connection is limited or non-existent, allowing farmers to operate independently. Furthermore, by not relying on the grid, farmers are not subject to electricity price fluctuations or potential power outages. However, these types of systems face operational, economic, and regulatory challenges.

Their generation capacity depends on weather conditions and the efficiency of the modules, which may be insufficient to meet annual energy demand, especially during

periods of intensive irrigation if they are not adequately sized. Added to this is the high cost of battery storage, which significantly increases the initial investment and maintenance costs. However, recent studies have demonstrated the viability of these installations (Babatunde *et al.*, 2020).

Brief cost comparison

Mérida-García *et al*. (2019) and Mantri *et al*. (2023) demonstrated that grid-connected SPVs have a lower levelized cost of energy (LCOE) compared to off-grid systems; however, both systems have lower LCOEs than those using fossil fuel generators. On the other hand, subsidized RABT and RAMT rates represent a significant barrier to the development of grid-connected SPVs, since a detailed analysis of the LCOE of these systems shows that their profitability depends on multiple factors, including installation and maintenance costs, and fluctuations in energy generation due to weather conditions.

The subsidized RABT rate is very similar to the DB1 and DB2 rates (Table 3). On the other hand, the RAMT rate has lower costs compared to the "General Medium-Voltage High-Demand" rate (GDMTO, from the Spanish *Gran Demanda en Media Tensión Ordinaria*) and "Hourly Medium-Voltage High Demand" rate (GDMTH, from the Spanish *Gran Demanda Media Tensión Horaria*) rates (CRE, 2024). Specifically, concerning the capacity charge, the RAMT rate is 42.48% and 48.93% lower than the corresponding charges for the GDMTO and GDMTH rates, respectively. As a result, when access to the electricity grid is available, it becomes evident that agricultural producers prefer a pumping system supplied by the grid rather than considering the option of SPV systems.

Table 3. Results of the consultation on final basic supply rates for the Bajío region 2024 (All values are expressed in Mexican pesos), (CRE, 2024).

Rate	Description	Schedule	Fixed charge $/month	Variable energy charge $/kWh	Variable charge for capacity $/kWh
DB1	Domestic Low Voltage up to 150 kWh-month	NA	36.26	2.2275	0.550
DB2	Domestic low voltage greater than 150 kWh-month	NA	36.26	2.0545	0.547
RABT	Low Voltage Agricultural Irrigation	NA	36.6	1.9876	0.634
RAMT	Medium Voltage Agricultural Irrigation	NA	362.6	0.9746	268.3
GDMTO	General Medium-Voltage High-Demand	NA	362.6	1.642	466.47
GDMTH	Hourly Medium-Voltage High Demand	Base	362.6	1.1199	525.42
		Medium		2.0050	
		High		2.2872	

Additional Challenges of SPV Systems in the Agricultural Sector

Another critical consideration in the implementation of these systems within the agricultural sector is land use. Traditional systems can occupy significant areas, thereby

reducing the land available for crop cultivation. This issue is particularly important in Guanajuato, where agricultural land represents a highly valuable resource. Effective implementation also requires careful planning to prevent shadows cast by the photovoltaic modules from decreasing agricultural productivity. Alternatives such as the use of non-arable land or floating structures on water bodies have been proposed as viable strategies to mitigate land-use impacts.

On the other hand, water resource management in the state represents an increasing challenge, particularly in terms of controlling and monitoring wells used for agricultural irrigation in rural areas that are difficult to access. Government institutions face serious difficulties in obtaining accurate data on these wells, due to a combination of complex factors.

One of the effects is the illegal exploitation of aquifers. In Guanajuato, clandestine wells have been drilled by farmers to secure a water supply, especially in regions where availability is limited (CONAGUA, 2024f). This unregulated use has led to significant overexploitation of aquifers, contributing to an alarming decline in groundwater levels in several areas of the state. Furthermore, insecurity in some regions prevents authorities from accessing these wells to carry out inspections and regulatory activities, as the state has experienced an increase in violence linked to organized crime.

The lack of control not only exacerbates the overexploitation of aquifers but also jeopardizes the sustainability of agriculture in the state. As a result, agricultural productivity in Guanajuato could reach precarious levels if these problems are not solved. The water crisis may affect not only food production but also the local economy, which depends mostly on agriculture. The need to implement effective regulation and conservation policies is becoming increasingly important to ensure the future of agriculture in the region.

Public policies for the development of SPV systems

In Mexico, the implementation of SPV systems for water pumping has been actively promoted. During the 2013–2015 period, the Shared Risk Trust Fund under the Ministry of Agriculture, Livestock, Rural Development, Fisheries, and Food supported the installation of 52 SPV systems, of which 41 were implemented in dairy farms, four in ecotourism facilities, three in the agricultural sector, three in agro-industrial operations, and one in swine facilities. The systems generate approximately 2,405 MWh per year, preventing the emission of 1,200 Mg of CO_2 into the atmosphere.

Recently, the Sectoral Program for Agriculture and Rural Development 2020–2024 (SADER, 2020) established the foundations for promoting renewable energies within "Priority Objective 3: Increase sustainable production practices in the agricultural and aquaculture-fisheries sector in response to agro-climatic risks," and specifically under "Priority Strategy 3.2: Promote adaptation and mitigation actions to climate change for comprehensive risk management; Specific Action 3.2.5: Encourage the use of and transition to renewable energies in agricultural, aquaculture, and fisheries activities."

As a result of these public policies, the National Commission for Arid Zones has promoted solar pumping through shared financing schemes. For example, in Quintana Roo, more than 2,487 SPV modules for agricultural pumping have been installed, benefiting at least seven communities. In turn, the Government of the State of Guanajuato, through the Ministry of Agriculture, Food, and Rural Development, and the Ministry of Agriculture and Rural Development (SADER, from the Spanish *Secretaría de Agricultura y Desarrollo Rural*), continually issues calls for proposals to access funding aimed at improving productivity in the agricultural sector, which includes the implementation of alternative energy sources.

However, as mentioned previously, greater knowledge is required to take advantage of these programs for the development of SPV systems applied to agricultural water pumping. Based on the authors' experience in conducting this research, there is a lack of information from the Mexican government and federal entities regarding the promotion, development, and installation of these types of systems. When addressing the development of the agricultural sector, most of the reported results focus on water harvesting, increased crop productivity, and managed subsidies, including the electricity rate subsidies, while overlooking the outcomes derived from the implementation of renewable energy sources.

PERSPECTIVE ON PVS SYSTEMS FOR AGRICULTURAL IRRIGATION IN THE STATE OF GUANAJUATO

The state of Guanajuato has experienced an 85% growth in distributed electricity generation capacity during the 2022–2024 period, ranking fourth nationwide, with an installed capacity of 290 MW (GTO, 2025a). Recently, five off-grid SPV systems with storage have been implemented in locations without access to electricity from the Federal Electricity Commission (CFE, from the Spanish *Comisión Federal de Electricidad*) grid. Such is the case of the community of El Refugio, where two of these systems were installed to power brick production kilns, one system in the Cuenca La Esperanza protected natural area, and two systems in Sierra de Lobos; however, their installed capacity is not reported (GTO, 2025b).

As a relevant outcome of the present research, it was found that there is no available information that would allow the establishment of a perspective or the performance of statistical or comparative analyses with other entities and/or countries. Government data only provide estimates regarding the number of well concessions, the volume of water granted under concession, and current consumption levels. The situation is even more critical in the case of information related to SPV systems for agricultural irrigation. For grid-connected systems, the CFE only reports data on interconnection requests without distinguishing those intended for agricultural irrigation. In the case of off-grid systems, there is no organization or bibliographic source that provides related data or information.

To overcome the aforementioned limitations, it is necessary to implement a series of strategic actions aimed at strengthening the management and utilization of SPV

systems applied to agricultural irrigation. First, it is proposed to design and implement a national system for registration and monitoring of these systems, integrating key information such as their location, installed capacity, configuration type (off-grid or grid-connected), associated water source, and both electricity and water consumption volumes. Likewise, it is essential to establish inter-institutional coordination between the CFE, CONAGUA, SADER, the National Energy Commission (formerly called Energy Regulatory Commission), and state and municipal governments to integrate and standardize the available data on water concessions, energy consumption, and photovoltaic technologies used in the agricultural sector.

Another priority measure is the incorporation of a specific category for agricultural use within the official reports on distributed generation and interconnection requests issued by CFE, which will allow for the clear identification of SPV systems intended for irrigation. Likewise, it is necessary to promote the development of technical studies and specialized surveys led by academic institutions and public organizations to obtain reliable and up-to-date data on the adoption, efficiency, and sustainability of these technologies in the agricultural sector. Finally, it is proposed to strengthen mandatory technical and operational reporting mechanisms as a requirement to access financial support, subsidies, or permits, ensuring the continuous update of a public, systematized, and periodically maintained database.

The implementation of these actions will enable, in the short and medium term, the performance of qualitative and quantitative analyses on SPV systems for agricultural irrigation in the state, thereby strengthening technical decision-making and the formulation of more effective and sustainable public policies in the agricultural sector.

CONCLUSIONS

In Guanajuato, agriculture relies primarily on groundwater well irrigation, which has led to the overexploitation of aquifers and recurring annual water deficits. Illegal well drilling and lack of supervision due to rural insecurity further exacerbate the challenges to agricultural sustainability. On the other hand, the use of SPV systems for agricultural water pumping has gained relevance as a sustainable alternative to address energy and environmental challenges. The high solar irradiance in the state favors the development of SPV systems; however, the high initial investment limits their adoption, particularly among small and medium-sized producers without access to financing.

Although off-grid SPV systems have been implemented in areas without access to the electricity network, the lack of specific information limits their evaluation and planning in agricultural irrigation. The available data do not allow for an accurate determination of the number, capacity, coverage, or efficiency of the systems used for irrigation. This information gap hinders the development of technical assessments, international comparisons, and the design of effective public policies. Consequently, it is essential to establish institutional mechanisms for the collection, systematization,

and publication of disaggregated data to enable more effective monitoring and promotion of solar energy adoption in the agricultural sector.

REFERENCES

Babatunde DE, Babatunde OM, Uzoamaka Emezirinwune M, Denwigwe IH, Okharedia TE, Omodara OJ. 2020. Feasibility analysis of an off-grid photovoltaic-battery energy system for a farm facility. International Journal of Electrical and Computer Engineering 10 (3): 2874–2883. https://doi.org/10.11591/ijece.v10i3.pp2874-2883

Cámara de Diputados. 2023. Ley de aguas nacionales. Diario Oficial de la Federación. Congreso de la Unión. Ciudad de México, México. https://www.diputados.gob.mx/LeyesBiblio/ref/lan.htm (Recuperado: septiembre 2025).

Carrausse R, de Sartre XA. 2023. Does agrivoltaism reconcile energy and agriculture? Lessons from a French case study. Energy, Sustainability and Society, 13 (8). https://doi.org/10.1186/s13705-023-00387-3

CFE (Comisión Federal de Electricidad). 2024a. Esquema tarifario vigente. Gobierno de México. Comisión Federal de Electricidad. Ciudad de México, México. https://app.cfe.mx/Aplicaciones/CCFE/Tarifas/TarifasCRENegocio/Negocio.aspx (Recuperado: septiembre 2025).

CFE (Comisión Federal de Electricidad). 2024b. Tarifa RABT. Gobierno de México. Comisión Federal de Electricidad. Ciudad de México, México. https://app.cfe.mx/Aplicaciones/CCFE/Tarifas/TarifasCRENegocio/Tarifas/RiegoAgricolaBT.aspx (Recuperado: septiembre 2025).

CFE (Comisión Federal de Electricidad). 2024c. Tarifa RAMT. Gobierno de México. Comisión Federal de Electricidad. Ciudad de México, México. https://app.cfe.mx/Aplicaciones/CCFE/Tarifas/TarifasCRENegocio/Tarifas/RiegoAgricolaMT.aspx (Recuperado: septiembre 2025).

CONAGUA (Comisión Nacional del Agua). 2018. Atlas del agua en México. Gobierno de México. Secretaría del Medio Ambiente y Recursos Naturales. Comisión Nacional del Agua. Ciudad de México, México. https://files.conagua.gob.mx/conagua/publicaciones/Publicaciones/AAM2018.pdf (Recuperado: septiembre 2025).

CONAGUA (Comisión Nacional del Agua). 2022. Estadísticas del agua en México 2021. Secretaría de Medio Ambiente y Recursos Naturales. Comisión Nacional del Agua. Ciudad de México, México. 349 p.

CONAGUA (Comisión Nacional del Agua). 2024a. Estadísticas agrícolas de los distritos de riego. Gobierno de México. Secretaría del Medio Ambiente y Recursos Naturales. Comisión Nacional del Agua. Ciudad de México, México. https://www.gob.mx/conagua/documentos/estadisticas-agricolas-de-los-distritos-de-riego (Recuperado: septiembre 2025).

CONAGUA (Comisión Nacional del Agua). 2024b. Sistema nacional de información del agua. Gobierno de México. Secretaría del Medio Ambiente y Recursos Naturales. Comisión Nacional del Agua. Ciudad de México, México. https://sinav30.conagua.gob.mx:8080/ (Recuperado: septiembre 2025).

CONAGUA (Comisión Nacional del Agua). 2024c. Usos del agua. Gobierno de México. Secretaría del Medio Ambiente y Recursos Naturales. Comisión Nacional del Agua. Ciudad de México, México. https://sinav30.conagua.gob.mx:8080/UsosAgua/#/totales (Recuperado: septiembre 2025).

CONAGUA (Comisión Nacional del Agua). 2024d. Sistema de información de acuíferos y cuencas. Gobierno de México. Secretaría del Medio Ambiente y Recursos Naturales. Comisión Nacional del Agua. Ciudad de México, México. https://sigagis.conagua.gob.mx/gas1/index.html (Recuperado: septiembre 2025).

CONAGUA (Comisión Nacional del Agua). 2024e. Aguas subterráneas. Gobierno de México. Secretaría del Medio Ambiente y Recursos Naturales. Comisión Nacional del Agua. Ciudad de México, México. https://www.gob.mx/conagua/acciones-y-programas/agua-subterranea (Recuperado: septiembre 2025).

CONAGUA (Comisión Nacional del Agua). 2024f. Clausura CONAGUA pozos irregulares en León, Guanajuato. Gobierno de México. Secretaría del Medio Ambiente y Recursos Naturales. Comisión Nacional del Agua. Ciudad de México, México. https://www.gob.mx/conagua/prensa/228578 (Recuperado: septiembre 2025).

Cota-Espericueta AD, Foster RE, Ross MP, Montúfar-Avilez O, Paredes-Rubio AR. 2004. Ten-year reliability assessment of photovoltaic water pumping systems in Mexico. Solar 2004: 9–14.

CRE (Comisión Reguladora de Energía). 2024. Memorias de cálculo de tarifas de suministro básico. Gobierno de México. Comisión Reguladora de Energía. Ciudad de México, México. https://www.gob.mx/cne/articulos/memorias-de-calculo-de-las-tarifas-electricas (Recuperado: septiembre 2025).

DNV (Det Norske Veritas). 2023. Energy transition outlook 2023. Bærum, Norway. https://www.dnv.com/energy-transition-outlook/download (Recuperado: septiembre 2025).

DOF (Diario Oficial de la Federación). 2017. RES/142/2017. RESOLUCIÓN de la Comisión Reguladora de Energía por la que expide las disposiciones administrativas de carácter general, los modelos de contrato, la metodología de cálculo de contraprestación y las especificaciones técnicas generales, aplicables a las centrales eléctricas de generación distribuida y generación limpia distribuida. Gobierno de México, Comisión Reguladora de Energía. Ciudad de México, México. https://www.cenace.gob.mx/Docs/16_MARCOREGULATORIO/GenDis/(DOF%202017-03-07%20CRE)%20RES-142-2017%20DACG%20Generaci%C3%B3n%20Distribuida.pdf (Recuperado: septiembre 2025).

FAO (Food and Agriculture Organization of the United Nations). 2024. GIEWS - Global information and early warning system. Rome, Italy. https://www.fao.org/giews/countrybrief/country.jsp?code=Mex (Recuperado: septiembre 2025).

GTO (Gobierno del Estado de Guanajuato). 2025a. Guanajuato 4 lugar a nivel nacional en generación distribuida mediante paneles solares. Guanajuato, México. https://boletines.guanajuato.gob.mx/2025/02/23/guanajuato-4-lugar-a-nivel-nacional-en-generacion-distribuida-mediante-paneles-solares/ (Recuperado: septiembre 2025).

GTO (Gobierno del Estado de Guanajuato). 2025b. Promueven sustentabilidad energética. Guanajuato, México. https://boletines.guanajuato.gob.mx/2024/12/26/promueven-la-sustentabilidad-energetica/ (Recuperado: septiembre 2025).

Guevara M, Manzini F, Sánchez-Juárez A. 2025. Technical and economic analysis for the implementation of photovoltaic systems in agricultural zones of Mexico City: A case study. Energy for Sustainable Development 87: 101743. https://doi.org/10.1016/j.esd.2025.101743

Guzmán-Soria E, Hernández-Martínez J, García-Salazar JA, Rebollar-Rebollar S, de la Garza-Carranza MT, Hernández-Soto D. 2009. Consumo de agua subterránea en Guanajuato, México. Agrociencia 43 (7): 749–761.

IEE (Instituto de Ecología del Estado de Guanajuato). 2024. Sistema de indicadores ambientales y de sustentabilidad. Guanajuato, México. https://smaot.guanajuato.gob.mx/sitio/micro/siaseg/agua.php (Recuperado: septiembre 2025).

Mantri SR, Kasibhatla RS, Chennapragada VKB. 2023. Grid-connected vs. off-grid solar water pumping systems for agriculture in India: A comparative study. Journal of Energy Sources, Part A: Recovery, Utilization, and Environmental Effects 46 (1): 6348–6362. https://doi.org/10.1080/15567036.2020.1745957

Matsumoto Y, Valdés M, Urbano JA, Kobayashi T, López G, Peña R. 2014. Global solar irradiation in north Mexico City and some comparisons with the south. Energy Procedia 57: 1179–1188. https://doi.org/10.1016/j.egypro.2014.10.105

Mérida-García A, Gallagher J, McNabola A, Camacho-Poyato E, Montesinos-Barrios P, Rodríguez-Díaz JA. 2019. Comparing the environmental and economic impacts of on- or off-grid solar photovoltaics with traditional energy sources for rural irrigation systems. Renewable Energy 140: 895–904. https://doi.org/10.1016/j.renene.2019.03.122

Molina A, Sánchez-López AM, Martínez-Jiménez E, Bárcenas-Cortés AL, Ponce P. 2025. Creation of Parcelas 5.0 using the 5S framework (social, sustainable, smart, sensing and safe) to improve traditional farming in Mexico. International Journal of Sustainable Engineering 18 (1). https://doi.org/10.1080/19397038.2025.2471306

NASA (National Aeronautics and Space Administration). 2024. NASA prediction of worldwide energy resources (POWER), data access viewer (DAV) v2.3.6. Washington, DC, USA. https://power.larc.nasa.gov/data-access-viewer/ (Recuperado: septiembre 2025).

Negera M, Dejen ZA, Melaku D, Tegegne D, Adamseged ME, Haileslassie A. 2025. Agricultural productivity of solar pump and water harvesting irrigation technologies and their impacts on smallholder farmers' income and food security: Evidence from Ethiopia. Sustainability 17 (4): 1486. https://doi.org/10.3390/su17041486

ONU (Organización de las Naciones Unidas). 2024. Programa para el Medio Ambiente: Siete formas de restaurar las tierras, detener la desertificación y combatir la sequía. Roma, Italia. https://www.unep.org/es/noticias-y-reportajes/reportajes/siete-formas-de-restaurar-las-tierras-detener-la-desertificacion-y (Recuperado: septiembre 2025).

SADER (Secretaría de Agricultura y Desarrollo Rural). 2020. Programa sectorial de Agricultura y Desarrollo Rural 2020-2024. Gobierno de México. Secretaría de Agricultura y Desarrollo Rural. Ciudad de México, México. https://www.gob.mx/cms/uploads/attachment/file/708557/PROGRAMA_SECTORIAL_2020_2024baja.pdf (Recuperado: septiembre 2025).

SADER (Secretaría de Agricultura y Desarrollo Rural). 2024. Evolución de la producción agrícola en Guanajuato. Gobierno de México. Secretaría de Agricultura y Desarrollo Rural. Ciudad de México, México. https://www.gob.mx/agricultura/guanajuato/articulos/evolucion-de-la-produccion-agricola-en-guanajuato?idiom=es (Recuperado: septiembre 2025).

Sarr A, Soro YM, Tossa AK, Diop L. 2023. Agrivoltaic, a synergistic co-location of agricultural and energy production in perpetual mutation: A comprehensive review. Processes 11 (3): 948. https://doi.org/10.3390/pr11030948

SIAP (Servicio de Información Agroalimentaria y Pesquera). 2024. Producción agrícola. Gobierno de México. Servicio de Información Agroalimentaria y Pesquera. Ciudad de México, México. https://www.gob.mx/agricultura/dgsiap/acciones-y-programas/produccion-agricola-404122 (Recuperado: septiembre 2025).

USDA (U.S. Department of Agriculture). 2024. Mexico: Grain and feed update. Washington, DC, USA. https://fas.usda.gov/data/mexico-grain-and-feed-update-25 (Recuperado: septiembre 2025).

Walston LJ, Barley T, Bhandari I, Campbell B, McCall J, Hartmann HM, Dolezal AG. 2022. Opportunities for agrivoltaic systems to achieve synergistic food-energy-environmental needs and address sustainability goals. Frontiers in Sustainable Food Systems 6: 1–13. https://doi.org/10.3389/fsufs.2022.932018

Yusuf I, Sanusi A. 2025. Reliability and performance optimization of solar-powered water irrigation system for rural small-scale farming. International Journal of Applied and Computational Mathematics 11 (2). https://doi.org/10.1007/s40819-025-01840-x